



저작자표시-비영리-변경금지 2.0 대한민국

이용자는 아래의 조건을 따르는 경우에 한하여 자유롭게

- 이 저작물을 복제, 배포, 전송, 전시, 공연 및 방송할 수 있습니다.

다음과 같은 조건을 따라야 합니다:



저작자표시. 귀하는 원저작자를 표시하여야 합니다.



비영리. 귀하는 이 저작물을 영리 목적으로 이용할 수 없습니다.



변경금지. 귀하는 이 저작물을 개작, 변형 또는 가공할 수 없습니다.

- 귀하는, 이 저작물의 재이용이나 배포의 경우, 이 저작물에 적용된 이용허락조건을 명확하게 나타내어야 합니다.
- 저작권자로부터 별도의 허가를 받으면 이러한 조건들은 적용되지 않습니다.

저작권법에 따른 이용자의 권리는 위의 내용에 의하여 영향을 받지 않습니다.

이것은 [이용허락규약\(Legal Code\)](#)을 이해하기 쉽게 요약한 것입니다.

[Disclaimer](#)

이학박사학위논문

**Development of New Catalytic Synthetic Methodologies:  
Lactam Synthesis, Cyanohydrin Dehydrogenation, and  
Photocatalytic Cyanation of Aryl Halides**

새로운 촉매적 유기 합성법 개발:  
락탐 합성, 사이아노하이드린 탈수소화 반응, 아릴  
할라이드의 사이안화 광촉매 반응

2018년 8월

서울대학교 대학원

화학부 유기화학전공

김 기 철



## **Abstract**

# **Development of New Catalytic Synthetic Methodologies: Lactam Synthesis, Cyanohydrin Dehydrogenation, and Photocatalytic Cyanation of Aryl Halides**

**Kicheol Kim**

Department of Chemistry

The Graduate School

Seoul National University

Development of an efficient green chemical methodology is significant for organic synthesis and human society. Most conventional synthetic methods, in spite of being efficient, suffer from several drawbacks: production of wastes and subsequent cost for their treatment, use of stoichiometric and/or hazardous reagents, harsh reaction conditions such as high temperature and high pressure, and prefunctionalization of substrates for high reactivity. Such downsides have to be resolved considering fossil fuel depletion, climate change, and environmental pollution. We also need efficient organic synthesis to improve commercial products and medicines.

Sustainable green chemistry has emerged as an inevitable discipline in the 21<sup>st</sup> century. This concept endeavors to reduce or eliminate the use and generation of hazardous substances at the molecular level.<sup>1</sup> Chemical processes and the production of materials should be designed following several criteria: prevention of waste, atom economy, less hazardous synthesis, energy efficiency, and reduction of derivatives. In these aspects, organometallic catalysis is a suitable tool for achieving green chemistry and efficient organic chemistry. In contrast to traditional synthetic methods, organometallic catalytic methods promote transformations via distinct mechanistic pathways operated by transition metal-ligand complexes in a catalytic manner. In this thesis, the development of atom- and step-economical, and efficient organic reactions of readily available feedstocks was explored using two major activation modes mediated by a rationally designed organometallic catalyst: alcohol activation and copper-based photocatalysis. This work is divided into three stages: establishment of a strategy on the basis of working mechanism (*organic synthesis*), design and syntheses of catalyst and ligand to achieve the desired reactivity (*organometallic chemistry*), and investigation of mechanism in terms of electronic and steric effects for further reactivity improvement (*catalysis*).

**Part I – Alcohol Activation and its Application for Lactam Synthesis via Tandem C–N Bond Formation and Dehydrogenation of Cyanohydrins (Chapter 1-3):** Dehydrogenation of alcohol as substrate-activating strategy in homogeneous transition metal catalysis affords a reactive and versatile carbonyl compound for further tandem transformation (Chapter 1).<sup>2</sup> In the absence of highly reactive reagents such as alkyl halides or oxidants, we could realize the dehydrogenative transformation of alcohols, concomitantly achieving atom economy and avoiding mutagenic reagents. Chapter 2 describes the development of

the first Ir-catalyzed N-substituted lactam synthesis. We identified a [Cp\*Ir] catalyst that is active for the synthesis of lactams from lactones and amines via dehydrogenative C–N bond formation. This method provides a step-economical and readily accessible way to produce *N*-substituted lactams from simple starting materials. Mechanistic studies indicate that the domino reaction—aminolysis of lactone, *N*-alkylation of a hydroxyamide with amine, and intramolecular transamidation of aminoamide—afforded lactams, offering a distinctive mechanistic insight different from those of non-catalytic lactam syntheses. Chapter 3 demonstrates the first Ru-catalyzed dehydrogenation of cyanohydrins under base-free conditions using an acceptor-less alcohol dehydrogenation (AAD) strategy. The ruthenium(II) arene complex bearing  $\eta^2$ -bidentate phosphine ligand promoted the kinetically controlled dehydrogenation reaction over the thermodynamically preferred elimination of hydrogen cyanide. The effects of ligands, coordination mode, and counteranions in the Ru catalyst were investigated to modulate catalytic activity and selectivity. Selective dehydrogenation occurred via the  $\beta$ -hydride elimination of experimentally observed ruthenium-alkoxide species.

**Part II – Copper-based Photocatalyst for Cross-Coupling Reactions and its Application for Cyanation of Aromatic Halides (Chapters 4-5):**

Photocatalysis has been highlighted as an environmentally benign activation mode for small molecules, compared to thermal activation in conventional organic reactions (Chapter 4). In this concept, photons activate a photocatalyst to mediate energy transfer or single-electron transfer (SET) with organic molecules. Cu-based photocatalysis stands as an alternative or complementary photocatalytic system to Ru- and Ir-based photoredox catalysis in terms of cost, stability, and activity.<sup>3</sup> Specifically, Cu(I) complexes can directly mediate cross-coupling reactions under

mild condition by participating in catalytic processes and promoting SET processes.<sup>4</sup> Chapter 5 describes the development of the first photoinduced Cu(I)-bisimine catalyzed cyanation of aryl halides at room temperature. This SET-mediated mild C(sp<sup>2</sup>)-cyanation reaction exhibited outstanding tolerance to diverse functional groups including free amino groups, carboxylic groups, and amino acids and high chemoselectivity against S<sub>N</sub>2-reactive alkyl chlorides, which were not achieved in previously developed two-electron-based Cu catalysis.

The development of novel and efficient synthetic methods using simple substrates in rationally designed catalytic systems is demonstrated via two substrate-activation modes: *alcohol activation* and *Cu-based photocatalysis*. Investigations of the synthetic utility and mechanism of the developed catalytic methods are also described in this dissertation.

## Reference

- (1) P. Anastas, N. Eghbali, *Chem. Soc. Rev.* **2010**, *39*, 301.
- (2) G. E. Dobereiner, R. H. Crabtree, *Chem. Rev.* **2010**, *110*, 681.
- (3) S. Paria, O. Reiser, *ChemCatChem* **2014**, *6*, 2477.
- (4) S. E. Creutz, K. J. Lotito, G. C. Fu, J. C. Peters, *Science* **2012**, *338*, 647.

**Keywords:** Organic chemistry, Organometallic catalysis, Green chemistry, Transition metal catalyst, Design of catalyst and ligand, Alcohol activation, Photocatalysis, Lactam, Acyl cyanide, Aromatic nitrile

**Student Number:** 2013-20256



# Table of Contents

Abstract .....	i
Table of Contents .....	v
List of Tables .....	xii
List of Schemes .....	xiii
List of Figures .....	xvii
List of Abbreviations .....	xviii

## **Part I – Alcohol Activation and its Application for Lactam Synthesis via Tandem C–N Bond Formation and Dehydrogenation of Cyanohydrins (Chapter 1-3)**

### **Chapter 1. Dehydrogenative Alcohol Activation for Oxidation of Alcohols and *N*-Alkylation of Amines**

1.1 Introduction .....	1
1.2 Oxidation of alcohols .....	3
1.2.1 Traditional methods using stoichiometric oxidants and the origin of reactivity .....	3
1.2.2 Catalytic methods using transition metal complexes: with hydrogen acceptors or acceptorless condition .....	5
1.2.3 Representative methods for acceptorless alcohol dehydrogenation: Rh, Ru, Ir and 1 <sup>st</sup> -row transition metal based catalytic systems .....	9
1.2.4 Selective AAD of primary alcohol to aldehyde .....	15
1.3 Redox-neutral alcohol activation: <i>N</i> -alkylation of amines with alcohols .....	17
1.3.1 Importance of organonitrogen compounds and their traditional syntheses .....	18

1.3.2 Representative homogeneous catalytic methods for <i>N</i> -alkylation of amines with alcohols: two major precious metal Ru- and Ir-based systems ..	20
1.3.3 Representative homogeneous catalytic methods for <i>N</i> -alkylation of amines with alcohols: base metal-based catalytic systems .....	28
1.4 Conclusion.....	32
1.5 References .....	33

## **Chapter 2. Iridium-Catalyzed Single-Step *N*-Substituted Lactam Synthesis from Lactones and Amines**

2.1 Introduction.....	39
2.2 Results and discussion .....	41
2.2.1 Optimization for lactam synthesis from lactones and amines .....	41
2.2.2 Substrate scope.....	44
2.2.3 Mechanistic studies .....	47
2.2.4 Chemoselectivity of the reaction of alcohols and amines for two different C–N bond formations: <i>N</i> -alkylation and amide formation.....	51
2.3 Conclusion.....	57
2.4 Experimental section.....	58
2.4.1 General considerations .....	58
2.4.2 General procedure for lactam synthesis from lactones and amines .....	59
2.4.3 Procedure for kinetic study .....	60
2.4.4 Characterization of compounds.....	61
2.5 References .....	69

## **Chapter 3. Acceptorless and Base-free Dehydrogenation of Cyanohydrin with ( $\eta^6$ -arene)halide(bidentate phosphine)ruthenium(II) Complex**

3.1 Introduction.....	73
-----------------------	----

3.2 Results and discussion .....	77
3.2.1 Optimization for dehydrogenation of cyanohydrins.....	77
3.2.2 The effects of the nature of the catalyst on the selective dehydrogenation.....	81
3.2.3 Substrate scope.....	84
3.2.4 Mechanistic studies .....	86
3.3 Conclusion.....	90
3.4 Experimental section.....	91
3.4.1 General considerations .....	91
3.4.2 Substrate and catalyst preparation.....	92
3.4.2.1 Preparation of cyanohydrins .....	92
3.4.2.2 Preparation of catalysts .....	93
3.4.2.2.1 Preparation of catalyst precursors.....	93
3.4.2.2.2 Preparation of dppe derivatives .....	93
3.4.2.2.3 Preparation of catalyst <b>5</b> .....	95
3.4.2.2.4 Preparation of <i>trans</i> -[RuCl <sub>2</sub> (PP) <sub>2</sub> ] .....	99
3.4.3 General procedure for acceptorless and base-free dehydrogenation of cyanohydrin and isolation .....	100
3.4.4 Mechanistic investigation.....	101
3.4.4.1 Substoichiometric reactions of [Ru(benzene)Cl <sub>2</sub> ] with dppe and <b>1a</b> [Figure 3.1] .....	101
3.4.4.2 Catalytic activity of <i>trans</i> -[RuCl <sub>2</sub> (PP) <sub>2</sub> ] .....	102
3.4.4.3 Coordination mode: the reaction of [Ru(benzene)Cl(dppe)]Cl with cyanohydrin <b>1m</b> [Figure 3.2–3.3] .....	103
3.4.5 Calculation .....	104
3.4.5.1 General computational method.....	104
3.4.5.2 References for computation .....	105

3.4.5.3 Raw energy data.....	107
3.4.6 Characterization of products .....	109
3.5 References .....	116

## **Part II – Copper-based Photocatalyst for Cross-Coupling Reactions and its Application for Cyanation of Aromatic Halides (Chapters 4-5)**

### **Chapter 4. Copper-based Photocatalysis for Cross-Coupling Reaction**

4.1 Introduction.....	121
4.2 Copper photocatalysis for organic synthesis .....	123
4.2.1 Electronic, geometric, and photophysical properties of copper(I) complexes.....	124
4.2.2 Copper photocatalysis for [2+2] cycloaddition and atom transfer radical addition (ATRA) .....	126
4.3 Copper-based photocatalysis for cross-coupling reactions .....	129
4.3.1 Pioneering works of Fu and Peters groups in copper photocatalysis for cross-coupling reactions .....	129
4.3.2 Mechanistic investigation of copper photocatalysis for cross-coupling reactions by Fu and Peters groups.....	140
4.3.3 Contributions of other groups in copper photocatalysis for cross-coupling reactions .....	145
4.4 Conclusion.....	147
4.5 References .....	148

### **Chapter 5. Photoinduced Copper(I)-Catalyzed Cyanation of Aromatic Halides at Room Temperature**

5.1 Introduction.....	152
-----------------------	-----

5.2 Results and discussion .....	154
5.2.1 Optimization for cyanation of aromatic halides .....	154
5.2.2 Substrate scope .....	156
5.2.3 Chemoselectivity of the method.....	160
5.2.4 Mechanistic investigation.....	161
5.3 Conclusion.....	165
5.4 Experimental section.....	166
5.4.1 General considerations .....	166
5.4.2 Catalyst and substrate preparation.....	167
5.4.2.1 Preparation of bisimines .....	167
5.4.2.2 Preparation of CuX-bisimine complexes .....	170
5.4.2.3 Preparation of substrate .....	172
5.4.3 Experimental setup and general procedure for photoinduced copper catalyzed cyanation of aryl halides .....	175
5.4.3.1 Photoreaction setup.....	175
5.4.3.2 General procedure.....	176
5.4.4 Additional screening tables .....	177
5.4.5 Reactivity comparison ([CuI(bisimine-CN)] and [CuI]).....	180
5.4.6 Mechanistic investigation (light-dark experiment, radical scavenger, kinetic profile, and kinetic order).....	181
5.4.6.1 Light-dark experiment (Figure 5.1) .....	181
5.4.6.2 Inhibition by radical scavenger .....	182
5.4.6.3 Kinetic profile (Figure 5.1).....	182
5.4.6.4 Kinetic order .....	183
5.4.7 Characterization of products .....	185
5.4.7.1 Protection of carboxylic groups.....	185
5.4.7.2 Protection of amino acid.....	186

5.4.7.3 Characterization of products.....	188
5.5 Notes and References.....	204

# List of Tables

## Chapter 2

**Table 2.1** Optimization of reaction conditions ..... 43

**Table 2.2** Direct lactam synthesis from lactones and amine..... 45

## Chapter 3

**Table 3.1** Optimization of reaction conditions..... 79

**Table 3.2** Raw energy data for optimized geometries..... 107

## Chapter 5

**Table 5.1** Optimization of reaction conditions..... 155

**Table 5.2** Cu catalysts (variation of X and bisimine ligands)..... 177

**Table 5.3** Cyanide source (nucleophilic, neutral, and electrophilic) ..... 178

**Table 5.4** Solvent..... 179

**Table 5.5** Reaction with simple CuI catalyst..... 180

# List of Schemes

## Chapter 1

<b>Scheme 1.1</b> Representative synthetic methods for aldehydes and ketones.....	2
<b>Scheme 1.2</b> Catalytic dehydrogenation of alcohols as an alcohol activation mode..	3
<b>Scheme 1.3</b> Traditional conditions for oxidation of alcohols .....	4
<b>Scheme 1.4</b> Catalytic dehydrogenation of alcohols: with a hydrogen acceptor, acceptorless method (AAD), and base free AAD method.....	5
<b>Scheme 1.5</b> Preliminary reactions of hetero-/homogeneous catalytic AD.....	7
<b>Scheme 1.6</b> Schematic view of homogeneous catalytic alcohol dehydrogenation ...	8
<b>Scheme 1.7</b> A) First catalytic example of AAD reactivity. B) Thermodynamic data of alcohol dehydrogenation .....	9
<b>Scheme 1.8</b> Two catalytic modes: outer-sphere and inner-sphere mechanism. Shvo catalyst following the outer-sphere mechanism .....	10
<b>Scheme 1.9</b> Application of Noyori's catalyst via microscopic reversibility .....	11
<b>Scheme 1.10</b> Representative examples of AAD catalytic systems .....	14
<b>Scheme 1.11</b> AAD of primary alcohols to aldehydes .....	16
<b>Scheme 1.12</b> Representative amine syntheses.....	19
<b>Scheme 1.13</b> First examples of N-alkylation of amines with alcohols in 1981.....	20
<b>Scheme 1.14</b> Improved catalytic systems before the 2000s.....	21
<b>Scheme 1.15</b> Works of the Beller group: Ru & monophosphine catalytic systems	22
<b>Scheme 1.16</b> Works of the Williams group: Ru & bidentate phosphine catalytic systems.....	23
<b>Scheme 1.17</b> N-alkylation of ammonia under the Milstein's catalytic systems.....	23



<b>Scheme 1.18</b> Works of the Fujita and Yamaguchi group: Cp*Ir-catalyzed <i>N</i> -alkylation .....	24
<b>Scheme 1.19</b> Newly designed Cp*Ir complexes and their catalysis.....	26
<b>Scheme 1.20</b> Use of carbohydrates in <i>N</i> -alkylation and large-scale reaction for pharmaceutically active compound synthesis .....	27
<b>Scheme 1.21</b> Cu-catalytic systems.....	28
<b>Scheme 1.22</b> Co-, Mn-, and Ni-catalytic systems.....	29
<b>Scheme 1.23</b> Fe-catalytic systems .....	31
 <b>Chapter 2</b>	
<b>Scheme 2.1</b> Conventional methods for <i>N</i> -substituted lactam synthesis.....	40
<b>Scheme 2.2</b> Research strategy and its background .....	41
<b>Scheme 2.3</b> Catalytic reactions of observed intermediates in the presence or absence of amines .....	49
<b>Scheme 2.4</b> Proposed catalytic cycle.....	50
<b>Scheme 2.5</b> Two pathways of hemiaminal reaction.....	51
<b>Scheme 2.6</b> The Milstein group: effort to control selectivity between amide and imine formation.....	52
<b>Scheme 2.7</b> The Mashima group: effort to control selectivity between amide or imine formation.....	54
<b>Scheme 2.8</b> The Crabtree group: effort to control selectivity between amide or amine formation .....	55
<b>Scheme 2.9</b> The Huynh group: effort to control selectivity between amide or amine formation.....	56

## Chapter 3

<b>Scheme 3.1</b> Thermodynamic consideration of the dehydrogenation of mandelonitrile .....	74
<b>Scheme 3.2</b> Thermal equilibration of cyanohydrins to aldehydes and benzoin condensation.....	75
<b>Scheme 3.3</b> Plausible elementary reaction step for dehydrogenation.....	81
<b>Scheme 3.4</b> Reactions of <b>1a</b> with modified [Ru(arene)X(ligand)]CA complexes. CA = counteranion. p-Tol = p-tolyl.....	83
<b>Scheme 3.5</b> Dehydrogenation of cyanohydrins .....	85
<b>Scheme 3.6</b> Mechanistic investigation.....	88
<b>Scheme 3.7</b> Plausible mechanism.....	89
<b>Scheme 3.8</b> Model reaction using mandelonitrile <b>1a</b> as substrate .....	104

## Chapter 4

<b>Scheme 4.1</b> Schematic view of photoredox catalysis and copper photocatalysis.	122
<b>Scheme 4.2</b> Representative copper photocatalysts .....	123
<b>Scheme 4.3</b> Photoexcitation of Cu(NN) complex and photophysical properties of Ru, Ir, Cu complexes.....	124
<b>Scheme 4.4</b> Early examples of copper photocatalysis.....	127
<b>Scheme 4.5</b> Visible light induced C–N bond formation via copper photocatalysis .....	128
<b>Scheme 4.6</b> First discovery of photoinduced copper catalyzed cross-coupling: Ullmann-type C–N bond formation .....	130
<b>Scheme 4.7</b> Catalytic version of this method and mechanism studies.....	132
<b>Scheme 4.8</b> Scope expansion in C–N bond formation .....	134

<b>Scheme 4.9</b> Various cross-coupling reactions beyond C–N bond formation.....	135
<b>Scheme 4.10</b> First asymmetric version of copper catalyzed cross-coupling reaction under visible light irradiation .....	137
<b>Scheme 4.11</b> Visible light induced C–N bond formation via copper photocatalysis .....	138
<b>Scheme 4.12</b> General mechanism of copper-based photocatalysis for cross-coupling.....	140
<b>Scheme 4.13</b> Preliminary mechanistic studies in C–N cross-coupling reactions .	141
<b>Scheme 4.14</b> Significant role of copper–thiolate in C–S cross-coupling process	142
<b>Scheme 4.15</b> Detailed mechanistic studies in C–S cross-coupling.....	143
<b>Scheme 4.16</b> Ackerman group: application to C–H activation.....	145
<b>Scheme 4.17</b> Hong group: application to chemoselective C(sp <sup>2</sup> )–cyanation .....	146
 <b>Chapter 5</b>	
<b>Scheme 5.1</b> Aromatic nitriles: utility and syntheses.....	153
<b>Scheme 5.2</b> Scope of aryl halides .....	157
<b>Scheme 5.3</b> Cu-catalyzed cyanation: our method and the method in (ref 10).....	159
<b>Scheme 5.4</b> Scope of aryl iodides with polar functional groups.....	159
<b>Scheme 5.5</b> Chemoselectivity to C(sp <sup>2</sup> ) cyanation over S <sub>N</sub> 2.....	160
<b>Scheme 5.6</b> Inhibition with radical scavenger .....	161
<b>Scheme 5.7</b> Plausible mechanism.....	164
<b>Scheme 5.8</b> Kinetic study .....	164

# List of Figures

## Chapter 2

**Figure 2.1** Reaction profiles monitored by  $^1\text{H}$  NMR spectroscopy.....48

**Figure 2.2** Stacked  $^1\text{H}$  NMR spectra of kinetic study..... 60

## Chapter 3

**Figure 3.1** Quantitative and qualitative analysis of substoichiometric reaction using  $^{31}\text{P}$  NMR ..... 101

**Figure 3.1** Qualitative analysis of stoichiometric reaction using  $^1\text{H}$  NMR ..... 103

**Figure 3.1** Qualitative analysis of substoichiometric reaction using  $^{31}\text{P}$  NMR .... 103

## Chapter 5

**Figure 5.1** Investigation of photocatalysis. A) light-dark experiment; B) reaction profile during catalysis ..... 162

**Figure 5.2** Pictures of reaction setup..... 175

**Figure 5.3**  $[\text{Ar-I}]$  dependent initial reaction profile..... 183

**Figure 5.4**  $[\text{Cu}]$  dependent initial reaction profile ..... 184

**Figure 5.5**  $[\text{CN}^-]$  dependent initial reaction profile ..... 184

## List of Abbreviations

Cp*	pentamethylcyclopentadienyl
AAD	acceptorless alcohol dehydrogenation
SET	single-electron transfer
S <sub>N</sub> 2	bimolecular nucleophilic substitution
PCC	pyridinium chlorochromate
DMSO	dimethyl sulfoxide
NCS	<i>N</i> -chlorosuccinimide
DMS	dimethyl sulfide
TEMPO	tetramethylpiperidine nitroxide
AD	alcohol dehydrogenation
PCy <sub>3</sub>	tricyclohexylphosphine
TON	turnover number
NHC	<i>N</i> -heterocyclic carbene
<i>p</i> -cymene	1-isopropyl-4-methylbenzene
dppe	1,2-bis(diphenylphosphino)ethane.
dppm	bis(diphenylphosphino)methane
dppb	1,4-bis(diphenylphosphino)butane
dcpe	1,2-bis(dicyclohexylphosphino)butane
CA	counteranion
OLED	organic light emitting diode
HOMO	highest occupied molecular orbital
MLCT	metal-to-ligand charge transfer
ISC	intersystem crossing
ATRA	atom transfer radical addition
E2	bimolecular elimination
NHP ester	<i>N</i> -hydroxyphthalimide (NHP) ester
BTTP	<i>tert</i> -butylimino-tri(pyrrolidino)phosphorene
TBACN	tetra- <i>n</i> -butylammonium cyanide

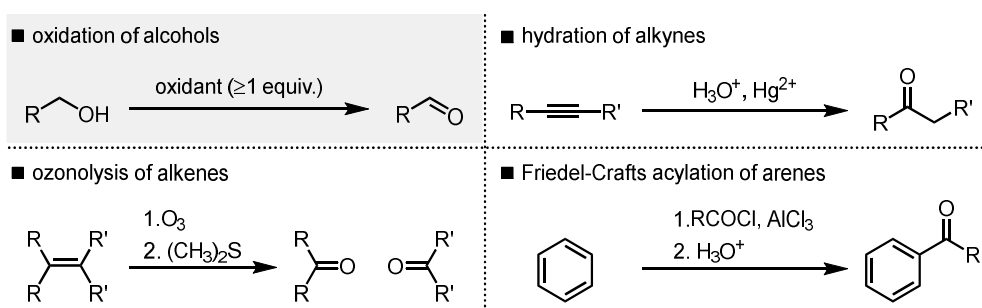
# Chapter 1. Dehydrogenative Alcohol Activation for Oxidation of Alcohols and *N*-Alkylation of Amines

## 1.1 Introduction

Replacement of highly reactive mutagenic reactants such as R–Br to less-reactive abundant reactants such as R–OH has drawn attention as a green-chemical synthetic method in organic synthesis. The utilization of readily available, less reactive compounds as substrates circumvents prefunctionalization to afford highly reactive reactants to avoid the subsequent generation of waste. Given that most reactions of intrinsically less reactive substrates include C–H bond activation, organometallic catalysis is one of the most attractive activation methods even in the absence of stoichiometric reactive reagents.

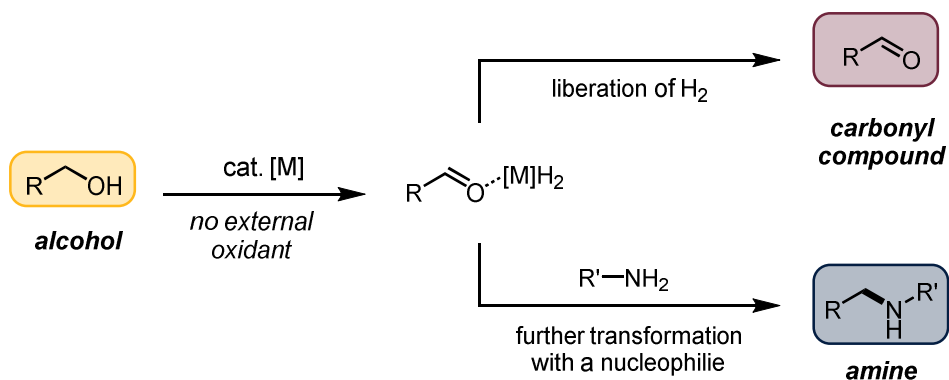
Organic carbonyl compounds are ubiquitous in nature and industry. In nature, these functionalities contribute to the flavors of foods and flowers and assist enzymatic processes. In addition, considerable amounts of these compounds are used as reagents and solvents for organic synthesis in academia and industry. The highly short, polar, and electrophilic carbon–oxygen double bond enables carbonyl compounds to act as both electrophiles and nucleophiles (*e.g.*, enol and enolate) under certain conditions. The carbonyl group indeed serves as the most versatile and important functional group in organic chemistry. Accordingly, a number of synthetic protocols for aldehydes and ketones have been developed: oxidation of alcohols, ozonolysis of alkenes, hydration of alkynes, and Friedel-Crafts acylation (Scheme 1.1). Oxidation of alcohols is a straightforward approach for producing aldehydes and ketones. Alcohols are readily available and versatile organic molecules. These

compounds can be obtained easily from nature (*e.g.* biomass, fermentation of sugar in the case of ethanol) and industry via the Ziegler process or hydration of alkenes. Stoichiometric amounts of mutagenic oxidants are required in conventional oxidation methods.



**Scheme 1.1** Representative synthetic methods for aldehydes and ketones

Since the early 2000s, catalytic dehydrogenation of alcohols without stoichiometric use of oxidants has been developed using organometallic catalytic systems. This catalysis has emerged as an alcohol activation mode for the net oxidation of alcohols and tandem transformations. In this chapter, two distinct transformations via catalytic alcohol activation will be introduced in detail, including their principal backgrounds and seminal examples: net-oxidation of alcohols and *N*-alkylation of amines with alcohols as alkylating reagents (Scheme 1.2).



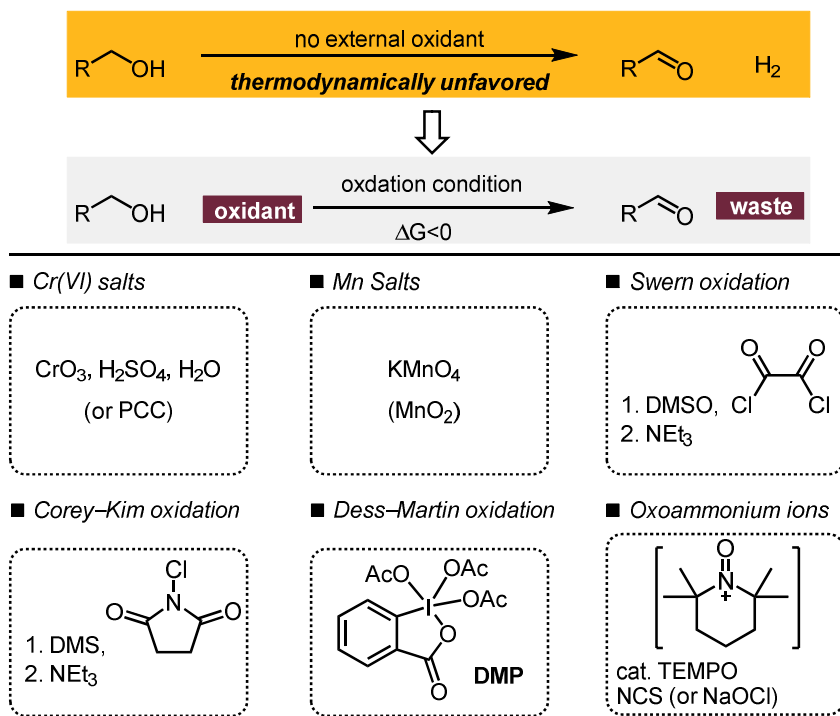
**Scheme 1.2** Catalytic dehydrogenation of alcohols as an alcohol activation mode

## 1.2 Oxidation of alcohols

### 1.2.1 Traditional methods using stoichiometric oxidants and the origin of reactivity

In terms of kinetics and thermodynamics, two major obstacles hinder the oxidation of alcohols. Alcohols are kinetically less labile compounds and dehydrogenation of alcohols is thermodynamically disfavored. Hence, (over)stoichiometric amounts of oxidants are needed to drive the oxidation of alcohols in conventional methods (Scheme 1.3). The use of oxidants has significant disadvantages in terms of cost, atom economy, selectivity (*e.g.*, overoxidation and other side reactions) and environmental aspects.





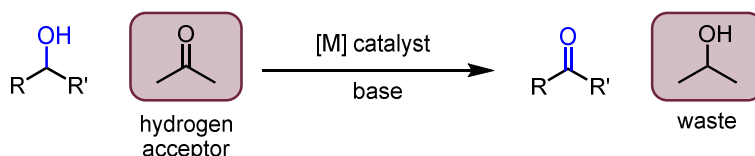
**Scheme 1.3** Traditional conditions for oxidation of alcohols

For example, Jones oxidation takes advantage of highly reactive hazardous Cr(VI) salts under acidic aqueous conditions. These conditions lead to overoxidation of primary alcohols to carboxylic acids. The alternative method using pyridinium chlorochromate (PCC) promotes selective oxidation to aldehydes and ketones, but it also poses toxicity and environmental hazards. Mn salts such as KMnO<sub>4</sub> and MnO<sub>2</sub> are also powerful oxidants but show lower selectivity than Cr(VI). Dimethyl sulfoxide (DMSO) and several electrophiles also mediate alcohol oxidation via sulfoxonium species. Representative methods include Swern oxidation (using oxalic chloride with DMSO) and Corey-Kim oxidation (using *N*-chlorosuccinimide (NCS) with dimethyl sulfide (DMS)). Dess-Martin oxidation using hypervalent iodine(V) reagent mediates a milder reaction with a wide functional group tolerance. However,

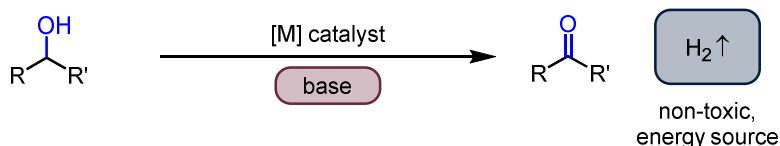
it also generates stoichiometric amounts of byproducts (*o*-iodobenzoic acid and acetic acids). Another oxidation method uses a catalytic amount of tetramethylpiperidine nitroxide (TEMPO) with sodium hypochlorite (NaOCl) via oxoammonium ion formation. This procedure shows the selectivity to primary alcohols over secondary alcohols. However, the method is limited in the use of a stoichiometric NaOCl and chlorinated solvents. The equivalent amount of sodium chloride waste is also produced concurrently for each catalytic cycle.

### 1.2.2 Catalytic methods using transition metal complexes: with hydrogen acceptors or acceptorless condition

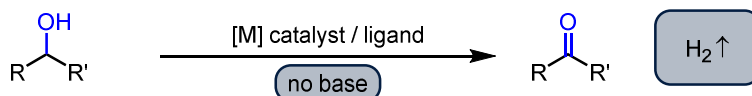
#### A. catalytic alcohol transfer dehydrogenation



#### B. acceptorless alcohol dehydrogenation (AAD)



#### C. base free AAD

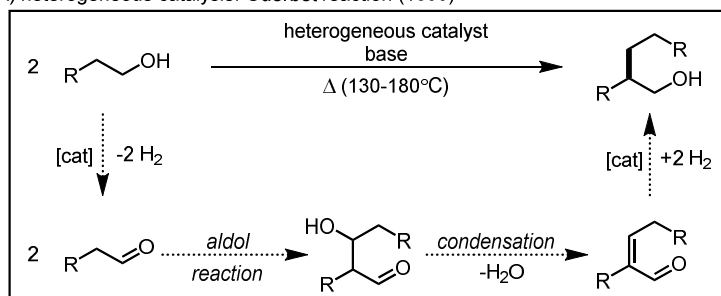


**Scheme 1.4** Catalytic dehydrogenation of alcohols: with a hydrogen acceptor, acceptorless method (AAD), and base free AAD method

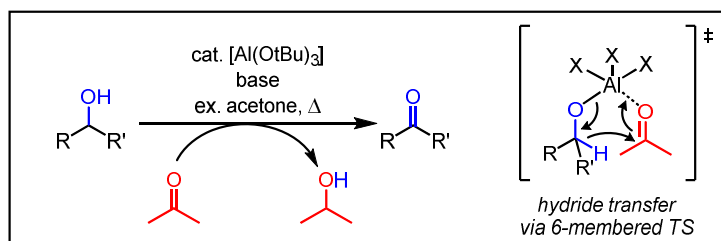
To overcome the green chemical and selectivity problems, catalytic alcohol dehydrogenation without the use of conventional oxidants has been extensively developed with transition metal catalysts.<sup>1</sup> The methods can be classified with several standards including whether a method requires the use of hydrogen acceptor or base (Scheme 1.4). Seminal preliminary reactions will be covered, prior to introduction of these catalytic methods.

Primitive investigation of catalytic alcohol dehydrogenation was reported using heterogeneous catalysis in the late 1800s (Scheme 1.5A).<sup>2</sup> The Guerbet group demonstrated the synthesis of  $\beta$ -branched primary alcohols via dehydrogenation of linear primary alcohols in a basic medium at 130–180 °C, using the heterogeneous hydrogen transfer catalyst. The reaction undergoes tandem transformations through dehydrogenation of alcohols to aldehydes – aldol condensation of aldehydes – transfer hydrogenation of unsaturated C–C and C–O bonds in the aldol adducts. In the field of homogeneous catalysis, the preliminary study of hydrogen-transfer reaction had arisen from the Oppenauer oxidation, which is the reverse version of Meerwein-Ponndorf-Verley reduction (Scheme 1.5B).<sup>3</sup> The reaction dehydrogenates secondary alcohols to form ketones in the presence of acetone using alkali or lanthanide alkoxide catalysts. In this reaction, the disfavored thermodynamics of alcohol dehydrogenation was compensated with the simultaneous, thermodynamically favored hydrogenation of acetone. Additionally, the kinetic barriers were relieved by a six-membered transition state, the [(alkoxide)Al(acetone)] species that promotes hydride transfer from alkoxide to the coordinated acetone.

- A) heterogeneous catalysis: Guerbet reaction (1899)



- B) homogeneous catalysis: Oppenauer oxidation (1937)

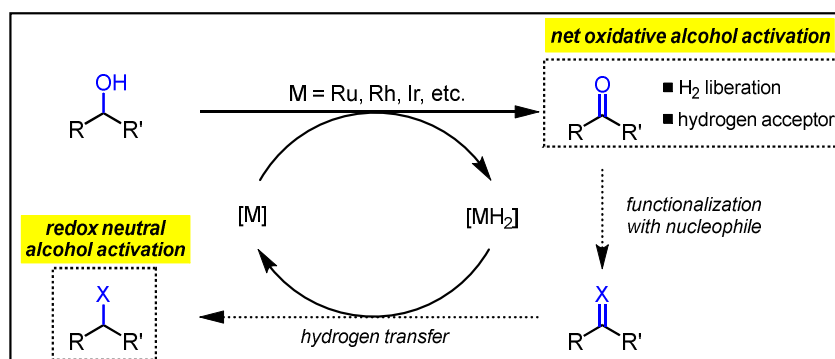


**Scheme 1.5** Preliminary reactions of hetero-/homogeneous catalytic AD

Homogeneous catalytic versions of alcohol dehydrogenation have been developed along with hydrogen transfer catalysis. Like its initial version (Oppenauer oxidation), the transfer of two hydrogens from an alcohol to a sacrificial hydrogen acceptor is promoted by transition metal catalysts in the activation mode (Scheme 1.6). Thermodynamics are allowed by the use of hydrogen acceptors that take part in reduction concomitantly to dehydrogenate alcohol. The difference of transition metal catalysts from aluminum alkoxides used in Oppenauer oxidation is that the former mediates C–H activation to form metal hydride species. One hydrogen is removed via the transition metal mediated activation of the hydric C–H bond adjacent to the -OH group, and the other hydrogen comes from the alcohol O–H proton. Afterward, the in situ-generated metal hydride can follow two pathways. First, it can liberate  $\text{H}_2$  so that the net oxidative alcohol activation is completed. The

transformation is specifically called acceptorless alcohol dehydrogenation (AAD), which is not very common in the field of alcohol dehydrogenation (AD). The absence of external oxidants makes AAD chemistry greener because it avoids the hazards associated with the oxidant and waste formation, and fulfils atom economy. Moreover, AAD is an alternative method in energy chemistry that has a potential for hydrogen storage. An open system at highly elevated temperature is generally applied for the extrusion of H<sub>2</sub>. Ultimately it entropically drives the enthalpically less-favored forward reaction and accelerates all the steps. This strategy can be also understood from the perspective of Le Chatelier's principle.

In other cases, in situ-generated organic carbonyls undergo further tandem transformations with various nucleophiles, especially amines, to construct valuable C–N bonds (*e.g.*, amide, imine, and amines). Further transfer hydrogenation of unsaturated adducts completes redox neutral alcohol activation and balances the thermodynamics. The initial dehydrogenation is endoergic and the resulting hydrogenation is exoergic to approximately the same extent as the first step. These tandem transformations are described in next section 1.3.

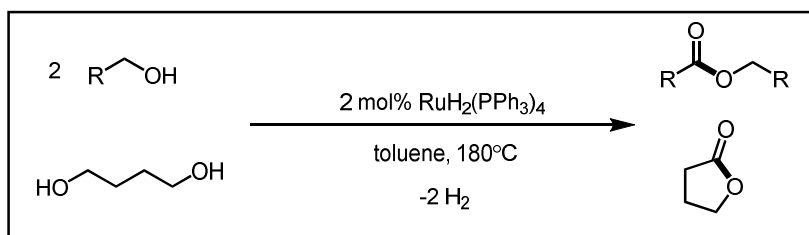


**Scheme 1.6** Schematic view of homogeneous catalytic alcohol dehydrogenation

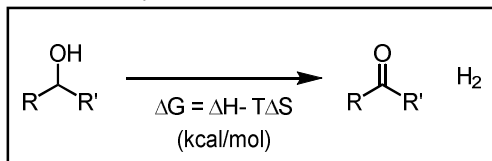
### 1.2.3 Representative methods for acceptorless alcohol dehydrogenation: Rh, Ru, Ir and 1<sup>st</sup>-row transition metal based catalytic systems

The Charman group reported the first acceptorless dehydrogenation reactivity in the reaction of isopropyl alcohol using the rhodium–tin complex in late 1960s.<sup>4</sup> The first homogeneous AAD catalytic reaction was developed by the Murahashi group (1981).<sup>5</sup> Transformation of alcohols (diols) into esters (lactones) is catalyzed by  $\text{RuH}_2(\text{PPh}_3)_4$  complex, albeit high temperature (180 °C) and moderate conversions (40–50% yields) (Scheme 1.7A). Since then, less common but several AAD examples mainly with secondary alcohols have been reported using Rh, Ru, and Ir based transition metal complexes. More powerful catalytic systems promote AAD with higher catalytic efficiency and wider range of alcohols including thermodynamically challenging primary alcohols such as ethanol and methanol ( $\Delta G^\circ = 6.4$  kcal/mol and 15.2 kcal/mol at 298 K, respectively) (Scheme 1.7B).<sup>1a</sup>

- A: the first catalytic version of AAD reactivity: Murahashi (1981)



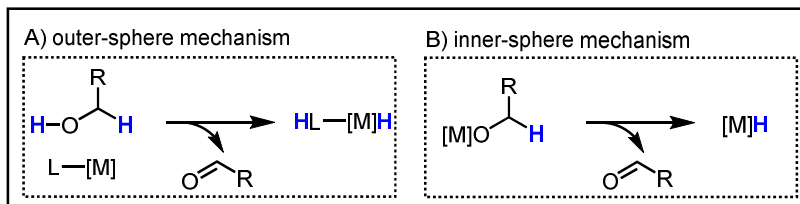
- B: thermodynamic data at 298K



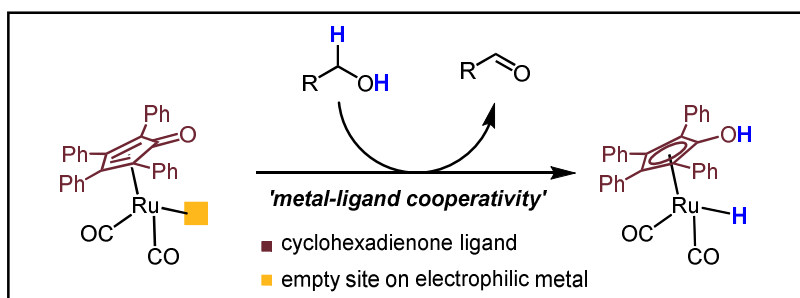
alcohol	$\Delta H^\circ$	$\Delta G^\circ$
MeOH	31.0	15.2
EtOH	19.4	6.4
iPrOH	16.4	-0.8
PhCH <sub>2</sub> OH	17.5	1.5

**Scheme 1.7** A) First catalytic example of AAD reactivity. B) Thermodynamic data of alcohol dehydrogenation

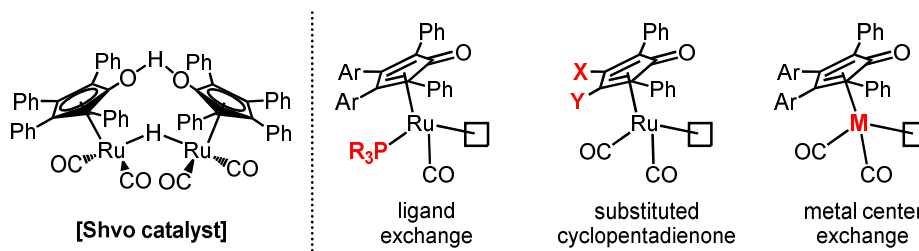
- two major activation pathways via transition metal catalysis



- Shvo's catalyst: outer-sphere mechanism & metal-ligand cooperativity



#### modification of Shvo catalyst

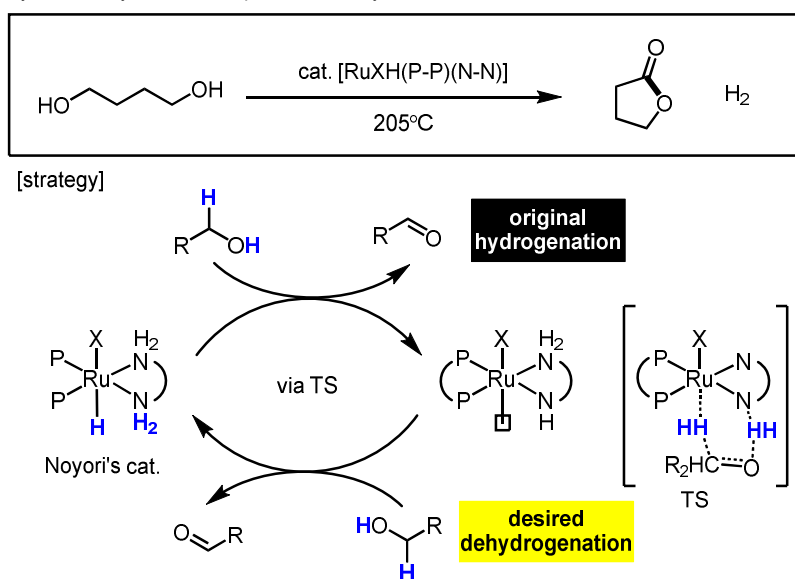


**Scheme 1.8** Two catalytic modes: outer-sphere and inner-sphere mechanism. Shvo catalyst following the outer-sphere mechanism

The Shvo group (1985)<sup>6</sup> and the Cole-Hamilton group (1988)<sup>7</sup> reported seminal examples of Ru catalysis, respectively following the outer-sphere and inner-sphere mechanisms. The Shvo catalyst is active for AAD following metal-ligand cooperation, where a non-innocent ligand directly participates in substrate activation (Scheme 1.8). A catalytically active monomer bearing a cyclopentadienone ligand abstracts two hydrogens from alcohols. In a concerted manner, a proton in the alcohol is abstracted by a pendant basic oxygen of the cyclopentadienone ligand and a hydride in the alcohol is abstracted by the electrophilic metal center in the 16 electron

complex. On the basis of the original Shvo catalyst, the modification of various factors in the complex (e.g., exchange of carbonyl ligand to another L-type ligand, substitution on cyclopentadienone ligand / exchange of metal center) was comprehensively attempted to improve catalytic activity.<sup>8</sup> Based on microscopic reversibility between hydrogenation (forward reaction) and dehydrogenation (backward reaction), Noyori's bisphosphine diamine ruthenium catalysts—which mediate hydrogenation via the outer-sphere mechanism—were also applied into the acceptorless dehydrogenation of diols to lactones (Scheme 1.9).<sup>9</sup> Beyond primary alcoholic substrates, the Ru-PNP pincer complex developed by the Milstein group catalyzed the dehydrogenation of secondary alcohols with low catalyst loading in the presence of catalytic NaOiPr base.<sup>10</sup>

■ Noyori's catalyst: microscopic reversibility



**Scheme 1.9** Application of Noyori's catalyst via microscopic reversibility



The Cole-Hamilton group reported the generation of H<sub>2</sub> from C1–C4 alcohols under [RuH<sub>2</sub>(N<sub>2</sub>)(PPh<sub>3</sub>)<sub>3</sub>] catalyst using excessive NaOH at 150 °C (Scheme 1.10A).<sup>7</sup> Despite the focus of the work on the release of H<sub>2</sub> from alcohols, the catalytic efficiency was explained by the high tendency to form ruthenium dihydrogen complex [Ru(H<sub>2</sub>)], which is likely to liberate H<sub>2</sub>. Since this pioneering work, numerous Ru-catalytic systems have been developed following the inner-sphere mechanism, where Ru-alkoxide species undergo β-H elimination to afford Ru-hydride species and carbonyl compound (Scheme 1.8). The Hulshof group demonstrated that Robinson catalyst, [Ru(CF<sub>3</sub>CO<sub>2</sub>)<sub>2</sub>(CO)(PPh<sub>3</sub>)<sub>2</sub>] mediates the catalytic AAD of secondary alcohols in the presence of catalytic trifluoroacetic acid CF<sub>3</sub>CO<sub>2</sub>H under the neat condition at 130 °C.<sup>11</sup> However, the reactions of primary alcohols showed low conversions and poor selectivity due to ‘decarbonylation with concomitant catalyst deactivation’ and ‘aldol condensation of corresponding aldehydes under the strong acid or basic conditions’. In 2005, the Beller group and the Williams group reported respectively seminal methods using simple Ru complexes and phosphine ligands under the basic conditions.<sup>12</sup> The Beller group reported that the combination of [RuCl<sub>3</sub>• nH<sub>2</sub>O] catalyst and PCy<sub>3</sub> ligand mediates AAD of 2-propanol below 100 °C with turnover frequencies >54(h<sup>-1</sup>). The Williams group reported the Grubbs 1st catalyst (or combination of [Ru(p-cymene)Cl]<sub>2</sub> and PPh<sub>3</sub>) promoted AAD of secondary alcohols. Even though osmium stands in the same group of periodic table with ruthenium, Os is much rarely exploited in homogeneous AAD than Ru. The Barrata group disclosed that Os-catalyzed AAD of secondary alcohols, even 5-en-3β-hydroxy steroids using catalytic KO<sup>t</sup>Bu at 130–145 °C (Scheme 1.10B).<sup>13</sup>

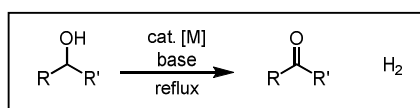
The Ir-based complexes also catalyze the AAD reactions with comparable activity to that of Ru-catalysts. The pioneering group in the Ir catalysis is Fujita and Yamaguchi group in Kyoto University, Japan. In 2007, this group developed the Cp\*Ir (Cp\*: Pentamethylcyclopentadienyl) bearing hydroxypyridine ligand-based catalytic system for AAD of secondary alcohols under the neutral conditions with high turnover numbers (TONs).<sup>14</sup> Introduction of 2-hydroxypyridine as a functional ligand onto Cp\*Ir complex promoted the loss of H<sub>2</sub> from metal hydride species. The metal hydride is generated by  $\beta$ -H elimination that is recognized as the most critical step in the catalytic dehydrogenation. In the dehydrogenation reaction of 1-phenylethanol, the Cp\*Ir complex with 2-hydroxypyridine ligand gave higher catalytic efficiency (54%, 2120 TON) than simple [Cp\*IrCl<sub>2</sub>]<sub>2</sub> complex (20% conversion, 170 TON).

To achieve the AAD in aqueous media, this group established the three design principles: (1) a strongly electron-donating ligand (*N*-heterocyclic carbene, NHC) which might be effective for dehydrogenation, (2) a chelating ligand to avoid a catalyst decomposition via a dissociation of the ligand, and (3) an ionic catalyst for high solubility in water.<sup>15</sup> The dicationic Ir-complex bearing the bidentate ligand that consisting of NHC and  $\alpha$ -hydroxypyridine moieties succeeded AAD under aqueous media. Interestingly, the reactions of primary alcohols afforded carboxylic acids instead of aldehydes or corresponding esters.

The Ir-PCP catalytic systems, which the Goldman group and the Jensen group comprehensively investigated for alkane dehydrogenation,<sup>16</sup> also mediated the AAD of secondary alcohols.<sup>17</sup> In the case of primary alcohols, rapid decarbonylation was observed to form the catalytically inactive iridium carbonyl species. Another Ir-

catalyst with the bifunctional dibenzobarrelene-based PCP pincer ligand was developed for AAD by the Gelman group (2011).<sup>18</sup> Under the lower catalyst loading and shortened reaction time, the method achieved dehydrogenation of primary alcohols (or diols) only to corresponding esters (or lactones).

■ Representative examples of catalytic AAD



A) simple Ru complexes

[RuH <sub>2</sub> (N <sub>2</sub> )(PPh <sub>3</sub> ) <sub>3</sub> ]	[Ru(CF <sub>3</sub> CO <sub>2</sub> ) <sub>2</sub> (CO)(PPh <sub>3</sub> ) <sub>2</sub> ]	[RuCl <sub>3</sub> , nH <sub>2</sub> O] PCy <sub>3</sub>	Grubbs 1st cat. or [Ru(p-cymene)Cl <sub>2</sub> ] <sub>2</sub> / PPh <sub>3</sub>
J. Cole-Hamilton ( <i>JSC CC</i> , 1988)	Hulshof ( <i>TL</i> , 2003)	Beller ( <i>TL</i> , 2005)	Williams ( <i>TL</i> , 2005)
ex. NaOH	only secondary alcohol cat. CF <sub>3</sub> CO <sub>2</sub> H	only secondary alcohol ex. NaOH	only secondary alcohol cat. LiOH

B) advanced complexes: pincer ligand, non-innocent ligand

Milstein ( <i>OM</i> , 2004)	Baratta ( <i>CEJ</i> , 2011)	Fujita & Yamaguchi ( <i>OL</i> , 2007)	Gelman ( <i>ACIE</i> , 2011)
only secondary alcohol cat. NaOPr	only secondary alcohol	only secondary alcohol no base	secondary alcohol : ketone primary alcohol : ester cat. Cs <sub>2</sub> CO <sub>3</sub>

C) non-precious transition metals

Hanson ( <i>JACS</i> , 2013)	Hong ( <i>ACS Catal</i> , 2014)	Jones ( <i>OM</i> , 2015)	Li & Lang ( <i>CCC</i> , 2017)
only secondary alcohol no base	only secondary alcohol cat. K <sub>2</sub> CO <sub>3</sub>	secondary alcohol : ketone primary alcohol : ester no base	secondary alcohol : ketone primary alcohol : aldehyde cat. KOH

**Scheme 1.10** Representative examples of AAD catalytic systems

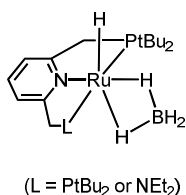
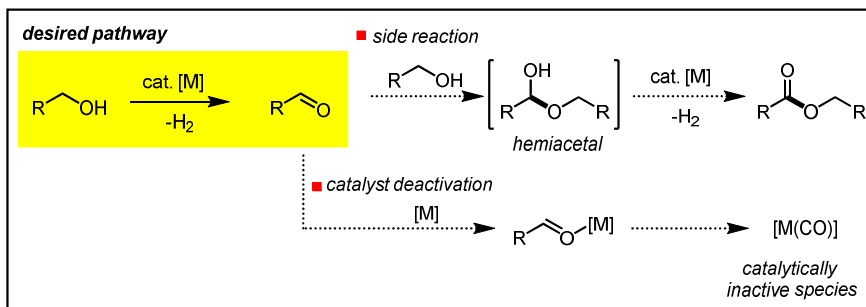
There are several accomplishments in base metal-based AAD catalysis, but the area is still in the stage of infancy. Because base metals are earth-abundant, cheap, and biocompatible, fewer health and environmental impacts are expected than precious metal; however, research on them is lacking compared to the tremendous advances with precious 4d- or 5d-metal complexes such as Ru and Pd.<sup>19</sup> However, base-metal catalysis promotes the release of H<sub>2</sub> from the metal due to their lower M–L bond strengths.<sup>1a</sup> A number of base metal catalysts including Co,<sup>20</sup> Fe,<sup>21</sup> Ni,<sup>22</sup> and Cu<sup>23</sup> mediate the AAD of secondary alcohols (Scheme 1. 10C). For example, the copper-(*N*-heterocycle thiolate) complex catalyzes the selective AAD of primary alcohols to aldehydes instead of the corresponding esters under mild reaction conditions (70 °C).

#### **1.2.4 Selective AAD of primary alcohol to aldehyde**

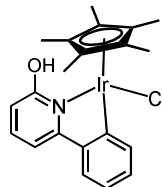
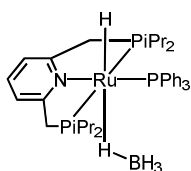
Selective AAD of primary alcohols to aldehydes is more challenging in homogeneous catalysis, although several examples using heterogeneous Ru, Ag, and Cu catalytic systems were reported (Scheme 1.11).<sup>24</sup> In the homogeneous catalytic AAD of primary alcohols, two major hurdles exist: side reaction and catalyst decomposition. Most catalysts often mediate further transformation to form esters. In the process, nucleophilic addition of a primary alcohol to an aldehyde affords hemiacetals and the subsequent dehydrogenation of hemiacetals produces esters. Moreover, catalysts are deactivated to form catalytically inactive carbonyl species via decarbonylation.

In Milstein's PNN or PNP pincer-ruthenium(II) hydrido borohydride catalysts, dehydrogenation of primary alcohols to aldehydes was observed albeit its low selectivity (toward aldehydes versus esters).<sup>25</sup> More improved catalytic systems following the metal-ligand cooperativity were reported by the Fujita and Yamaguchi group using the Ir complex. The preliminary catalytic systems were on the basis of  $[\text{Cp}^*\text{Ir}]$  complexes bearing the C,N-chelate ligand, 6-phenyl-2-pyridone derivatives.<sup>26</sup> The modified water-soluble complex bearing the bipyridine-based functional ligand catalyzes the greener dehydrogenation of both secondary and primary alcohols to ketone and aldehydes, respectively, in water.<sup>27</sup> Reuse of the water-soluble catalyst is also accomplished by a very simple procedure, organic-aqueous phase separation.

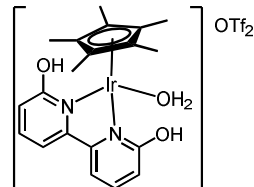
■ AAD of primary alcohols to aldehyde



Milstein (2011)



(2011)



(2012)

Fujita & Yamaguchi

**Scheme 1.11** AAD of primary alcohols to aldehydes

### 1.3 Redox-neutral alcohol activation: *N*-alkylation of amines with alcohols

Along with the development of an alcohol dehydrogenation method, the redox neutral *N*-alkylation of amines with alcohols has been thoroughly explored via the hydrogen transfer strategy (Scheme 1.2).<sup>28</sup>

According to the ACS Green Chemistry Institute Pharmaceutical Roundtable, the pharmaceutical industry chose ‘the alcohol(-OH) activation for nucleophilic substitution to synthetically versatile functionalities (halide, sulfonate esters, and nitrogen)’ as one of the most important reactions that must be improved in terms of green chemistry.<sup>29</sup> Since the hydroxyl group in alcohols is a very poor leaving group, harsh activation conditions such as excess Brønsted or Lewis acid are essential for substitution. In this context, catalytic alcohol activation has received attention as an alternative.<sup>30</sup> This method converts less-reactive alcohols to reactive carbonyl species, which undergo further transformation. Specifically, in the reaction of amines, nucleophilic addition forms hemiaminals, which can undergo selective condensation to form imines. Subsequently, the catalyst transfers hydrogen to imine, thus affording an *N*-alkylated amine. This strategy is termed “hydrogen autotransfer process”, “borrowing hydrogen methodology”, or “hydrogen transfer”. Its application to the *N*-alkylation of amines with alcohols is mainly described in this section.

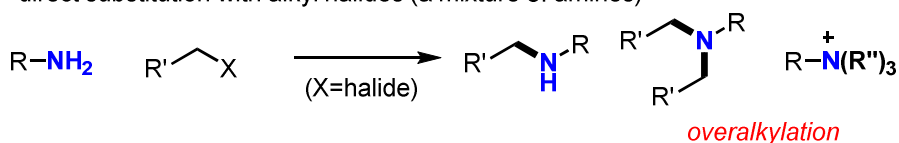
### 1.3.1. Importance of organonitrogen compounds and their traditional syntheses

Amines and other organonitrogen compounds (amides, amino acids) are ubiquitous organic molecules. They are essential as amino acids, peptides, and alkaloids in biochemistry. As amines exhibit high physiological activities, their medicinal applications are reported, including their use in decongestants, anesthetics, sedatives, and stimulants.

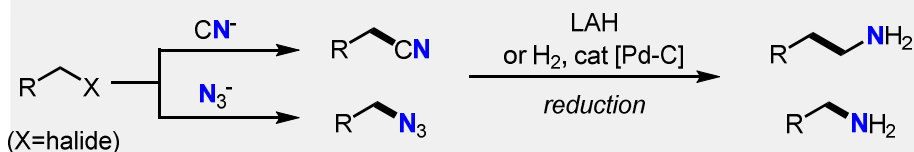
Therefore, a number of conventional syntheses were well-documented (Scheme 1.12). As organonitrogen compounds are highly nucleophilic, alkylating nitrogen with alkyl halides is quite reactive, but not clean producing a mixture of over-alkylation products. As a result, the indirect alkylation methods through cyanation (or azidation) of alkyl halides with cyanide (or azide) and subsequent reduction (LAH or catalytic hydrogenation using  $H_2$  and Pd-C catalyst) are frequently used for primary amine synthesis. The Gabriel synthesis is also widely used for primary amine synthesis via a non-reductive pathway utilizing a readily available phthalimide as a nitrogen surrogate. Hofmann rearrangement of amides and Curtius rearrangement of acyl azides also produce primary amines via liberation of  $CO_2$  from isocyanate intermediate. More general procedure is reductive amination of aldehydes and ketones. Condensation to imine (when  $NH_3$  and primary amines are used) and iminium ion (when secondary amines are used) is followed by reduction to give various types of amines. In these conventional organic syntheses, numerous synthetic and green chemical drawbacks exist: poor selectivity, use of stoichiometric activating reagents, harsh reaction conditions, generation of (over)stoichiometric waste, and its disposal. The catalytic methods with transition metal complexes have been widely developed showing improved efficiency,

selectivity and atom-economy: Ullmann or Buchwald-Hartwig amination with aryl halides, hydroamination of C=C unsaturated bonds, and *N*-alkylation of amines with alcohols.

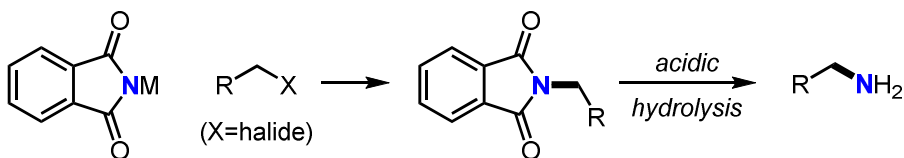
- direct substitution with alkyl halides (a mixture of amines)



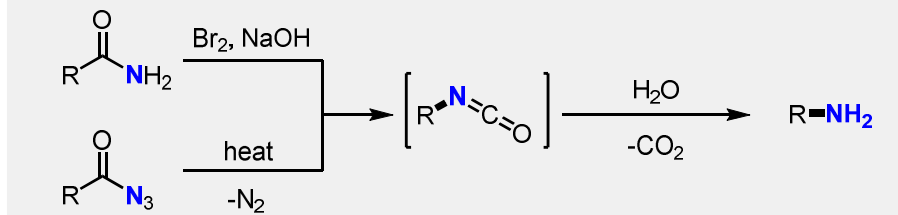
- indirect alkylation (primary amine)



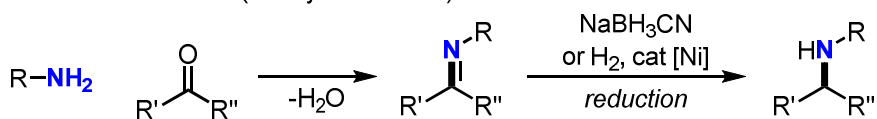
- Gabriel synthesis (primary amine)



- Hofmann rearrangement & Curtius rearrangement (primary amine)



- reductive amination (*N*-alkylated amine)



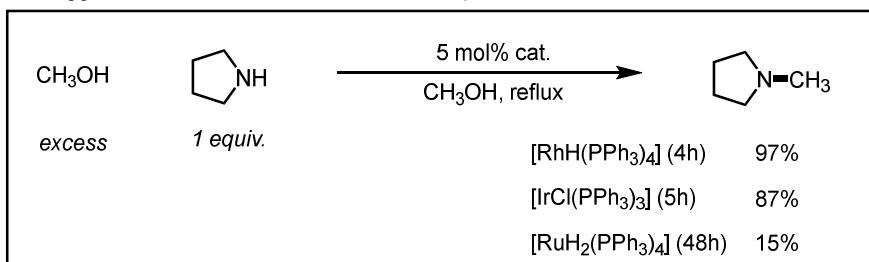
**Scheme 1.12** Representative amine syntheses



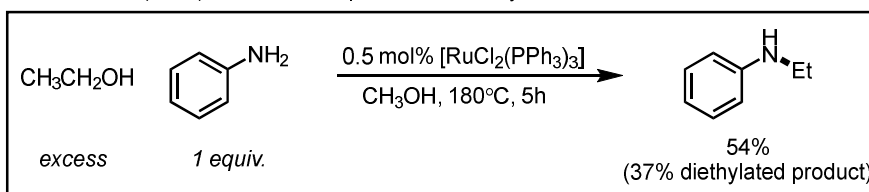
### 1.3.2. Representative homogeneous catalytic methods for *N*-alkylation of amines with alcohols: two major precious metal Ru- and Ir-based systems

In 1981, the Grigg group reported the first homogeneous catalytic *N*-alkylation of amines with alcohols using Rh, Ir, and Ru catalysts after reporting  $\text{RhH}(\text{PPh}_3)_4$  complex catalyzed transfer hydrogenation of aldimines with 2-propanol (Scheme 1.13).<sup>31</sup> The Watanabe group also demonstrated the similar reactivity using Ru(II) catalytic systems in the same year.<sup>32</sup> Since the seminal studies (1981), diverse Ru- and Ir-based catalytic systems have been developed for synthesis of various scope of amines (from primary amine to heterocycles) and even amides (from linear amide to cyclic imides). The improved activities was realized involving milder conditions, wider substrate scope, lower catalyst loading, higher selectivity, and base metal center instead of precious metals.

- Grigg (1981): the first example with Rh catalyst



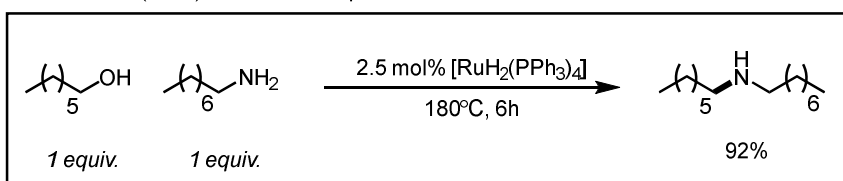
- Watanabe (1981): the first example with Ru catalyst



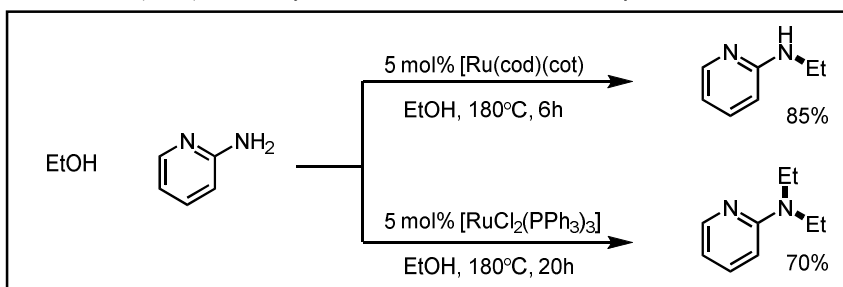
**Scheme 1.13** First examples of *N*-alkylation of amines with alcohols in 1981

In terms of alcohol equivalent, the Murahashi group (1982) reported the improved procedure using alcohols as limiting reactants, in contrast to the previous methods which use excess amounts of alcohols (Scheme 1.14).<sup>33</sup> In 1996, the Watanabe group studied controlling selectivity between monoalkylation and dialkylation.<sup>34</sup> They speculated that further alkylation of secondary amine products is difficult to take place because it requires iminium cation formation that is unfavorable especially in nonpolar solvents. The ligand along a metal center would promote or inhibit further alkylations, although the origin of ligand effect is unclear.

- Murahashi (1982): the use of 1 equiv. of alcohol



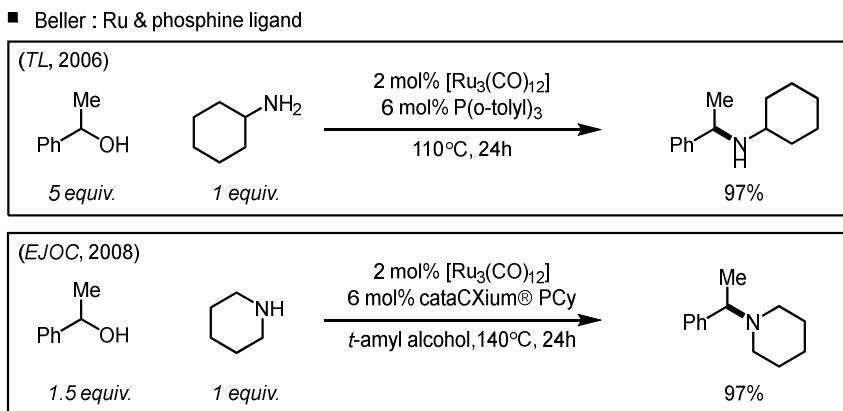
- Watanabe (1996): selectivity control between mono- and di-alkylations



**Scheme 1.14** Improved catalytic systems before the 2000s

The Beller group (2006) expanded alcohol scopes to more difficult secondary alcohols using the combination of Ru<sub>3</sub>(CO)<sub>12</sub> complex and bulky phosphine ligand, tri(*o*-tolyl)phosphine (Scheme 1.15).<sup>35</sup> With the bulkier phosphine ligand, cataCXium® PCy, the reactions of secondary amine with secondary alcohols were also achieved for tertiary amine synthesis.<sup>36</sup> Because of this difficulty in

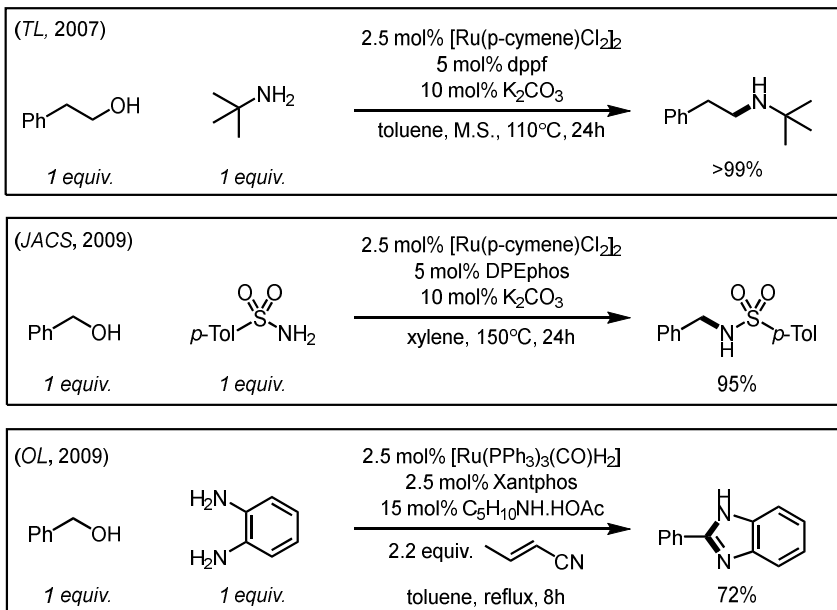
transfer hydrogenation of C=N bonds, excessive alcohols which serve as hydrogen donors were necessary.



**Scheme 1.15** Works of the Beller group: Ru & monophosphine catalytic systems

Another pioneer group, the Williams group have endeavored to improve the methods using the combination of Ru complexes and bidentate ligands (Scheme 1.16). In 2007, the combination of  $[\text{Ru}(\text{p-cymene})\text{Cl}_2]_2$  and bidentate dppf ligand in the presence of catalytic  $\text{K}_2\text{CO}_3$  base realized *N*-alkylation of sterically hindered amine under the milder conditions (low temperature).<sup>37</sup> In 2009, they expanded *N*-surrogate scope to sulfonamides by applying the combination of  $[\text{Ru}(\text{p-cymene})\text{Cl}_2]_2$  and another bidentate DPEphos ligand under more harsh conditions, reflux of xylene.<sup>38</sup> On the basis of their previously developed catalytic system for the transfer dehydrogenation of alcohols ( $[\text{Ru}(\text{PPh}_3)_3(\text{CO})\text{H}_2]$  and bidentate Xantphos ligand), benzimidazole synthesis was achieved following *N*-alkylation and further hydrogen transfer using crotononitrile as a hydride acceptor. The catalytic use of piperidinium acetate,  $\text{C}_5\text{H}_{10}\text{NH}\cdot\text{HOAc}$  would activate imine intermediates to corresponding iminiums to facilitate the desired cyclization.<sup>39</sup>

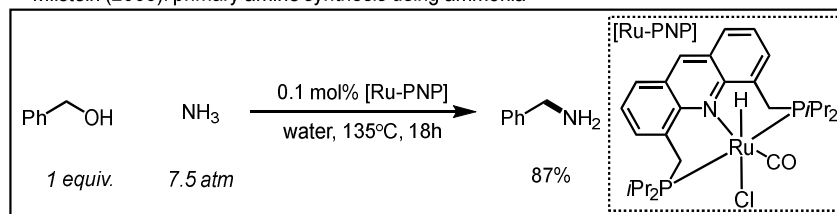
■ Williams: Ru & bidentate ligand



**Scheme 1.16** Works of the Williams group: Ru & bidentate phosphine catalytic systems

Ammonia is recognized as a challenging N-source in reactions with alkyl halides, since more nucleophilic primary amine products compete for *N*-alkylation. By applying hydrogen autotransfer, the Milstein group (2008) achieved primary amine synthesis via *N*-alkylation of  $\text{NH}_3$  with alcohols using a Ru-acridine-derived PNP pincer complex (Scheme 1. 17).<sup>40</sup> The rationally designed bulky ligand renders the catalytic system air-stable and selective for coordination to  $\text{NH}_3$  rather than amines, even under mild and non-basic conditions.

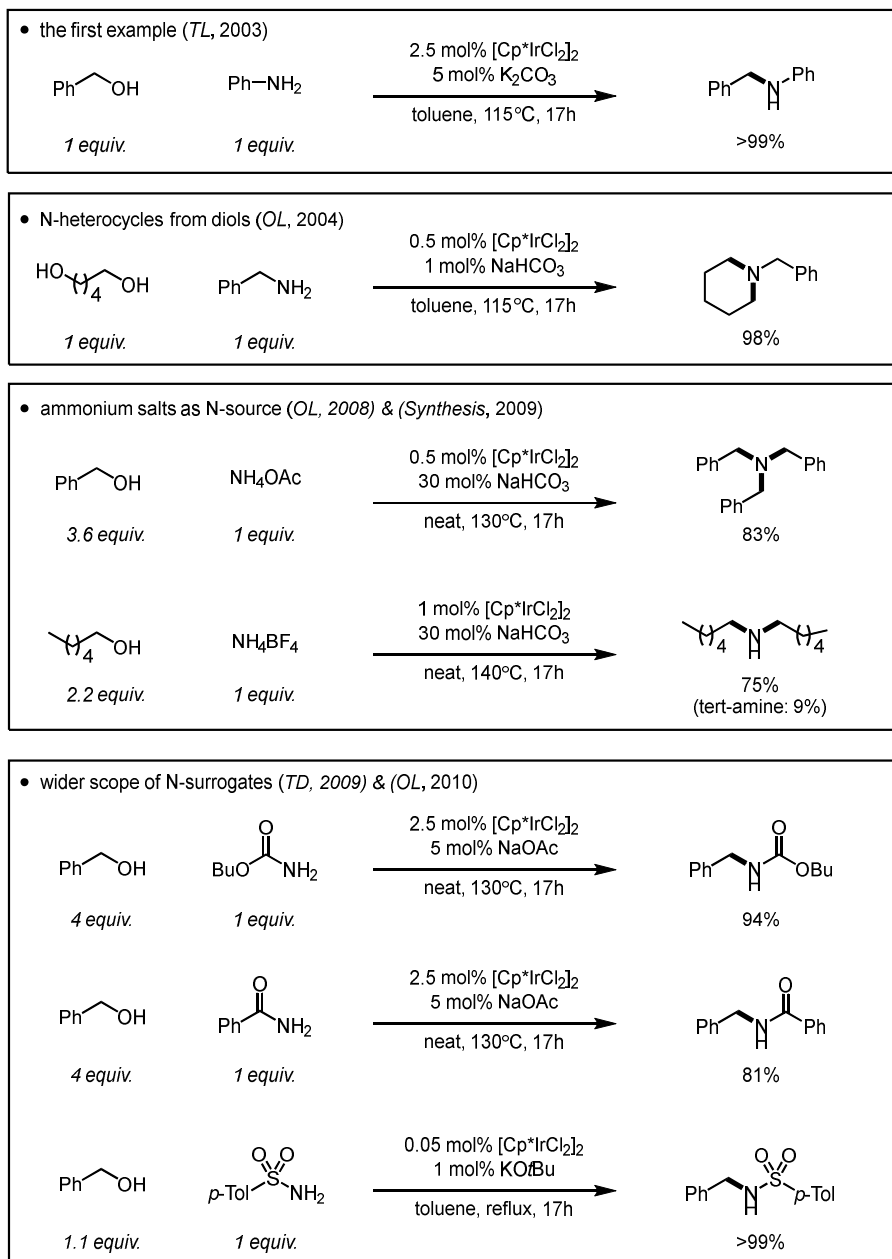
■ Milstein (2008): primary amine synthesis using ammonia



**Scheme 1.17** *N*-alkylation of ammonia under the Milstein's catalytic systems

Ir complexes have shown comparable or complementary reactivities for *N*-alkylation of amines with alcohols. Among those, Cp\*Ir complexes showed superior activities similar to their status in the AAD catalysis.

■ Fujita & Yamaguchi

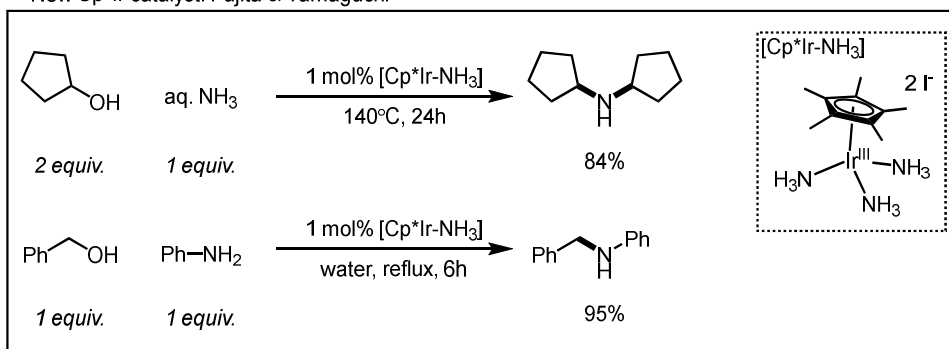


**Scheme 1.18** Works of the Fujita and Yamaguchi group: Cp\*Ir-catalyzed *N*-alkylation

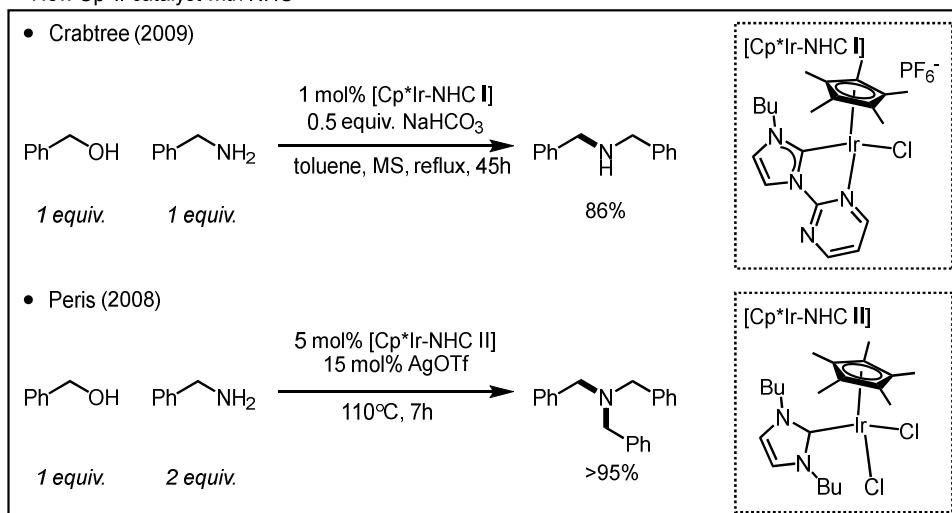
The Fujita and Yamaguchi group reported  $[\text{Cp}^*\text{IrCl}_2]_2$  catalyzed *N*-alkylation of amines with alcohols, inspired by their previous investigation of  $\text{Cp}^*\text{Ir}$  for hydrogen-transfer reactions and Oppenauer-type oxidation (Scheme 1.18).<sup>41</sup> The reactions of various substrates (alcohols: primary and secondary alcohols; amines: primary and secondary amines) proceeded to afford the corresponding *N*-alkylated products. *N*-Alkylation of amines with diols<sup>42</sup> or aminoalcohols<sup>43</sup> efficiently afforded *N*-heterocycles under the  $\text{Cp}^*\text{Ir}$  catalyst and basic conditions. In the same manner, the Madsen group realized piperazine synthesis from diamines and diols using  $[\text{Cp}^*\text{IrCl}_2]_2$  and  $\text{NaHCO}_3$  catalytic conditions.<sup>44</sup> The first selective catalytic method for di- and tri-alkylamine synthesis from ammonium salts was developed using  $\text{Cp}^*\text{Ir}$  catalyst under rather harsh conditions (130–140 °C).<sup>45</sup> In the reactions of primary alcohols (benzyl alcohols), the exclusive synthesis of tertiary amines was observed using ammonium acetate as N-source. On the contrary, the reactions of secondary alcohols and linear primary alcohols with ammonium tetrafluoroborate as N-source resulted in selective synthesis of secondary amines. Less nucleophilic amine surrogates such as carbamates, amides, sulfonamides were also compatible with the  $\text{Cp}^*\text{Ir}$  catalyzed *N*-alkylation with alcohols.<sup>46</sup> In 2010s, new  $\text{Cp}^*\text{Ir}$  type complexes bearing  $\text{NH}_3$  ligands were developed and applied successfully to *N*-alkylation of  $\text{NH}_3$  and amines (Scheme 1.19).<sup>47</sup> The water-soluble and air-stable  $[\text{Cp}^*\text{Ir-NH}_3]$  catalyst mediates the reaction under greener aqueous medium. Moreover, it could be recycled by a simple procedure maintaining high activity. Regarding that the NHC-metal complexes are catalytically active for transfer hydrogenation with C=O and C=N bonds, the Crabtree group and the Peris group respectively prepared  $[\text{Cp}^*\text{Ir}(\text{NHC})]$  catalysts and applied those complexes for *N*-

alkylation.<sup>48</sup> In Crabtree's report (2009), the air-stable Ir complex [Cp\*Ir-NHC **I**] with the chelating pyrimidine-functionalized NHC ligand catalyzes the desired reaction under mild basic conditions instead of using strong base such as KOH in general methods.<sup>48a</sup> In Peris' report (2008), [Cp\*Ir-NHC **II**] mediates the *N*-alkylation under the base-free conditions utilizing catalytic silver triflate.<sup>48b</sup>

■ New Cp\*Ir catalyst: Fujita & Yamaguchi



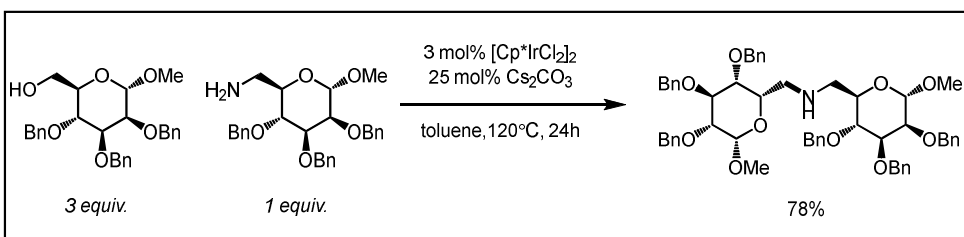
■ New Cp\*Ir catalyst with NHC



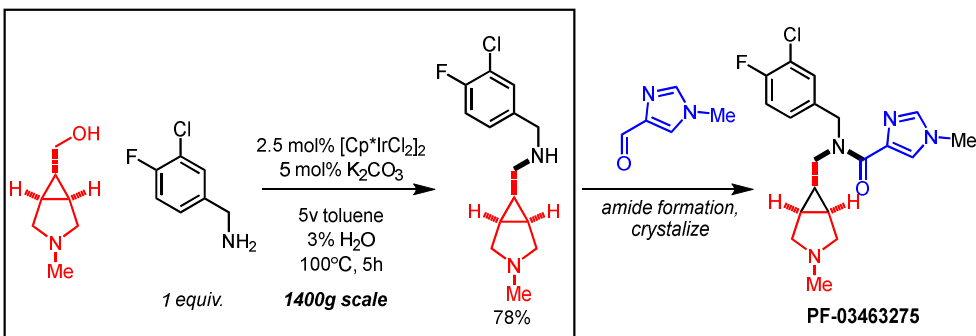
**Scheme 1.19** Newly designed Cp\*Ir complexes and their catalysis

The substrate scope was even expanded to cheap, renewable, and densely functionalized potential building blocks: carbohydrates (Scheme 1.20).<sup>49</sup> Despite their advantages in green chemistry and organic synthesis, utilization of these compounds as alcohol substrates is challenging because the electron-poor alcoholic carbons in carbohydrates are less reactive to oxidation. The Cp\*Ir catalytic system successfully mediated *N*-alkylation of carbohydrate amines with carbohydrate alcohols under the basic condition. Moreover, kilogram-scale application was achieved in the synthesis of the pharmaceutically active compound, PF-03463275 that is a GlyT1 inhibitor used for the treatment of schizophrenia.<sup>50</sup>

■ *N*-substituted aminosugar synthesis



■ large scale synthesis for pharmaceutical-compound preparation

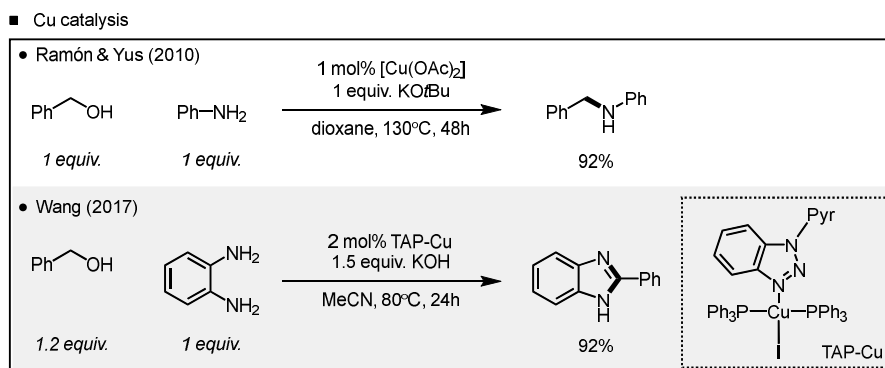


**Scheme 1.20** Use of carbohydrates in *N*-alkylation and large-scale reaction for pharmaceutically active compound synthesis



### 1.3.3. Representative homogeneous catalytic methods for *N*-alkylation of amines with alcohols: base metal-based catalytic systems

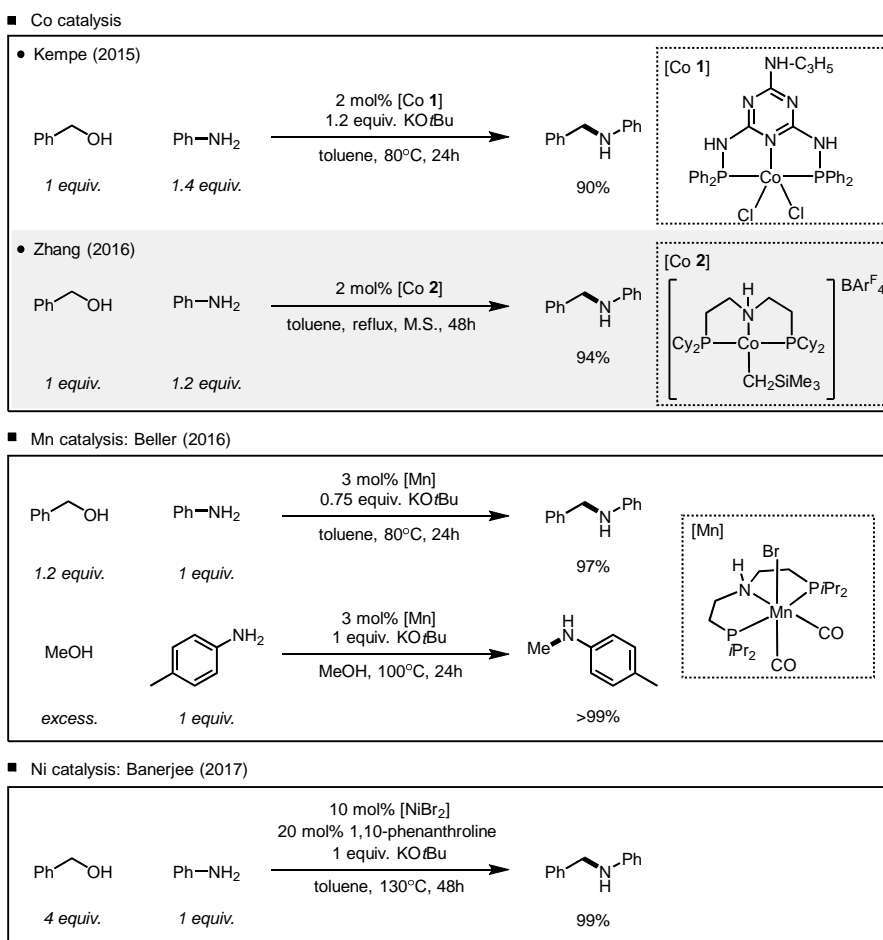
To substitute highly active and selective precious metal catalysts with base metal catalysts, various groups have tried to find appropriate conditions to modify the capricious nature of base metals. The Ramón and Yus group (2010) reported Cu(II) acetate catalyzed *N*-monoalkylation of less nucleophilic amino groups including (hetero)aromatic amines and sulfonamides (Scheme 1.21).<sup>51</sup> In 2017, the triazole-phosphine copper (TAP-Cu) catalytic system was developed for direct imidazole synthesis from diamines and alcohols using *N*-alkylation strategy.<sup>52</sup> The triazole-phosphine ligand serves a critical role in hydrogen transfer catalysis by formation of the catalytically active copper hydride species.



**Scheme 1.21** Cu-catalytic systems

The Kempe group (2015) reported the first Co-catalyzed *N*-alkylation of (hetero)aromatic amines with aliphatic and benzyl alcohols (Scheme 1.22).<sup>53</sup> The Co complex with PN<sub>5</sub>P ligand bearing the triazine backbone, [Co **1**] mediated the reactions under mild conditions (80 °C) with low catalyst loading (2 mol%). Another Co-PNP pincer complex, [Co **2**] promoted base-free *N*-alkylation of aliphatic and

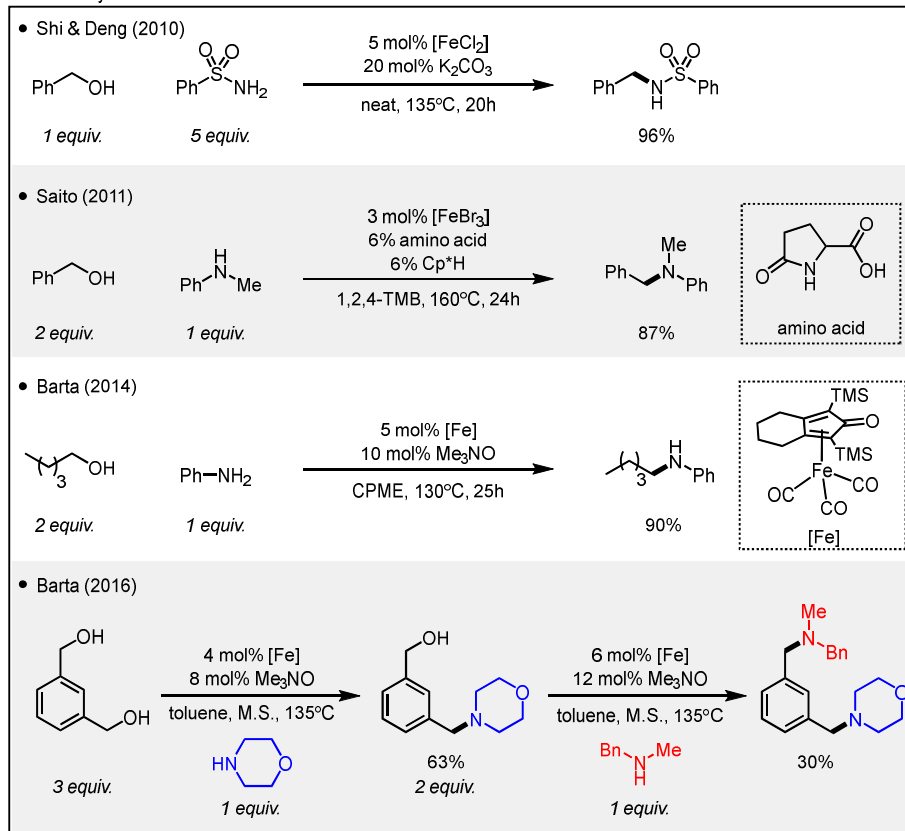
aromatic amines with alcohols in the presence of molecular sieves.<sup>54</sup> The Beller group (2016) reported Mn-PNP pincer complex-catalyzed *N*-alkylation of amines with alcohols including methanol under mild conditions (80–100 °C).<sup>55</sup> This method shows wide functional group tolerance to halides, thioether, heteroaromatics, and reducible olefins. The Banerjee group (2017) developed the first Ni-catalytic system for *N*-alkylation of anilines with a variety of alcohols.<sup>56</sup> Mechanistic studies indicate that the abstraction of  $\beta$ -hydrogen of alcohol, the rate-limiting step furnished [NiH] species that is active for further transfer hydrogenation.



**Scheme 1.22** Co-, Mn-, and Ni-catalytic systems

Among base metals, iron has some distinctive advantages;<sup>57</sup> As Fe is one of the most abundant metal in earth (second to aluminum), cost issue cannot be problem in Fe catalysis. As Fe compounds are incorporated in biological systems, relatively less toxicity was observed in numerous Fe complexes, which is attractive to cosmetic, pharmaceutical and food industries. In 2010, the Shi and Deng group reported the first Fe-catalyzed *N*-alkylation of sulfonamide with alcohols following Fe(0)/Fe(II) pathways (Scheme 1.23).<sup>58</sup> The Saito group (2011) also demonstrated Fe-catalyzed *N*-alkylation of amines with alcohols in the presence of catalytic amino acid (DL-pyroglutamic acid) and Cp\*H.<sup>59</sup> The proposed mechanism involves substitution (S<sub>N</sub>) onto the C(sp<sup>3</sup>) bearing a hydroxy group of alcohol, instead of conventional “borrowing hydrogen” mechanism. The Barta group (2014) developed bifunctional Fe-cyclopentadienone complex catalyzed *N*-alkylation method.<sup>60</sup> Further studies achieved the one-pot synthesis of nonsymmetric tertiary amines, sequential functionalization of diols with different secondary amines.<sup>61</sup>

■ Fe catalysis



Scheme 1.23 Fe-catalytic systems

## 1.4 Conclusion

In this chapter, dehydrogenative alcohol activation is described, especially in terms of the oxidation of alcohols and *N*-alkylation of amines with alcohols. Within diverse organometallic catalytic systems, remarkable improvements in activity, selectivity, substrate scope and reaction conditions have been accomplished by ligand design (especially bifunctional ligands) and the substitution of precious metal centers with base metals.

Alcohol dehydrogenation catalysis was initiated by the introduction of hydrogen acceptors, which obviates the use of toxic inorganic oxidants. Moreover, delicately designed catalytic systems achieved thermodynamically unfavorable alcohol dehydrogenation under acceptor-free conditions (AAD). In recent decades, many groups have made efforts to develop rather mild methods (*e.g.* base-free condition), for application to biomass conversion, or developing base-metal catalysis. In the context of alcohol dehydrogenation catalysis, the *N*-alkylation of amines with alcohols following a hydrogen auto-transfer pathway has been widely investigated for the construction of versatile C–N bonds. Recently, highly selective *N*-monomethylation of amines with methanol was developed using a Ru-MACHO catalytic system by the Hong group.<sup>62</sup> Many groups have actively tried to improve catalytic methods to cover the challenging alcohol substrates, utilize base metal centers, and impart high selectivity.

## 1.5 References

- (1) (a) R. H. Crabtree, *Chem. Rev.* **2017**, *117*, 9228. (b) C. Gunanathan, D. Milstein, *Science* **2013**, *341*, 1229712. (c) G. E. Dobereiner, R. H. Crabtree, *Chem. Rev.* **2010**, *110*, 681.
- (2) M. Guerbet, *CR Hebd Seances Acad Sci* **1899**, *128*, 1002.
- (3) R. V. Oppenauer, *Recl. Trav. Chim. Pays-Bas* **1937**, *56*, 137.
- (4) (a) H. B. Charman, *Nature* **1966**, *212*, 278. (b) H. B. Charman, *J. Chem. Soc. B* **1970**, 584.
- (5) S.-I. Murahashi, K.-i. Ito, T. Naota, Y. Maeda, *Tetrahedron Lett.* **1981**, *22*, 5327.
- (6) Y. Blum, Y. Shvo, D. F. Chodosh, *Inorganica Chim. Acta* **1985**, *97*, L25.
- (7) D. Morton, D. J. Cole-Hamilton, *J. Chem. Soc., Chem. Commun.* **1988**, 1154.
- (8) B. L. Conley, M. K. Pennington-Boggio, E. Boz, T. J. Williams, *Chem. Rev.* **2010**, *110*, 2294.
- (9) (a) J. Zhao, J. F. Hartwig, *Organometallics* **2005**, *24*, 2441. (b) R. Noyori, M. Yamakawa, S. Hashiguchi, *J. Org. Chem.* **2001**, *66*, 7931.
- (10) J. Zhang, M. Gandelman, L. J. W. Shimon, H. Rozenberg, D. Milstein, *Organometallics* **2004**, *23*, 4026.
- (11) G. B. W. L. Ligthart, R. H. Meijer, M. P. J. Donners, J. Meuldijk, J. A. J. M. Vekemans, L. A. Hulshof, *Tetrahedron Lett.* **2003**, *44*, 1507.
- (12) (a) H. Junge, M. Beller, *Tetrahedron Lett.* **2005**, *46*, 1031. (b) G. R. A. Adair, J. M. J. Williams, *Tetrahedron Lett.* **2005**, *46*, 8233.
- (13) W. Baratta, G. Bossi, E. Putignano, P. Rigo, *Chem. Eur. J.* **2011**, *17*, 3474.
- (14) K.-i. Fujita, N. Tanino, R. Yamaguchi, *Org. Lett.* **2007**, *9*, 109.
- (15) K.-i. Fujita, R. Tamura, Y. Tanaka, M. Yoshida, M. Onoda, R. Yamaguchi, *ACS*

*Catal.* **2017**, *7*, 7226.

(16) J. Choi, A. H. R. MacArthur, M. Brookhart, A. S. Goldman, *Chem. Rev.* **2011**, *111*, 1761.

(17) A. V. Polukeev, P. V. Petrovskii, A. S. Peregudov, M. G. Ezernitskaya, A. A. Koridze, *Organometallics* **2013**, *32*, 1000.

(18) S. Musa, I. Shaposhnikov, S. Cohen, D. Gelman, *Angew. Chem. Int. Ed.* **2011**, *50*, 3533.

(19) P. Chirik, R. Morris, *Acc. Chem. Res.* **2015**, *48*, 2495.

(20) (a) G. Zhang, K. V. Vasudevan, B. L. Scott, S. K. Hanson, *J. Am. Chem. Soc.* **2013**, *135*, 8668. (b) G. Zhang, S. K. Hanson, *Org. Lett.* **2013**, *15*, 650.

(21) H. Song, B. Kang, S. H. Hong, *ACS Catal.* **2014**, *4*, 2889.

(22) S. Chakraborty, P. E. Piszal, W. W. Brennessel, W. D. Jones, *Organometallics* **2015**, *34*, 5203.

(23) D. W. Tan, H. X. Li, M. J. Zhang, J. L. Yao, J. P. Lang, *ChemCatChem* **2017**, *9*, 1113.

(24) (a) J. H. Choi, N. Kim, Y. J. Shin, J. H. Park, J. Park, *Tetrahedron Lett.* **2004**, *45*, 4607. (b) W.-H. Kim, I. S. Park, J. Park, *Org. Lett.* **2006**, *8*, 2543. (c) T. Mitsudome, Y. Mikami, H. Funai, T. Mizugaki, K. Jitsukawa, K. Kaneda, *Angew. Chem. Int. Ed.* **2008**, *47*, 138. (d) T. Mitsudome, Y. Mikami, K. Ebata, T. Mizugaki, K. Jitsukawa, K. Kaneda, *Chem. Commun.* **2008**, 4804. (e) K. i. Shimizu, K. Sugino, K. Sawabe, A. Satsuma, *Chem. Eur. J.* **2009**, *15*, 2341.

(25) J. Zhang, E. Balaraman, G. Leitus, D. Milstein, *Organometallics* **2011**, *30*, 5716.

(26) K.-i. Fujita, T. Yoshida, Y. Imori, R. Yamaguchi, *Org. Lett.* **2011**, *13*, 2278.

(27) R. Kawahara, K.-i. Fujita, R. Yamaguchi, *J. Am. Chem. Soc.* **2012**, *134*, 3643.

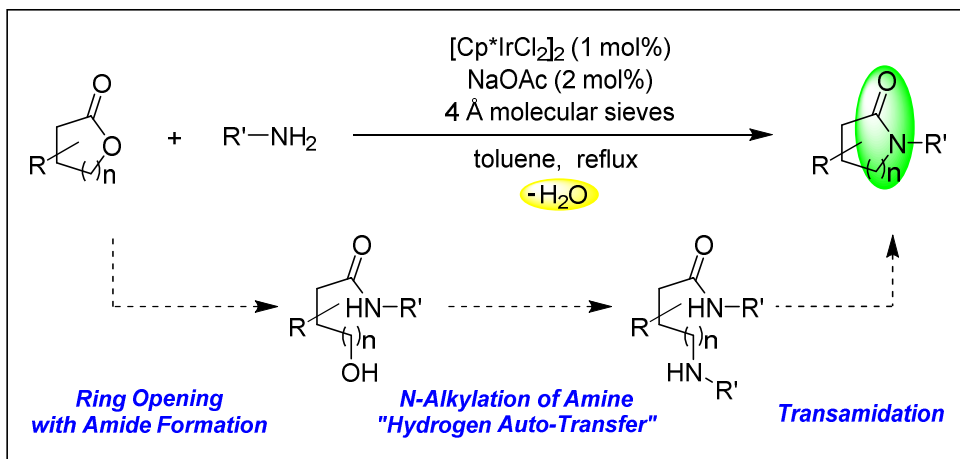
- (28) X. Ma, C. Su, Q. Xu, *Top. Curr. Chem.* **2016**, 374, 27.
- (29) D. J. C. Constable, P. J. Dunn, J. D. Hayler, G. R. Humphrey, J. J. L. Leazer, R. J. Linderman, K. Lorenz, J. Manley, B. A. Pearlman, A. Wells, A. Zaks, T. Y. Zhang, *Green Chem.* **2007**, 9, 411.
- (30) A. J. A. Watson, J. M. J. Williams, *Science* **2010**, 329, 635.
- (31) (a) R. Grigg, T. R. B. Mitchell, S. Sutthivaiyakit, N. Tongpenyai, *J. Chem. Soc., Chem. Commun.* **1981**, 611. (b) R. Grigg, T. R. B. Mitchell, N. Tongpenyai, *Synthesis* **1981**, 1981, 442.
- (32) Y. Watanabe, Y. Tsuji, Y. Ohsugi, *Tetrahedron Lett.* **1981**, 22, 2667.
- (33) S.-I. Murahashi, K. Kondo, T. Hakata, *Tetrahedron Lett.* **1982**, 23, 229.
- (34) Y. Watanabe, Y. Morisaki, T. Kondo, T.-a. Mitsudo, *J. Org. Chem.* **1996**, 61, 4214.
- (35) A. Tillack, D. Hollmann, D. Michalik, M. Beller, *Tetrahedron Lett.* **2006**, 47, 8881.
- (36) A. Tillack, D. Hollmann, K. Mevius, D. Michalik, S. Bähn, M. Beller, *Eur. J. Org. Chem.* **2008**, 2008, 4745.
- (37) M. H. S. A. Hamid, J. M. J. Williams, *Chem. Commun.* **2007**, 725.
- (38) M. H. S. A. Hamid, C. L. Allen, G. W. Lamb, A. C. Maxwell, H. C. Maytum, A. J. A. Watson, J. M. J. Williams, *J. Am. Chem. Soc.* **2009**, 131, 1766.
- (39) A. J. Blacker, M. M. Farah, M. I. Hall, S. P. Marsden, O. Saidi, J. M. J. Williams, *Org. Lett.* **2009**, 11, 2039.
- (40) C. Gunanathan, D. Milstein, *Angew. Chem. Int. Ed.* **2008**, 47, 8661.
- (41) (a) K.-i. Fujita, Z. Li, N. Ozeki, R. Yamaguchi, *Tetrahedron Lett.* **2003**, 44, 2687.  
(b) K.-i. Fujita, S. Furukawa, R. Yamaguchi, *J. Organomet. Chem.* **2002**, 649, 289.



- (c) K.-i. Fujita, K. Yamamoto, R. Yamaguchi, *Org. Lett.* **2002**, *4*, 2691.
- (42) (a) K.-i. Fujita, T. Fujii, R. Yamaguchi, *Org. Lett.* **2004**, *6*, 3525. (b) K.-i. Fujita, T. Fujii, A. Komatsubara, Y. Enoki, R. Yamaguchi, *Heterocycles* **2007**, *74*, 673.
- (43) K.-i. Fujita, Y. Kida, R. Yamaguchi, *Heterocycles* **2009**, *77*, 1371.
- (44) L. U. Nordstrom, R. Madsen, *Chem. Commun.* **2007**, 5034.
- (45) (a) R. Yamaguchi, Z. Mingwen, S. Kawagoe, C. Asai, K.-i. Fujita, *Synthesis* **2009**, *2009*, 1220. (b) R. Yamaguchi, S. Kawagoe, C. Asai, K.-i. Fujita, *Org. Lett.* **2008**, *10*, 181.
- (46) (a) K.-i. Fujita, A. Komatsubara, R. Yamaguchi, *Tetrahedron* **2009**, *65*, 3624. (b) M. Zhu, K.-i. Fujita, R. Yamaguchi, *Org. Lett.* **2010**, *12*, 1336.
- (47) (a) R. Kawahara, K.-i. Fujita, R. Yamaguchi, *J. Am. Chem. Soc.* **2010**, *132*, 15108. (b) R. Kawahara, K. i. Fujita, R. Yamaguchi, *Adv. Synth. Catal.* **2011**, *353*, 1161.
- (48) (a) D. Gnanamgari, E. L. O. Sauer, N. D. Schley, C. Butler, C. D. Incarvito, R. H. Crabtree, *Organometallics* **2009**, *28*, 321. (b) A. Prades, R. Corberán, M. Poyatos, E. Peris, *Chem. Eur. J.* **2008**, *14*, 11474.
- (49) I. Cumpstey, S. Agrawal, K. E. Borbas, B. Martin-Matute, *Chem. Commun.* **2011**, *47*, 7827.
- (50) M. A. Berliner, S. P. A. Dubant, T. Makowski, K. Ng, B. Sitter, C. Wager, Y. Zhang, *Org. Process Res. Dev.* **2011**, *15*, 1052.
- (51) A. Martínez-Asencio, D. J. Ramón, M. Yus, *Tetrahedron Lett.* **2010**, *51*, 325.
- (52) Z. Xu, D. S. Wang, X. Yu, Y. Yang, D. Wang, *Adv. Synth. Catal.* **2017**, *359*, 3332.
- (53) S. Rösler, M. Ertl, T. Irrgang, R. Kempe, *Angew. Chem. Int. Ed.* **2015**, *54*, 15046.

- (54) G. Zhang, Z. Yin, S. Zheng, *Org. Lett.* **2016**, *18*, 300.
- (55) S. Elangovan, J. Neumann, J.-B. Sortais, K. Junge, C. Darcel, M. Beller, *Nat. Commun.* **2016**, *7*, 12641.
- (56) M. Vellakkaran, K. Singh, D. Banerjee, *ACS Catal.* **2017**, *7*, 8152.
- (57) I. Bauer, H.-J. Knölker, *Chem. Rev.* **2015**, *115*, 3170.
- (58) X. Cui, F. Shi, Y. Zhang, Y. Deng, *Tetrahedron Lett.* **2010**, *51*, 2048.
- (59) Y. Zhao, S. W. Foo, S. Saito, *Angew. Chem. Int. Ed.* **2011**, *50*, 3006.
- (60) T. Yan, B. L. Feringa, K. Barta, *Nat. Commun.* **2014**, *5*, 5602.
- (61) T. Yan, B. L. Feringa, K. Barta, *ACS Catal.* **2016**, *6*, 381.
- (62) C. Geunho, H. S. Hyeok, *Angew. Chem. Int. Ed.* **2018**, *57*, 6166.

## Chapter 2. Iridium-Catalyzed Single-Step *N*-Substituted Lactam Synthesis from Lactones and Amines\*

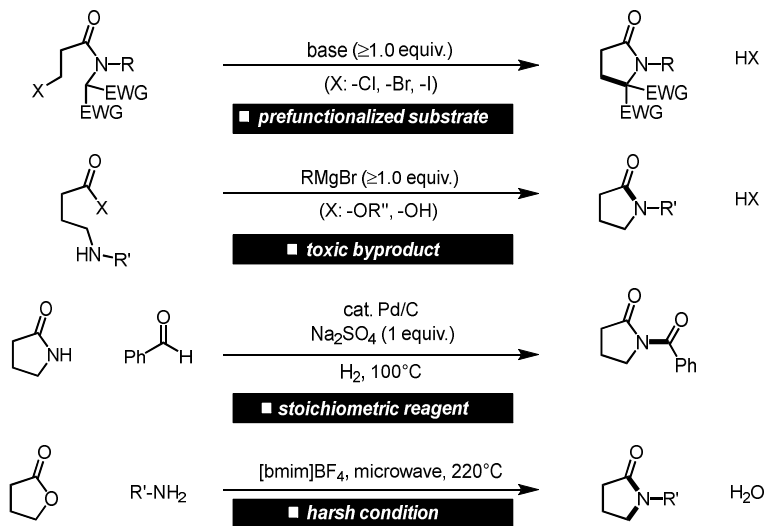


\* The majority of this work has been published: Kicheol Kim and Soon Hyeok Hong\*, *J. Org. Chem.* **2015**, *80*, 4152-4156.

## 2.1 Introduction

Lactams are one of the fundamental functional molecules in organic chemistry.<sup>1</sup> They serve as pharmacophores in antibiotics, antipsychotics, drug candidates, and intermediates in the synthesis of dopamine receptors.<sup>2</sup> Moreover, they can be used as the monomers of versatile synthetic polymers such as poly(1-vinylpyrrolidin-2-one) derivatives.<sup>3</sup> Conventional synthetic methods for lactam include the intramolecular condensation of amino acid derivatives under extremely high temperature conditions and the use of activating reagents such as Grignard reagents<sup>4</sup> and Brønsted acids<sup>5</sup> (Scheme 2.1). Moreover, the intramolecular cyclization of haloamides with Brønsted bases affords lactams.<sup>6</sup> Among these methods, the lactamization of lactones with amines is a straightforward approach because the substrates are readily available without any prefunctionalization. However, the previous methods for this reaction suffer from harsh temperature (220–270 °C) or high pressure,<sup>7</sup> require stoichiometric amounts of activating reagents,<sup>8</sup> and multistep reactions.<sup>9</sup> Moreover, catalytic methods also suffer from the use of prefunctionalized substrates.<sup>10</sup> Herein, we report the first Ir-catalyzed *N*-substituted lactam synthesis from readily available lactones and amines. Mechanistic investigations indicated that three distinct C–N bond transformation reactions occurred sequentially.

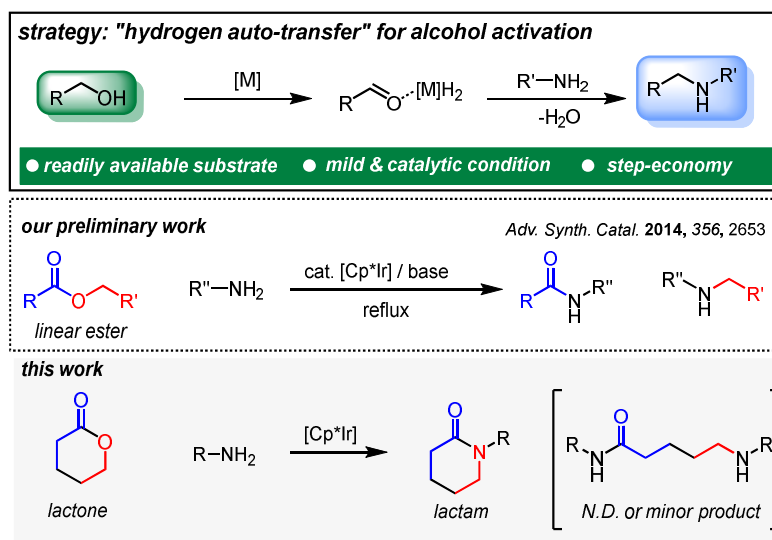
Conventional Methods: major drawbacks in synthetic and green-chemical view



**Scheme 2.1** Conventional methods for *N*-substituted lactam synthesis

## 2.2 Results and discussion

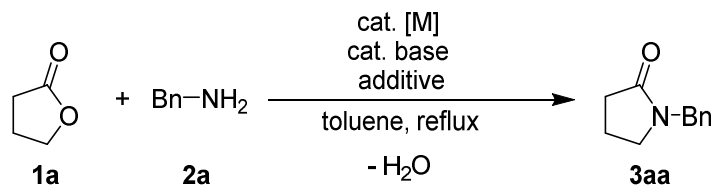
### 2.2.1 Optimization for lactam synthesis from lactones and amines



**Scheme 2.2** Research strategy and its background

Ir-catalyzed amination of alcohols using “hydrogen autotransfer” has been extensively explored in the last decade (Scheme 2.2).<sup>11</sup> Our group recently reported a tandem synthesis of amides and secondary amines from linear esters and amines via hydrogen autotransfer using the [Cp\*Ir] catalytic system.<sup>12</sup> Inspired by the results, we expected that aminoamides can be synthesized by the ring-opening reaction of lactones. The reaction of  $\gamma$ -butyrolactone (**1a**) with benzylamine (**2a**) using the reported Ir catalyst<sup>12</sup> afforded the corresponding lactam, 1-benzyl-2-pyrrolidinone (**3aa**) in 39% yield instead of the aminoamide (entry 5, Table 2.1). Encouraged by the unexpected result, the reaction conditions were optimized for the selective lactamization with several Ru and Ir complexes, which are well known for dehydrogenative C–N bond formation reactions (Table 2.1).<sup>11h,13</sup> A combination of

$[\text{Cp}^*\text{IrCl}_2]_2$  and a base was identified as the best precatalyst with an additional amount of amine (1.5–2 equiv) to achieve good yields (entries 5–7). The use of molecular sieves as drying agents increased the efficiency of the reaction by removing  $\text{H}_2\text{O}$  by-product (entry 8). The addition of X- or L-type ligands did not improve the yield (entries 9 and 10). Both  $[\text{Cp}^*\text{IrCl}_2]_2$  and NaOAc were essential for the efficient conversion (entries 11 and 12).

**Table 2.1** Optimization of reaction conditions<sup>a</sup>

entry	<b>2a/1a</b>	[M] (mol %)	Base (mol %)	additives	yield (%) <sup>b</sup>
1	2.0	[RuH <sub>2</sub> (PPh <sub>3</sub> ) <sub>4</sub> ] (5)	NaH (20)	<b>4</b> , CH <sub>3</sub> CN <sup>c</sup>	0
2	2.0	[Cp*IrCl <sub>2</sub> ] <sub>2</sub> (1)	NaHCO <sub>3</sub> (2)	-	16
3	2.0	[Ru(p-cymene)Cl <sub>2</sub> ] <sub>2</sub> (5)	-	dppf <sup>d</sup>	1
4	2.0	[Sc(OTf) <sub>3</sub> ] (5)	-	-	1
5	1.0	[Cp*IrCl <sub>2</sub> ] <sub>2</sub> (1)	NaOAc (2)	-	39
6	1.5	[Cp*IrCl <sub>2</sub> ] <sub>2</sub> (1)	NaOAc (2)	-	59
7	2.0	[Cp*IrCl <sub>2</sub> ] <sub>2</sub> (1)	NaOAc (2)	-	63
8	2.0	[Cp*IrCl <sub>2</sub> ] <sub>2</sub> (1)	NaOAc (2)	4 Å M.S. <sup>e</sup>	77
9	2.0	[Cp*IrCl <sub>2</sub> ] <sub>2</sub> (1)	NaOAc (2)	<b>5</b> <sup>f</sup>	8
10	2.0	[Cp*IrCl <sub>2</sub> ] <sub>2</sub> (1)	NaOAc (2)	<b>4</b> , CH <sub>3</sub> CN <sup>g</sup>	53
11	2.0	-	NaOAc (2)	4 Å M.S. <sup>e</sup>	0
12	2.0	[Cp*IrCl <sub>2</sub> ] <sub>2</sub> (1)	-	4 Å M.S. <sup>e</sup>	26

<sup>a</sup>Standard reaction conditions: **1a** (0.25 mmol, 1.0 equiv), **2a** (0.5 mmol, 2.0 equiv), [M] (1 mol %), toluene (0.6 mL), reflux, and 36 h. <sup>b</sup>Determined by GC using dodecane as the internal standard. <sup>c</sup>1,3-diisopropylimidazolium bromide (**4**, 5 mol %), CH<sub>3</sub>CN (5 mol %). <sup>d</sup>dppf = 1,1'-bis(diphenylphosphino)ferrocene (10 mol %) <sup>e</sup>4 Å molecular sieves (ca. 20 mg). <sup>f</sup>tri(*p*-tolyl)phosphine (**5**, 2 mol %). <sup>g</sup>**4** (2 mol %), CH<sub>3</sub>CN (2 mol %).

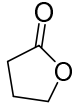
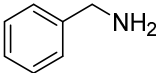
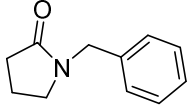
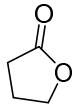
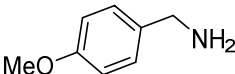
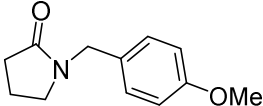
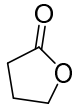
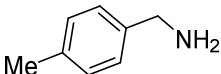
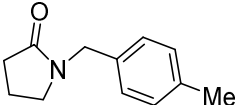
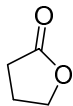
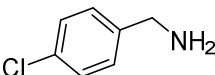
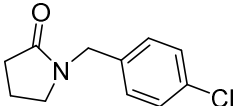
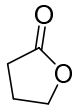
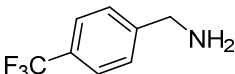
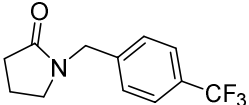
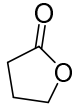
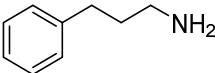
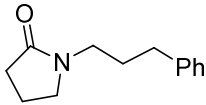
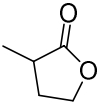
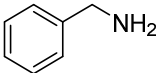
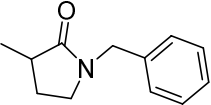


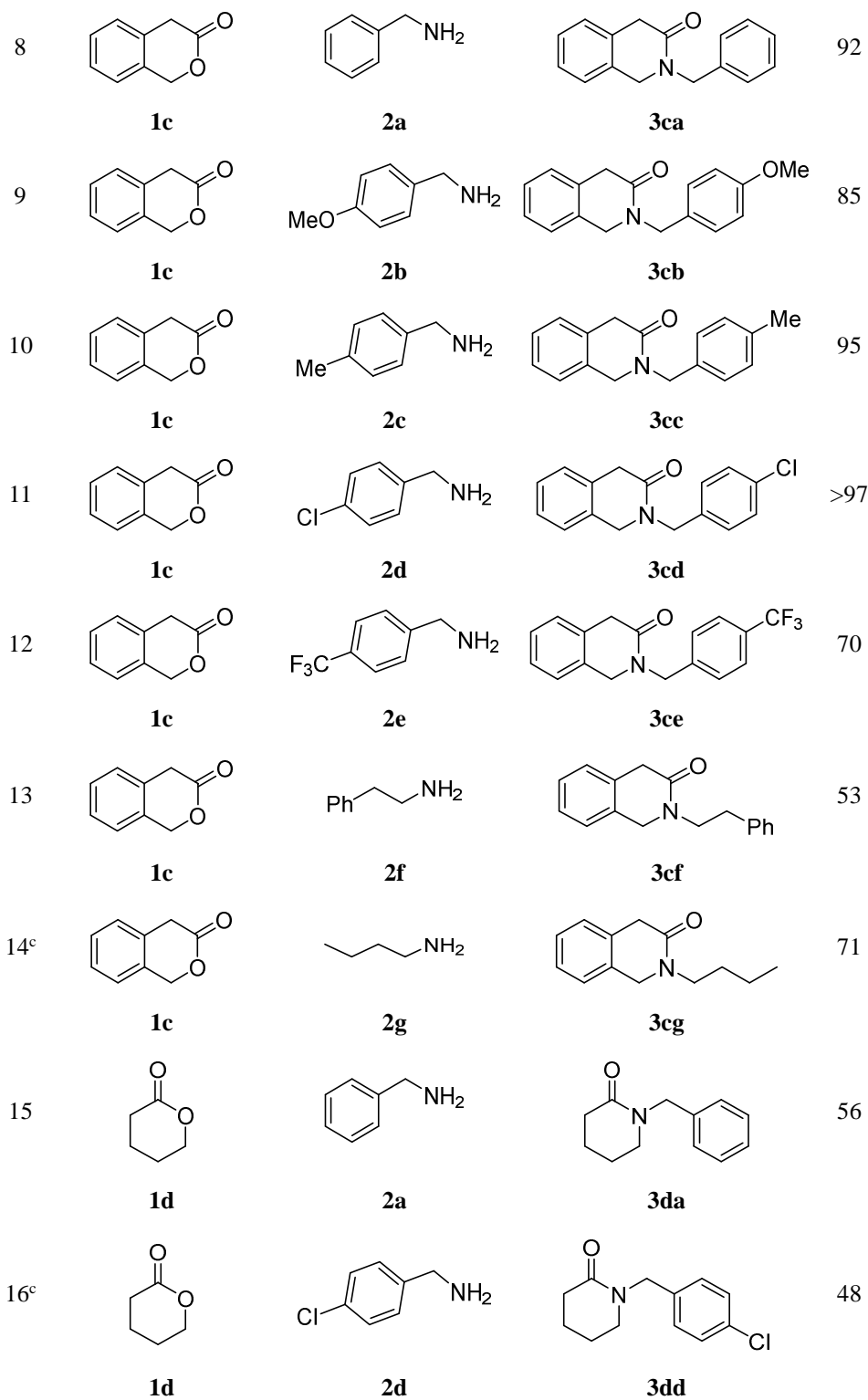
### 2.2.2 Substrate scope

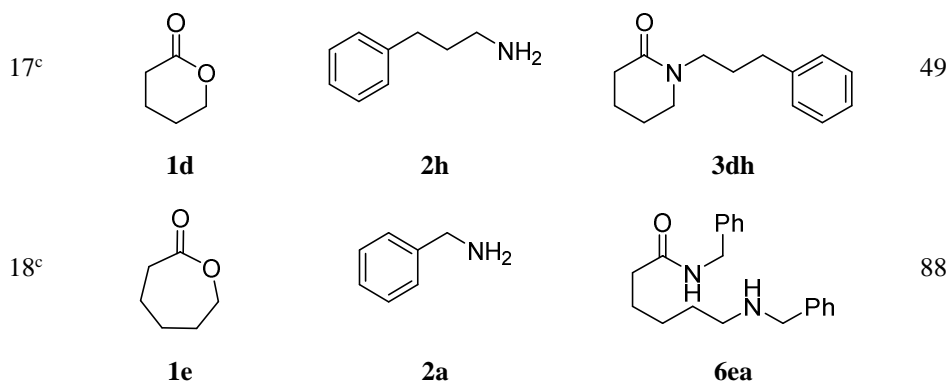
With the optimized reaction conditions, the method was attempted for the synthesis of diverse *N*-substituted lactams (Table 2.2). The reactions of **1a** with a variety of benzylamines and 3-phenylpropylamine **2h** afforded the corresponding lactams in fair-to-very good yields (entries 1–6). Electron-deficient benzylamines resulted in slightly higher conversion than electron-rich benzylamines (entries 4 and 5). The reactions of  $\alpha$ -branched primary amines such (S)-(-)- $\alpha$ -methylbenzylamine with **1a** did not give the corresponding lactams but only produced the corresponding hydroxyamides and/or aminoamides. The  $\alpha$ -methyl substituent on butyrolactone did not interfere with the reaction (entry 7). The reactions of 3-isochromanone **1c** with benzylamines and aliphatic amines proceeded smoothly to afford the corresponding lactams in fair-to-excellent yields (entries 8–14). In the lactamization of **1c**, both electron-rich and electron-deficient benzylamines participated in the reaction efficiently. The catalytic system tolerated various functional groups including ether, alkyl, chloro, and trifluoromethyl groups. Trifluoromethylated lactam **3ae** and **3ce**, potential building blocks for pharmaceutical compounds,<sup>14,15</sup> were synthesized efficiently (entries 5 and 12). Linear aliphatic amine **2g** was lactamized with **1c** in 71% yield (entry 14). To gain further insight into the effect of lactone ring size, the reactions of  $\delta$ -valerolactone (**1d**) and  $\epsilon$ -caprolactone (**1e**) with **2a** were conducted. The reaction of six-membered lactone **1d** resulted in a reduced yield (56%) with dibenzylamine as the by-product (entry 15). Inefficient reactions were caused by the homocoupling reaction of amines, producing secondary amines.<sup>16</sup> The reaction of  $\epsilon$ -caprolactone (**1e**) afforded only the corresponding aminoamide **6ea** in 88% yield, indicating that an aminoamide may be the intermediate before the intramolecular

transamidation to furnish the corresponding lactam (entry 18).

**Table 2.2** Direct lactam synthesis from lactones and amines<sup>a</sup>

entry	lactone	amine	product	yield (%) <sup>b</sup>
1				65
	<b>1a</b>	<b>2a</b>	<b>3aa</b>	
2 <sup>c</sup>				62
	<b>1a</b>	<b>2b</b>	<b>3ab</b>	
3 <sup>c</sup>				65
	<b>1a</b>	<b>2c</b>	<b>3ac</b>	
4 <sup>c</sup>				80
	<b>1a</b>	<b>2d</b>	<b>3ad</b>	
5 <sup>c</sup>				86
	<b>1a</b>	<b>2e</b>	<b>3ae</b>	
6 <sup>c</sup>				>97
	<b>1a</b>	<b>2h</b>	<b>3ah</b>	
7 <sup>c</sup>				72
	<b>1b</b>	<b>2a</b>	<b>3ba</b>	





<sup>a</sup>Reaction conditions: lactone (0.5 mmol, 1.0 equiv), amine (1.0 mmol, 2.0 equiv), [Cp\*IrCl<sub>2</sub>]<sub>2</sub> (1 mol %), NaOAc (2 mol %), 4 Å molecular sieves, toluene (1.2 mL), reflux, and 36 h in a 5 mL Schlenk tube. <sup>b</sup>Isolated yield. <sup>c</sup>[Cp\*IrCl<sub>2</sub>]<sub>2</sub> (2 mol %) and NaOAc (4 mol %) were used.

### 2.2.3 Mechanistic studies

To understand the reaction mechanism, the reactions of **1a** with **2a** were monitored by <sup>1</sup>H NMR spectroscopy (Figure 2.1). At the initial stage, hydroxyamide **A** was generated along with the consumption of **1a** and **2a**. Subsequently, the amounts of aminoamide **B** and lactam **3aa** increased with the decrease in the amounts of **1a**, **2a**, and **A**. After ~5 h, both the amounts of **A** and **B** gradually decreased, while the amount of **3aa** continuously increased. The concentration of **2a** started to increase after ~10 h and finally remained almost constant at ~40% of the initial concentration.

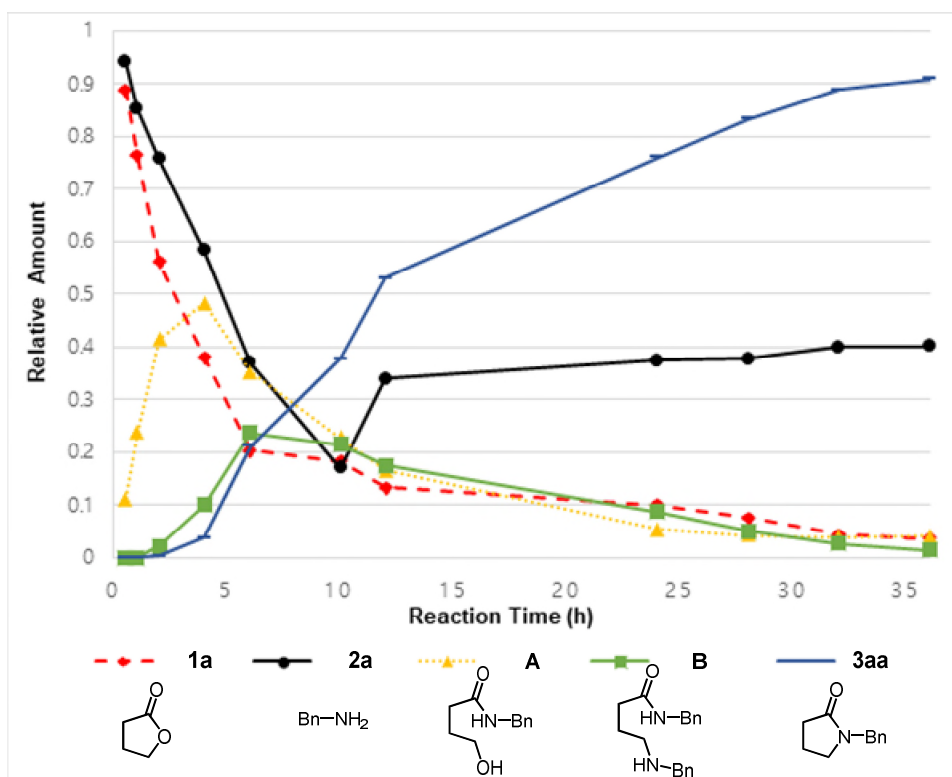
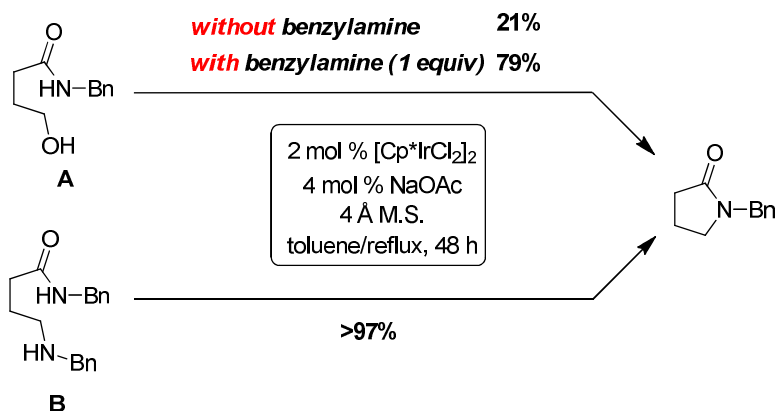


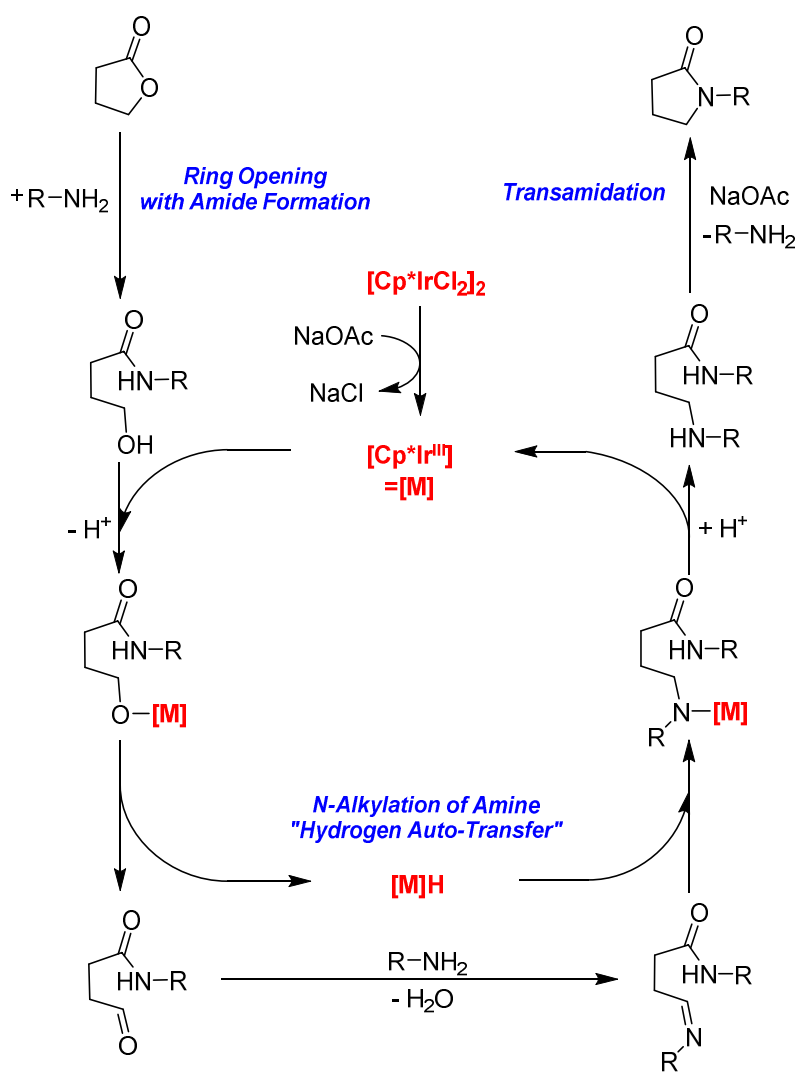
**Figure 2.1** Reaction profiles monitored by  $^1\text{H}$  NMR spectroscopy. Relative amount is the ratio of the observed integration value to its original 1 equiv value. Lactone (**1a**, 0.25 mmol, 1.0 equiv), amine (**2a**, 2.0 equiv),  $[\text{Cp}^*\text{IrCl}_2]_2$  (1 mol %), NaOAc (2 mol %), toluene- $d_8$  (0.6 mL), reflux in a screw-capped NMR tube.



**Scheme 2.3** Catalytic reactions of observed intermediates in the presence or absence of amines

To confirm the intermediacy of hydroxyamide and aminoamide in the mechanism of the reaction, independent reactions with **A** and **B** were performed under the catalytic conditions. Hydroxyamide **A** may be formed by the nucleophilic addition of amine to the carbonyl carbon of lactone and ring-opening process. When **A** alone was subjected to these reaction conditions, a small amount (21%) of **3aa** was obtained (Scheme 2.3). This result indicates that the direct intramolecular cyclization of hydroxyamides to lactams via the *N*-alkylation of amides is unlikely in our cases. In the catalytic *N*-alkylations of amides with alcohols, only primary amides were generally applicable even under harsh reaction conditions.<sup>17</sup> Considering that an amine is needed for the *N*-alkylation of amine with **A** to afford the second intermediate candidate **B**, 1 equiv of **2a** was added to the reaction of **A**. The reaction smoothly afforded **3aa** in 79% yield. Aminoamide **B** was efficiently transformed to **3aa** in quantitative yield under the reaction conditions. The intramolecular transamidation reaction even occurred quantitatively only with catalytic amount of NaOAc (4 mol %) and 4 Å molecular sieves, without using

$[\text{Cp}^*\text{IrCl}_2]_2$ . These results including the reaction profiles indicate that the last step in the reaction pathway is the intramolecular transamidation of aminoamide.

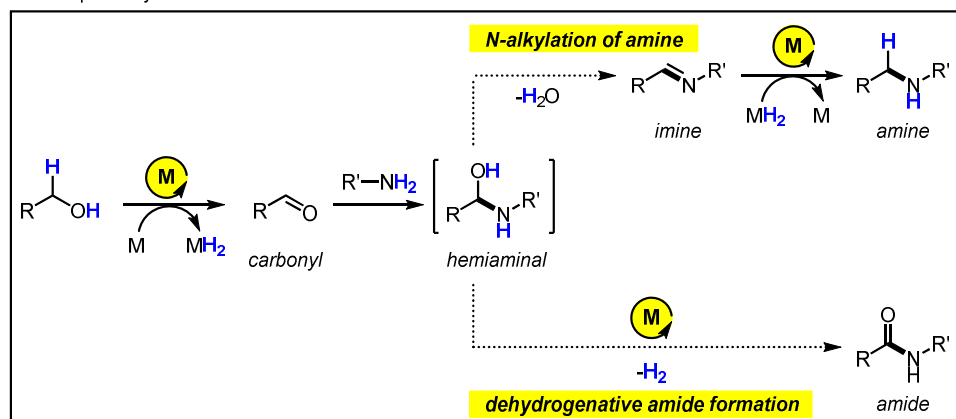


**Scheme 2.4** Proposed catalytic cycle

Based on the results, a mechanism that involves three sequential chemical transformations is proposed (Scheme 2.4). At the initial stage, the carbonyl group of lactone is aminolyzed by an amine, generating the corresponding hydroxyamide. Then, the Ir-catalyzed *N*-alkylation of an amine with the hydroxyamide via “hydrogen autotransfer” affords the corresponding aminoamide.<sup>11g,18</sup> Finally, the aminoamide undergoes intramolecular transamidation to afford the corresponding lactam. Ir catalysis is necessary for *N*-alkylation of an amine with the hydroxyamide, whereas the aminolysis of lactone with amine and transamidation of aminoamide occurred without Ir complex.

#### 2.2.4. Chemoselectivity of the reaction of alcohols and amines for two different C–N bond formations: *N*-alkylation and amide formation

■ Two pathways from hemiaminal intermediate



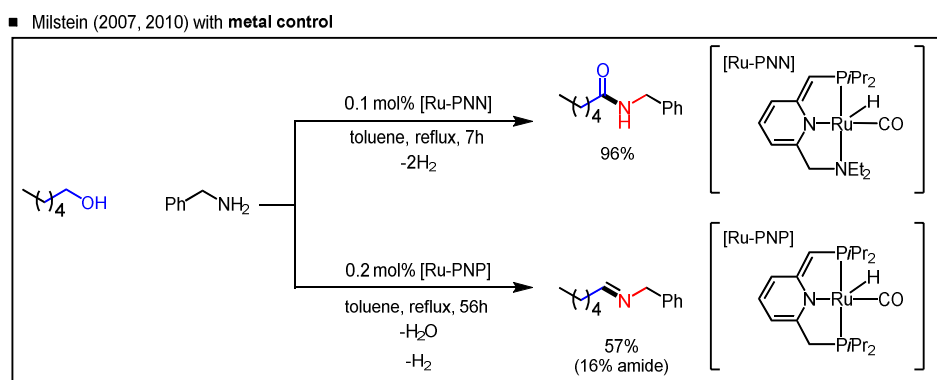
**Scheme 2.5** Two pathways of hemiaminal reaction

The major step in catalysis is the *N*-alkylation of an amine with a hydroxyamide intermediate (Scheme 2.4). An alcohol is dehydrogenated to form a carbonyl by a catalyst, which forms either a free carbonyl compound or a metal-coordinated



carbonyl species (Scheme 2.5). The resulting carbonyl species forms a labile hemiaminal intermediate via nucleophilic attack of the amine. Reactions of the hemiaminal diverge into two pathways: “dehydration and further transfer hydrogenation to afford an amine” and “catalytic dehydrogenation to afford an amide”. Therefore, the release or retention of H<sub>2</sub> in metal hydride species is critical for determining the selectivities toward two valuable C–N adducts. However, to the best of our knowledge, no universal principle to kinetically control selectivity has been elucidated. Only thermodynamically driving strategies were established: open condition to liberate H<sub>2</sub> for dehydrogenative amidation and the use of drying reagents such as molecular sieves for dehydrative amination. In this section, several examples of controlling selectivity are introduced by varying the catalyst, base, and other conditions.

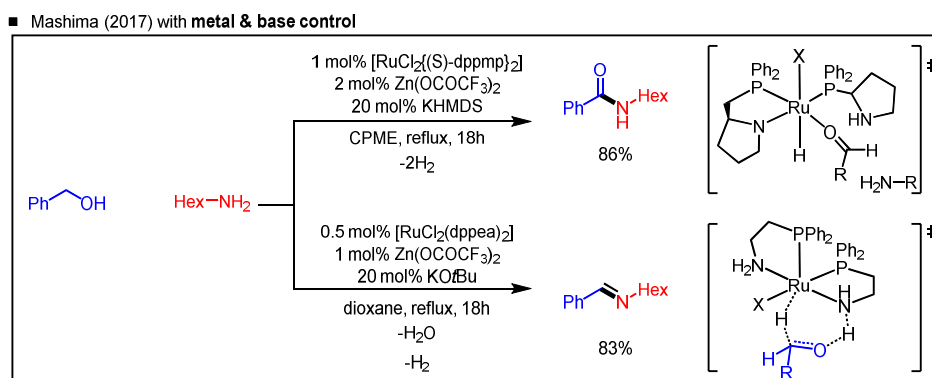
Seminal works controlling selectivity toward amide or imine formation were reported by the Milstein group and the Mashima group, respectively. The Milstein group (2007) reported base-free dehydrogenative amidation from alcohols and amines using a Ru–PNN pincer complex.<sup>19</sup> This group developed a selective



**Scheme 2.6** The Milstein group: effort to control selectivity between amide and imine formation

imine formation from the same reactants using a modified Ru–PNP pincer complex.<sup>20</sup> The reactions of *n*-hexylalcohol with benzyl amine in the presence of [Ru–PNN] and [Ru–PNP] complexes resulted in distinct chemoselectivity: [Ru–PNN] (major product: amide, 96%) and [Ru–PNP] (major product: imine 57%) (Scheme 2.6). The Ru-dearomatized pincer complex activated the alcohol to a metal-alkoxide concurrently with aromatization of the pincer ligand. The resulting metal-alkoxide species underwent  $\beta$ -H elimination to afford the metal-hydride species bearing the aldehyde ligand. These metal-aldehyde complexes followed two pathways: liberation of the aldehyde or attack of an amine to the coordinated aldehyde. When the former pathway took place, the reactive aldehyde coupled with an amine to generate the labile hemiaminal intermediate. The labile hemiaminal intermediate was likely to be condensed to imine when heated. In the case of the latter pathway, the metal-hemiaminalato species was in situ generated and further  $\beta$ -H elimination resulted in amide formation. The key factor determining the selectivities of structurally similar [Ru–PNN] (with amide selectivity) and [Ru–PNP] (with imine selectivity) complexes might be the hemilability of the arm in the ligand. While the strongly coordinating phosphine arm in [Ru–PNP] facilitated the dissociation of aldehyde, the hemilabile amino arm in [Ru–PNN] enabled the coordinating aldehyde to react with an amine for amide synthesis. Considering that the other two sterically different Ru–PNP complexes showed similar activities, steric hindrance was not a critical factor for selectivity.<sup>20</sup> The Mashima group (2017) also reported the control of selectivity between amide or imine formations by changing bases and ligands in Ru complexes bearing PN-chelating ligands.<sup>21</sup> The reactions of benzyl alcohols with *n*-hexylamine on [RuCl<sub>2</sub>P((S)-dppmp)<sub>2</sub>] / KHMDS and

$[\text{RuCl}_2(\text{dppea})_2]$  /  $\text{KO}t\text{Bu}$  showed the distinct chemoselectivity:  $[\text{RuCl}_2\text{P}((\text{S})\text{-dppmp})_2]$  (major product: amide, 86%) and  $[\text{RuCl}_2(\text{dppea})_2]$  (major product: imine 83%) (Scheme 2.7). Comprehensive experimental studies including kinetic profile, Hammett plot study using various alcohols, and KIE study of alcohols indicated certain rate-limiting steps for each selective amide and imine formation. In contrast to the Milstein work, the bulkiness of the pyrrolidine arm in the (S)-dppmp ligand made hemilabile ligation possible for selective amide formation.

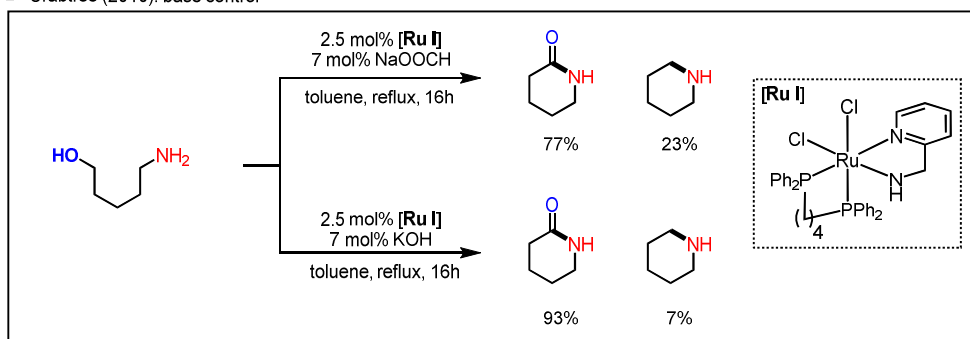


**Scheme 2.7** The Mashima group: effort to control selectivity between amide or imine formation

A more straightforward approach to control the selectivity between the amine and amide formation is to tune other conditions within a single well-defined catalyst. Two seminal examples were reported by the Crabtree group and the Huynh group. The Crabtree group studied reactions of 5-amino-1-pentanol using a **[Ru I]** complex at 110 °C by modifying the base.<sup>22</sup> Though two bases furnished amide as the major product, the catalytic system with sodium formate ( $\text{NaHCO}_2$ ) resulted in a higher amount of imine product than that with potassium hydroxide (23% vs. 7%).

On the basis of both theoretical and experimental investigations, the Crabtree group found several significant factors for catalytic activity and selectivity. First, high temperature was necessary for the continuous generation of an empty coordination site and  $\beta$ -H elimination. Second, selective formation of amide resulted from nucleophilic attack of an amine on the coordinated aldehyde. In addition, ruthenium monohydrides are implicated in this catalysis. Lastly, in selective amine formation, a hemiaminal was liberated from metal and H<sub>2</sub> was retained on the metal to further transfer-hydrogenate the in situ-generated imine.

■ Crabtree (2010): base control

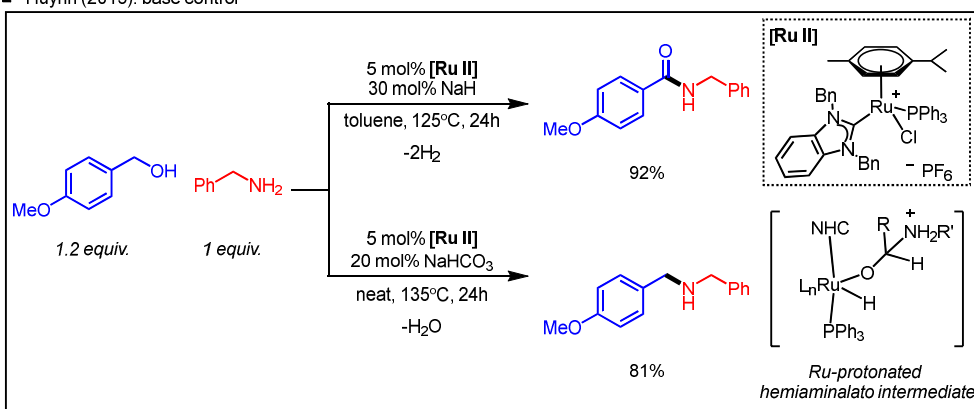


**Scheme 2.8** The Crabtree group: effort to control selectivity between amide or amine formation

The Huynh group (2015) demonstrated base-controlled selective dehydrogenative amidation (with sodium hydride) and amination (with sodium bicarbonate) using the single well-defined, cationic benzimidazolone-2-ylidene ruthenium complex, [Ru II] (Scheme 2.9).<sup>23</sup> NMR study of the catalytic system indicated that dissociation of *p*-cymene resulted in a catalytically active ruthenium hydride species bearing the *N*-heterocyclic carbene ligand and phosphine ligand. The

selectivity was determined at the reaction of a ruthenium-protonated hemiaminalato complex generated from nucleophilic attack of an amine on the coordinated aldehyde in  $[\text{RuH}(\text{NHC})(\text{PPh}_3)]$  complex. While proton transfer to hydrido led to the formation of an amide with liberation of  $\text{H}_2$ , proton-transfer-to-alkoxido led to the formation of an amine. In detail, formation of amine resulted from successive transformations involving imine formation from hemiaminal intermediate and transfer hydrogenation of the imine by a ruthenium hydride species.

■ Huynh (2015): base control



**Scheme 2.9** The Huynh group: effort to control selectivity between amide or amine formation

### 2.3 Conclusion

A catalytic lactam synthesis was developed from lactones and amines using the readily available Ir complex  $[\text{Cp}^*\text{IrCl}_2]_2$  and sodium acetate. Mechanistic studies revealed an interesting domino reaction involving the following sequence of reactions: aminolysis of lactone, *N*-alkylation of amine with hydroxyamide, and intramolecular transamidation of aminoamide. The literature study covers several examples of the control of selectivity between amide and amine (or imine) formation from the hemiaminal intermediate.

## 2.4 Experimental section

### 2.4.1 General considerations

Unless otherwise noted, all the reactions were carried out using standard Schlenk techniques or in an Ar-filled glove box. NMR spectra were recorded in CDCl<sub>3</sub> or toluene-*d*<sub>8</sub>, and residual solvent signals were used as the reference. Chemical shifts are reported in ppm, and coupling constants are reported in Hz. Multiplicity is indicated by one or more of the following: s (singlet), d (doublet), t (triplet), q (quartet), quin (quintet), sext (sextet), and m (multiplet). High Resolution Mass Spectrometry (HRMS) was performed by using the fast atom bombardment (FAB) ionization mode, the electrospray ionization (ESI) Q-TOF mode, and electron ionization (EI) mode. GC analysis was carried out using a GC system equipped with an HP-5 column and FID detector. NHC precursor (1,3-diisopropylimidazolium bromide),<sup>24</sup> *N*-benzyl-4-hydroxybutanamide (A),<sup>7a</sup> and *N*-benzyl-4-(benzylamino)butanamide (B)<sup>7a</sup> were prepared based on literature procedures. Other chemicals were purchased from commercial suppliers and used as received without further purification.

#### 2.4.2 General procedure for lactam synthesis from lactones and amines

Inside an Ar-filled glove box, 1 mol % of  $[\text{Cp}^*\text{IrCl}_2]_2$  (3.98 mg, 0.005 mmol), 2 mol % NaOAc (0.82 mg, 0.010 mmol), 4 Å molecular sieves (*ca.* 35 mg), and toluene (1.2 mL) were added to an oven-dried 5 mL Schlenk tube equipped with a magnetic spin bar and septum. After the tube with the catalytic system was removed from the box, 0.50 mmol of lactone and 1.00 mmol of amine were added to the tube under Ar flow using the Schlenk technique. Then, the reaction mixture was stirred at 110 °C for 36 h before cooling down to room temperature. All the volatiles were removed in *vacuo*, and the resulting residue was purified by flash column chromatography (hexane/EtOAc = 4:1 v/v or DCM/MeOH = 30:1 v/v) to afford the corresponding lactam.



### 2.4.3 Procedure for kinetic study

Inside an Ar-filled glove box, 1 mol % of  $[\text{Cp}^*\text{IrCl}_2]_2$  (1.99 mg, 0.0025 mmol), 2 mol % NaOAc (0.41 mg, 0.005 mmol), and toluene- $d_8$  (0.6 mL) were added to a screw-capped NMR tube. After the tube with the catalytic system was removed from the box,  $\gamma$ -butyrolactone (1a, 19.2  $\mu\text{L}$ , 0.25 mmol) and benzylamine (1b, 54.6  $\mu\text{L}$ , 0.50 mmol) were added to the tube under Ar flow. Then, the reaction mixture was heated at 110  $^\circ\text{C}$  for due reaction time (*e.g.* 30 mins from 0 h to 0.5 h) before cooling down to room temperature. The NMR reaction tube was sequentially analyzed with  $^1\text{H}$  NMR spectroscopy. Then, the reaction mixture was heated again at 110  $^\circ\text{C}$  for another due reaction time (*e.g.* 30 mins from 0.5 h to 1.0 h). Repetitive analyses using  $^1\text{H}$  NMR spectroscopy were continued until the overall reaction time reached 36 h (Figure 2.2).

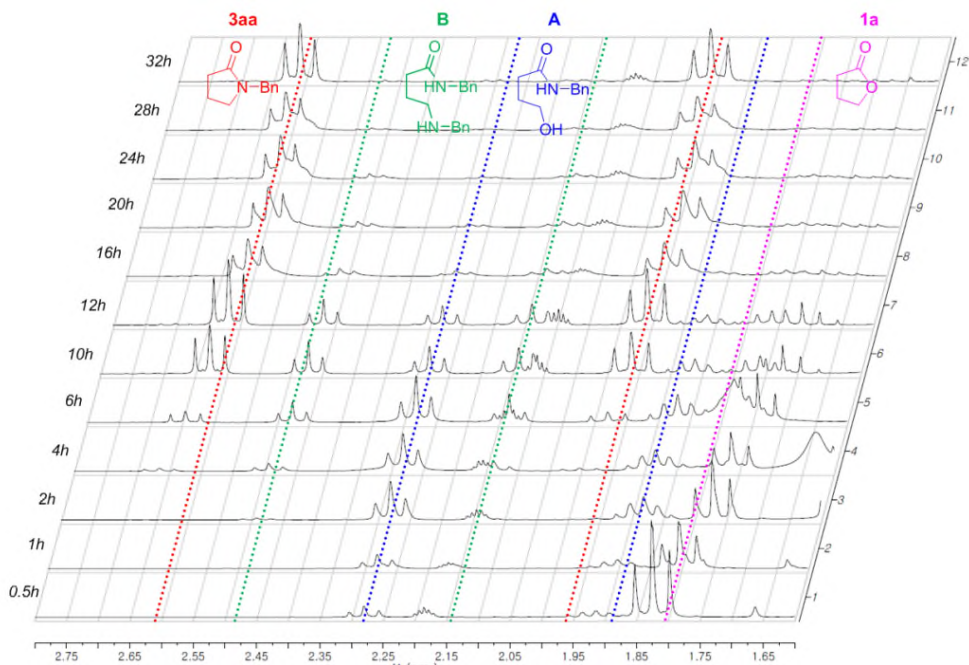
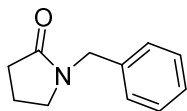
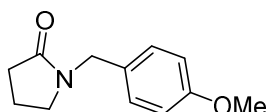


**Figure 2.2** Stacked  $^1\text{H}$  NMR spectra of kinetic study

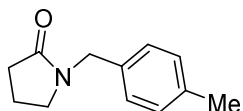
#### 2.4.4 Characterization of compounds



**1-(Phenylmethyl)-2-pyrrolidinone (3aa):** Yellow liquid (57 mg, 65%).  $^1\text{H}$  NMR (300 MHz,  $\text{CDCl}_3$ )  $\delta$  = 7.29-7.15 (m, 5H), 4.38 (s, 2H), 3.20 (t,  $J=7.5$  Hz, 2H), 2.39 (t,  $J=8.3$  Hz, 2H), 1.92 (quin,  $J=7.9$  Hz, 2H). The spectral data were consistent with those reported in the literature.<sup>25</sup>

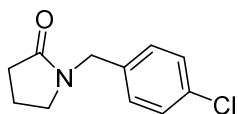


**1-[(4-Methoxyphenyl)methyl]-2-pyrrolidinone (3ab):** Brown liquid (64 mg, 62%).  $^1\text{H}$  NMR (499 MHz,  $\text{CDCl}_3$ )  $\delta$  = 7.18 (d,  $J=8.8$  Hz, 2H), 6.86 (d,  $J=8.8$  Hz, 2H), 4.39 (s, 2H), 3.81 (s, 3H), 3.25 (t,  $J=7.1$  Hz, 2H), 2.43 (t,  $J=8.1$  Hz, 2H), 1.98 (quin,  $J=7.7$  Hz, 2H). The spectral data were consistent with those reported in the literature.<sup>26</sup>



**1-[(4-Methylphenyl)methyl]-2-pyrrolidinone (3ac):** Brown liquid (62 mg, 65%). IR (neat): 1679, 1514, 1461, 1423, 1285, 1261, 806, 754, 662  $\text{cm}^{-1}$ ;  $^1\text{H}$  NMR (499 MHz,  $\text{CDCl}_3$ )  $\delta$  = 7.14 (s, 4H), 4.42 (s, 2H), 3.25 (t,  $J=7.1$  Hz, 2H), 2.46 (t,  $J=8.1$  Hz, 2H), 2.34 (s, 3H), 1.98 (quin,  $J=7.6$  Hz, 2H);  $^{13}\text{C}$  NMR (75 MHz,  $\text{CDCl}_3$ )  $\delta$

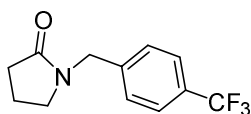
=174.8, 137.2, 133.5, 129.3, 128.1, 46.5, 46.2, 30.9, 21.0, 17.6; HRMS–EI (m/z) [M]<sup>+</sup> calcd for C<sub>12</sub>H<sub>15</sub>NO, 189.1154; found: 189.1153.



**1-[(4-Chlorophenyl)methyl]-2-pyrrolidinone (3ad):** Brown liquid (84 mg, 80%).

<sup>1</sup>H NMR (499 MHz, CDCl<sub>3</sub>) δ = 7.31 (d, *J*=8.3 Hz, 2H), 7.19 (d, *J*=8.8 Hz, 2H), 4.43 (s, 2H), 3.26 (t, *J*=7.2 Hz, 2H), 2.45 (t, *J*=8.3 Hz, 2H), 2.01 (quin, *J*=7.6 Hz, 2H).

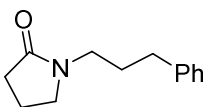
The spectral data were consistent with those reported in the literature.<sup>27</sup>



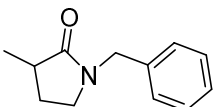
**1-[(4-Trifluoromethylphenyl)methyl]-2-pyrrolidinone (3ae):** Yellow liquid (105

mg, 86%). IR (neat): 1683, 1417, 1323, 1291, 1161, 1110, 1065, 1018, 819 cm<sup>-1</sup>; <sup>1</sup>H NMR (499 MHz, CDCl<sub>3</sub>) δ = 7.60 (d, *J*=8.3 Hz, 2H), 7.37 (d, *J*=8.3 Hz, 2H), 4.51 (s, 2H), 3.29 (t, *J*=7.3 Hz, 2H), 2.47 (t, *J*=8.3 Hz, 2H), 2.04 (quin, *J*=7.5 Hz, 2H);

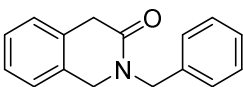
<sup>13</sup>C NMR (101 MHz, CDCl<sub>3</sub>) δ = 174.7, 140.5, 129.2 (q, *J*=32.0 Hz), 127.8, 125.1 (q, *J*=3.8 Hz), 124.5 (q, *J*=271.6 Hz), 46.3, 45.6, 30.3, 17.3; <sup>19</sup>F NMR (376 MHz, CDCl<sub>3</sub>) δ = -62.67; HRMS–ESI (m/z) [M+Na]<sup>+</sup> calcd for C<sub>12</sub>H<sub>12</sub>F<sub>3</sub>NNaO, 266.0763; found: 266.0764.



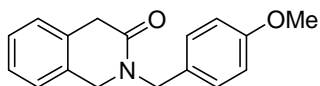
**1-(3-phenylpropyl)-2-pyrrolidinone (3ah):** Yellow liquid (101 mg, >97%).  $^1\text{H}$  NMR (499 MHz,  $\text{CDCl}_3$ )  $\delta$  = 7.31-7.27 (m, 2H), 7.22-7.17 (m, 3H), 3.35 (t,  $J=7.8$  Hz, 4H), 2.64 (t,  $J=7.8$  Hz, 2H), 2.37 (t,  $J=8.3$  Hz, 2H), 1.98 (quin,  $J=7.3$  Hz, 2H), 1.86 (quin,  $J=7.7$  Hz, 2H). The spectral data were consistent with those reported in the literature.<sup>28</sup>



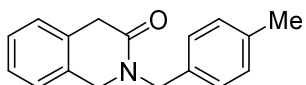
**3-Methyl-1-(phenylmethyl)-2-pyrrolidinone (3ba):** Brown liquid (68 mg, 72%).  $^1\text{H}$  NMR (499 MHz,  $\text{CDCl}_3$ ) 7.36 - 7.23 (m, 5H), 4.50 - 4.42 (m, 2H), 3.21 - 3.13 (m, 2H), 2.52 (sext,  $J = 7.8$  Hz, 1 H), 2.26 - 2.16 (m, 1H), 1.65 - 1.55 (m, 1H), 1.25 (d,  $J=7.3$  Hz, 3H) ; HRMS-EI (m/z)  $[\text{M}]^+$  calcd for  $\text{C}_{12}\text{H}_{15}\text{NO}$ , 189.1154; found: 189.1153. The spectral data were consistent with those reported in the literature.<sup>29</sup>



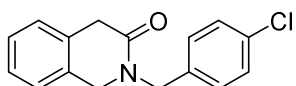
**1,4-Dihydro-2-(phenylmethyl)-3(2H)-isoquinolinone (3ca):** Brown liquid (109 mg, 92%).  $^1\text{H}$  NMR (300 MHz,  $\text{CDCl}_3$ )  $\delta$  = 7.41-7.09 (m, 9H), 4.79 (s, 2H), 4.41 (s, 2H), 3.74 (s, 2H). The spectral data were consistent with those reported in the literature.<sup>30</sup>



**1,4-Dihydro-2-(4-methoxyphenylmethyl)-3(2H)-isoquinolinone (3cb):** Yellow liquid (114 mg, 85%). IR (neat): 1711, 1667, 1611, 1512, 1460, 1334, 1285, 1246, 1176, 1032, 820, 741  $\text{cm}^{-1}$ ;  $^1\text{H}$  NMR (499 MHz,  $\text{CDCl}_3$ )  $\delta$  = 7.32 (m, 5H), 7.12 (d,  $J=7.8$  Hz, 1H), 6.90 (d,  $J=8.3$  Hz, 2H), 4.73 (s, 2H), 4.40 (s., 2H), 3.82 (s, 3H), 3.72 (s, 2H);  $^{13}\text{C}$  NMR (101 MHz,  $\text{CDCl}_3$ )  $\delta$  = 169.0, 159.1, 132.0, 131.1, 129.4, 128.6, 127.5, 127.2, 126.6, 125.1, 114.1, 55.3, 50.0, 49.4, 37.3; HRMS–FAB ( $m/z$ )  $[\text{M}+\text{H}]^+$  calcd for  $\text{C}_{17}\text{H}_{18}\text{NO}_2$ , 268.1338; found: 268.1338.

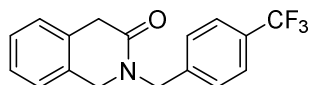


**1,4-Dihydro-2-(4-methylphenylmethyl)-3(2H)-isoquinolinone (3cc):** Yellow liquid (119 mg, 95%). IR (neat): 1711, 1669, 1430, 1380, 1349, 1309, 1284, 1248, 1047, 741, 697  $\text{cm}^{-1}$ ;  $^1\text{H}$  NMR (499 MHz,  $\text{CDCl}_3$ )  $\delta$  = 7.28-7.08 (m, 8H), 4.73 (s, 2H), 4.38 (s, 2H), 3.71 (s, 2H), 2.34 (s, 3H);  $^{13}\text{C}$  NMR (101 MHz,  $\text{CDCl}_3$ )  $\delta$  = 169.0, 137.2, 133.5, 132.1, 131.2, 129.3, 128.0, 127.5, 127.2, 126.5, 125.1, 50.1, 49.7, 37.3, 21.1; HRMS–FAB ( $m/z$ )  $[\text{M}+\text{H}]^+$  calcd for  $\text{C}_{17}\text{H}_{18}\text{NO}$ , 252.1388; found: 252.1386.



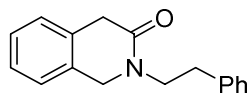
**1,4-Dihydro-2-(4-chlorophenylmethyl)-3(2H)-isoquinolinone (3cd):** Yellow liquid (135 mg, >97%). IR (neat): 1639, 1491, 1408, 1348, 1284, 1090, 1048, 1015,

881, 740, 698  $\text{cm}^{-1}$ ;  $^1\text{H}$  NMR (499 MHz,  $\text{CDCl}_3$ )  $\delta$  = 7.32-7.20 (m, 7H), 7.10 (d, 1H), 4.74 (s, 2H), 4.40 (s, 2H), 3.72 (s, 2H);  $^{13}\text{C}$  NMR (75 MHz,  $\text{CDCl}_3$ )  $\delta$  = 169.0, 135.2, 133.4, 132.0, 131.0, 129.3, 128.9, 127.6, 127.3, 126.6, 125.1, 50.2, 49.3, 37.3; HRMS-FAB ( $m/z$ )  $[\text{M}+\text{H}]^+$  calcd for  $\text{C}_{16}\text{H}_{15}\text{ClNO}$ , 272.0842; found: 272.0848.



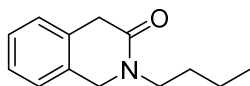
**1,4-Dihydro-2-(4-trifluoromethylphenylmethyl)-3(2H)-isoquinolinone (3ce):**

Dark yellow liquid (107 mg, 70%). IR (neat): 1670, 1326, 1286, 1162, 1112, 1067, 1048, 745  $\text{cm}^{-1}$ ;  $^1\text{H}$  NMR (499 MHz,  $\text{CDCl}_3$ )  $\delta$  7.59 (d,  $J=8.3$  Hz, 2H), 7.53(t,  $J=7.8$  Hz, 1H), 7.39 (d,  $J=8.3$  Hz, 2H), 7.25-7.18 (m, 2H), 7.10 (d,  $J=7.3$  Hz, 1H), 4.82 (s, 2H) 4.41 (s, 2H), 3.73(s, 2H);  $^{13}\text{C}$  NMR (101 MHz,  $\text{CDCl}_3$ )  $\delta$  = 169.3, 140.7, 131.9, 130.8, 128.1, 127.7, 127.3, 126.7, 125.7, 125.7, 125.6, 125.1, 50.5, 49.7, 37.3;  $^{19}\text{F}$  NMR (376 MHz,  $\text{CDCl}_3$ )  $\delta$  = -62.58; HRMS-CI ( $m/z$ )  $[\text{M}+\text{H}]^+$  calcd for  $\text{C}_{17}\text{H}_{15}\text{F}_3\text{NO}$ , 306.1106; found: 306.1109.

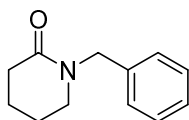


**1,4-Dihydro-2-(2-phenylethyl)-3(2H)-isoquinolinone (3cf):** Orange liquid (53 mg, 53%). IR (neat): 1712, 1664, 1455, 1390, 1352, 1287, 1269, 1146, 1048, 751, 700  $\text{cm}^{-1}$ ;  $^1\text{H}$  NMR (300 MHz,  $\text{CDCl}_3$ )  $\delta$  = 7.32-7.17 (m, 8H), 7.07 (d,  $J=7.0$  Hz, 1H), 4.32 (s, 2H) 3.78 (t,  $J=7.4$  Hz, 2H), 3.62 (s, 2H), 2.95 (t,  $J=7.3$  Hz, 2H);  $^{13}\text{C}$  NMR (75 MHz,  $\text{CDCl}_3$ )  $\delta$  = 168.8, 139.0, 132.4, 131.5, 128.8, 128.5, 127.5, 127.1, 126.4,

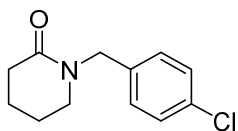
126.4, 125.0, 51.8, 49.1, 37.7, 33.9; HRMS–EI (m/z) [M]<sup>+</sup> calcd for C<sub>17</sub>H<sub>17</sub>NO, 251.1310; found: 251.1310.



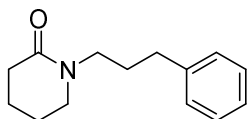
**1,4-Dihydro-2-butyl-3(2H)-isoquinolinone (3cg):** Brown liquid (72 mg, 71%). IR (neat): 1711, 1665, 1602, 1353, 1247, 1223, 740, 685 cm<sup>-1</sup>; <sup>1</sup>H NMR (499 MHz, CDCl<sub>3</sub>) δ = 7.29-7.15 (m, 4H), 4.46 (s, 2H), 3.61 (s, 2H), 3.52 (t, *J*=7.3 Hz, 2H), 1.58 (quin, *J* = 7.3 Hz, 2H), 1.35 (sext, *J*=7.3 Hz, 2H), 0.94 (t, *J*=7.3 Hz, 3H); <sup>13</sup>C NMR (75 MHz, CDCl<sub>3</sub>) δ = 168.7, 132.6, 131.6, 127.5, 127.2, 126.5, 125.0, 50.9, 46.7, 37.6, 29.5, 20.1, 13.9; HRMS–EI (m/z) [M]<sup>+</sup> calcd for C<sub>13</sub>H<sub>17</sub>NO, 203.1310; found: 203.1311.



**1-(Phenylmethyl)-2-piperidinone (3da):** Orange liquid (53 mg, 56%). <sup>1</sup>H NMR (499 MHz, CDCl<sub>3</sub>) δ = 7.33-7.23 (m, 5H), 4.55 (s, 2H), 3.18 (t, *J*=5.9 Hz, 2H); 2.46 (t, *J*=6.4 Hz 2H), 1.77(m, 4H). The spectral data were consistent with those reported in the literature.<sup>22</sup>

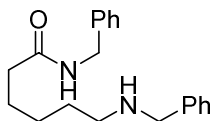


**1-[(4-Chlorophenyl)methyl]-2-piperidinone (3dd):** Brown liquid (54 mg, 48%). IR (neat): 1630, 1492, 1465, 1447, 1409, 1284, 1252, 1175, 1089, 1015, 829, 800, 655  $\text{cm}^{-1}$ ;  $^1\text{H}$  NMR (499 MHz,  $\text{CDCl}_3$ )  $\delta$  = 7.29 (d,  $J=8.3$  Hz, 2H), 7.19 (d,  $J=8.3$  Hz, 2H), 4.59 (s, 2H), 3.19 (t,  $J=5.4$  Hz, 2H), 2.45 (t,  $J=6.1$  Hz, 2H), 1.77 (m, 4H);  $^{13}\text{C}$  NMR (126 MHz,  $\text{CDCl}_3$ )  $\delta$  = 169.8, 135.7, 129.6, 128.9, 128.1, 49.3, 47.2, 32.2, 23.0, 21.2; HRMS–FAB ( $m/z$ )  $[\text{M}+\text{H}]^+$  calcd for  $\text{C}_{12}\text{H}_{15}\text{ClNO}$ , 224.0842; found: 224.0843.



**1-[3-phenylpropyl]-2-piperidinone (3dh):** Yellow liquid (54 mg, 49%). IR (neat): 2942, 1635, 1494, 1451, 1353, 1171, 731, 699  $\text{cm}^{-1}$ ;  $^1\text{H}$  NMR (499 MHz,  $\text{CDCl}_3$ )  $\delta$  = 7.31-7.26 (m, 2H), 7.23-7.17 (m, 3H), 3.43 (t,  $J=7.3$  Hz, 2H), 3.24 (t,  $J=5.9$  Hz, 2H), 2.64 (t,  $J=7.8$  Hz, 2H), 2.36 (t,  $J=5.8$  Hz, 2H), 1.89 (q,  $J=7.8$  Hz, 2H), 1.76 (q,  $J=3.0$  Hz, 4H);  $^{13}\text{C}$  NMR (75 MHz,  $\text{CDCl}_3$ )  $\delta$  = 169.5, 141.6, 128.2, 128.2, 125.7, 47.7, 46.8, 33.1, 32.2, 28.4, 23.1, 21.2; HRMS–EI ( $m/z$ )  $[\text{M}]^+$  calcd for  $\text{C}_{14}\text{H}_{19}\text{NO}$ , 217.1467; found: 217.1469





**N-(Phenylmethyl)-6-[(phenylmethyl)amino]-hexanamide (6ea):** Yellowish solid (137 mg, 88%). IR (neat): 1632, 1548, 1452, 727, 693  $\text{cm}^{-1}$ ;  $^1\text{H}$  NMR (300MHz,  $\text{CDCl}_3$ )  $\delta$  = 7.38 - 7.21 (m, 10H), 6.05 (br. s., amide proton, 1H), 4.41 (d,  $J$  = 5.7 Hz, 2H), 3.79 (s, 2H), 3.22 (br. s., amine proton, 1H), 2.64 (t,  $J$  = 7.2 Hz, 2H), 2.20 (s,  $J$  = 7.5 Hz, 2H), 1.66 (quin,  $J$  = 7.5 Hz, 2H), 1.57 (quin,  $J$  = 7.2 Hz, 2H), 1.36 (quin,  $J$  = 7.9 Hz, 2H);  $^{13}\text{C}$  NMR (75 MHz,  $\text{CDCl}_3$ )  $\delta$  = 172.8, 138.8, 138.4, 128.6, 128.4, 128.4, 127.8, 127.4, 127.2, 53.5, 48.6, 43.5, 36.4, 28.9, 26.7, 25.3; HRMS–EI ( $m/z$ )  $[\text{M}]^+$  calcd for  $\text{C}_{20}\text{H}_{26}\text{N}_2\text{O}$ , 310.2045; found: 310.2043.

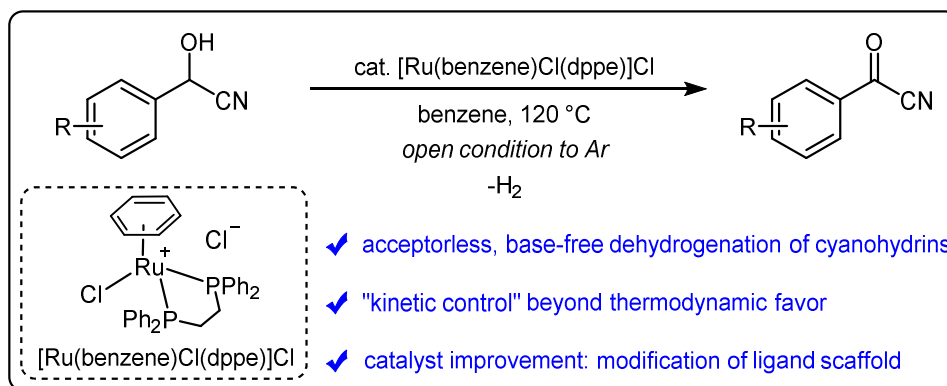
## 2.5 References

- (1) (a) A. S. Touchy, S. M. A. Hakim Siddiki, K. Kon, K.-i. Shimizu, *ACS Catalysis* **2014**, *4*, 3045. (b) M. A. Ogliaruso, J. F. Wolfe, *Synthesis of lactones and lactams* Wiley, Chichester New York, **1993**. (c) M. B. Smith, *Science of Synthesis* **2005**, *21*, 647.
- (2) (a) A. H. Abadi, S. Lankow, B. Hoefgen, M. Decker, M. U. Kassack, J. Lehmann, *Arch. Pharm.* **2002**, *335*, 367. (b) Y. Nishimura, H. Adachi, T. Satoh, E. Shitara, H. Nakamura, F. Kojima, T. Takeuchi, *J. Org. Chem.* **2000**, *65*, 4871. (c) T. Witt, F. J. Hock, J. Lehmann, *J. Med. Chem.* **2000**, *43*, 2079. (d) E. J. Neafsey, R. Albores, D. Gearhart, G. Kindel, K. Raikoff, F. Tamayo, M. A. Collins, *Brain Res.* **1995**, *675*, 279. (e) W. Dürckheimer, J. Blumbach, R. Lattrell, K. H. Scheunemann, *Angew. Chem. Int. Ed.* **1985**, *24*, 180.
- (3) (a) M. Bencini, E. Ranucci, P. Ferruti, A. Manfredi, *Macromol. Rapid Commun.* **2006**, *27*, 1060. (b) K. Dachs, E. Schwartz, *Angew. Chem. Int. Ed.* **1962**, *1*, 430.
- (4) R. H. Earle, D. T. Hurst, M. Viney, *J. Chem. Soc. (C)* **1969**, 2093.
- (5) P. G. Gassman, T. J. Van Bergen, *J. Am. Chem. Soc.* **1973**, *95*, 2718.
- (6) (a) T. Okawara, K. Harada, *J. Org. Chem.* **1972**, *37*, 3286. (b) B. G. Chatterjee, V. Venkateswara Rao, *Tetrahedron* **1967**, *23*, 487.
- (7) (a) M. Decker, T. T. H. Nguyen, J. Lehmann, *Tetrahedron* **2004**, *60*, 4567. (b) F. B. Zienty, G. W. Steahly, *J. Am. Chem. Soc.* **1947**, *69*, 715. (c) E. Späth, J. Lintner, *Berichte der deutschen chemischen Gesellschaft (A and B Series)* **1936**, *69*, 2727.
- (8) K. M. Orrling, X. Wu, F. Russo, M. Larhed, *J. Org. Chem.* **2008**, *73*, 8627.
- (9) N. H. Kawahata, J. Brookes, G. M. Makara, *Tetrahedron Lett.* **2002**, *43*, 7221.
- (10) (a) B. P. Babu, Y. Endo, J.-E. Bäckvall, *Chem. Eur. J.* **2012**, *18*, 11524. (b) J.

- Zhang, S. H. Hong, *Org. Lett.* **2012**, *14*, 4646. (c) K.-i. Fujita, Y. Takahashi, M. Owaki, K. Yamamoto, R. Yamaguchi, *Org. Lett.* **2004**, *6*, 2785.
- (11) (a) P. Fristrup, M. Tursky, R. Madsen, *Org. Biomol. Chem.* **2012**, *10*, 2569. (b) O. Saidi, A. J. Blacker, M. M. Farah, S. P. Marsden, J. M. J. Williams, *Chem. Commun.* **2010**, *46*, 1541. (c) O. Saidi, A. J. Blacker, G. W. Lamb, S. P. Marsden, J. E. Taylor, J. M. J. Williams, *Org. Process Res. Dev.* **2010**, *14*, 1046. (d) K.-i. Fujita, Y. Enoki, R. Yamaguchi, *Tetrahedron* **2008**, *64*, 1943. (e) K.-i. Fujita, R. Yamaguchi, *Synlett* **2005**, *2005*, 560. (f) K.-i. Fujita, T. Fujii, R. Yamaguchi, *Org. Lett.* **2004**, *6*, 3525. (g) K.-i. Fujita, Z. Li, N. Ozeki, R. Yamaguchi, *Tetrahedron Lett.* **2003**, *44*, 2687. (h) K.-i. Fujita, K. Yamamoto, R. Yamaguchi, *Org. Lett.* **2002**, *4*, 2691.
- (12) J. Lee, S. Muthaiah, S. H. Hong, *Adv. Synth. Catal.* **2014**, *356*, 2653.
- (13) (a) M. H. S. A. Hamid, J. M. J. Williams, *Chem. Commun.* **2007**, 725. (b) S. E. Eldred, D. A. Stone, S. H. Gellman, S. S. Stahl, *J. Am. Chem. Soc.* **2003**, *125*, 3422.
- (14) K. Müller, C. Faeh, F. Diederich, *Science* **2007**, *317*, 1881.
- (15) F. M. Awadallah, F. Müller, J. Lehmann, A. H. Abadi, *Bioorg. Med. Chem.* **2007**, *15*, 5811.
- (16) L. L. R. Lorentz-Petersen, P. Jensen, R. Madsen, *Synthesis* **2009**, *2009*, 4110.
- (17) (a) U. Jana, S. Maiti, S. Biswas, *Tetrahedron Lett.* **2008**, *49*, 858. (b) Uuml, Jingping, Y. Ishimura, N. Nagato, *Nippon Kagaku Kaishi* **1996**, *1996*, 525. (c) J. Qu, Y. Ishimura, N. Nagato, *Nippon Kagaku Kaishi* **1996**, *1996*, 256. (d) Y. Watanabe, T. Ohta, Y. Tsuji, *Bull. Chem. Soc. Jpn.* **1983**, *56*, 2647.
- (18) D. Balcells, A. Nova, E. Clot, D. Gnanamgari, R. H. Crabtree, O. Eisenstein, *Organometallics* **2008**, *27*, 2529.
- (19) C. Gunanathan, Y. Ben-David, D. Milstein, *Science* **2007**, *317*, 790.

- (20) B. Gnanaprakasam, J. Zhang, D. Milstein, *Angew. Chem. Int. Ed.* **2010**, *49*, 1468.
- (21) T. Higuchi, R. Tagawa, A. Iimuro, S. Akiyama, H. Nagae, K. Mashima, *Chem. Eur. J.* **2017**, *23*, 12795.
- (22) A. Nova, D. Balcells, N. D. Schley, G. E. Dobereiner, R. H. Crabtree, O. Eisenstein, *Organometallics* **2010**, *29*, 6548.
- (23) X. Xie, H. V. Huynh, *ACS Catal.* **2015**, *5*, 4143.
- (24) O. V. Starikova, G. V. Dolgushin, L. I. Larina, P. E. Ushakov, T. N. Komarova, V. A. Lopyrev, *Russ. J. Org. Chem.* **2003**, *39*, 1467.
- (25) J. Mun, M. B. Smith, *Synth. Commun.* **2007**, *37*, 813.
- (26) J. A. Weitgenant, I. Katsuyama, M. A. Bigi, S. J. Corden, J. T. Markiewicz, A. P. R. Zabell, K. T. Homan, O. Wiest, C. V. Stauffacher, P. Helquist, *Heterocycles* **2006**, *70*, 599.
- (27) Y. T. Oh, K. Senda, T. Hata, H. Urabe, *Tetrahedron Lett.* **2011**, *52*, 2458.
- (28) B. Fanté, Y. Soro, S. Siaka, J. Marrot, J.-M. Coustard, *Synth. Commun.* **2014**, *44*, 2377.
- (29) Y. Nakao, H. Idei, K. S. Kanyiva, T. Hiyama, *J. Am. Chem. Soc.* **2009**, *131*, 5070.
- (30) C. Bouaudeau, A. Parlier, H. Rudler, *J. Org. Chem.* **1997**, *62*, 7247.

### Chapter 3. Acceptorless and Base-free Dehydrogenation of Cyanohydrin with ( $\eta^6$ -arene)halide(bidentate phosphine)ruthenium(II) Complex\*

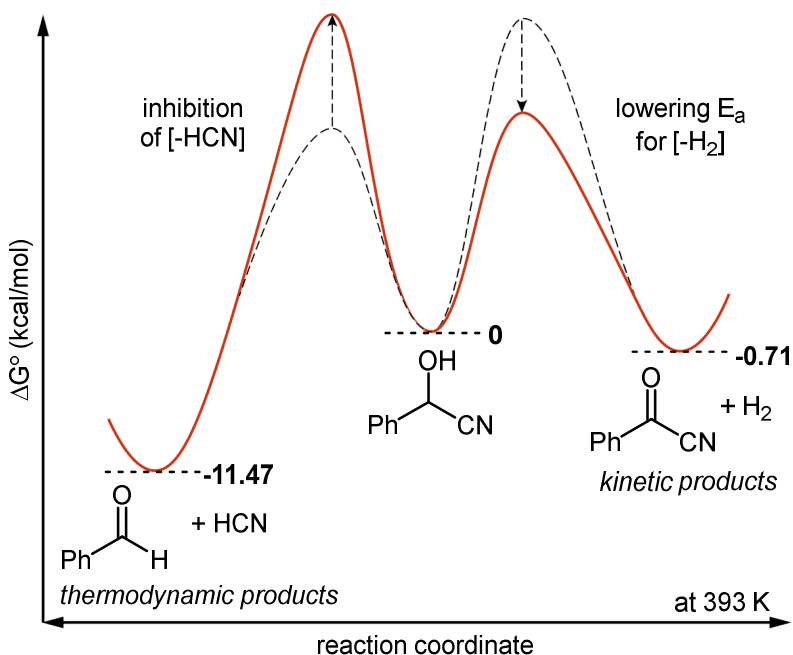


\* The majority of this work has been published: Kicheol Kim, Adhitya Mangala Putra Moeljadi, Hajime Hirao,\* and Soon Hyeok Hong\*, *Adv. Synth. Catal.* **2017**, 359, 3292–3298.

### 3.1 Introduction

Acyl cyanides are among the most versatile building blocks especially in regard to heterocycle synthesis.<sup>1</sup> The enhanced electrophilicity of the carbonyl carbon in acyl cyanides allows for various transformations with nucleophiles. Representative synthetic methods for acyl cyanides include cyanation of acyl halides with cyanide sources,<sup>2</sup> catalytic cyanocarbonylation of aryl iodides,<sup>3</sup> and dehydrogenation of cyanohydrin.<sup>4</sup> Compared to the former two methods which require prefunctionalized substrates and toxic reagents such as metal cyanide and/or carbon monoxide, the dehydrogenation of cyanohydrins is straightforward because easily accessible cyanohydrins can be used. However, to the best of our knowledge, stoichiometric oxidants are inevitably utilized in all reported methods for the dehydrogenation of cyanohydrins including a mild catalytic method developed by the Murahashi group.<sup>4a,b</sup>

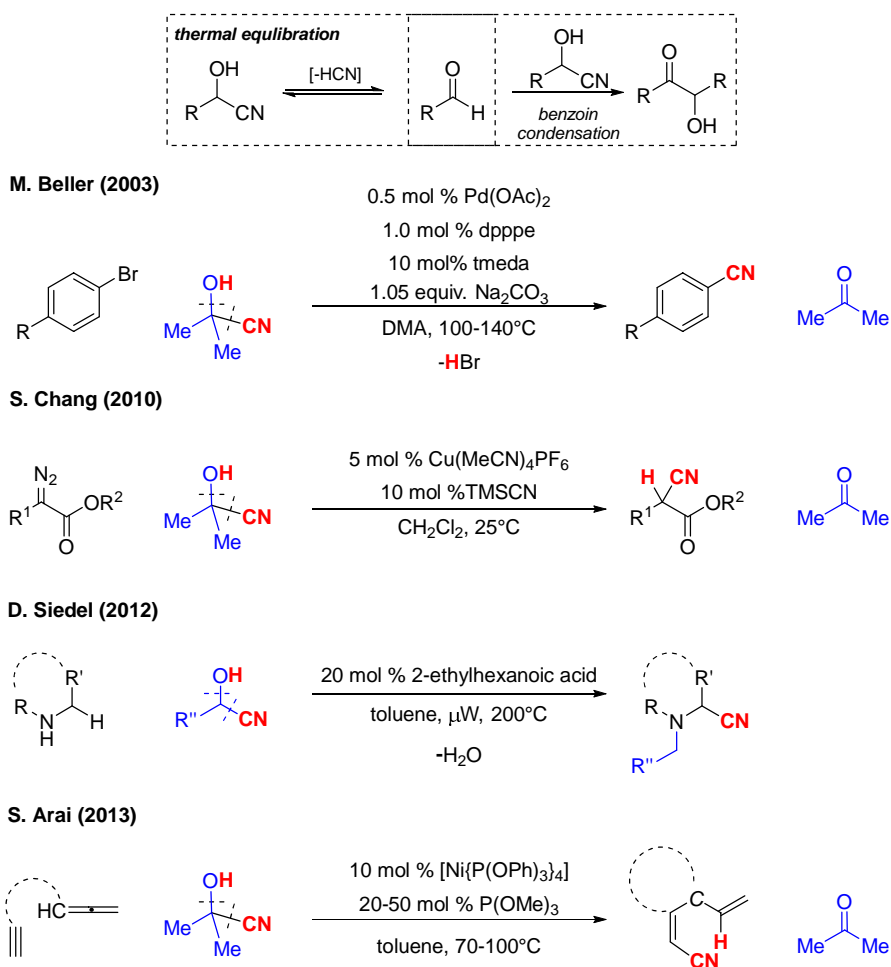
The oxidation of alcohols to carbonyl-containing compounds is a fundamental transformation in organic chemistry. Conventional methods for this oxidation reaction require (over)stoichiometric amounts of oxidants such as toxic Cr(VI),<sup>5</sup> Mn salts,<sup>6</sup> oxalic chloride with DMSO,<sup>7</sup> hypervalent iodine,<sup>8</sup> H<sub>2</sub>O<sub>2</sub>,<sup>9</sup> and O<sub>2</sub> with transition metal catalysts.<sup>10</sup> The use of such oxidants has major disadvantages in terms of cost, atom economy, and environmental aspects. Acceptorless alcohol dehydrogenation (AAD) producing hydrogen as the sole byproduct has been highlighted as an alternative approach.<sup>11</sup> However, most conditions for AAD require the use of a base to activate the precatalyst or alcohol.<sup>12</sup> This drawback restricts the utility because the base can corrode industrial facilities and disrupt stereoselectivity, especially with base-sensitive carbonyl compounds.<sup>13</sup>



**Scheme 3.1** Thermodynamic consideration of the dehydrogenation of mandelonitrile

For the synthesis of acyl cyanide from cyanohydrins under base-free conditions, the most challenging issue in AAD reactions is the thermodynamic preference towards aldehydes via elimination of hydrogen cyanide. DFT calculations have revealed that the elimination of hydrogen cyanide is thermodynamically more favored ( $\Delta G^\circ = -8.32$  kcal/mol at 298 K;  $-11.47$  kcal/mol at 393 K) than dehydrogenation ( $\Delta G^\circ = 1.85$  kcal/mol at 298 K;  $-0.71$  kcal/mol at 393 K), in the reaction of mandelonitrile in benzene (Scheme 3.1). In this context, cyanohydrins have been exploited as a HCN source in (hydro)cyanation reactions (Scheme 3.2).<sup>14</sup> In 2003, the Beller group reported Pd-catalyzed cyanation of aryl halides using acetone cyanohydrin as a cyanide source without deactivation of Pd catalyst by slow dosage of the cyanohydrin.<sup>14e</sup> In 2010, the Chang group reported Cu-catalyzed hydrocyanation of  $\alpha$ -aryl diazoesters using acetone cyanohydrin as a source of

HCN.<sup>14d</sup> In 2012, the Siedel group reported a redox-neutral transformation of amines via reductive *N*-alkylation and an oxidative  $\alpha$ -cyanation with cyanohydrins as source of corresponding aldehydes and cyanides.<sup>14c</sup> In 2013, the Arai group demonstrated Ni-catalyzed hydrocyanative cyclization and three-component cross-coupling reaction with allenes and alkynes using acetone cyanohydrin as a source of HCN.<sup>14b</sup> Benzoin condensation could also occur in the presence of in situ generated aldehydes and HCN from cyanohydrins.<sup>15</sup>



**Scheme 3.2** Thermal equilibration of cyanohydrins to aldehydes and benzoin condensation



To promote the targeted dehydrogenation of cyanohydrin instead of the elimination of hydrogen cyanide, kinetic control at higher temperatures induced by a catalyst is essential. Herein, we report acceptorless and base-free catalytic systems for the dehydrogenation of cyanohydrins with ruthenium-bidentate phosphine complexes, based on previous studies on AAD in the oxidative transformation of alcohols.<sup>16,17</sup> Electronic properties of the ruthenium complexes were modified to promote the dehydrogenation rather than the thermodynamically favored elimination of hydrogen cyanide.

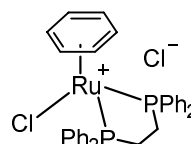
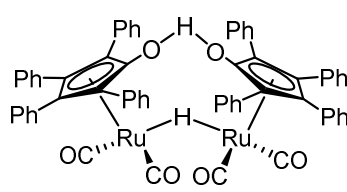
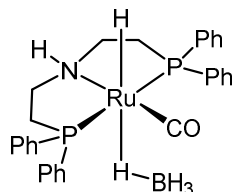
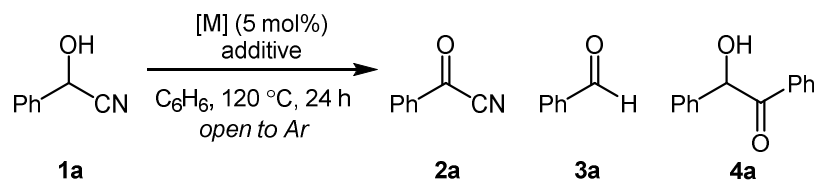
## 3.2 Results and discussion

### 3.2.1 Optimization for dehydrogenation of cyanohydrins

In order to identify an efficient catalytic system, the dehydrogenation of mandelonitrile **1a** was carried out using previously reported conditions for AAD and hydrogen transfer reactions between carbonyls and alcohols (Table 3.1). The reactions were refluxed at 120 °C, because the desired dehydrogenation of cyanohydrin is thermodynamically allowed ( $\Delta G^\circ = -0.71$  kcal/mol) at this temperature. An open system to argon atmosphere was used to drive the desired dehydrogenation entropically by release of dihydrogen.<sup>18</sup> An NHC-Ru(II)-based catalytic system for amide formation with nitriles and alcohols via hydrogen transfer only afforded benzoin adduct **4a** (entry 1).<sup>17</sup> Because bases promote the formation of aldehydes from cyanohydrins in benzoin condensations, the use of a base should be avoided to obviate this undesired reaction. A previously developed Fe(III)-based catalyst for dehydrogenations gave the aldehyde as the major product, and produced the desired acyl cyanide in a poor yield (10%, entry 2).<sup>19</sup> These results indicated that the appropriate catalyst might be able to induce kinetic control of the reaction despite the poor yields obtained in the initial studies.  $[\text{RuCl}_2(\text{PPh}_3)]$  and  $[\text{Ru-MACHO}^{\text{TM}}\text{-BH}]$  catalysts for methanol dehydrogenation were not selective towards **2a**, affording **3a** in quantitative yields (entries 3 and 7).<sup>20</sup> Several complexes known to be active in the base-free dehydrogenation of alcohols exhibited exclusive selectivity towards aldehyde **3a** (entries 4–6).<sup>16e</sup> Ru-based catalytic systems known for their metal-ligand bifunctionality also showed poor reactivity in the dehydrogenation (entries 7–9).<sup>21</sup> Inspired by a ruthenium/phosphine catalytic system for hydrogen transfers,<sup>22</sup> monophosphine and bidentate P-based or N-based ligands were screened with  $[\text{Ru}(\text{p-}$

cymene)Cl<sub>2</sub>]<sub>2</sub> and [Ru(benzene)Cl<sub>2</sub>]<sub>2</sub> complexes (entries 10–16). Excellent reactivities were observed from [Ru(benzene)Cl<sub>2</sub>]<sub>2</sub> and bidentate phosphine ligands (entries 13–16). In the control of temperature, 120 °C is optimal in accordance with our thermodynamic hypothesis for reflux condition (entries 17-19). Reaction under higher temperature (130 °C) gave a sudden evaporation of solution due to the open condition. Unfortunately, the results from the in situ catalytic systems were not reproducible. In situ generation of an active catalyst from a catalyst precursor and ligand could limit the precise control over the nature of the catalyst.<sup>23</sup> To our delight, the well-defined complex, [Ru(benzene)Cl(dppe)]Cl, **5A** showed excellent, consistent activity and selectivity in the dehydrogenation (entry 20). The presence of a ruthenium complex and dppe ligand was essential for high efficiency and selectivity (entries 21–23).

**Table 3.1** Optimization of reaction conditions<sup>a</sup>



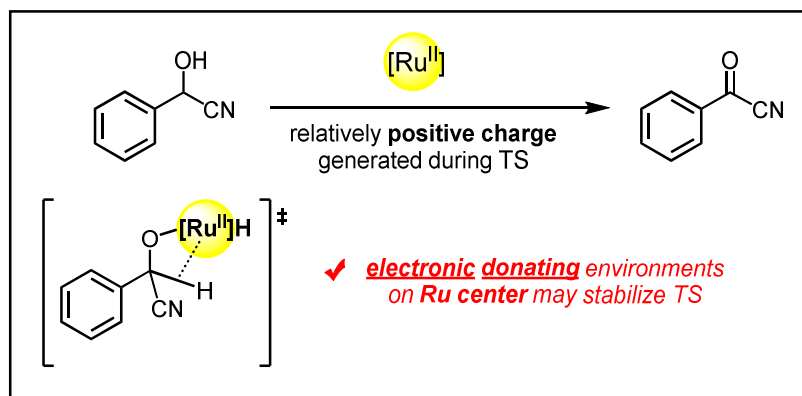
entry	[M]	Additive [mol%]	Conv [%]	2a [%]	3a/4a [%]
1	[RuH <sub>2</sub> (PPh <sub>3</sub> ) <sub>4</sub> ]	NHC <sup>[b]</sup> (5) / NaH (20)	100	0	0/60
2	[Fe(acac) <sub>3</sub> ]	1,10-phenanthroline (5) / K <sub>2</sub> CO <sub>3</sub> (5)	100	10	90/0
3	[RuCl <sub>2</sub> (PPh <sub>3</sub> ) <sub>3</sub> ]	-	100	0	100/0
4	RuH <sub>2</sub> CO(PPh <sub>3</sub> ) <sub>3</sub>	-	100	0	100/0
5	RuHClCO(PPh <sub>3</sub> ) <sub>3</sub>	-	100	0	100/0
6	Ru <sub>3</sub> (CO) <sub>12</sub>	-	78	0	78/0
7	Ru-MACHO™-BH	-	100	0	100/0
8	Shvo's catalyst	-	28	28	0/0
9	RuCl <sub>2</sub> (Ph <sub>2</sub> PCH <sub>2</sub> CH <sub>2</sub> NH <sub>2</sub> ) <sub>2</sub>	-	50	0	50/0
10	[Ru(p-cymene)Cl <sub>2</sub> ] <sub>2</sub>	tri(p-tolyl)phosphine (5)	89	28	61/0
11	[Ru(p-cymene)Cl <sub>2</sub> ] <sub>2</sub>	dppe (5)	65	0	65/0
12	[Ru(p-cymene)Cl <sub>2</sub> ] <sub>2</sub>	1,10-phenanthroline (5)	18	0	18/0
13	[Ru(benzene)Cl <sub>2</sub> ] <sub>2</sub>	dppe (5)	100	100	0/0
14	[Ru(benzene)Cl <sub>2</sub> ] <sub>2</sub>	dppm (5)	7	0	7/0
15	[Ru(benzene)Cl <sub>2</sub> ] <sub>2</sub>	dppb (5)	97	92	5/0
16	[Ru(benzene)Cl <sub>2</sub> ] <sub>2</sub>	dcpe (5)	100	97	3/0
17	[Ru(benzene)Cl <sub>2</sub> ] <sub>2</sub>	dppe (5)	21	0	21/0

18	[Ru(benzene)Cl <sub>2</sub> ] <sub>2</sub>	dppe (5)	90	46	44/0
19	[Ru(benzene)Cl <sub>2</sub> ] <sub>2</sub>	dppe (5)	100	45	55/0
20	<b>5A</b>	-	100	95	5/0
21	-	-	11	0	11/0
22	-	dppe (5)	26	0	26/0
23	[Ru(benzene)Cl <sub>2</sub> ] <sub>2</sub>	-	89	0	89/0

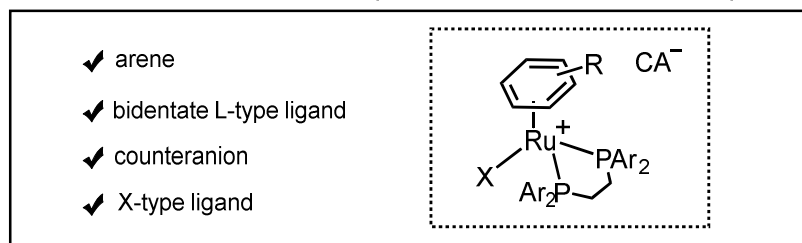
[a] Conditions: **1a** (0.25 mmol, 1 equiv.), [M] (5 mol%), benzene (1.25 mL), 120 °C, and 24 h under open conditions with an argon atmosphere. Average yield of two runs and determined by <sup>1</sup>H NMR using dibromethane as the internal standard. [b]NHC = 1,3-diisopropylimidazolium bromide. [c] Room temperature. [d] 90 °C. [e] 110 °C. p-cymene = 1-isopropyl-4-methylbenzene. dppe = 1,2-bis(diphenylphosphino)ethane. dppm = bis(diphenylphosphino)methane. dppb = 1,4-bis(diphenylphosphino)butane. dcpe = 1,2-bis(dicyclohexylphosphino)butane.

### 3.2.2 The effects of the nature of the catalyst on the selective dehydrogenation

#### ■ plausible pathway for dehydrogenation: $\beta$ -H elimination



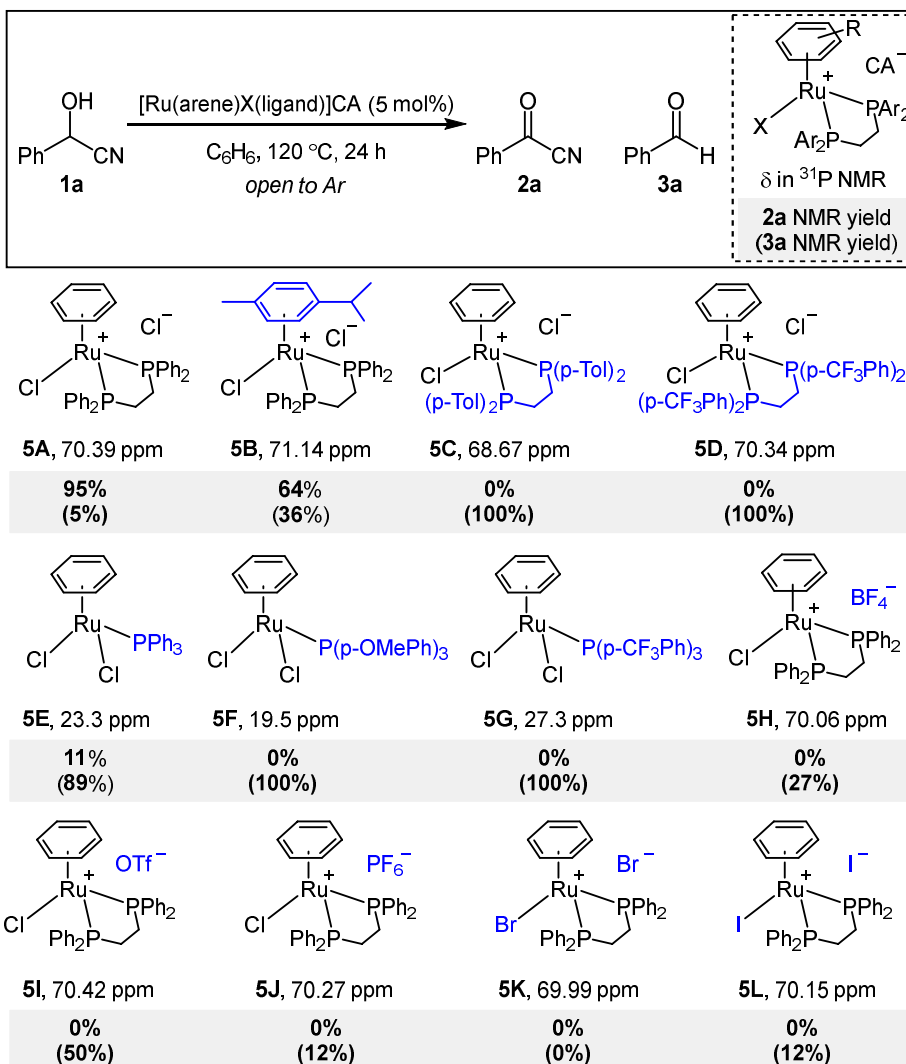
#### ■ 4 significant factors in Ru catalyst: electronic effect on reactivity



**Scheme 3.3** Plausible elementary reaction step for dehydrogenation

To understand the effects of the nature of the catalyst on the selective dehydrogenation, several Ru complexes were synthesized and tested.  $\beta$ -H elimination, the general rate-limiting step in the catalytic dehydrogenation of alcohols, can be facilitated by an electron-rich metal center (Scheme 3.3).<sup>24</sup> Therefore, the selectivity was likely controlled by the electronic environment around the metal center.<sup>25</sup> In complex **5A**, the  $\eta^6$ -arene,  $\eta^2$ -bidentate phosphine ligand, counteranion, and X-type ligands can be modified to control the electronic property of the metal center (Scheme 3.4). The Ru complex with p-cymene ligand **5B** exhibited diminished selectivity in the reaction, affording **2a** in 64% yield.  $\eta^2$ -

Bidentate phosphine ligands except dppe produced aldehyde **3a** exclusively (**5C** and **5D**). To investigate the role of bidentate ligands on the catalytic activity, [Ru(benzene)Cl<sub>2</sub>(phosphine)] complexes were compared (**5E–5G**). Notably, [Ru(benzene)Cl<sub>2</sub>(phosphine)] complexes with electron-donating ligands exhibited higher catalytic activities and lower stabilities in the transfer hydrogenation of acetophenone with isopropanol.<sup>22c</sup> **5E** produced acyl cyanide **2a** in a poor yield (11%). In addition, other counteranions such as tetrafluoroborate (**5H**), trifluoromethanesulfonate (**5I**), and hexafluorophosphate (**5J**), and X-type ligands including bromide (**5K**) and iodide (**5L**) resulted in poor selectivity. Although it is difficult to directly correlate specific catalyst properties and selectivity towards dehydrogenation, the kinetic selectivity was indeed affected by the nature of the catalyst.

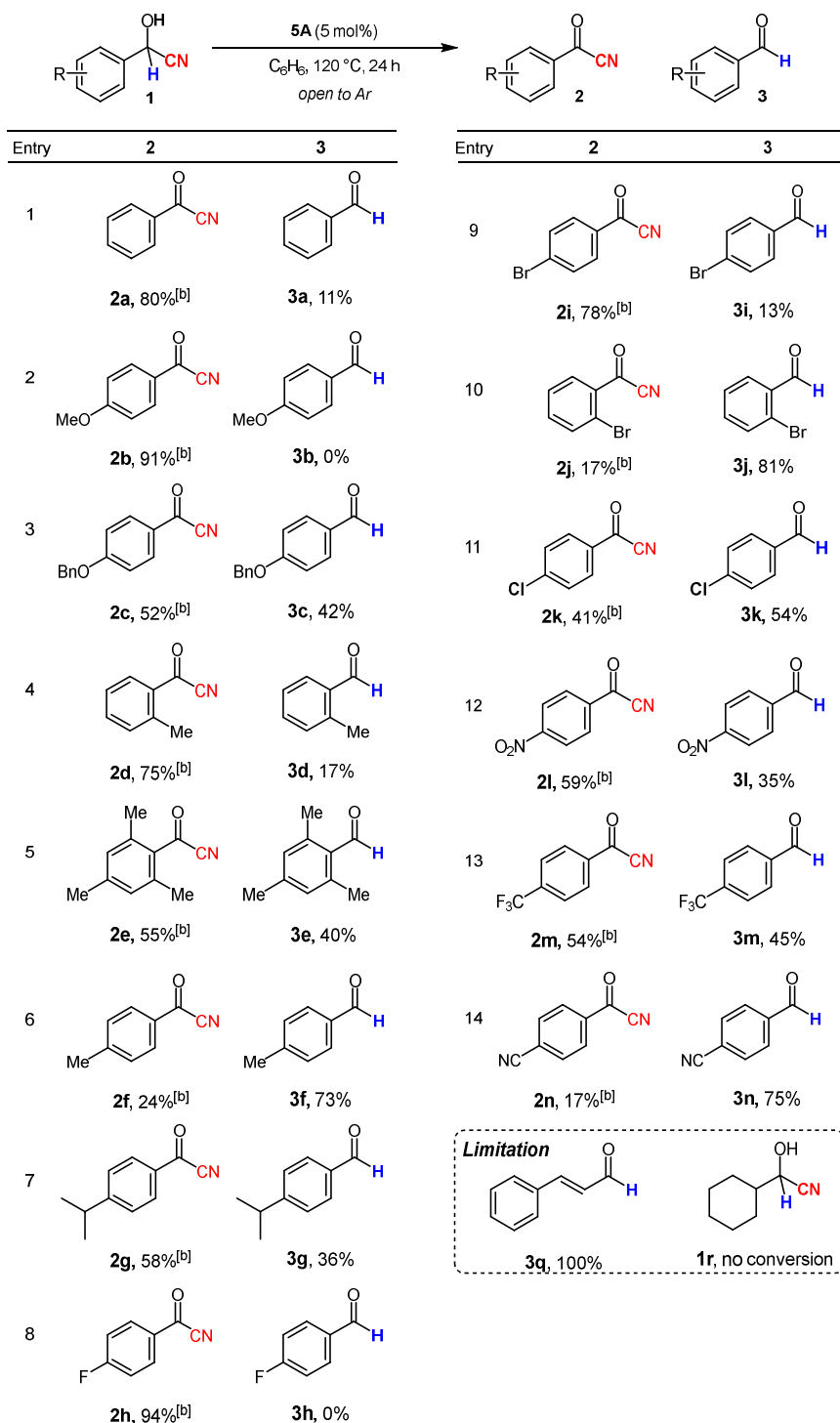


**Scheme 3.4** Reactions of **1a** with modified [Ru(arene)X(ligand)]CA complexes. CA = counteranion. p-Tol = p-tolyl



### 3.2.3 Substrate scope

The scope and limitations of the dehydrogenation were investigated with complex **5A** (Scheme 3.5). Most cyanohydrins were completely converted into their corresponding acyl cyanides and/or aldehydes. The selectivity between dehydrogenation and elimination of hydrogen cyanide also depended on the substrates. As the crude products are too susceptible to hydrolysis during silica column chromatography,<sup>4b</sup> they were isolated as the corresponding carboxylic acids after hydrolysis in a mixture of water and ethyl acetate.<sup>26</sup> In the reactions with benzyl cyanohydrins, various functional groups including ether (MeO-, **2b** and BnO-, **2c**), alkyl (Me-, **2d–2f** and iPr-, **2g**), fluoro (**2h**), bromo (**2i**, **2j**), chloro (**2k**), nitro (**2l**), trifluoromethyl (**2m**), and cyano (**2n**) group afforded the corresponding acyl cyanides. However, benzyl cyanohydrins bearing dimethylamino groups (**3o**), naphthyl cyanohydrins (**3p**), and  $\alpha,\beta$ -unsaturated cyanohydrins (**3q**) only produced the corresponding aldehydes. The reaction with 2-cyclohexyl-2-hydroxyacetonitrile (**1r**) did not proceed.

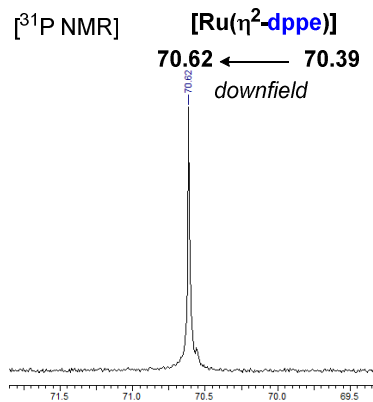
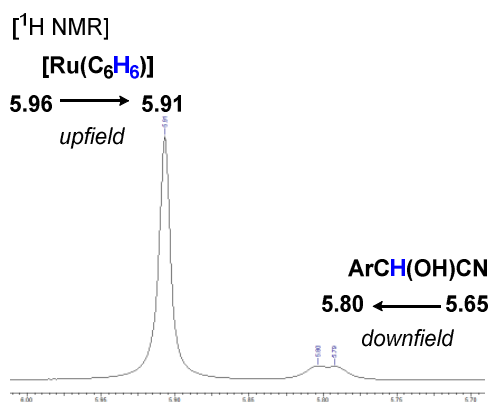
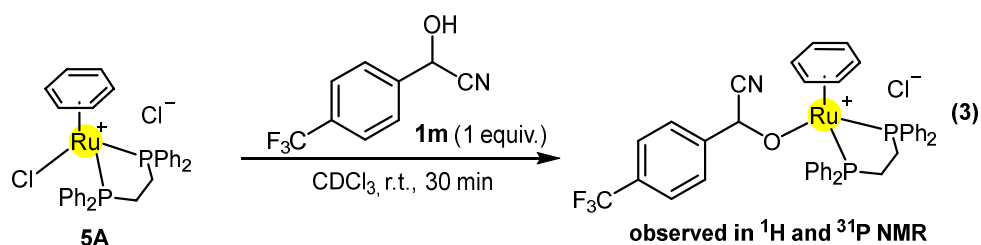
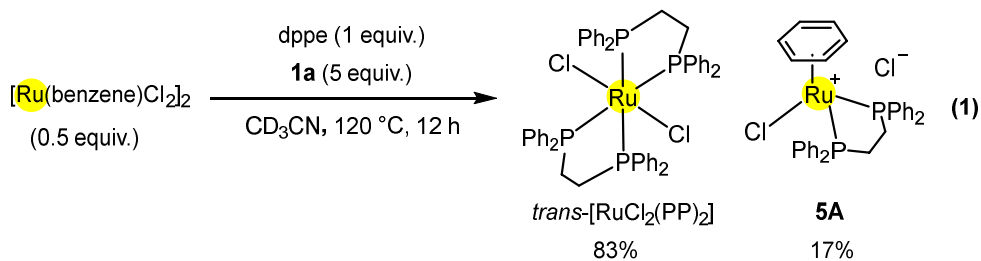


**Scheme 3.5** Dehydrogenation of cyanohydrins. <sup>[a]</sup> Reaction conditions: **1** (0.25 mmol, 1 equiv.), **5A** (5 mol%), benzene (1.25 mL), 120 °C, and 24 h under open to argon atmosphere. Isolated yields. <sup>[b]</sup> Isolated yields of the corresponding carboxylic acid.

### 3.2.4 Mechanistic studies

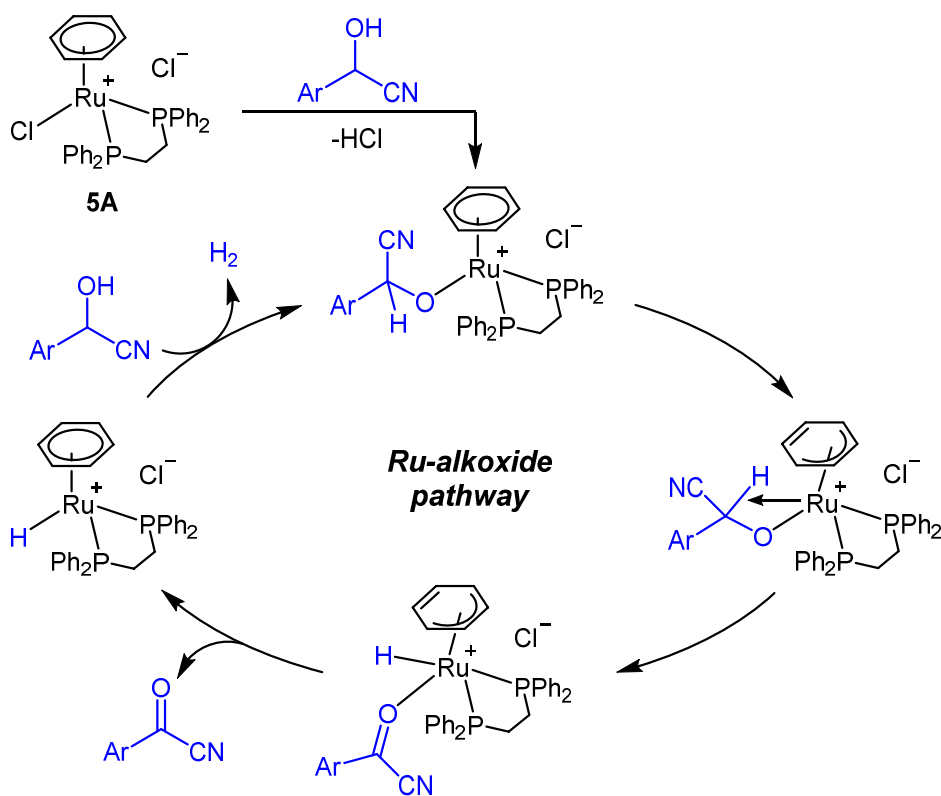
In order to further investigate the subtle reaction selectivity, mechanism, and active catalytic intermediates, the reaction of  $[\text{Ru}(\text{benzene})\text{Cl}_2]_2$  with dppe and **1a** was conducted in  $\text{CD}_3\text{CN}$  ([Eq. 1], Scheme 3.6). In the  $^{31}\text{P}$  NMR spectrum, *trans*- $[\text{RuCl}_2(\text{dppe})_2]$  was detected as the major product along with catalytically active **5A** as a minor product (ratio = 4.9:1). The major product, *trans*- $[\text{RuCl}_2(\text{dppe})_2]$ , could be generated via arene dissociation from  $[\text{Ru}(\text{benzene})\text{Cl}_2]_2$ .<sup>27</sup> *Trans*- $[\text{RuCl}_2(\text{dppe})_2]$  was independently prepared and subjected to the reaction with **1a**. However, it was catalytically inactive with no conversion of **1a** ([Eq. 2], Scheme 3.6). The observed irreproducibility of the in-situ catalytic system (Table 3.1) was likely due to the formation of catalytically inactive *trans*- $[\text{RuCl}_2(\text{dppe})_2]$  rather than **5A**. Notably, the addition of cyanohydrin to **5A** (Scheme 3.5), which is hardly soluble in benzene, prompted the sudden solubilization of **5A**, implying possible coordination of the cyanohydrin to the Ru center. Next, stoichiometric amounts of **5A** and **1m** were reacted to investigate the possible binding mode of the cyanohydrin ([Eq. 3], Scheme 3.6). Yi and co-workers reported that exchange of the  $\eta^6$ -arene ligand with a benzamide substrate in cationic  $[(\eta^6\text{-arene})\text{Ru}]$  complexes was important for the activation of the substrate.<sup>28</sup> However, in this case, only a halide exchange, resulting in the  $[(\text{alkoxide})\text{Ru}]$  complex, was observed without any exchange of the arene ring. In  $^1\text{H}$  NMR, a downfield chemical shift of the  $\alpha$ -hydrogen in the cyanohydrin and an upfield shift of the hydrogens in  $\eta^6$ -benzene were observed. The down field shift of the  $\alpha$ -hydrogen in cyanohydrin indicated the decreased electron density via coordination to the ruthenium center. Regarding the binding of  $\eta^6$ -arenes to transition metals, upfield chemical shifts of the hydrogens of the  $\eta^6$ -benzene ligand in  $^1\text{H}$  NMR

are known to be induced from a more electron-poor metal center via enhanced  $\pi$ -donation.<sup>29</sup> In the case of the observed intermediate, the decreased electron density around the metal center might be induced by a weaker electron donor, as alkoxide ligand have a low trans effect.<sup>30</sup> Similarly, a downfield chemical shift of the dppe ligand was observed in <sup>31</sup>P NMR. These changes in chemical shifts indicate coordination of the deprotonated cyanohydrin as an alkoxide upon displacement of the chloride ligand. No free benzene from the  $[(\eta^6\text{-benzene})\text{Ru}]$  complex was observed, confirming the lack of exchange of the  $\eta^6$ -arene ligand.



**Scheme 3.6** Mechanistic investigation

On the basis of the experimental results, a plausible reaction mechanism that involves the previously proposed Ru-alkoxide pathway<sup>11b</sup> instead of arene-exchange is proposed (Scheme 3.7). Ligand exchange between chloride and cyanohydrin moieties produces a Ru-alkoxide species. Subsequently, the Ru-alkoxide complex undergoes  $\beta$ -hydride elimination with ring-slippage of the  $\eta^6$ -arene to give the desired acyl cyanide and Ru-hydride species.<sup>27b,31</sup> Other alternative pathway for  $\beta$ -hydride elimination is also possible via dissociation of one phosphine donor in the chelating dppe ligand. Dehydrogenation of the ruthenium hydride species with an additional cyanohydrin completes the catalytic cycle.



**Scheme 3.7** Plausible mechanism.

### **3.3 Conclusion**

In summary, the first acceptorless and base-free dehydrogenation of cyanohydrins was demonstrated in the synthesis of acyl cyanides. Subtle electronic modulation of the catalysts promoted the targeted dehydrogenation reactions producing synthetically useful acyl cyanides, over the thermodynamically preferred formation of aldehydes by elimination of hydrogen cyanide.

### 3.4 Experimental section

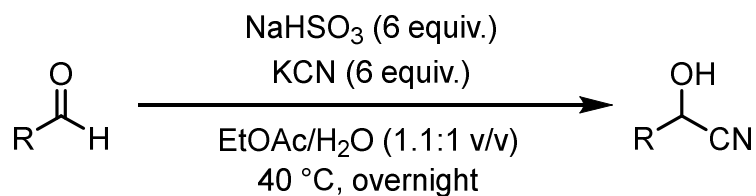
#### 3.4.1 General considerations

Unless otherwise noted, reagents were purchased from commercial suppliers and used as received without further purification: KCN (Alfa) were ground using a mortar. Benzene (anhydrous, Aldrich) was deoxygenated by bubbling argon without further drying. Unless otherwise specified, the reactions were carried out under magnetic stirring in an oven-dried 25 mL Schlenk tube equipped with a rubber septum under an inert argon atmosphere. NMR spectra were recorded in  $\text{CDCl}_3$ ,  $\text{CD}_3\text{OD}$ , dimethyl sulfoxide- $d_6$  and the residual solvent signals were used as the reference. The NMR spectral data were processed using the ACD/NMR Processor Academic Edition and Mnova NMR processor. Chemical shifts are reported in ppm, and coupling constants are reported in Hz. Multiplicity is indicated by one or more of the following: s (singlet), d (doublet), t (triplet), q (quartet), quin (quintet), sep (septet), and m (multiplet).



### 3.4.2 Substrate and catalyst preparation

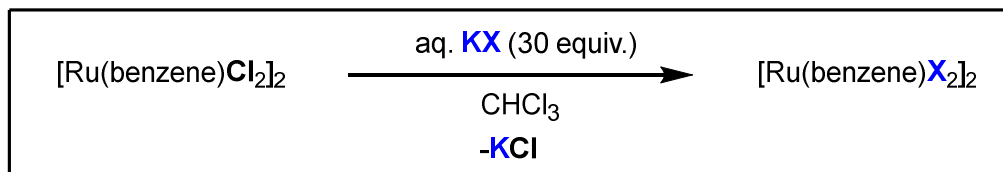
#### 3.4.2.1 Preparation of cyanohydrins



Following the procedure slightly modified from literature method,<sup>32</sup> potassium cyanide (60 mmol, 6 equiv) was added to a stirring mixture of distilled water (15 mL) and EtOAc (17 mL). Once dissolved, sodium bisulfite (NaHSO<sub>3</sub>, 60 mmol, 6 equiv) was added and stirring continued. To this mixture, aldehyde was added (10 mmol, 1 equiv), the flask was then sealed with an outlet and stirred vigorously at 40 °C for 20 h. The reaction was poured into 20 mL distilled water, washed with distilled water (2 x 20 mL), then brine (20 mL). The organic layer was dried over MgSO<sub>4</sub> and concentrated. The residue was purified by column chromatography using a mixture of hexane/ethyl acetate.

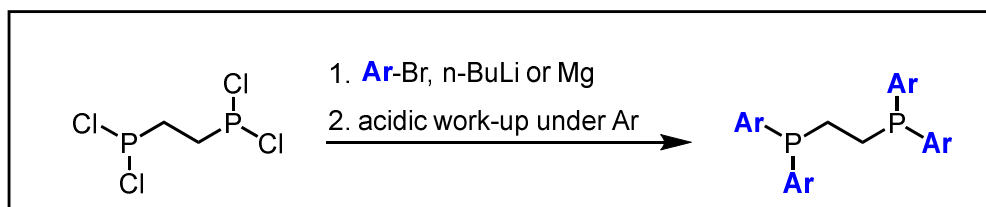
### 3.4.2.2 Preparation of catalysts

#### 3.4.2.2.1 Prerparation of catalyst precursors



Following the literature procedure,<sup>33</sup> solution of potassium halide (12.5 mmol) in water (10 mL) was added to a solution of  $[\text{Ru}(\text{benzene})\text{Cl}_2]_2$  (0.41 mmol) in chloroform (10 mL), and the mixture was stirred vigorously for 2 days. The phases were separated, and a red solid was obtained after evaporation of chloroform and dried under vacuum for 4 days to remove remained water. It is noteworthy to note that the complexes were hardly soluble in chloroform.

#### 3.4.2.2.2 Preparation of dppe derivatives



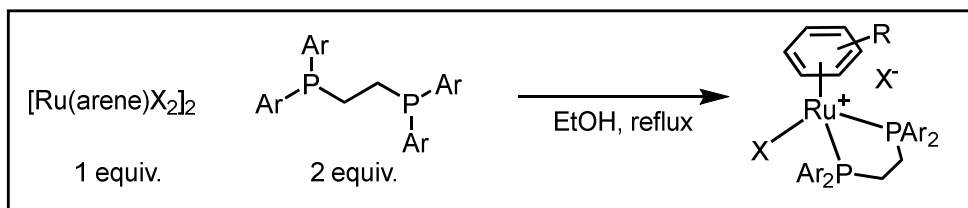
**1,2-Bis[di(p-tolyl)phosphino]ethane:** Following the literature procedure,<sup>34</sup> a solution of 1,2-bis[dichlorophosphino]ethane in ether (10 mL) was added slowly to the p-tolyl magnesium bromide at -30 °C for 2 h. When the addition was complete,

the flask was allowed to warm to 10 °C and the excess Grignard reagents were hydrolysed with saturated ammonium chloride solution. The ether layer was siphoned from the flask under Ar gas using cannular transfer and dried over anhydrous Na<sub>2</sub>SO<sub>4</sub> for 16 h. The mixture was then filtered and concentrated under vacuo. The compounds were precipitated with MeOH and recrystallized by dissolving in THF and adding MeOH. A white solid. 22% isolated yield. <sup>1</sup>H NMR (CDCl<sub>3</sub>, 400 MHz): δ ppm = 7.46 (m, 8 H), 7.33 (m, 8 H), 2.57 (m, 12 H), 2.27 (m., 4 H). <sup>31</sup>P NMR (CDCl<sub>3</sub>, 162 MHz): δ ppm = -20.10. The spectral data were consistent with those reported in the literature.<sup>35</sup>

**1,2-Bis[di(p-trifluoromethylphenyl)phosphino]ethane:** Following the literature,<sup>35</sup> a solution of n-butyl lithium (15 mmol, 4.4 equiv.) in hexane was added dropwise over 1 h to a stirred solution of 4-trifluoromethylphenyl bromide (15 mmol, 4.4 equiv.) in Et<sub>2</sub>O (55 mL) at 20 °C. The mixture was cooled to -70 °C, stirred, and a solution of 1,2-bis[dichlorophosphino]ethane (3.41 mmol, 1 equiv) in Et<sub>2</sub>O (120 mL) was added dropwise during 1 h. The reactants were allowed to warm to 20 °C and stirred for 12 h until a white precipitate was formed. The reaction mixture was quenched with water, and the ethereal layer was separated and dried over anhydrous Na<sub>2</sub>SO<sub>4</sub> under Ar. The white precipitate was filtered off, washed with MeOH, and dried under vacuo. A white solid. 32% isolated yield. <sup>1</sup>H NMR (CDCl<sub>3</sub>, 400 MHz): δ ppm = 7.58 (d, *J* = 7.8 Hz, 8 H), 7.42 (br. s., 8 H), 2.13 (t, *J* = 4.3 Hz, 4 H). <sup>31</sup>P NMR (CDCl<sub>3</sub>, 162 MHz): δ ppm = -13.14. The spectral data were consistent with those reported in the literature.<sup>35</sup>

### 3.4.2.2.3 Preparation of catalysts 5

The chemical shift in  $^{31}\text{P}$  NMR was calculated using triphenylphosphine oxide as an internal standard ( $\delta = 29.30$  ppm).



Following the literature procedure,<sup>36</sup>  $[\text{Ru}(\text{arene})\text{X}(\text{bidentate phosphine})]\text{X}$  complexes were prepared. To a suspension of  $[\text{Ru}(\text{arene})\text{X}_2]_2$  (0.5 mmol, 1 equiv) in ethanol (35 mL), 1,2-bis(diarylphosphino)ethane (1 mmol, 2 equiv) was added and the mixture was refluxed until a yellow solution was obtained. The solution was filtered and the solvent evaporated to reduce the volume to 2 mL; by adding cooled diethylether a yellow solid was obtained. This was filtered, washed with diethylether and dried under reduced pressure.

**$[\text{Ru}(\text{benzene})\text{Cl}(\text{dppe})]\text{Cl}$  (5A)**: yellow solid.  $^1\text{H}$  NMR ( $\text{CDCl}_3$ , 499 MHz):  $\delta$  ppm = 7.32 - 7.79 (m, 20 H), 6.10 (s, 6 H), 2.83 - 2.97 (m, 2 H), 2.46 - 2.60 (m, 2 H).  $^{31}\text{P}$  NMR ( $\text{CDCl}_3$ , 162 MHz):  $\delta$  ppm = 70.40. The spectral data were consistent with those reported in the literature.<sup>37</sup>

**$[\text{Ru}(\text{p-cymene})\text{Cl}(\text{dppe})]\text{Cl}$  (5B)**: yellow solid.  $^1\text{H}$  NMR ( $\text{CDCl}_3$ , 499 MHz):  $\delta$  ppm = 7.33 - 7.73 (m, 20 H), 6.19 (d,  $J = 5.4$  Hz, 2 H), 6.08 (d,  $J = 5.9$  Hz, 2 H), 2.92 - 3.02 (m, 2 H), 2.47 - 2.56 (m, 2 H), 2.34 - 2.41 (m, 1 H), 1.21 (s, 3 H), 0.83 (d,  $J =$

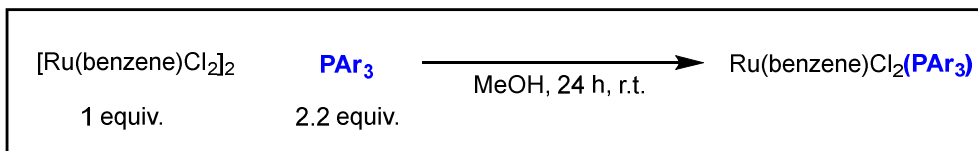
6.8 Hz, 6 H).  $^{31}\text{P}$  NMR ( $\text{CDCl}_3$ , 162 MHz):  $\delta$  ppm = 71.14. The spectral data were consistent with those reported in the literature.<sup>38</sup>

**[Ru(benzene)Cl(1,2-bis[di(p-tolyl)phosphino]ethane)]Cl (5C)**: yellow solid.  $^1\text{H}$  NMR ( $\text{CDCl}_3$ , 400MHz):  $\delta$  ppm = 7.18 - 7.61 (m, 16 H), 6.04 (s, 6 H), 2.75 - 2.87 (m, 2 H), 2.32 - 2.48 ppm (m, 14 H).  $^{31}\text{P}$  NMR ( $\text{CDCl}_3$ , 162 MHz):  $\delta$  ppm = 68.67.

**[Ru(benzene)Cl(1,2-bis[di(p-trifluoromethyl)phosphino]ethane)]Cl (5D)**: yellow solid.  $^1\text{H}$  NMR ( $\text{CDCl}_3$ , 400MHz):  $\delta$  ppm = 7.57 - 8.03 (m, 16 H), 6.10 (br. s., 6 H), 2.86 (br. s., 2 H), 2.42 ppm (br. s., 2 H).  $^{31}\text{P}$  NMR ( $\text{CDCl}_3$ , 162 MHz):  $\delta$  ppm = 70.34.

**[Ru(benzene)Br(dppe)]Br (5K)**: dark yellow solid.  $^1\text{H}$  NMR ( $\text{CDCl}_3$ , 400MHz):  $\delta$  ppm = 7.71 - 7.86 (m, 4 H), 7.43 - 7.63 (m, 12 H), 7.29 - 7.39 (m, 4 H), 6.12 (s, 6 H), 3.01 (m, 2 H), 2.66 ppm (m, 2 H).  $^{31}\text{P}$  NMR ( $\text{CDCl}_3$ , 162 MHz):  $\delta$  ppm = 69.99.

**[Ru(benzene)I(dppe)]I (5L)**: light brown solid.  $^1\text{H}$  NMR ( $\text{CDCl}_3$ , 400MHz):  $\delta$  ppm = 7.25 - 7.75 (m, 20 H), 6.16 (s, 6 H), 3.19 (m, 2 H), 2.89 ppm (m, 2 H).  $^{31}\text{P}$  NMR ( $\text{CDCl}_3$ , 162 MHz):  $\delta$  ppm = 70.15.



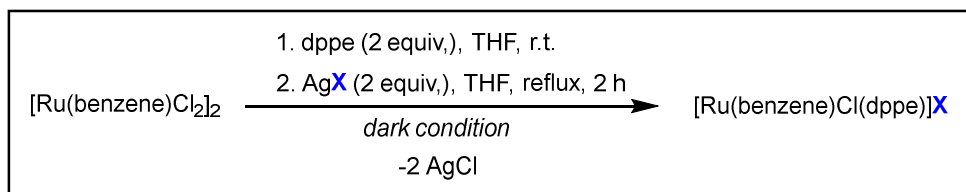
Following the literature protocol,<sup>22c</sup> a mixture of  $[\text{Ru}(\text{benzene})\text{Cl}_2]_2$  (0.20 mmol, 1 equiv.) and monophosphine (0.44 mmol, 2.2 equiv.) in methanol (50 mL) was stirred at room temperature for 24 h. The solid substances were slowly dissolved and the color of solution changed to orange-red. At the end of the reaction, a trace amount of insoluble substance was removed by filtration. The filtrate was concentrated to 5 mL and stored in a refrigerator overnight to form red crystals. The product was filtered, washed with diethyl, and dried under vacuum.

**$[\text{Ru}(\text{benzene})\text{Cl}_2\text{PPh}_3]$  (5E):** red solid.  $^1\text{H}$  NMR ( $\text{CDCl}_3$ , 499MHz):  $\delta$  ppm = 7.73 - 7.79 (m, 6 H), 7.37 - 7.48 (m, 10 H), 5.41 (s, 6 H). The spectral data were consistent with those reported in the literature.<sup>22c</sup>

**$[\text{Ru}(\text{benzene})\text{Cl}_2\text{P}(\text{p-OMePh})_3]$  (5F):** red solid.  $^1\text{H}$  NMR ( $\text{CDCl}_3$ , 499 MHz):  $\delta$  ppm = 7.63 - 7.69 (m, 6 H), 6.90 (d,  $J = 8.8$  Hz, 6 H), 5.40 (s, 6 H), 3.83 (s, 9 H). The spectral data were consistent with those reported in the literature.<sup>22c</sup>

**$[\text{Ru}(\text{benzene})\text{Cl}_2\text{P}(\text{p-CF}_3\text{Ph})_3]$  (5G):** orange solid.  $^1\text{H}$  NMR ( $\text{CDCl}_3$ , 499 MHz):  $\delta$  ppm = 7.88 - 7.94 (m, 7 H), 7.70 (d,  $J = 7.8$  Hz, 6 H), 5.48 (s, 6 H). The spectral data

were consistent with those reported in the literature.<sup>22c</sup>



Following the procedure slightly modified from literature method,<sup>39</sup>  $[\text{Ru}(\text{benzene})\text{Cl}_2]_2$  (0.3 mmol, 1 equiv.) and dppe (0.6 mmol, 1 equiv.) in THF (7 mL) was placed in a Schlenk tube along with a magnetic stir bar in the glove box. The Schlenk tube was then sequentially evacuated and purged with argon. The suspension was stirred for 10 min, when a solution of AgX (0.6 mmol, 2 equiv.) in THF (4 mL) was added. The mixture was heated at reflux temperature for 1 h, during which time the color changed to dark yellow. Using cannular transfer, the solid AgCl was filtered through fritted glass, and the dark yellow filtrate was collected. The THF solvent was removed in vacuo, and the residue was extracted with diethyl ether to give the product as yellow solid.

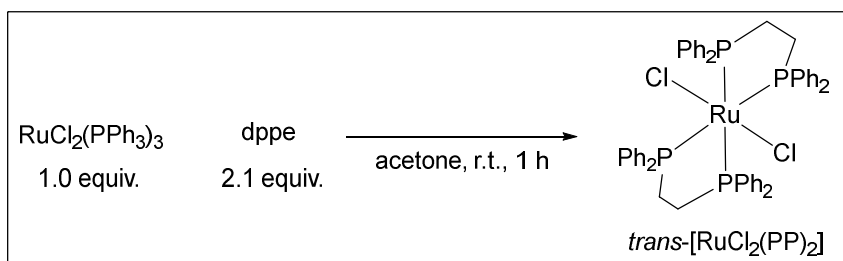
**$[\text{Ru}(\text{benzene})\text{Cl}(\text{dppe})]\text{BF}_4$  (5H)**: yellow solid.  $^1\text{H}$  NMR ( $\text{CDCl}_3$ , 499 MHz):  $\delta$  ppm = 7.27 - 7.77 (m, 20 H), 5.95 (s, 6 H), 2.89 (m, 2 H), 2.46 (m, 2 H).  $^{31}\text{P}$  NMR ( $\text{CDCl}_3$ , 162 MHz):  $\delta$  ppm = 70.06.  $^{19}\text{F}$  NMR ( $\text{CDCl}_3$ , 376 MHz):  $\delta$  = -152.73 ppm (s).

**$[\text{Ru}(\text{benzene})\text{Cl}(\text{dppe})]\text{OTf}$  (5I)**: yellow solid.  $^1\text{H}$  NMR ( $\text{CDCl}_3$ , 499 MHz):  $\delta$  ppm = 7.28 - 7.79 (m, 20 H), 5.96 (s, 6 H), 2.91 (m, 2 H), 2.48 (m, 2 H).  $^{31}\text{P}$  NMR ( $\text{CDCl}_3$ ,

162 MHz):  $\delta$  ppm = 70.42.  $^{19}\text{F}$  NMR ( $\text{CDCl}_3$ , 376 MHz):  $\delta$  ppm = -78.14 (s).

**[Ru(benzene)Cl(dppe)]PF<sub>6</sub> (5J)**: yellow solid.  $^1\text{H}$  NMR ( $\text{CDCl}_3$ , 499 MHz):  $\delta$  ppm = 7.27 - 7.82 (m, 20 H), 5.91 (s, 6 H), 2.88 (m, 2 H), 2.47 (m, 2 H).  $^{31}\text{P}$  NMR ( $\text{CDCl}_3$ , 162 MHz):  $\delta$  ppm = 70.27.  $^{19}\text{F}$  NMR ( $\text{CDCl}_3$ , 376 MHz):  $\delta$  ppm = -71.97(s), -73.87(s), -78.15 (s).

#### 3.4.2.2.4. Preparation of *trans*-[RuCl<sub>2</sub>(PP)<sub>2</sub>]



Following the literature protocol,<sup>40</sup> A suspension of RuCl<sub>2</sub>(PPh<sub>3</sub>)<sub>3</sub> (3.59 g, 3.75 mmol, 1.0 equiv.) and dppe (3.14 g, 7.89 mmol, 2.1 equiv.) in acetone (40 mL) was stirred for 1 h at room temperature. The resulting yellow precipitate was collected by filtration, washed with acetone and dried in vacuo.

***Trans*-[RuCl<sub>2</sub>(PP)<sub>2</sub>]** : yellow solid.  $^1\text{H}$  NMR ( $\text{CDCl}_3$ , 400 MHz):  $\delta$  ppm = 7.29 (m, 16 H), 7.21 (t,  $J$  = 7.2 Hz, 8 H), 7.01 (t,  $J$  = 7.6 Hz, 16 H), 2.75 (br. s., 8 H).  $^{31}\text{P}$  NMR ( $\text{CDCl}_3$ , 162 MHz):  $\delta$  ppm = 46.10. The spectral data were consistent with those reported in the literature.<sup>40</sup>



### 3.4.3 General procedure for acceptorless and base-free dehydrogenation of cyanohydrin and isolation

To an oven-dried 25 mL Schlenk tube equipped with a stir bar, [Ru(benzene)Cl(dppe)] (5.0 mol%, 8.1 mg) and (if solid) cyanohydrin (1 equiv., 0.25 mmol) were added in an Ar-filled glovebox. The reaction tube was capped with a 14/20 septum after benzene (1.25 mL) was added via syringe. After removal from the glovebox, the reaction tube was sealed with a metal-wire (If the cyanohydrin was liquid, it was added via microsyringe at this time). The tube was connected to an Ar line after evacuation/Ar purging three times. The resulting mixture was stirred vigorously and heated to 120 °C for 24 h. Then, the reaction mixture was transferred into a round-bottom flask using CH<sub>2</sub>Cl<sub>2</sub> and concentrated under reduced pressure. The reaction mixture was hydrolyzed in a mixture of water/ethyl acetate (1:1 v/v) for 24 h. The organic phase was extracted from aqueous mixture (3 x 4 mL of ethyl acetate), washed with brine (4 mL). The organic layer was dried over Na<sub>2</sub>SO<sub>4</sub> and concentrated. The residue was purified by column chromatography using a mixture of hexane/ethyl acetate.

### 3.4.4 Mechanistic investigation

#### 3.4.4.1 Substoichiometric reactions of $[\text{Ru}(\text{benzene})\text{Cl}_2]$ with dppe and 1a

##### [Figure 3.1]

To an oven-dried screw-capped NMR tube,  $[\text{Ru}(\text{benzene})\text{Cl}_2]$  (0.02 mmol, 10 mol%, 10.0 mg) and 1a (0.2 mmol, 1 equiv., 26.6 mg) were added in an Ar-filled glovebox. The reaction tube was sealed after  $\text{CD}_3\text{CN}$  (1.2 mL) was added via a syringe. After removing from the glovebox, the reaction tube was sealed again with Teflon tape. The resulting mixture was heated at 120 °C for 12 h. Subsequently, quantitative and qualitative analysis of the reaction mixture was carried out by  $^{31}\text{P}$  NMR.

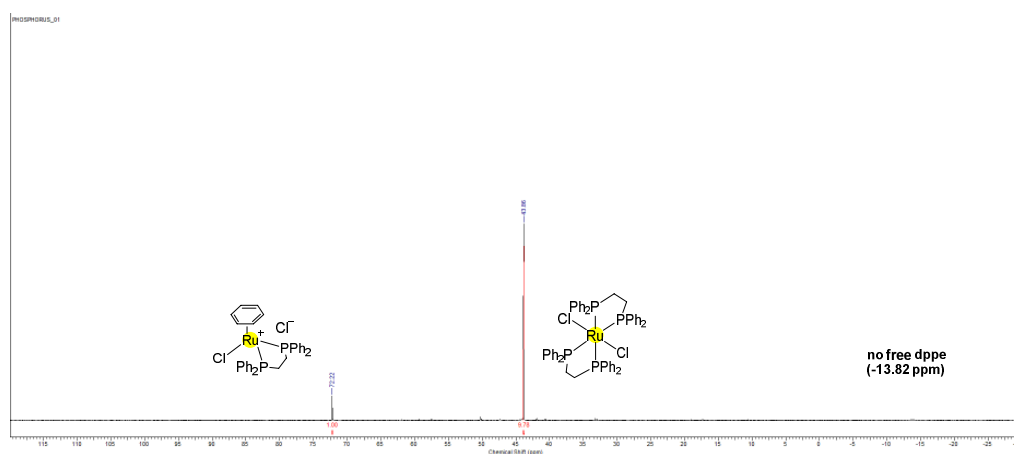


**Figure 3.1** Quantitative and qualitative analysis of substoichiometric reaction using  $^{31}\text{P}$  NMR.

#### 3.4.4.2 Catalytic activity of *trans*-[RuCl<sub>2</sub>(PP)<sub>2</sub>]

To an oven-dried 25mL Schlenk tube equipped with a stir bar, *trans*-[RuCl<sub>2</sub>(PP)<sub>2</sub>] (5 mol%, 12.11 mg) and **1a** (1 equiv., 0.25 mmol) were added in an Ar-filled glovebox. The reaction tube was capped with a 14/20 septum after benzene (1.25 mL) was added via a syringe. After removing from the glovebox, the reaction tube was sealed again with metal-wire. The Schlenk tube was connected to Ar line after purging the line with Ar three times for 5 minutes. The resulting mixture was stirred vigorously and heated at 120 °C for 24 h. Then, the reaction mixture was transferred to a round-bottom flask using CH<sub>2</sub>Cl<sub>2</sub> and then concentrated under reduced pressure. The crude mixture was directly analyzed by <sup>1</sup>H NMR.

### 3.4.4.3 Coordination mode: the reaction of [Ru(benzene)Cl(dppe)]Cl with cyanohydrin **1m** [Figure 3.2–3.3]

To an oven-dried screw-capped NMR tube, [Ru(benzene)Cl(dppe)]Cl (0.025 mmol, 1 equiv., 16.2 mg) was added in an Ar-filled glovebox. After removing from the glovebox, the reaction tube was filled with 2-hydroxy-2-(4-trifluoromethylphenyl)acetonitrile **1m** (0.025 mmol, 1 equiv., 5.0 mg) in CDCl<sub>3</sub> (0.6 mL) via syringe. The resulting mixture was kept at room temperature for 30 min. Subsequently, qualitative analysis of the reaction mixture was carried out by <sup>1</sup>H and <sup>31</sup>P NMR.

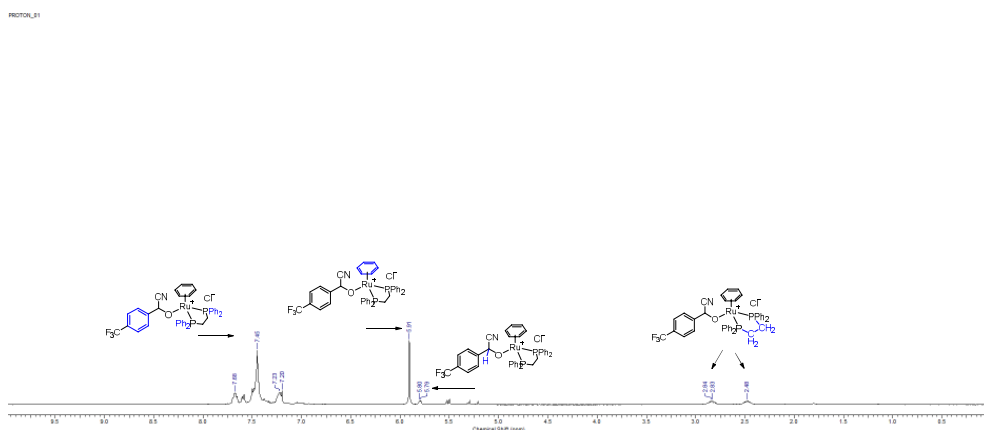


**Figure 3.2** Qualitative analysis of stoichiometric reaction using <sup>1</sup>H NMR.

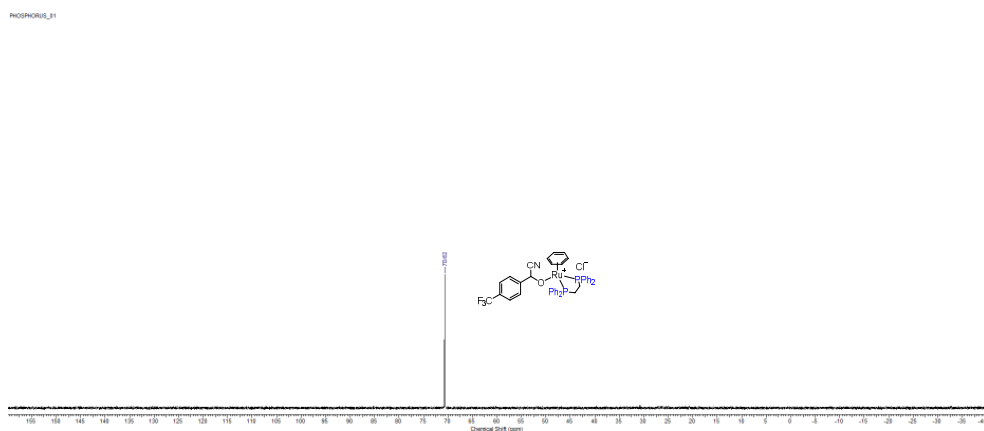


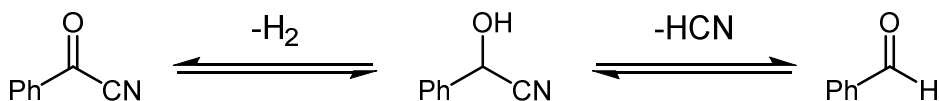
**Figure 3.3** Qualitative analysis of substoichiometric reaction using <sup>31</sup>P NMR.

### 3.4.5 Calculation<sup>†</sup>

#### 3.4.5.1 General computational method

DFT calculations were carried out using Gaussian09 software package<sup>S1</sup> to determine the relative Gibbs free energies for the formation of thermodynamic and kinetic products. Geometry optimization and frequency calculations were initially performed at the unrestricted B3LYP/6-311+G(df,p) level.<sup>S2-4</sup> Subsequently, single-point energy calculations with the Def2TZVP triple zeta basis set of Ahlrics and coworkers were performed on the optimized geometry in order to obtain a refined energy data.<sup>S5</sup> The effect of benzene solvent was included using the IEFPCM-SCRF model in all calculations.<sup>S6</sup>

Mandelonitrile **1a** was considered as the model substrate in free energy calculations. The elimination of a hydrogen molecule from substrate **1a** results in the formation of **2a**, while the elimination of hydrogen cyanide results in the formation of benzaldehyde **3a** (Scheme 3.8).



**Scheme 3.8** Model reaction using mandelonitrile **1a** as substrate.

---

<sup>†</sup> The entire work in this section **3.4.5** has been conducted by Adhitya Mangala Putra Moeljadi and Hajime Hirao.

### 3.4.5.2 References for computation

(S1) *Gaussian 09, Revision D.01*, Frisch, M. J., Trucks, G. W., Schlegel, H. B., Scuseria, G. E., Robb, M. A., Cheeseman, J. R., Scalmani, G., Barone, V., Mennucci, B., Petersson, G. A., Nakatsuji, H., Caricato, M., Li, X., Hratchian, H. P., Izmaylov, A. F., Bloino, J., Zheng, G., Sonnenberg, J. L., Hada, M., Ehara, M., Toyota, K., Fukuda, R., Hasegawa, J., Ishida, M., Nakajima, T., Honda, Y., Kitao, O., Nakai, H., Vreven, T., Montgomery, J. A., Jr., Peralta, J. E., Ogliaro, F., Bearpark, M., Heyd, J. J., Brothers, E., Kudin, K. N., Staroverov, V. N., Kobayashi, R., Normand, J., Raghavachari, K., Rendell, A., Burant, J. C., Iyengar, S. S., Tomasi, J., Cossi, M., Rega, N., Millam, M. J., Klene, M.; Knox, J. E., Cross, J. B., Bakken, V., Adamo, C., Jaramillo, J., Gomperts, R., Stratmann, R. E., Yazyev, O., Austin, A. J., Cammi, R., Pomelli, C., Ochterski, J. W., Martin, R. L., Morokuma, K., Zakrzewski, V. G., Voth, G. A., Salvador, P., Dannenberg, J. J., Dapprich, S., Daniels, A. D., Farkas, Ö., Foresman, J. B., Ortiz, J. V., Cioslowski, J., Fox, D. J. Gaussian, Inc., Wallingford CT, **2009**.

(S2) (a) Becke, A. D. *J. Chem. Phys.* **1993**, *98*, 5648. (b) Lee, C., Yang, W., Parr, R. G. *Phys. Rev. B* **1988**, *37*, 785. (c) Vosko, S. H., Wilk, L., Nusair, M. *Can. J. Phys.* **1980**, *58*, 1200.

(S3) (a) Grimme, S., Ehrlich, S., Goerigk, L. *J. Comput. Chem.* **2011**, *32*, 1456. (b) Grimme, S., Antony, J., Ehrlich, S., Krieg, H. *J. Chem. Phys.* **2010**, *132*, 154104. (c) Johnson, E. R., Becke, A. D. *J. Chem. Phys.* **2006**, *124*, 174104. (d) Becke, A. D., Johnson, E. R. *J. Chem. Phys.* **2005**, *123*, 154101. (e) Johnson, E. R., Becke, A. D. *J. Chem. Phys.* **2005**, *123*, 024101.

(S4) (a) Hehre, W., Radom, L., Schleyer, P. v. R., Pople, J. *Ab Initio Molecular Orbital Theory*; John Wiley & Sons: New York, **1986**. (b) Clark, T., Chandrasekhar, J., Spitznagel, G. W., Schleyer, P. v. R. *J. Comput. Chem.* **1983**, *4*, 294. (c) Krishnan, R., Binkley, J. S., Seeger, R., Pople, J. A. *J. Chem. Phys.* **1980**, *72*, 650. (d) Hariharan, P. C., Pople, J. A. *Theor. Chim. Acta* **1973**, *28*, 213.

(S5) (a) Weigend, F., Ahlrichs, R. *Phys. Chem. Chem. Phys.* **2005**, *7*, 3297. (b) Weigend, F. *Phys. Chem. Chem. Phys.* **2006**, *8*, 1057.

(S6) Tomasi, J., Mennucci, B., Cammi, R. *Chem. Rev.* **2005**, *105*, 2999.

### 3.4.5.3 Raw energy data

**Table 3.2** Raw energy data for optimized geometries

Structure	E(B1) [hartree]	ZPE [hartree]	G <sub>corr</sub> [hartree]	E(B2) [hartree]
H <sub>2</sub>	-1.1796394914	0.010061	-0.001430	-1.1797155590
HCN	-93.4603769752	0.016378	-0.002981	-93.4674751752
<b>1a</b>	-439.1523195600	0.131351	0.096172	-439.1854380550
<b>2a</b>	-437.9457585390	0.108314	0.074703	-437.9798700110
<b>3a</b>	-345.6845666680	0.109574	0.078993	-345.7110589250

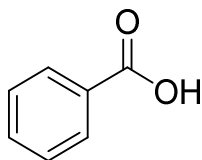


### 3.4.5.4 XYZ coordinates of optimized geometries

==== **1a** ====

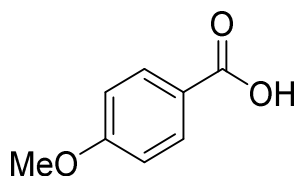
C	-3.088654	-0.069116	0.390652
C	-1.701909	-0.055083	0.465751
C	-0.994237	1.088283	0.092774
C	-1.683292	2.211150	-0.357234
C	-3.073218	2.194403	-0.436970
C	-3.776564	1.055046	-0.062426
H	-3.634486	-0.958562	0.682983
H	-1.168019	-0.930096	0.817916
H	-1.136429	3.102767	-0.644650
H	-3.603412	3.071857	-0.788235
H	-4.858656	1.040698	-0.122767
C	0.517174	1.118364	0.193967
O	0.893060	0.894690	1.548553
C	1.136753	0.104878	-0.690870
N	1.647269	-0.671882	-1.371287
H	0.874221	2.095739	-0.152659

### 3.4.6 Characterization of products



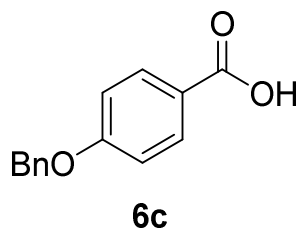
**6a**

**Benzoic acid (6a):** white solid (24 mg, 0.20 mmol, 80% isolated yield).  $^1\text{H}$  NMR ( $\text{CDCl}_3$ , 499MHz):  $\delta$  ppm = 8.14 (d,  $J=7.3$  Hz, 2 H), 7.63 (t,  $J=7.3$  Hz, 1 H), 7.50 (t,  $J=7.6$  Hz, 2 H).  $^{13}\text{C}$  NMR ( $\text{CDCl}_3$ , 126MHz):  $\delta$  ppm = 171.8, 133.8, 130.2, 129.3, 128.5. The spectral data were consistent with those reported in the literature.<sup>41</sup>

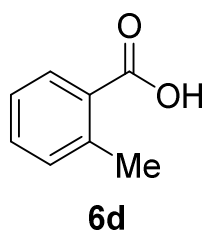


**6b**

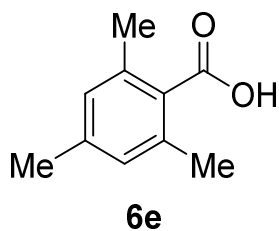
**4-Methoxybenzoic acid (6b):** white solid (35mg, 0.23 mmol, 91% isolated yield).  $^1\text{H}$  NMR ( $\text{CD}_3\text{OD}$ , 300MHz):  $\delta$  ppm = 7.97 (d,  $J=9.0$  Hz, 2 H), 6.97 (d,  $J=9.0$  Hz, 2 H), 3.85 ppm (s, 3 H).  $^{13}\text{C}$  NMR ( $\text{CD}_3\text{OD}$ , 75MHz):  $\delta$  ppm = 169.9, 165.2, 133.0, 124.2, 114.8, 56.1. The spectral data were consistent with those reported in the literature.<sup>41</sup>



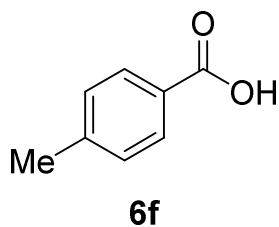
**4-Benzyloxybenzoic acid (6c):** white solid (30 mg, 0.13 mmol, 52% isolated yield).  $^1\text{H}$  NMR ( $\text{CDCl}_3$ , 300MHz):  $\delta$  ppm = 8.08 (d,  $J=8.7$  Hz, 2 H), 7.35 - 7.50 (m, 5 H), 7.03 (d,  $J=8.9$  Hz, 2 H), 5.15 (s, 2 H).  $^{13}\text{C}$  NMR ( $\text{CDCl}_3$ , 75MHz):  $\delta$  ppm = 171.3, 163.1, 136.1, 132.4, 128.7, 128.2, 127.5, 121.9, 114.6, 70.1. The spectral data were consistent with those reported in the literature.<sup>42</sup>



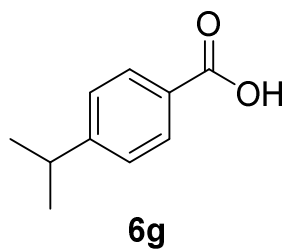
**2-Methylbenzoic acid (6d):** white solid (26 mg, 0.19 mmol, 75% isolated yield).  $^1\text{H}$  NMR ( $\text{CDCl}_3$ , 300MHz):  $\delta$  ppm = 8.08 (dd,  $J=8.2$ , 1.4 Hz, 1 H), 7.47 (td,  $J=7.5$ , 1.5 Hz, 1 H), 7.30 (t,  $J=7.1$  Hz, 2 H), 2.68 (s, 3 H).  $^{13}\text{C}$  NMR ( $\text{CDCl}_3$ , 75MHz):  $\delta$  ppm = 172.9, 141.3, 132.9, 131.9, 131.6, 128.3, 125.8, 22.1. The spectral data were consistent with those reported in the literature.<sup>43</sup>



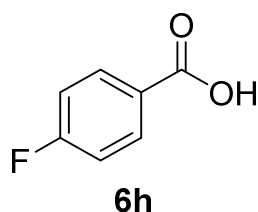
**2,4,6-Trimethylbenzoic acid (6e):** white solid (23 mg, 0.14 mmol, 55% isolated yield).  $^1\text{H}$  NMR ( $\text{CDCl}_3$ , 300MHz):  $\delta$  ppm = 6.91 (s, 2 H), 2.44 (s, 6 H), 2.32 (s, 3 H).  $^{13}\text{C}$  NMR ( $\text{CDCl}_3$ , 75MHz):  $\delta$  ppm = 175.7, 140.1, 136.2, 129.2, 128.8, 21.1, 20.3. The spectral data were consistent with those reported in the literature.<sup>42</sup>



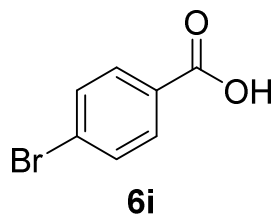
**4-Methylbenzoic acid (6f):** white solid (8 mg, 0.06 mmol, 24% isolated yield).  $^1\text{H}$  NMR ( $\text{CD}_3\text{OD}$ , 300MHz):  $\delta$  ppm = 7.90 (d,  $J=7.3$  Hz, 2 H), 7.27 (d,  $J=7.9$  Hz, 2 H), 2.40 (s, 3 H).  $^{13}\text{C}$  NMR ( $\text{CD}_3\text{OD}$ , 75MHz):  $\delta$  ppm = 170.2, 145.1, 131.0, 130.2, 129.2, 21.7. The spectral data were consistent with those reported in the literature.<sup>41</sup>



**4-Isopropylbenzoic acid (6g)**: white solid (24 mg, 0.15 mmol, 58% isolated yield).  $^1\text{H}$  NMR ( $\text{CD}_3\text{OD}$ , 499MHz):  $\delta$  ppm = 7.94 (d,  $J=7.8$  Hz, 2 H), 7.33 (d,  $J=8.3$  Hz, 2 H), 2.97 (sep,  $J=6.9$  Hz, 1 H), 1.27 ppm (d,  $J=6.8$  Hz, 6 H).  $^{13}\text{C}$  NMR ( $\text{CD}_3\text{OD}$ , 126MHz):  $\delta$  ppm = 170.2, 155.9, 131.1, 129.6, 127.7, 35.6, 24.3. The spectral data were consistent with those reported in the literature.<sup>41</sup>

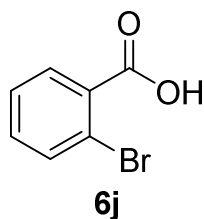


**4-Fluorobenzoic acid (6h)**: white solid (33 mg, 0.24 mmol, 94% isolated yield).  $^1\text{H}$  NMR ( $\text{CDCl}_3$ , 300MHz):  $\delta$  ppm = 8.15 (dd,  $J=9.0, 5.5$  Hz, 2 H), 7.17 (t,  $J=8.7$  Hz, 2 H).  $^{13}\text{C}$  NMR ( $\text{CDCl}_3$ , 75MHz):  $\delta$  ppm = 171.1, 166.4 (d,  $J=255.4$  Hz), 132.9 (d,  $J=9.6$  Hz), 125.5 (d,  $J=2.9$  Hz), 115.7 (d,  $J=22.1$  Hz). The spectral data were consistent with those reported in the literature.<sup>41</sup>

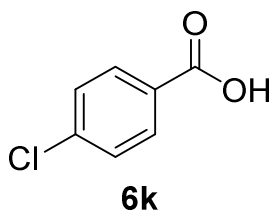


**4-Bromobenzoic acid (6i)**: white solid (39 mg, 0.20 mmol, 78% isolated yield).  $^1\text{H}$  NMR ( $\text{CD}_3\text{OD}$ , 300MHz):  $\delta$  ppm = 7.92 (m, 2 H), 7.64 (m, 2 H).  $^{13}\text{C}$  NMR ( $\text{CD}_3\text{OD}$ , 75MHz):  $\delta$  ppm = 169.0, 133.0, 132.6, 131.3, 128.9. The spectral data were

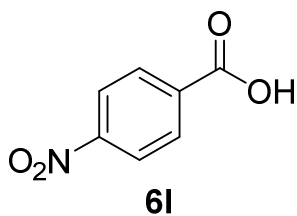
consistent with those reported in the literature.<sup>41</sup>



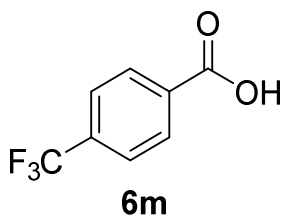
**2-Bromobenzoic acid (6j):** white solid (9 mg, 0.04 mmol, 17% isolated yield). <sup>1</sup>H NMR (CDCl<sub>3</sub>, 300MHz): δ ppm = 8.01 (m, 1 H), 7.73 (m, 1 H), 7.36 - 7.48 ppm (m, 2 H). <sup>13</sup>C NMR (CDCl<sub>3</sub>, 75MHz): δ ppm = 170.6, 134.9, 133.5, 132.4, 130.4, 127.3, 122.6. The spectral data were consistent with those reported in the literature.<sup>44</sup>



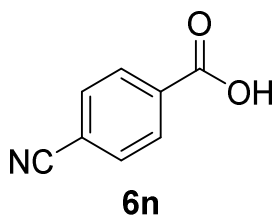
**4-Chlorobenzoic acid (6k):** white solid (16 mg, 0.10 mmol, 41% isolated yield). <sup>1</sup>H NMR (CD<sub>3</sub>OD, 300MHz): δ ppm = 7.99 (m, 2 H), 7.47 (m, 2 H). <sup>13</sup>C NMR (CD<sub>3</sub>OD, 75MHz): δ ppm = 168.9, 140.4, 132.5, 130.8, 129.9. The spectral data were consistent with those reported in the literature.<sup>41</sup>



**4-Nitrobenzoic acid (6l):** yellow solid (25 mg, 0.15 mmol, 59% isolated yield).  $^1\text{H}$  NMR ( $\text{CD}_3\text{OD}$ , 499MHz):  $\delta$  ppm = 8.31 (d,  $J=8.8$  Hz, 2 H), 8.22 (d,  $J=8.8$  Hz, 2 H).  $^{13}\text{C}$  NMR ( $\text{CD}_3\text{OD}$ , 126MHz):  $\delta$  ppm = 167.7, 152.1, 137.8, 132.1, 124.7. The spectral data were consistent with those reported in the literature.<sup>45</sup>



**4-(Trifluoromethyl)benzoic acid (6m):** white solid (26 mg, 0.14 mmol, 54% isolated yield).  $^1\text{H}$  NMR ( $\text{CD}_3\text{OD}$ , 300MHz):  $\delta$  ppm = .  $^{13}\text{C}$  NMR ( $\text{CD}_3\text{OD}$ , 75MHz):  $\delta$  ppm = 168.4, 135.9, 135.4 (q,  $J=32.3$  Hz), 131.5, 126.6 (q,  $J=126.6$  Hz), 125.4 (q,  $J=271.7$  Hz). The spectral data were consistent with those reported in the literature.<sup>41</sup>



**4-Cyanobenzoic acid (6n):** white solid (6 mg, 0.04 mmol, 17% isolated yield).  $^1\text{H}$

NMR (CD<sub>3</sub>OD, 499MHz):  $\delta$  ppm = 8.16 (d,  $J=8.8$  Hz, 2 H), 7.85 (d,  $J=8.8$  Hz, 2 H).

<sup>13</sup>C NMR (CD<sub>3</sub>OD, 126MHz):  $\delta$  ppm = 168.0, 136.3, 133.6, 131.5, 119.2, 117.4. The spectral data were consistent with those reported in the literature.<sup>44</sup>



### 3.5 References

- (1) (a) Z. P. Demko, K. B. Sharpless, *Angew. Chem. Int. Ed.* **2002**, *41*, 2113. (b) S. Hünig, R. Schaller, *Angew. Chem. Int. Ed.* **1982**, *21*, 36.
- (2) (a) G. A. Olah, M. Arvanaghi, G. K. Surya Prakash, *Synthesis* **1983**, *1983*, 636. (b) U. Hertenstein, S. Hünig, H. Reichelt, R. Schaller, *Chem. Ber.* **1982**, *115*, 261. (c) K. Haase, H. M. R. Hoffmann, *Angew. Chem. Int. Ed.* **1982**, *21*, 83. (d) K. Herrmann, G. Simchen, *Synthesis* **1979**, *1979*, 204. (e) E. C. Taylor, J. G. Andrade, K. C. John, A. McKillop, *J. Org. Chem.* **1978**, *43*, 2280. (f) M. E. Childs, W. P. Weber, *J. Org. Chem.* **1976**, *41*, 3486.
- (3) M. Tanaka, *Bull. Chem. Soc. Jpn.* **1981**, *54*, 637.
- (4) (a) S.-I. Murahashi, T. Naota, *Synthesis* **1993**, *1993*, 433. (b) S.-I. Murahashi, T. Naota, N. Nakajima, *Tetrahedron Lett.* **1985**, *26*, 925. (c) J. Thesing, D. Witzel, A. Brehm, *Angew. Chem.* **1956**, *68*, 425.
- (5) (a) D. G. Lee, U. A. Spitzer, *J. Org. Chem.* **1970**, *35*, 3589. (b) J. R. Holum, *J. Org. Chem.* **1961**, *26*, 4814.
- (6) R. J. Highet, W. C. Wildman, *J. Am. Chem. Soc.* **1955**, *77*, 4399.
- (7) K. Omura, D. Swern, *Tetrahedron* **1978**, *34*, 1651.
- (8) D. B. Dess, J. C. Martin, *J. Org. Chem.* **1983**, *48*, 4155.
- (9) (a) B. Join, K. Möller, C. Ziebart, K. Schröder, D. Gördes, K. Thurow, A. Spannenberg, K. Junge, M. Beller, *Adv. Synth. Catal.* **2011**, *353*, 3023. (b) R. Noyori, M. Aoki, K. Sato, *Chem. Commun.* **2003**, 1977.
- (10) (a) M. S. Sigman, D. R. Jensen, *Acc. Chem. Res.* **2006**, *39*, 221. (b) R. A. Sheldon, I. W. C. E. Arends, G.-J. ten Brink, A. Dijksman, *Acc. Chem. Res.* **2002**, *35*, 774. (c) G. Csajernyik, A. H. Éll, L. Fadini, B. Pugin, J.-E. Bäckvall, *J. Org. Chem.*

2002, 67, 1657.

(11) (a) C. Gunanathan, D. Milstein, *Science* **2013**, 341. (b) G. E. Dobereiner, R. H. Crabtree, *Chem. Rev.* **2010**, 110, 681. (c) A. Friedrich, S. Schneider, *ChemCatChem* **2009**, 1, 72.

(12) C. A. Sandoval, T. Ohkuma, K. Muñiz, R. Noyori, *J. Am. Chem. Soc.* **2003**, 125, 13490.

(13) (a) M. C. Carrión, F. Sepúlveda, F. A. Jalón, B. R. Manzano, A. M. Rodríguez, *Organometallics* **2009**, 28, 3822. (b) M. A. Esteruelas, C. García-Yebra, E. Oñate, *Organometallics* **2008**, 27, 3029. (c) Z.-R. Dong, Y.-Y. Li, J.-S. Chen, B.-Z. Li, Y. Xing, J.-X. Gao, *Org. Lett.* **2005**, 7, 1043. (d) K. Abdur-Rashid, S. E. Clapham, A. Hadzovic, J. N. Harvey, A. J. Lough, R. H. Morris, *J. Am. Chem. Soc.* **2002**, 124, 15104. (e) T. Ohkuma, M. Koizumi, K. Muñiz, G. Hilt, C. Kabuto, R. Noyori, *J. Am. Chem. Soc.* **2002**, 124, 6508.

(14) (a) K. J. Powell, L.-C. Han, P. Sharma, J. E. Moses, *Org. Lett.* **2014**, 16, 2158. (b) S. Arai, Y. Amako, X. Yang, A. Nishida, *Angew. Chem. Int. Ed.* **2013**, 52, 8147. (c) L. Ma, W. Chen, D. Seidel, *J. Am. Chem. Soc.* **2012**, 134, 15305. (d) E. J. Park, S. Lee, S. Chang, *J. Org. Chem.* **2010**, 75, 2760. (e) S. Mark, Z. Alexander, B. Matthias, *Angew. Chem. Int. Ed.* **2003**, 42, 1661.

(15) R. Adams, C. S. Marvel, *Org. Synth.* **1921**, 1, 33.

(16) (a) D. Kim, B. Kang, S. H. Hong, *Org. Chem. Front.* **2016**, 3, 475. (b) S. H. Kim, S. H. Hong, *Org. Lett.* **2016**, 18, 212. (c) K. Kim, B. Kang, S. H. Hong, *Tetrahedron* **2015**, 71, 4565. (d) B. Kang, S. H. Hong, *Adv. Synth. Catal.* **2015**, 357, 834. (e) S. Muthaiah, S. H. Hong, *Adv. Synth. Catal.* **2012**, 354, 3045.

(17) B. Kang, Z. Fu, S. H. Hong, *J. Am. Chem. Soc.* **2013**, 135, 11704.

- (18) (a) J. Zhao, J. F. Hartwig, *Organometallics* **2005**, *24*, 2441. (b) T. Aoki, R. H. Crabtree, *Organometallics* **1993**, *12*, 294.
- (19) H. Song, B. Kang, S. H. Hong, *ACS Catal.* **2014**, *4*, 2889.
- (20) (a) A. Monney, E. Barsch, P. Sponholz, H. Junge, R. Ludwig, M. Beller, *Chem. Commun.* **2014**, *50*, 707. (b) L.-C. Yang, T. Ishida, T. Yamakawa, S. Shinoda, *J. Mol. Catal. A: Chem.* **1996**, *108*, 87.
- (21) (a) B. L. Conley, M. K. Pennington-Boggio, E. Boz, T. J. Williams, *Chem. Rev.* **2010**, *110*, 2294. (b) L. A. Saudan, C. M. Saudan, C. Debieux, P. Wyss, *Angew. Chem. Int. Ed.* **2007**, *46*, 7473.
- (22) (a) A. Grabulosa, A. Mannu, E. Alberico, S. Denurra, S. Gladiali, G. Muller, *J. Mol. Catal. A: Chem.* **2012**, *363–364*, 49. (b) T. Marimuthu, H. B. Friedrich, *ChemCatChem* **2012**, *4*, 2090. (c) L. Wang, Q. Yang, H.-Y. Fu, H. Chen, M.-L. Yuan, R.-X. Li, *Appl. Organomet. Chem.* **2011**, *25*, 626. (d) M. H. S. A. Hamid, J. M. J. Williams, *Chem. Commun.* **2007**, 725. (e) R. Cerón-Camacho, V. Gómez-Benítez, R. Le Lagadec, D. Morales-Morales, R. A. Toscano, *J. Mol. Catal. A: Chem.* **2006**, *247*, 124. (f) M. T. Reetz, X. Li, *J. Am. Chem. Soc.* **2006**, *128*, 1044. (g) P. Crochet, M. A. Fernández-Zumel, C. Beauquis, J. Gimeno, *Inorg. Chim. Acta* **2003**, *356*, 114. (h) V. Cadierno, P. Crochet, J. n. García-Álvarez, S. E. García-Garrido, J. Gimeno, *J. Organomet. Chem.* **2002**, *663*, 32.
- (23) (a) C. J. Copley, I. C. Lennon, R. McCague, J. A. Ramsden, A. Zanotti-Gerosa, *Tetrahedron Lett.* **2001**, *42*, 7481. (b) J. A. Wiles, S. H. Bergens, K. P. M. Vanhessche, D. A. Dobbs, V. Rautenstrauch, *Angew. Chem. Int. Ed.* **2001**, *40*, 914. (c) D. A. Dobbs, K. P. M. Vanhessche, E. Brazi, V. Rautenstrauch, J.-Y. Lenoir, J.-P. Genêt, J. Wiles, S. H. Bergens, *Angew. Chem. Int. Ed.* **2000**, *39*, 1992.

- (24) (a) J. F. Hartwig, *Organotransition Metal Chemistry: From Bonding to Catalysis*, University Science Books, Sausalito, **2010**. (b) D. Tanaka, S. P. Romeril, A. G. Myers, *J. Am. Chem. Soc.* **2005**, *127*, 10323.
- (25) J. A. Mueller, C. P. Goller, M. S. Sigman, *J. Am. Chem. Soc.* **2004**, *126*, 9724.
- (26) Y. Sugiura, Y. Tachikawa, Y. Nagasawa, N. Tada, A. Itoh, *RSC Advances* **2015**, *5*, 70883.
- (27) (a) L. Delaude, S. Delfosse, A. Richel, A. Demonceau, A. F. Noels, *Chem. Commun.* **2003**, 1526. (b) T. J. Geldbach, P. S. Pregosin, *Helv. Chim. Acta* **2002**, *85*, 3937.
- (28) K.-H. Kwon, D. W. Lee, C. S. Yi, *Organometallics* **2010**, *29*, 5748.
- (29) (a) D. V. Simion, T. S. Sorensen, *J. Am. Chem. Soc.* **1996**, *118*, 7345. (b) J. T. Price, T. S. Sorensen, *Can. J. Chem.* **1968**, *46*, 515.
- (30) B. J. Coe, S. J. Glenwright, *Coord. Chem. Rev.* **2000**, *203*, 5.
- (31) (a) A. L. Noffke, A. Habtemariam, A. M. Pizarro, P. J. Sadler, *Chem. Commun.* **2012**, *48*, 5219. (b) K. Y. Ghebreyessus, J. H. Nelson, *J. Organomet. Chem.* **2003**, *669*, 48.
- (32) J. A. Malona, K. Cariou, A. J. Frontier, *J. Am. Chem. Soc.* **2009**, *131*, 7560.
- (33) M. G. Mendoza-Ferri, C. G. Hartinger, A. A. Nazarov, R. E. Eichinger, M. A. Jakupec, K. Severin, B. K. Keppler, *Organometallics* **2009**, *28*, 6260.
- (34) R. J. Burt, J. Chatt, W. Hussain, G. J. Leigh, *J. Organomet. Chem.* **1979**, *182*, 203.
- (35) J. Chatt, W. Hussain, G. J. Leigh, H. M. Ali, C. J. Picket, D. A. Rankin, *J. Chem. Soc., Dalton Trans.* **1985**, 1131.
- (36) F. Faraone, G. A. Loprete, G. Tresoldi, *Inorg. Chim. Acta* **1979**, *34*, L251.

- (37) D. E. Fogg, B. R. James, *J. Organomet. Chem.* **1993**, 462, C21.
- (38) C. Daguinet, R. Scopelliti, P. J. Dyson, *Organometallics* **2004**, 23, 4849.
- (39) F. L. Joslin, D. M. Roundhill, *Organometallics* **1992**, 11, 1749.
- (40) M. A. Fox, J. E. Harris, S. Heider, V. Pérez-Gregorio, M. E. Zakrzewska, J. D. Farmer, D. S. Yufit, J. A. K. Howard, P. J. Low, *J. Organomet. Chem.* **2009**, 694, 2350.
- (41) G. Urgoitia, R. SanMartin, M. T. Herrero, E. Dominguez, *Chem. Commun.* **2015**, 51, 4799.
- (42) J. N. Moorthy, K. N. Parida, *J. Org. Chem.* **2014**, 79, 11431.
- (43) G. Urgoitia, R. SanMartin, M. T. Herrero, E. Domínguez, *Adv. Synth. Catal.* **2016**, 358, 1150.
- (44) M. Berger, R. Chauhan, C. A. B. Rodrigues, N. Maulide, *Chem. Eur. J.* **2016**, 22, 16805.
- (45) P. Saisaha, L. Buettner, M. van der Meer, R. Hage, B. L. Feringa, W. R. Browne, J. W. de Boer, *Adv. Synth. Catal.* **2013**, 355, 2591.

# Chapter 4. Copper-based Photocatalysis for Cross-Coupling Reaction

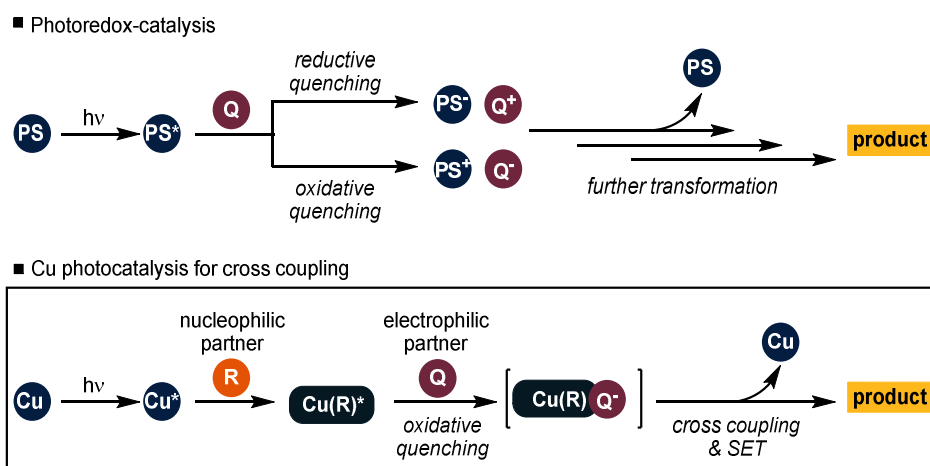
## 4.1 Introduction

The development of novel activation modes for small molecules is one of the most important issues in catalysis and synthetic organic chemistry. Since Ciamician dreamed of “photochemistry of the future” in 1912,<sup>1</sup> the photon has been recognized as an environmentally benign and new energy source to activate small molecules instead of heat, which inevitably utilizes unsustainable fossil fuel.

In the field of photochemistry, the investigation of photophysical properties (*e.g.*, absorption and emission wavelength, lifetime, and redox property) of photosensitizers is predominantly carried out for their application in water splitting, photovoltaic cells, organic light emitting diodes (OLEDs), and energy storage.<sup>2</sup> On the basis of these fundamental studies, synthetic chemists exploit photosensitizers for the catalytic activation of small organic molecules. Notably, this activation mode has opened an era of photocatalysis along with the splendid achievement in photosensitizers and dyes in the last decades. Through this activation, photoexcited photosensitizers with long lifetime and/or high redox activity (*e.g.*, Ru(bpy)<sub>3</sub>Cl<sub>2</sub>) interact with organic molecules via bimolecular energy- or electron-transfer processes. Photoredox catalysis with the aid of Ru(II) and Ir(III)-based polypyridyl complexes has been intensively explored in the field.<sup>3</sup> The electronically excited states generated by irradiation of closed-shell photosensitizers exhibit enhanced redox activities. These abilities make the photosensitizers potent single-

electron-transfer reagents, which serve simultaneously as stronger oxidants and stronger reductants than their corresponding ground states. Redox reaction of the photoexcited states with organic molecules triggers unique and efficient catalytic processes for organic synthesis.

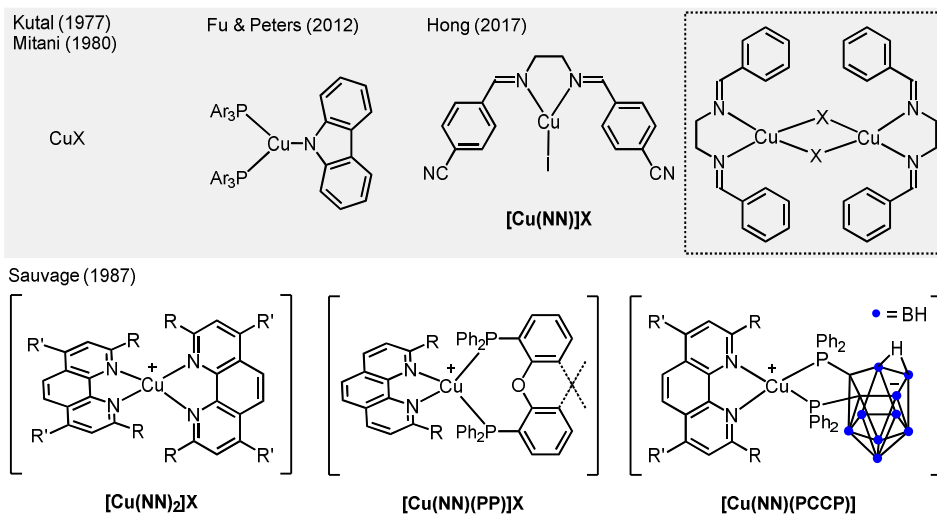
Less common but inexpensive and nontoxic Cu-based photocatalysts for synthetic organic chemistry are described in this chapter. Notably, certain Cu-based photocatalytic systems directly engage in cross-coupling reactions as well as single electron transfer (SET) with organic compounds (Scheme 4.1). This feature of Cu-based photocatalysis is complementary to general Ru- and Ir-based photocatalysts, which generally promotes only the redox process. With this novel catalytic tool, various cross-coupling reactions that are not possible with the previously established method have been realized with a wide range of organic nucleophiles and electrophiles.



**Scheme 4.1** Schematic view of photoredox catalysis and copper photocatalysis

## 4.2 Copper-based photocatalysis for organic synthesis

### ■ Representative examples of Cu photocatalysts



**Scheme 4.2** Representative copper photocatalysts

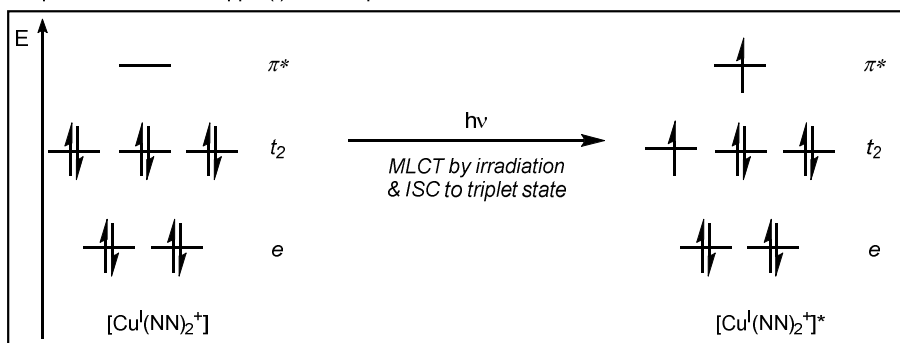
The photoredox catalysis has been flourished with Ru- and Ir-based organometallic complexes. Despite their stability and activity, their high cost and toxicity limit utilization of photoredox catalysis in large scale synthesis and pharmaceutical field. In the efforts to develop inexpensive and nontoxic photosensitizers, Cu complexes have received attention as sustainable alternatives. Because of the key features including strong reducing power, sufficient lifetime, and high luminescence in the excited state of the certain Cu complexes (*e.g.*,  $[\text{Cu}^{\text{I}}(\text{dap})_2]\text{Cl}$ ), application of Cu complexes has been desired for practical purposes including photocatalytic water splitting, solar cells, and OLED.<sup>4</sup> However, their utilization for photoredox catalysis is rare albeit with the early works by the Kutal group (1977) for [2+2] cycloaddition and the Mitani group (1980) for ATRA of unactivated alkyl halides to alkenes.<sup>5</sup> In this section, the competency of Cu complexes as photocatalysts will be discussed



using their electron configurations and photophysical properties. In addition, several representative examples for [2+2] cycloaddition and ATRA reactions promoted by several Cu(I) photocatalysts will be described (Scheme 4.2).

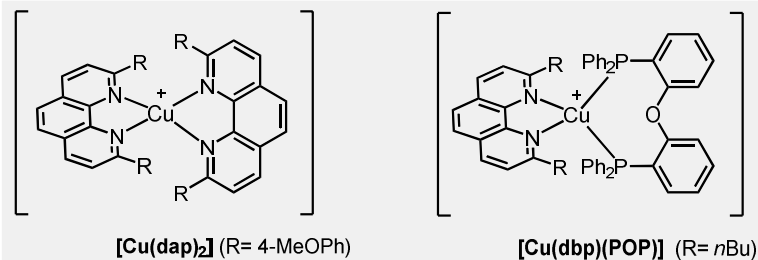
#### 4.2.1 Electronic, geometric, and photophysical properties of copper(I) complexes

■ photoexcitation of copper(I)-NN complexes



■ photophysical properties of several Ru, Ir, Cu complexes

	$E_{1/2}$ ( $M^*/M^+$ ) (V)	$E_{1/2}$ ( $M^+/M$ ) (V)	$E_{1/2}$ ( $M^*/M$ ) (V)	$\lambda_{max}$ (nm)	lifetime of excited state (ns)
$[Ru(bpy)_3]^{2+}$	-0.81	+1.29	-1.33	452	1100
$[Ir(dF(CF_3)ppy)_2(dtbbpy)]^+$	-0.89	+1.69	-1.37	380	2300
<i>fac</i> - $Ir(ppy)_3$	-1.73	+0.77	-2.19	375	1900
$[Cu(dap)_2]^+$	-1.43	+0.62	-	437	270
$[Cu(dbp)(POP)]^+$	-	-	-	378	16100



**Scheme 4.3** Photoexcitation of Cu(NN) complex and photophysical properties of Ru, Ir, and Cu complexes

Among the two common oxidation states (+1 and +2) of Cu complexes, Cu(I) shows intrinsically superior photochemical and photophysical properties.<sup>6</sup> Cu(I) complexes can be divided into anionic complexes, neutral clusters and cationic complexes. Cationic complexes and clusters show attractive photophysical properties (*e.g.*, luminescence), unlike anionic complexes. Among cationic complexes, the most extensively investigated ligand systems are bidentate imine ligands (NN-type, *e.g.*, 1,10-phenanthroline) and bidentate phosphine ligands (PP-type). In the electronic configurations of homoleptic  $[\text{Cu}^{\text{I}}(\text{NN})_2]^+$  and heteroleptic  $[\text{Cu}^{\text{I}}(\text{NN})(\text{PP})]^+$  complexes, complete filling of 3*d* orbitals (*d*<sup>10</sup> configuration) leads to symmetric localization of electronic charge and distorted tetrahedral geometry by minimizing electrostatic repulsions.<sup>6</sup> When these complexes are irradiated, an electron on the metal-centered *t*<sub>2</sub> orbital (HOMO) is excited to the ligand-centered  $\pi^*$  orbital (Scheme 4.3). This process is called metal-to-ligand charge transfer (MLCT). The initially generated singlet MLCT state undergoes rapid intersystem crossing (ISC) to attain the lowest energy triplet MLCT state, which exhibits long lifetime to mediate SET with organic molecules. In terms of photophysical properties, the photoexcited states of Cu(I)-phenanthroline complexes  $[\text{Cu}(\text{NN})_2]^+$  serve as potent reductants like  $[\text{Ru}(\text{bpy})_3]^{2+}$ , showing high oxidation potential ( $[\text{Cu}(\text{NN})_2]^+$ : -1.65V;  $[\text{Ru}(\text{bpy})_3]^{2+}$ : -0.81V versus SCE in MeCN at 298 K).<sup>7</sup> However, these complexes are known to be incompetent oxidants unlike Ru- and Ir-perpyridyl complexes, and their low tendencies to reduce ground-state Cu(I) species have been observed.

The prominent feature of Cu(I) complexes is the lifetime of the excited state, which is crucial for engaging electron transfer. Apparently,  $[\text{Cu}^{\text{I}}(\text{dap})_2]^+$  shows a short lifetime of its excited state (5–10 times lower) compared to the relevant Ru and

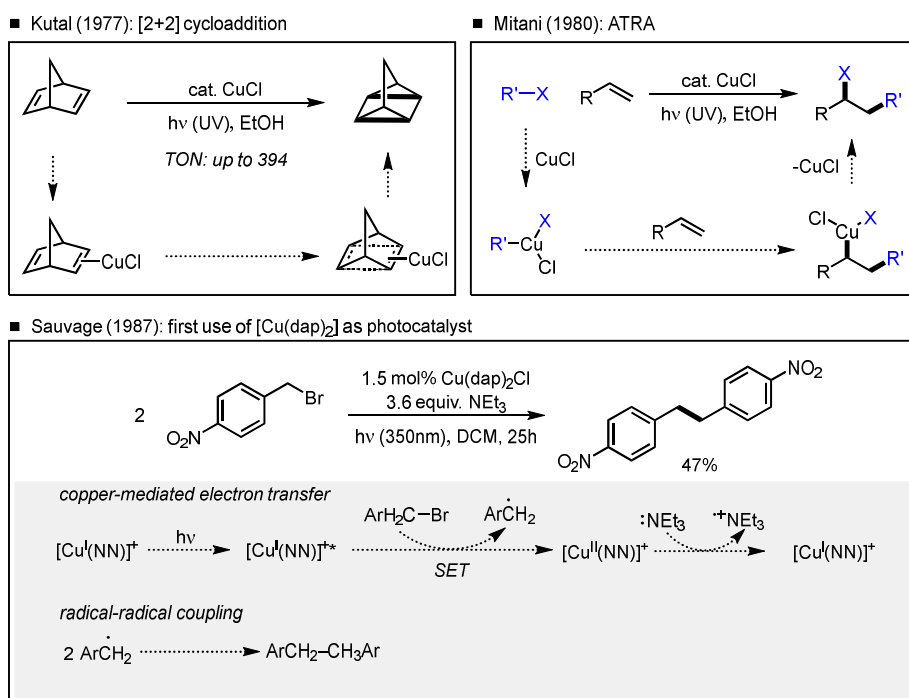
Ir complexes. This can be explained by the reorganization of geometry in the excited state, where the tetrahedral structure is changed to square planar geometry resulting in exciplex quenching.<sup>8</sup> To prevent structural relaxation in the excited state and lengthen the lifetime of the excited state, ligand modifications have been tried; substitution on 2,9-positions of phenanthroline ligands and exchange of one NN-type ligand with bulky bidentate phosphine ligands in  $[\text{Cu}^{\text{I}}(\text{NN})]^+$  complex are representative examples (Scheme 4.2).<sup>9</sup> The significant merit in Cu photocatalysis is the relative ease in tuning the electronic and steric natures of the chelating ligand, which ultimately affect the photoredox properties of the Cu photosensitizer.

#### **4.2.2 Copper-based photocatalysis for [2+2] cycloaddition and atom transfer radical addition (ATRA)**

In 1977, the Kutal group reported Cu-catalyzed isomerization of norbornadiene to quadricyclene via [2+2] cycloaddition under UV irradiation (Scheme 4.4).<sup>5b,10</sup> This process was promoted presumably via a CuCl-norbornadiene  $\pi$ -complex. In 1980, the Mitani group demonstrated photo-induced Cu-catalyzed addition of alkyl halides to alkenes under UV irradiation, which is the preliminary example of atom transfer radical addition (ATRA) reactions.<sup>5c</sup> With the result that radical quencher did not hamper the conversion, the mechanism involving a Cu(III) species was proposed;<sup>11</sup> photochemically facilitated oxidative addition of  $\text{Cu}(\text{I})^*$  to alkyl halide affords a catalytically active Cu(III) intermediate. Within the Cu(III) intermediate, migratory insertion of alkyl moiety to alkene and subsequent reductive elimination give rise to the product. The first catalytic use of  $\text{Cu}(\text{dap})_2\text{Cl}$ , the most popularly used copper

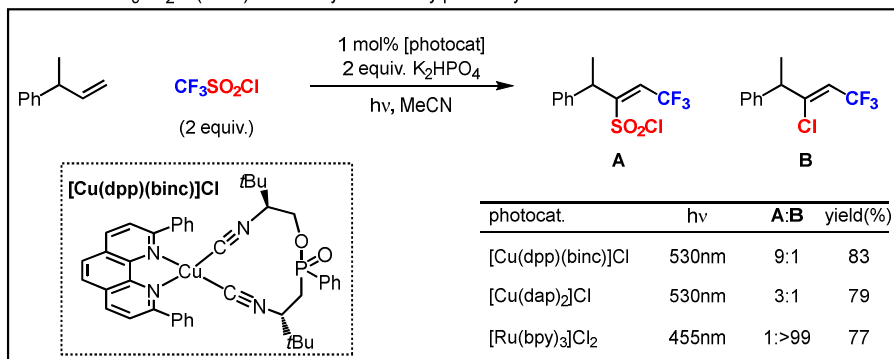
photocatalyst, was reported for reductive coupling of benzyl bromides by the Sauvage group.<sup>12</sup> In contrast to two former preliminary works of the Kutal group and the Mitani group, this catalytic system mediated direct electron transfer with organic molecule (via oxidative quenching). The reaction of 5-nitrobenzyl bromide with the catalytic system furnished a corresponding benzyl radical under near visible light irradiation (>350 nm). The resulting Cu(II) species is reduced to Cu(I) by a sacrificial electron donor, NEt<sub>3</sub>.

Inspired by the seminal works of the Mitani group and the Sauvage group, the Reiser group which is one of the pioneers in Cu-photocatalysis, and other groups have expanded Cu-catalyzed ATRA into a variety of organic halides and alkenes.<sup>4-5</sup> For example, photo-induced Cu-catalyzed ATRA with trifluoromethanesulfonyl



**Scheme 4.4** Early examples of copper photocatalysis

■ ATRA of CF<sub>3</sub>SO<sub>2</sub>Cl (2015): selectivity variation by photocatalyst



**Scheme 4.5** Visible light induced C–N bond formation via copper photocatalysis

chloride CF<sub>3</sub>SO<sub>2</sub>Cl were developed using various photocatalysts to control reactivity (Scheme 4.5).<sup>13</sup> Sterically less demanding [Cu(dpp)(binc)]Cl complex bearing a bis(isonitrile) ligand resulted in higher selectivity toward chlorosulfonation over chlorination (9:1, 83% yield). However, sterically bulkier Cu-complexes [Cu(dap)<sub>2</sub>]Cl led to increased reactivity toward chlorination (3:1, 79% yield). In the reactions, a copper-ligand species engaged in the SO<sub>2</sub>Cl transfer into the product, wherein steric effect affected whether a radical attacks chlorine or sulfur. It is worthwhile to note that [Ru(bpy)<sub>3</sub>]Cl<sub>2</sub> showed the converse selectivity to chlorination.<sup>13b,14</sup>

In summary, Cu photosensitizers have received attention as complementary photocatalysts to common Ru- and Ir-based complexes. With the advantage of strong reduction ability of Cu(I) excited state, Cu-based photocatalysis successfully promoted various organic transformations including [2+2]-cycloaddition and ATRA reactions.

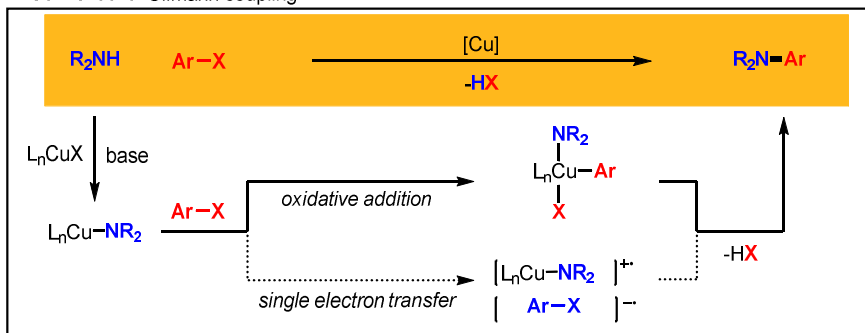
### 4.3 Copper-based photocatalysis for cross-coupling reactions

Cross-coupling chemistry is a powerful tool for constructing a variety of carbon–carbon and carbon–heteroatom bonds. In spite of remarkable achievements in transition metal-catalyzed cross-coupling reactions, the development of more mild, selective, and efficient catalytic systems based on earth-abundant metal complexes is still a challenge. In this section, on the basis of pioneering work reported by the Fu and Peters groups, the progress and principle of photo-induced Cu-catalyzed cross-coupling reactions will be introduced. Additional examples for the application of this methods developed by other groups will also be described.

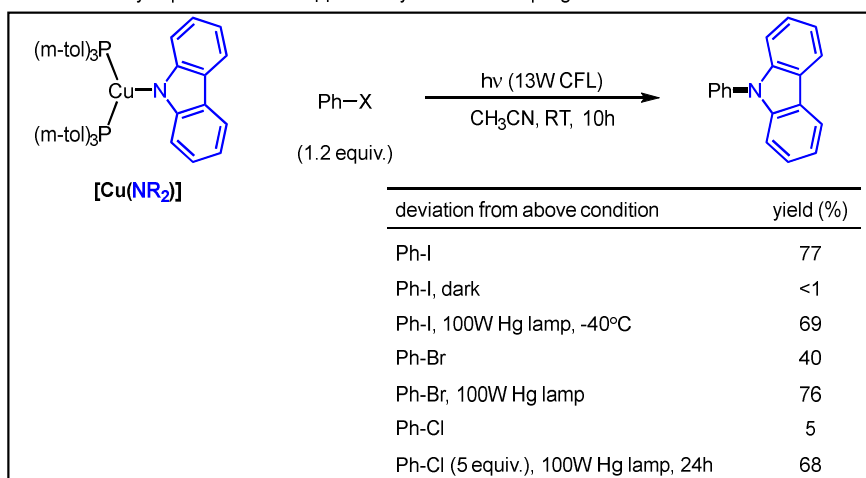
#### 4.3.1 Pioneering works of Fu and Peters groups in copper photocatalysis for cross-coupling reactions

Since the Fu and Peters groups reported the first discovery of a photo-induced Cu-catalyzed Ullmann-type *N*-arylation under unusually mild conditions ( $\leq 0^\circ\text{C}$ ),<sup>15</sup> these two groups together have thoroughly investigated “expansion of the substrate scopes to various nucleophiles (nitrogen: carbazoles, indoles, imidazoles, amides, aliphatic amines, and carbamates / sulfur: thiols, / oxygen: phenol, / carbon: cyanide) and electrophiles (aryl, alkyl, alkenyl, and alkynyl halides)”,<sup>15-16</sup> “irradiation by visible-light from ultra-violet light”,<sup>16f-h,17</sup> “asymmetric version”,<sup>17</sup> and “mechanistic studies”.<sup>18</sup>

■ Conventional Ullmann coupling



■ The discovery of photoinduced copper catalyzed cross-coupling reaction



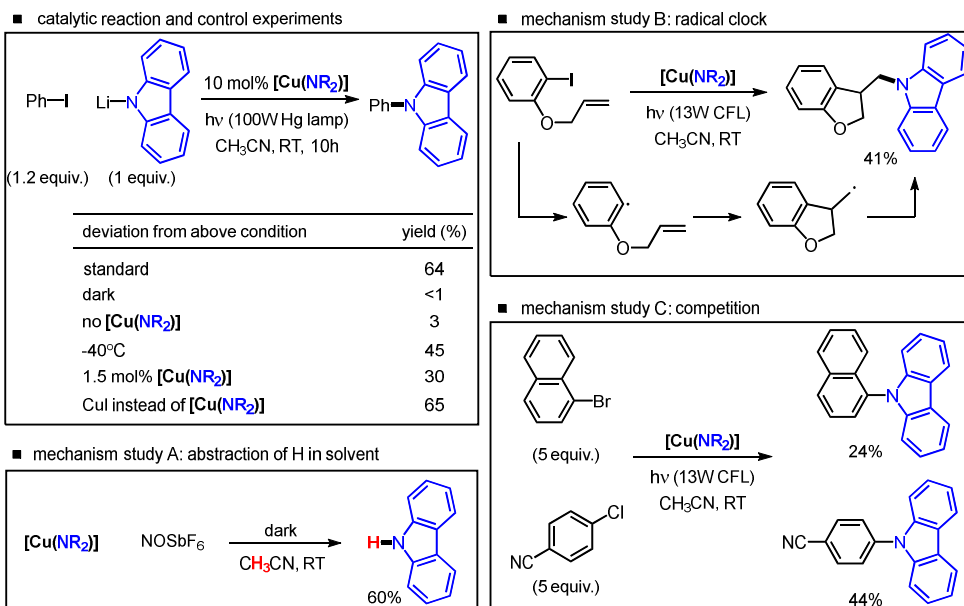
**Scheme 4.6** First discovery of photo-induced copper-catalyzed cross-coupling: Ullmann-type C–N bond formation

In 2012, the first photoinduced Cu-catalyzed cross-coupling reaction was reported for highly mild Ullmann type *N*-arylation of carbazole species (Scheme 4.6).<sup>15</sup> Ullmann reaction is a powerful method for C–N bond formation in the presence of stoichiometric copper salt under heating condition (> 180°C). Despite its improvement in reaction efficiency, the elucidation of the mechanism in Cu-mediated Ullmann process is not fully accomplished but suggests a Cu–NR<sub>2</sub> complex as a key species. Major proposal for its mechanism is oxidative addition of Cu(I) species with aryl halide to form Cu(III) adduct and subsequent reductive elimination

to furnish the product. Though one calculation result suggested SET process, no direct experimental evidence was reported before this work. In their preliminary study,  $(\text{PPh}_3)_2\text{Cu}(\text{cabazolide})$  species was proven photoluminescent when irradiated in 300–400 nm region.<sup>19</sup> On the basis of the observation, the Fu and Peters groups hypothesized that  $\text{Cu-NR}_2$  species could reveal the SET reactivity of Ullmann reaction but also mediate C–N bond formation under irradiation. At the outset, a similar but much soluble copper complex  $[(\text{P}(m\text{-tol})_3)_2\text{Cu}(\text{cabazolide})]$   $[\text{Cu}(\text{NR}_2)]$  was prepared and applied to the reaction with iodobenzene under photo-irradiation (13W CFL), which successfully furnished the C–N adduct with high yield (77%). Irradiation is essential for the conversion, regarding that no conversion was obtained under dark condition. Even at low temperature ( $-40\text{ }^\circ\text{C}$ ), reaction proceeded quite well under rather harsh irradiation (69% yield). It is worthwhile to note that previously reported cross-coupling reactions of carbazole with iodobenzene require at least  $90\text{ }^\circ\text{C}$  heating conditions. Even aryl bromide and chloride bearing stronger carbon–halide bonds are reactive under the method, although the modified conditions such as intense irradiation or excessive use of coupling partner are necessary for high conversion. In terms of electrochemistry, the conversion seems reasonable in the accordance of reduction potentials ( $\text{Ph-I}$ ,  $-1.91\text{ V}$ ;  $\text{Ph-Br}$ ,  $-2.43\text{ V}$ ;  $\text{Ph-Cl}$ ,  $-2.76\text{ V}$  vs. SCE in DMF;  $[\text{Cu}(\text{NR}_2)]$ ,  $-2.6\text{ V}$  vs. SCE in  $\text{CH}_3\text{CN}$  on a platinum electrode).

Continuous turnover to achieve catalytic Ullmann type reaction was successful in the reaction of lithium carbazolide with iodobenzene at  $-40\text{ }^\circ\text{C}$  (Scheme 4.7). Like the stoichiometric reaction, both irradiation and catalyst are essential for





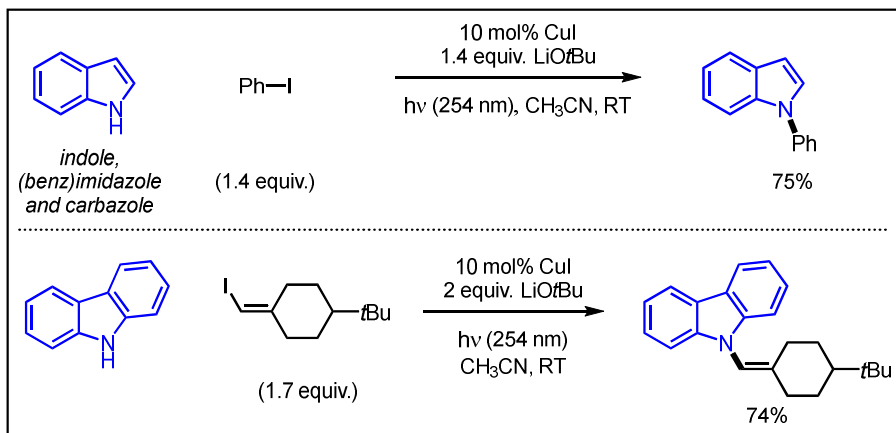
**Scheme 4.7** Catalytic version of this method and mechanism studies

the catalytic reaction. In the presence of stoichiometric lithium carbazolidate as a N-source, simple copper iodide salt is catalytically active instead of [Cu(NR<sub>2</sub>)]. Comprehensive investigations were carried out to shed light on the mechanism of the photo-induced Cu-catalytic system. On the basis of the observation of side products (carbazole, Ph-H, NCCH<sub>2</sub>-CH<sub>2</sub>CN, iodobiphenyl), SET process was proposed for plausible mechanism. In order to confirm whether a Cu(II) species which is in situ-generated from copper radical cation in SET engages in the catalysis, low temperature (77 K) electron paramagnetic resonance (EPR) was conducted in the reaction of [Cu(NR<sub>2</sub>)] with iodobenzene at -40 °C under 100W Hg lamp irradiation. In EPR spectrum, the strongly anisotropic *g*-values indicate that metalloradical Cu(II) species is certainly generated during catalysis. The chemical oxidation of [Cu(NR<sub>2</sub>)] under the oxidant Magic Blue, [tris(4-bromophenyl)aminium hexachloridoantimonate] gave the similar results, which

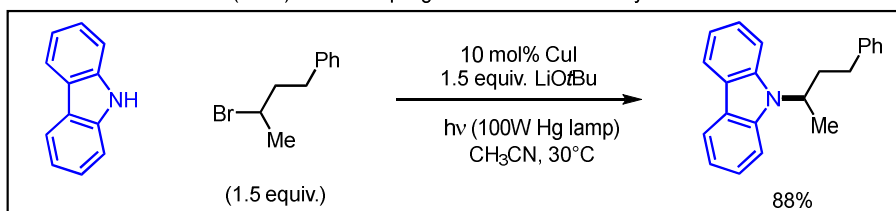
advocates the existence of Cu(II) species. Further studies to demonstrate radical intermediacy were conducted; First, oxidative condition to generate copper carbazole radical cation was adopted to check whether carbazole is generated or not. The reaction resulted in moderate amount of carbazole (60%), which was also observed as a side product from SET process. Next, the reaction of radical clock on aryl iodide, 2-(allyloxy)iodobenzene also exclusively afforded a cyclized product. Additionally, the competition reaction with two different aryl halides to distinguish between concerted oxidative addition and SET pathway was conducted using 1-bromonaphthalene and 4-chlorobenzonitrile (in the same molar ratio). If the concerted oxidative addition occurs, a C–X bond cleavage may prefer to weaker C–Br bond in 1-bromonaphthalene. However, if SET process takes place, 4-chlorobenzonitrile (-2.03 V vs. SCE in DMF) should be more reactive than 1-bromonaphthalene (-2.17 V). The reaction furnished the major product generated from the aryl chloride, which indicates a radical intermediacy and SET process in the catalysis. This seminal work established the mechanistic principles and potential for further application to other cross-coupling reactions.

In 2013, a variety of amine surrogates and electrophiles (amine surrogates: *N*-heterocycles including indoles, imidazoles, and benzimidazoles; electrophiles: hindered/deactivated/heterocyclic Ar–I, an Ar–Br, an activated Ar–Cl, alkenyl halides, and an alkynyl bromide) were also applied under CuI catalyst and LiO*t*Bu base under UV irradiation (Scheme 4.8). In 2013 and 2014, cross-coupling reactions of carbazoles and amides with alkyl iodides and alkyl bromides were demonstrated

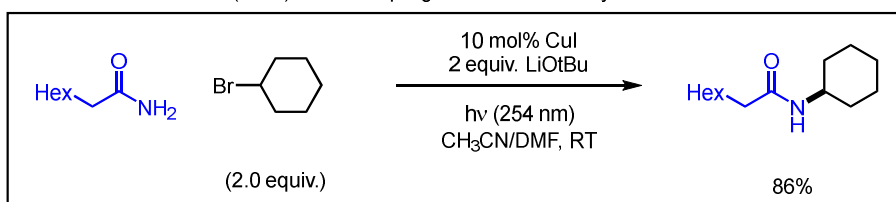
■ C-N bond construction (2013): cross coupling of N-heterocycles with aryl/alkenyl/alkynyl halides



■ C-N bond construction (2013): cross coupling of carbazoles with alkyl halide



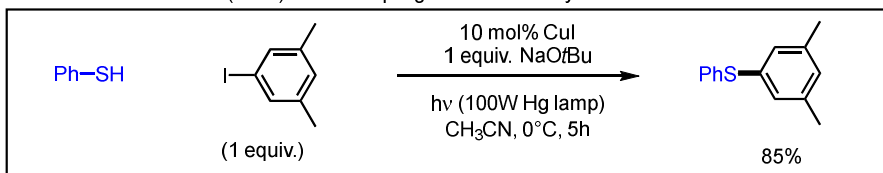
■ C-N bond construction (2014): cross coupling of amides with alkyl halides



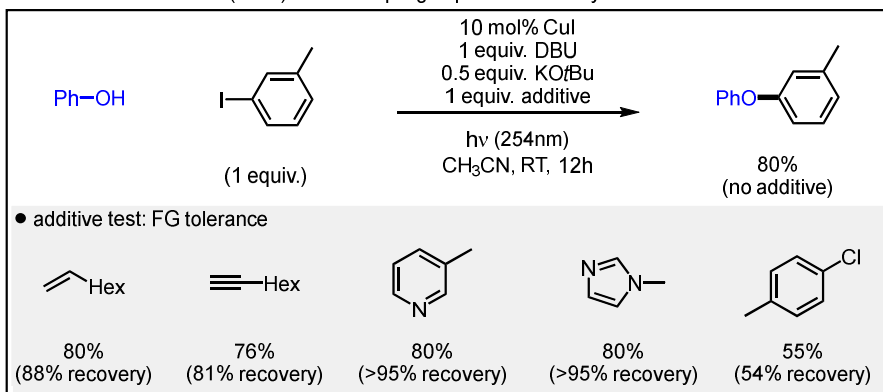
**Scheme 4.8** Scope expansion in C–N bond formation

using this photocatalytic method.<sup>16a,i</sup> Although reactions with amines and alkyl halides via S<sub>N</sub>2 pathway are classic and highly effective C–N bond formation method, sterically hindered primary and secondary alkyl electrophiles require elevated temperature. However, the present copper photocatalytic system enables the reaction of these challenging electrophiles at 0 °C to room temperature.

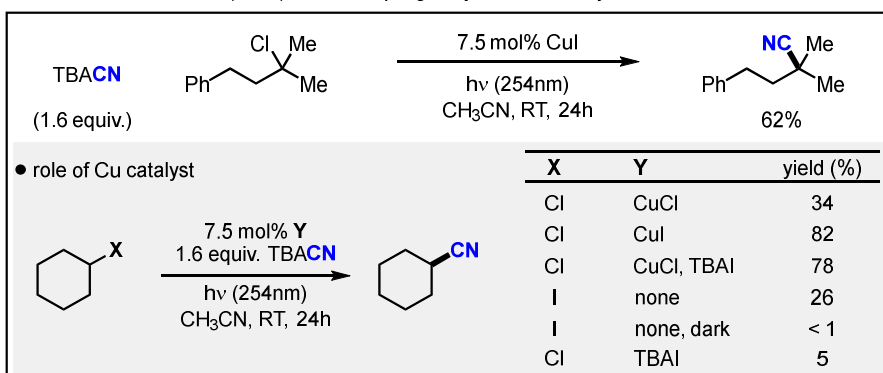
■ C-S bond construction (2013): cross coupling of thiols with aryl halides



■ C-O bond construction (2014): cross coupling of phenols with aryl halides



■ C-C bond construction (2015): cross coupling of cyanide with alkyl halides

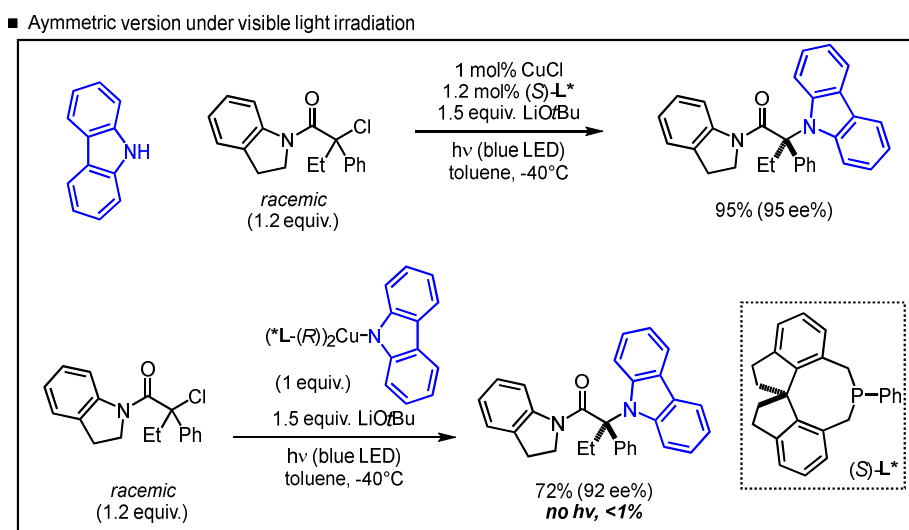


**Scheme 4.9** Various cross-coupling reactions beyond C–N bond formation

The notable advantage of the method is the use of a single set of catalytic conditions (simple copper catalyst and base under irradiation by readily available light sources) for the cross-coupling of a broad range of nucleophiles with a wide array of alkyl and aryl halides in mild condition (Scheme 4.9). In 2013, construction of C(sp<sup>2</sup>)–S bond was achieved from thiols and unactivated aryl iodides, aryl bromides and an activated aryl chloride at very mild condition (0 °C) using the

method.<sup>16b</sup> Likewise, C(sp<sup>2</sup>)-O bond construction for synthesis of diaryl ethers, which are substantial functionalities in pharmaceutical, agrochemical, and polymers, was also achieved at room temperature.<sup>16d</sup> Previously reported methods for C-O bond forming cross-coupling reactions require elevated temperature ( $\geq 60$  °C) even in the presence of highly active Pd catalysis. In this report (2014), wide functional group tolerance was demonstrated by additive tests in the reactions of phenol with 3-iodotoluene. When alkene, alkyne, pyridine, imidazole, and benzoxazole are present, nearly no inhibition was observed along with the additive intact in most cases. However, 4-chlorotoluene and 2-propionylfuran inhibited the conversion concomitantly with loss of additive. Moreover, this method was applied to C(sp<sup>3</sup>)-C bond formation for aliphatic nitrile synthesis from cyanide and unactivated secondary alkyl halides in 2015.<sup>16e</sup> Representative synthetic protocol for aliphatic nitrile is S<sub>N</sub>2 reaction but it suffers from side reactions including bimolecular elimination (E2). Notably, the photo-induced Cu-catalytic system promoted the reaction under mild condition (room temperature), while previous cyanations with unactivated secondary alkyl chlorides proceeded efficiently only at temperature above 75 °C. Regarding the superior activity of CuI over CuCl, additional study in the reactions of cyclohexyl chloride was conducted to elucidate the role of CuI. The combination of CuCl with TBAI that may in situ generate CuI via anion exchange resulted in the similar reactivity (82%) with sole CuI (78%). Regarding the potential process with alkyl iodide which can be generated from S<sub>N</sub>2 displacement of alkyl chloride with free iodide, the reactions of alkyl iodides showed diminished reactivity (26%) under the original condition and shut down under dark condition. As C(sp<sup>3</sup>)-I bond cleavage is likely to occur under 254 nm irradiation, copper-free condition

may occur. However, the reaction of cyclohexyl chloride with TBAI furnished only negligible amount of the product in the absence of Cu, which demonstrates the critical role of Cu catalyst.

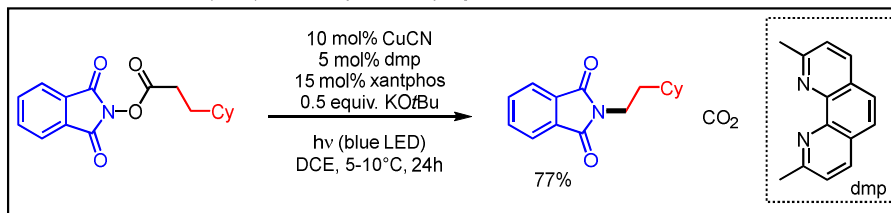


**Scheme 4.10** First asymmetric version of copper catalyzed cross-coupling reaction under visible light irradiation

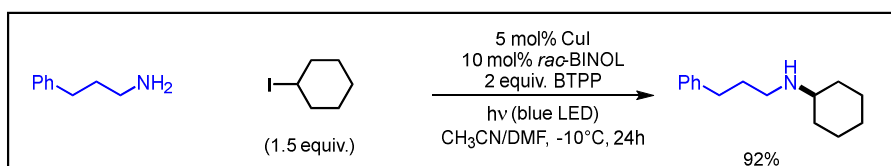
In 2016, there were two significant improvements achieved in the photo-induced Cu catalytic systems: asymmetric version and visible light irradiation instead of harsh UV light (Scheme 4.10).<sup>17</sup> Although several asymmetric variants of organic reactions were mediated by Ru- and Ir-based photoredox catalysis, photo-induced Cu-catalyzed asymmetric formation of such C–N bonds was uncommon. The Fu and Peters groups realized the Cu-catalyzed enantioconvergent cross-coupling reactions of racemic tertiary alkyl halides with amines under visible light irradiation by adopting a chiral phosphine ligand **L\***. A Cu-nucleophile adduct bearing the chiral ligand [(**L\***)<sub>2</sub>Cu(carbazolide)], which was independently prepared

and structurally characterized by X-ray single crystallography, was active for the stereoselective transformation.

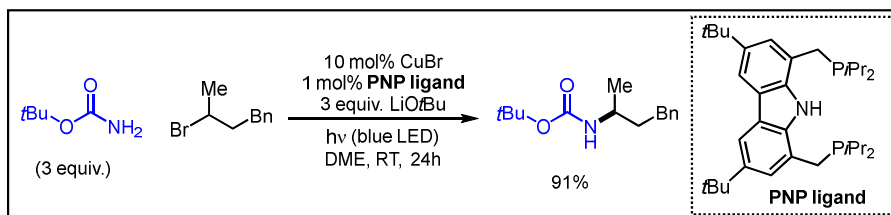
■ C-N bond construction (2017): decarboxylative coupling with NHP esters



■ C-N bond construction (2017): monoalkylation of primary amine with alkyl iodides



■ C-N bond construction (2017): monoalkylation of carbamates with alkyl halides



**Scheme 4.11** Visible light induced C–N bond formation via copper photocatalysis

Inspired by the seminal work (2016), the combination of Cu catalyst and additional ligand system promoted rather challenging cross-coupling reactions under mild visible light irradiation (Scheme 4.11). In 2017, the establishment of C–N bond using *N*-hydroxyphthalimide (NHP) esters as both organic radical and amine sources was demonstrated by applying this Cu-based photocatalysis.<sup>16f</sup> In the comparison of the Curtius rearrangement of acyl azides, where carboxylic acids are used as substrates like the Cu-based photocatalysis, the catalytic system (combination of

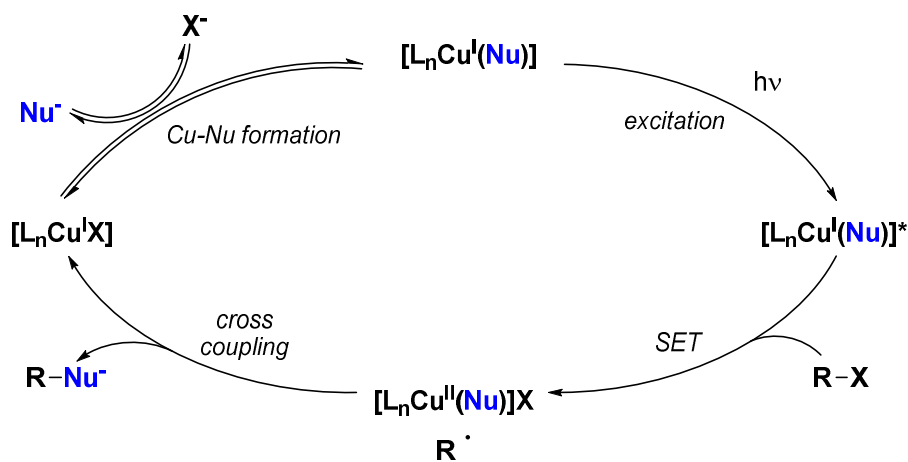
copper cyanide, 2,9-dimehtyl phenanthroline ligand, and xantphos ligand) poses no explosive hazard.

In the scope of nucleophiles in the all of the reported coupling reactions using this method, the nucleophilic site is a part of  $\pi$  systems (N: carbazole, indole, and imidazole; S: aryl thiol; O: phenol; C: cyanide) and other nucleophiles without  $\pi$  system were unsuccessful. Probably, the relevance between  $\pi$  system and reactivity is induced at the step of initial photoexcitation and/or electron transfer from a photoexcited state to an electrophile.

However, the combination of *rac*-BINOL ligand and *tert*-butylimino-tri(pyrrolidino)phosphorene (BTTP) base enabled the visible light induced Cu-catalyzed monoalkylation of primary amines with alkyl iodides.<sup>16g</sup> Another challenging nucleophiles, carbamates were also applied successfully into this type of cross-coupling reactions with unactivated secondary alkyl bromides.<sup>16h</sup> The combination of copper bromide (10 mol%) and carbazole-based PNP-pincer ligand **PNP ligand** (1 mol%) with different loadings may enable the catalytic conversion by promoting the out-of-cage bond formation process rather than the in-cage bond formation. The detailed mechanistic discussion will be described in following paragraphs.



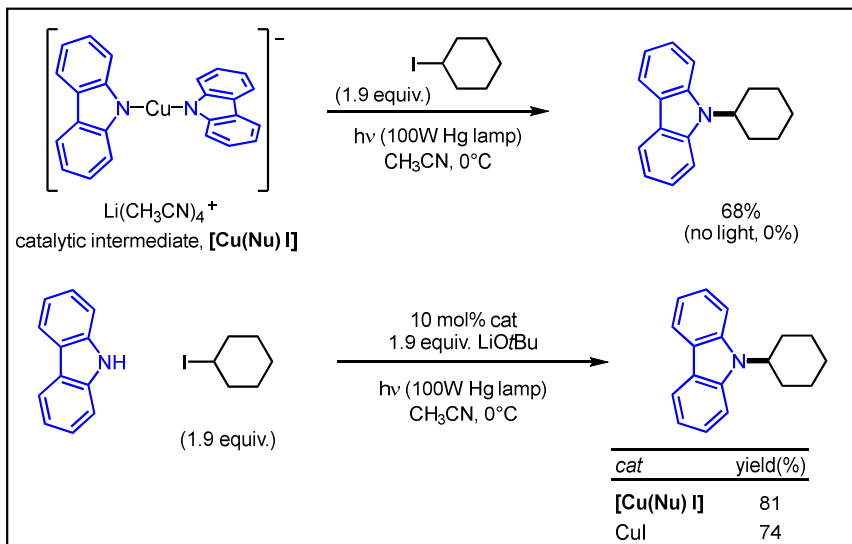
### 4.3.2 Mechanistic investigation of copper photocatalysis for cross-coupling reactions by Fu and Peters groups



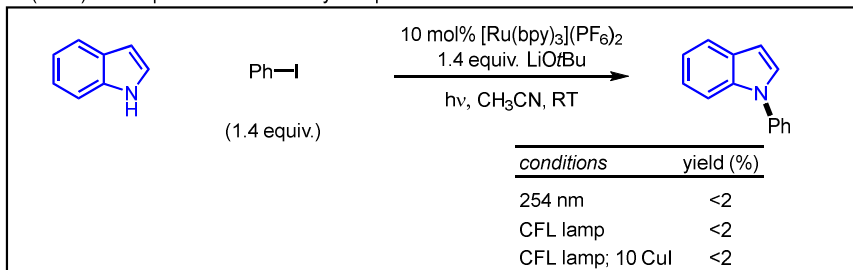
**Scheme 4.12** General mechanism of copper-based photocatalysis for cross-coupling

Outlined is the generally proposed mechanism in copper-based photocatalytic cross-coupling reactions (Scheme 4.12): formation of a Cu(I)-nucleophile complex by anion exchange, photoexcitation of a Cu(I)-nucleophile complex, SET with an organic electrophile ( $R-X$ ) to afford a Cu(II)-nucleophile complex and an organic radical ( $R\cdot$ ). These two intermediates couple to form the desired product ( $R-Nu$ ) and regenerate a Cu(I)-halide complex. The preliminary studies in line with Scheme 4.7 were carried out in each cross-coupling reaction (Scheme 4.13). The Cu(I)-nucleophile complex  $[Cu(Nu) I]$  directly undergoes cross-coupling with alkyl iodide only under irradiation.<sup>16a</sup> Besides,  $[Cu(Nu) I]$  was catalytically competent, showing similar activity to the original copper iodide catalyst. Regarding electron transfer, photoredox catalysis also transfers electrons with organic molecules but did not directly engage in inner-sphere bond-forming

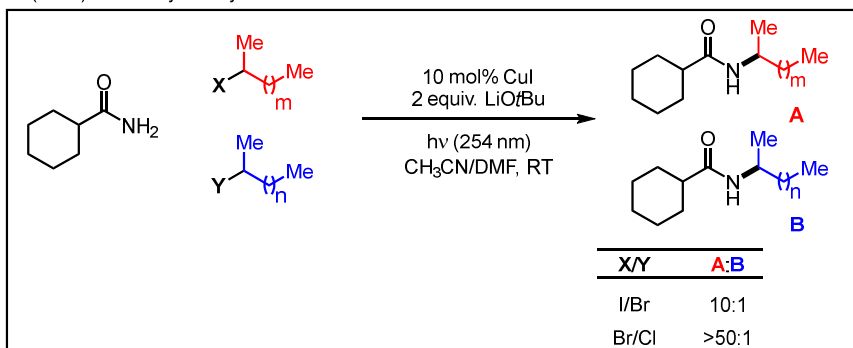
- (2013) Cu(Nu) species: catalytically active in cycle



- (2013) inner-sphere mechanism by comparison



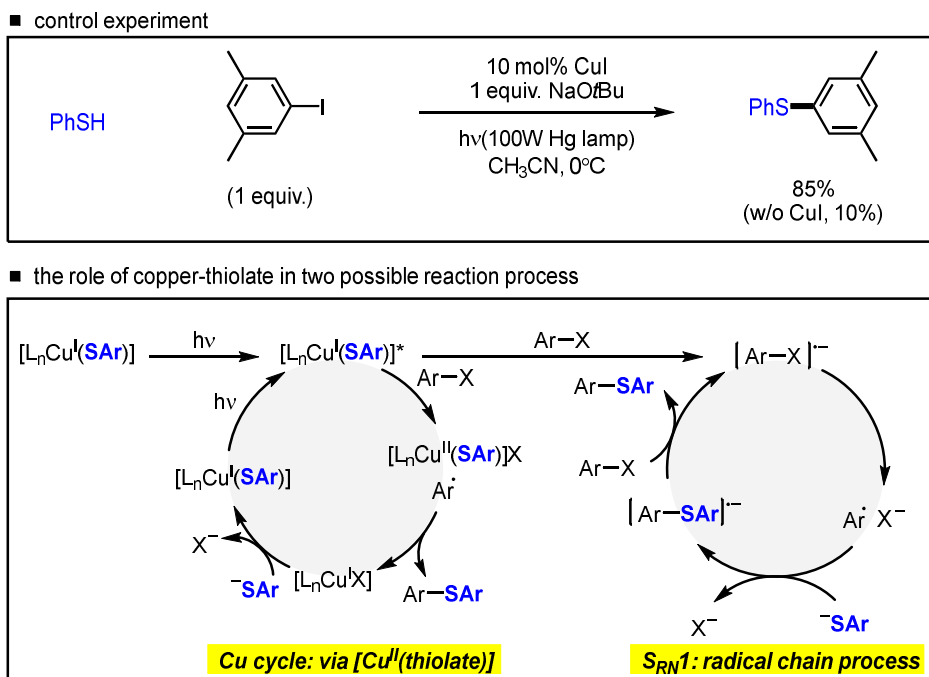
- (2014) selectivity of alkyl halides



**Scheme 4.13** Preliminary mechanistic studies in C–N cross-coupling reactions

processes. As a control experiment, [Ru(bpy)<sub>3</sub>](PF<sub>6</sub>)<sub>2</sub> was used as a catalyst instead of CuI in the reaction with indole and iodobenzene for Ullmann-type C–N bond formation under the standard conditions, but was not competent at all. Competition

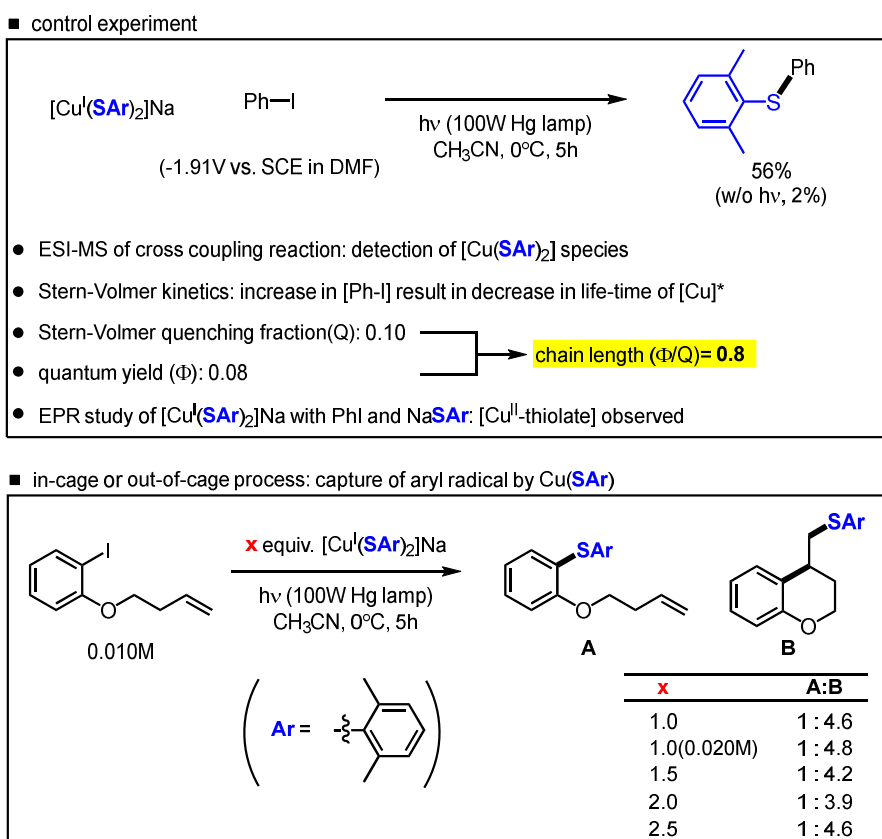
reactions of cyclohexanecarboxamide with two different alkyl halides were carried out to investigate reactivity tendencies in alkyl halides.<sup>16i</sup> The reactivity order (Alk-X: I > Br > Cl) was in accordance with the propensity for electron transfer and single-electron reduction.<sup>20</sup>



**Scheme 4.14** Significant role of copper–thiolate in C–S cross-coupling process

Further detailed mechanistic investigations were conducted in 2016 and 2017.<sup>18</sup> In the cross-coupling of aryl thiols and aryl halides,<sup>16b,18a</sup> comprehensive investigation of the role of copper–thiolate and each elementary step in photocatalysis was carried out (Scheme 4.14).<sup>18a</sup> The model reaction of photo-induced C–S cross-coupling proceeded more rapidly in the presence of Cu catalyst than in its absence. As the reaction mixture was heterogeneous, which indicated the

existence of sodium thiolate NaSAr, a lower amount of NaSAr might undergo C–S bond formation via copper-free pathway. In the  $S_{RN}1$  pathway—which was the most viable among copper-free processes—a photoexcited Cu(I)–thiolate engaged in the pathway as the initiating electron donor to aryl halide. As a result of electron transfer, a radical anion was generated that took part in a chain reaction to form thioether. On the other hand, photoexcited Cu(I)–thiolate also engaged in a common Cu-mediated photocatalytic cycle. In this aspect, a Cu(I)–thiolate complex  $[CuI(SAr)_2]Na$ , which was detected from ESI–MS under cross-coupling conditions, was prepared and investigated by a variety of analysis tools.



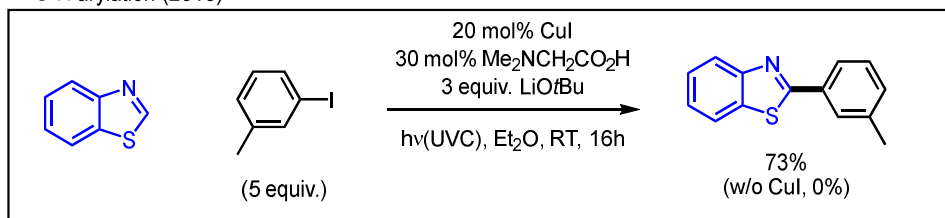
**Scheme 4.15** Detailed mechanistic studies in C–S cross-coupling

$[\text{Cu}^{\text{I}}(\text{SAr})_2]\text{Na}$  is active for cross-coupling with Ph-I (56% yield) at 0 °C, verifying its competency as this model complex for photo-induced copper-mediated S-arylation (Scheme 4.15). In terms of electrochemistry,  $[\text{Cu}^{\text{I}}(\text{SAr})_2]\text{Na}$  exhibits its excited-state reduction potential (around -2.6 V) on the basis of cyclic voltammetry. In terms of photoredox properties, it is excited under irradiation (365 nm) and luminesces with lifetime (approximately 7  $\mu\text{s}$ ) by transient luminescence spectroscopy. By Stern-Volmer kinetics, photoexcited state of  $[\text{Cu}^{\text{I}}(\text{SAr})_2]\text{Na}$  is quenched by Ph-I, which is reasonable regarding their reduction potential (Ph-I: -1.91 V vs. SCE in DMF). By actinometry, the quantum yield ( $\Phi$ ) for the stoichiometric coupling of  $[\text{Cu}^{\text{I}}(\text{SAr})_2]\text{Na}$  with Ph-I when irradiated at 365 nm is 0.08. This value can be induced either by a non-chain or a chain mechanism with rapid termination.<sup>21</sup> Chain length value (0.8) calculated by accommodating Stern-Volmer quenching fraction (Q) and quantum yield ( $\Phi$ ) indicated that less than one product molecule was generated from transfer of one electron, which implies non-chain process. EPR and optical spectroscopy data suggest that a copper(II)-thiolate species is formed when  $[\text{Cu}^{\text{I}}(\text{SAr})_2]\text{Na}$  is subjected to the mixture of Ph-I and NaSAr under irradiation. Moreover, under the chemical condition to induce aryl radical generation through the use of an aryldiazonium salt, two independent reactions in the presence of copper(I)-thiolates and copper(II)-thiolates were carried out. The results showed that cross-coupling is more facile with a copper(II)-thiolate, which advocates competency of copper(II) thiolate in catalytic cycle. To determine whether the photocatalysis follows an in-cage or out-of-cage process, relationship between the amount of  $[\text{Cu}^{\text{I}}(\text{SAr})_2]\text{Na}$  and the ratio of uncyclized/cyclized products using aryl iodide bearing radical clock was studied. If in-cage process in the proposed

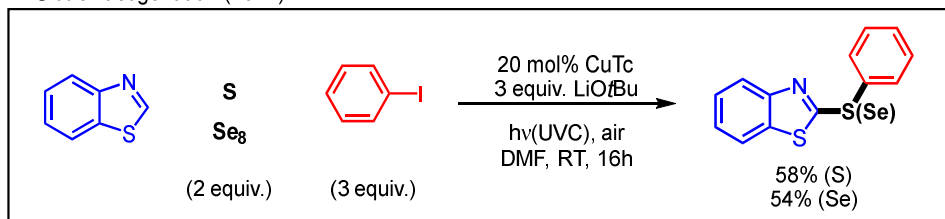
mechanism occurs, the product ratio should remain constant regardless of variation in the quantity of  $[\text{Cu}^{\text{I}}(\text{SAr})_2]\text{Na}$  or the concentration. If out-of-cage process takes place, the product ratio should depend on two factors as two reactants must encounter each other. Since the ratios in any case remain almost constant, the process may undergo in-cage-process during catalytic cycle. In 2017, the mechanism of photoinduced copper catalyzed alkylation of carbazoles was demonstrated as ‘out-of-cage process’ by a variety of analysis tools which were introduced above.<sup>18b</sup>

#### 4.3.3 Contributions of other groups in copper photocatalysis for cross-coupling reactions

##### ■ C-H arylation (2016)



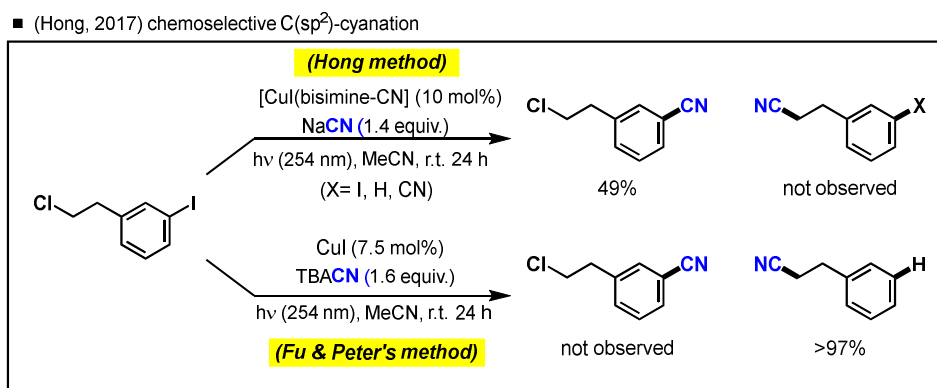
##### ■ C-H chalcogenation (2017)



**Scheme 4.16** Ackerman group: application to C–H activation

The Ackerman group expanded the scope of the photoinduced Cu-catalyzed cross-coupling reactions to C–H activation (Scheme 4. 16). If an aryl nucleophile is generated under transition metal catalysis at basic conditions, the photoinduced Cu-

catalyzed cross-coupling reaction will be operated. In the presence of CuI and the amino acid ligand, C–H arylations of benzothiazoles, benzoxazoles, oxadiazoles, and even non-aromatic oxazolines with aryl iodides were achieved.<sup>22</sup> This method is highly mild while the previously reported Cu-catalytic methods required harsh conditions (120–160 °C). In 2017, the same group also achieved C–H chalcogenation (S and Se) of (benzo)thiazoles under the very similar Cu-based photocatalytic system.<sup>23</sup>



**Scheme 4.17** Hong group: application to chemoselective C(sp<sup>2</sup>)-cyanation

The Hong group realized chemoselective and mild cyanation of aryl halide using an easily accessible Cu(I)-bisimine complex as a photocatalyst at room temperature by applying the same strategy (Scheme 4.17).<sup>24</sup> Notably, the Cu(I)-bisimine complex showed chemoselectivity to C(sp<sup>2</sup>)-cyanation over C(sp<sup>3</sup>)-cyanation, which can occur via either S<sub>N</sub>2 process or SET process reported in the work of the Fu and Peters groups.<sup>16c</sup> The detail of this method will be depicted in Chapter 5.

#### 4.4 Conclusion

In this chapter, the key features of photo-induced Cu-based catalytic systems for cross-coupling were introduced along with representative examples: the generality of a single catalytic system (copper(I) complex, base, and irradiation), rather mild conditions compared to previously reported methods (-40 °C to room temperature), wide functional group tolerance, and novel mechanism via both electron transfer to organic electrophile and direct participation in the bond formation step as nucleophile source. Recently, more delicate designs of catalytic systems have expanded this activation strategy toward an asymmetric version, C–H activation, and challenging substrates.



## 4.5 References

- (1) G. Ciamician, *Science* **1912**, *36*, 385.
- (2) J. J. Douglas, J. D. Nguyen, K. P. Cole, C. R. J. Stephenson, *Aldrichimica Acta* **2014**, *47*, 15.
- (3) (a) J. W. Tucker, C. R. J. Stephenson, *J. Org. Chem.* **2012**, *77*, 1617. (b) C. Stephenson, T. Yoon, *Acc. Chem. Res.* **2016**, *49*, 2059. (c) C. K. Prier, D. A. Rankic, D. W. C. MacMillan, *Chem. Rev.* **2013**, *113*, 5322. (d) J. M. R. Narayanam, C. R. J. Stephenson, *Chem. Soc. Rev.* **2011**, *40*, 102.
- (4) S. Paria, O. Reiser, *ChemCatChem* **2014**, *6*, 2477.
- (5) (a) O. Reiser, *Acc. Chem. Res.* **2016**, *49*, 1990. (b) D. P. Schwendiman, C. Kutal, *J. Am. Chem. Soc.* **1977**, *99*, 5677. (c) M. Mitani, M. Nakayama, K. Koyama, *Tetrahedron Lett.* **1980**, *21*, 4457.
- (6) N. Armaroli, G. Accorsi, F. Cardinali, A. Listorti, in *Photochemistry and Photophysics of Coordination Compounds I* (Eds.: V. Balzani, S. Campagna), Springer Berlin Heidelberg, Berlin, Heidelberg, **2007**, pp. 69.
- (7) D. R. McMillin, K. M. McNett, *Chem. Rev.* **1998**, *98*, 1201.
- (8) A. Lavie-Cambot, M. Cantuel, Y. Leydet, G. Jonusauskas, D. M. Bassani, N. D. McClenaghan, *Coord. Chem. Rev.* **2008**, *252*, 2572.
- (9) (a) B.-T. Ahn, D. R. McMillin, *Inorg. Chem.* **1978**, *17*, 2253. (b) D. R. McMillin, M. T. Buckner, B. T. Ahn, *Inorg. Chem.* **1977**, *16*, 943. (c) D. G. Cuttell, S.-M. Kuang, P. E. Fanwick, D. R. McMillin, R. A. Walton, *J. Am. Chem. Soc.* **2002**, *124*, 6.
- (10) P. A. Grutsch, C. Kutal, *J. Am. Chem. Soc.* **1979**, *101*, 4228.
- (11) M. Mitani, I. Kato, K. Koyama, *J. Am. Chem. Soc.* **1983**, *105*, 6719.
- (12) J.-M. Kern, J.-P. Sauvage, *J. Chem. Soc., Chem. Commun.* **1987**, 546.

- (13) (a) X. J. Tang, W. R. Dolbier, *Angew. Chem. Int. Ed.* **2015**, *54*, 4246. (b) D. B. Bagal, G. Kachkovskiy, M. Knorn, T. Rawner, B. M. Bhanage, O. Reiser, *Angew. Chem. Int. Ed.* **2015**, *54*, 6999.
- (14) S. H. Oh, Y. R. Malpani, N. Ha, Y.-S. Jung, S. B. Han, *Org. Lett.* **2014**, *16*, 1310.
- (15) S. E. Creutz, K. J. Lotito, G. C. Fu, J. C. Peters, *Science* **2012**, *338*, 647.
- (16) (a) A. C. Bissember, R. J. Lundgren, S. E. Creutz, J. C. Peters, G. C. Fu, *Angew. Chem. Int. Ed.* **2013**, *52*, 5129. (b) C. Uyeda, Y. Tan, G. C. Fu, J. C. Peters, *J. Am. Chem. Soc.* **2013**, *135*, 9548. (c) D. T. Ziegler, J. Choi, J. M. Muñoz-Molina, A. C. Bissember, J. C. Peters, G. C. Fu, *J. Am. Chem. Soc.* **2013**, *135*, 13107. (d) Y. Tan, J. M. Muñoz-Molina, G. C. Fu, J. C. Peters, *Chem. Sci.* **2014**, *5*, 2831. (e) T. S. Ratani, S. Bachman, G. C. Fu, J. C. Peters, *J. Am. Chem. Soc.* **2015**, *137*, 13902. (f) W. Zhao, R. P. Wurz, J. C. Peters, G. C. Fu, *J. Am. Chem. Soc.* **2017**, *139*, 12153. (g) C. D. Matier, J. Schwaben, J. C. Peters, G. C. Fu, *J. Am. Chem. Soc.* **2017**, *139*, 17707. (h) J. M. Ahn, J. C. Peters, G. C. Fu, *J. Am. Chem. Soc.* **2017**, *139*, 18101. (i) H.-Q. Do, S. Bachman, A. C. Bissember, J. C. Peters, G. C. Fu, *J. Am. Chem. Soc.* **2014**, *136*, 2162.
- (17) Q. M. Kainz, C. D. Matier, A. Bartoszewicz, S. L. Zultanski, J. C. Peters, G. C. Fu, *Science* **2016**, *351*, 681.
- (18) (a) M. W. Johnson, K. I. Hannoun, Y. Tan, G. C. Fu, J. C. Peters, *Chem. Sci.* **2016**, *7*, 4091. (b) J. M. Ahn, T. S. Ratani, K. I. Hannoun, G. C. Fu, J. C. Peters, *J. Am. Chem. Soc.* **2017**, *139*, 12716.
- (19) K. J. Lotito, J. C. Peters, *Chem. Commun.* **2010**, *46*, 3690.
- (20) (a) C. P. Andrieux, I. Gallardo, J. M. Savaent, K. B. Su, *J. Am. Chem. Soc.* **1986**, *108*, 638. (b) A. A. Isse, C. Y. Lin, M. L. Coote, A. Gennaro, *The Journal of Physical*

*Chemistry B* **2011**, *115*, 678.

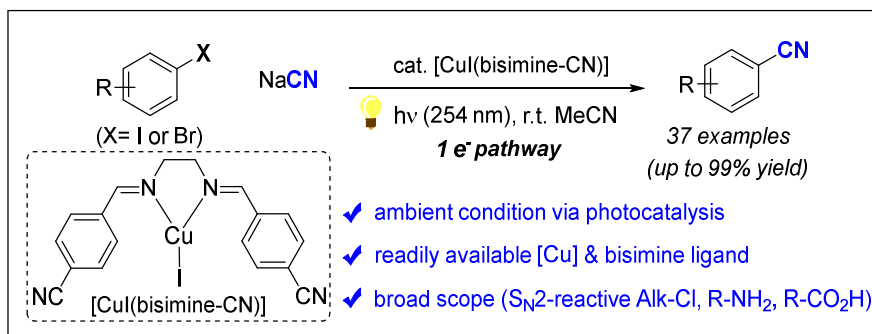
(21) M. A. Cismesia, T. P. Yoon, *Chem. Sci.* **2015**, *6*, 5426.

(22) F. Yang, J. Koeller, L. Ackermann, *Angew. Chem. Int. Ed.* **2016**, *55*, 4759.

(23) P. Gandeepan, J. Mo, L. Ackermann, *Chem. Commun.* **2017**, *53*, 5906.

(24) K. Kim, S. H. Hong, *Adv. Synth. Catal.* **2017**, *359*, 2345.

## Chapter 5. Photoinduced Copper(I)-Catalyzed Cyanation of Aromatic Halides at Room Temperature\*



\* The majority of this work has been published: Kicheol Kim and Soon Hyeok Hong\*, *Adv. Synth. Catal.* **2017**, 359, 2345 – 2351.

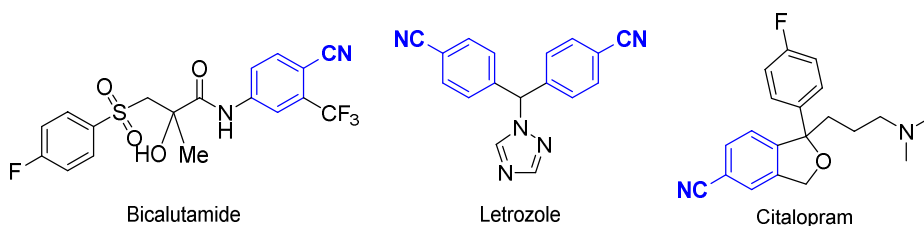
## 5.1 Introduction

Aromatic nitriles have gained significant attention as versatile synthetic intermediates and functional motifs in dyes, pharmaceuticals, and agrochemicals (Scheme 5.1A).<sup>1</sup> Because of their importance, various synthetic protocols have been developed following “addition of one carbon onto the target aromatic ring” concept (Scheme 5.1B).<sup>2</sup> Among the traditional methods, the Rosenmund–von Braun reaction is efficient, but suffers from the use of excess CuCN, tedious purification of the Cu wastes, and high temperature (150–280 °C).<sup>3</sup> Another common method, the Sandmeyer reaction involving the diazotization of anilines suffers from explosion hazard. In industry, ammoxidation with toluene derivatives under high-pressure O<sub>2</sub> and toxic NH<sub>3</sub> at highly elevated temperature (300–550 °C) is commonly used but restricted to a narrow scope due to such harsh conditions.<sup>4</sup>

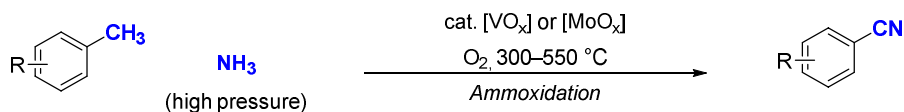
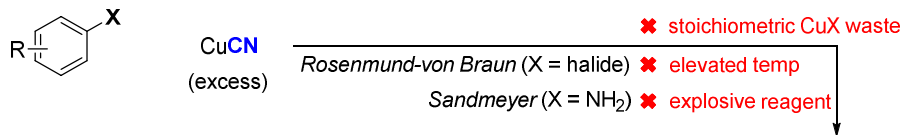
In aromatic nitrile synthesis, catalytic cyanation of aryl (pseudo)halides has been achieved using mainly Pd,<sup>1a,1b,5</sup> Ni,<sup>6</sup> and Cu<sup>7</sup> complexes based on the conventional reactivity of aryl electrophiles with nucleophilic cyanides at elevated temperature. Other catalytic methods via oxidative nitrogenation or C–H cyanation have also been developed.<sup>8</sup> With the advantages of low cost and chemical diversity,<sup>9</sup> Cu-catalyzed C(sp<sup>2</sup>) cyanation methods have been actively developed in the last decade based on a two-electron pathway utilizing Cu<sup>n+</sup>/Cu<sup>(n+2)+</sup> catalytic cycles.<sup>[6]</sup> The CuI and diamine ligand-based catalytic system, developed by the Buchwald group, has shown the widest scope of aryl bromides with a high activity among the reported Cu-based catalysts for sp<sup>2</sup> cyanation.<sup>10</sup> Inspired by recent developments by Fu and Peters,<sup>11,12</sup> we envisioned that photoinduced Cu-catalyzed SET may expand the scope of the reaction, especially with polar and coordinating substrates that could

interfere with two-electron-based inner-sphere-type catalytic systems. Herein, we report the first photoinduced Cu(I)-catalyzed cyanation of aryl halides with readily available NaCN at ambient temperature. Notably, this protocol is compatible with diverse aryl halides, polar reactive functional groups including free amino and carboxylic acid groups, and even S<sub>N</sub>2-reactive alkyl chlorides.

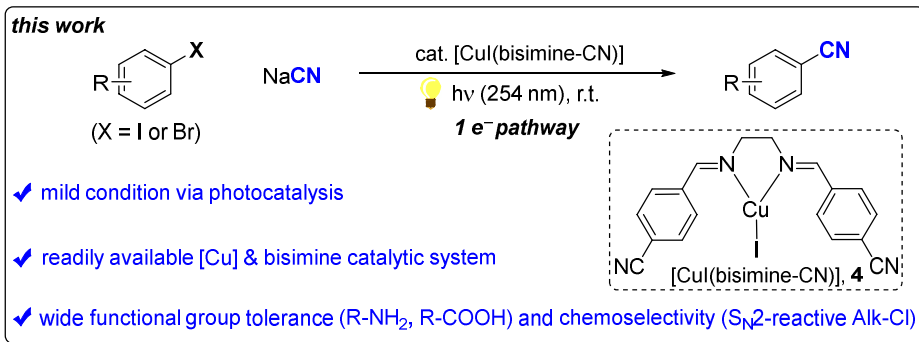
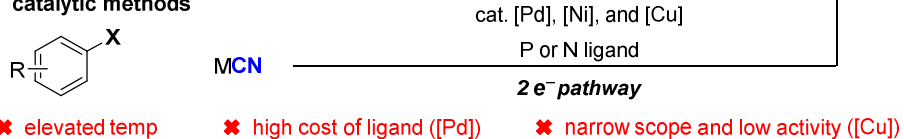
### A) aromatic nitriles in bioactive molecules



### B) stoichiometric methods



### catalytic methods



**Scheme 5.1** Aromatic nitriles: utility and syntheses

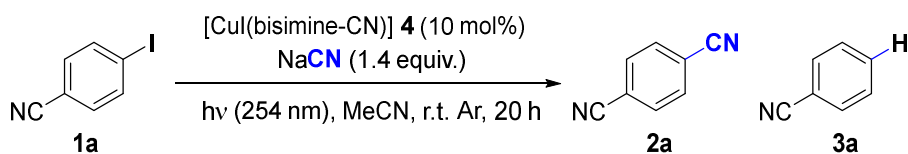
## 5.2 Results and discussion

### 5.2.1 Optimization for cyanation of aromatic halides

Recently, the Lectka group reported that bisimine ligands were especially effective in Cu(I)-catalyzed  $\text{sp}^3$  C–H fluorination via SET.<sup>13</sup> We envisioned that such bisimine ligands would improve catalytic activity by preventing the formation of inactive metal percyanides<sup>14</sup> and by varying the solubility and electronic properties of the catalysts.<sup>14a</sup> Inspired by the photoinduced Cu-catalyzed C( $\text{sp}^3$ ) cyanation of secondary alkyl chlorides,<sup>11,15</sup> the reaction of 4-iodobenzonitrile **1a** with tetra-*n*-butylammonium cyanide (TBACN) was conducted using [CuI(bisimine-CN)] **4** as the photocatalyst under UV-C irradiation ( $\lambda_{\text{max}} = 254$  nm). The desired product **2a** was obtained in a moderate yield at room temperature (entry 1, Table 5.1). To our delight, readily available NaCN was identified as the best cyanide source among the tested cyanide sources including  $\text{K}_4[\text{Fe}(\text{CN})_6]$  (entry 2, see Table 5.3 for further details). Simple Cu(I) salts gave lower yields, especially in the reactions with other aryl iodide (entries 3–5).<sup>16</sup> Visible-light irradiation was not effective (entry 6). With the exclusion of Cu, light, or cyanide the reaction did not produce any product (entries 7–9). Recently, MeCN was reported as a nucleophilic cyanide source when Cu catalysts and oxidants such as  $\text{O}_2$  and TEMPO were used.<sup>17</sup> However, the reaction did not produce the cyanated product without NaCN (entry 9). To our delight, the reaction was comparatively efficient even in presence of air and moisture, demonstrating excellent tolerance of the developed conditions (entries 10 and 11). Reductive dehalogenated product **3a** was observed as the by-product probably by the abstraction of one hydrogen from the solvent by the generated aryl radical. Thus, a

deuterated solvent with stronger C–D bonds than C–H bonds was used to prevent the side reaction, but a diminished yield was obtained (entry 12).

**Table 5.1** Optimization of reaction conditions<sup>a</sup>



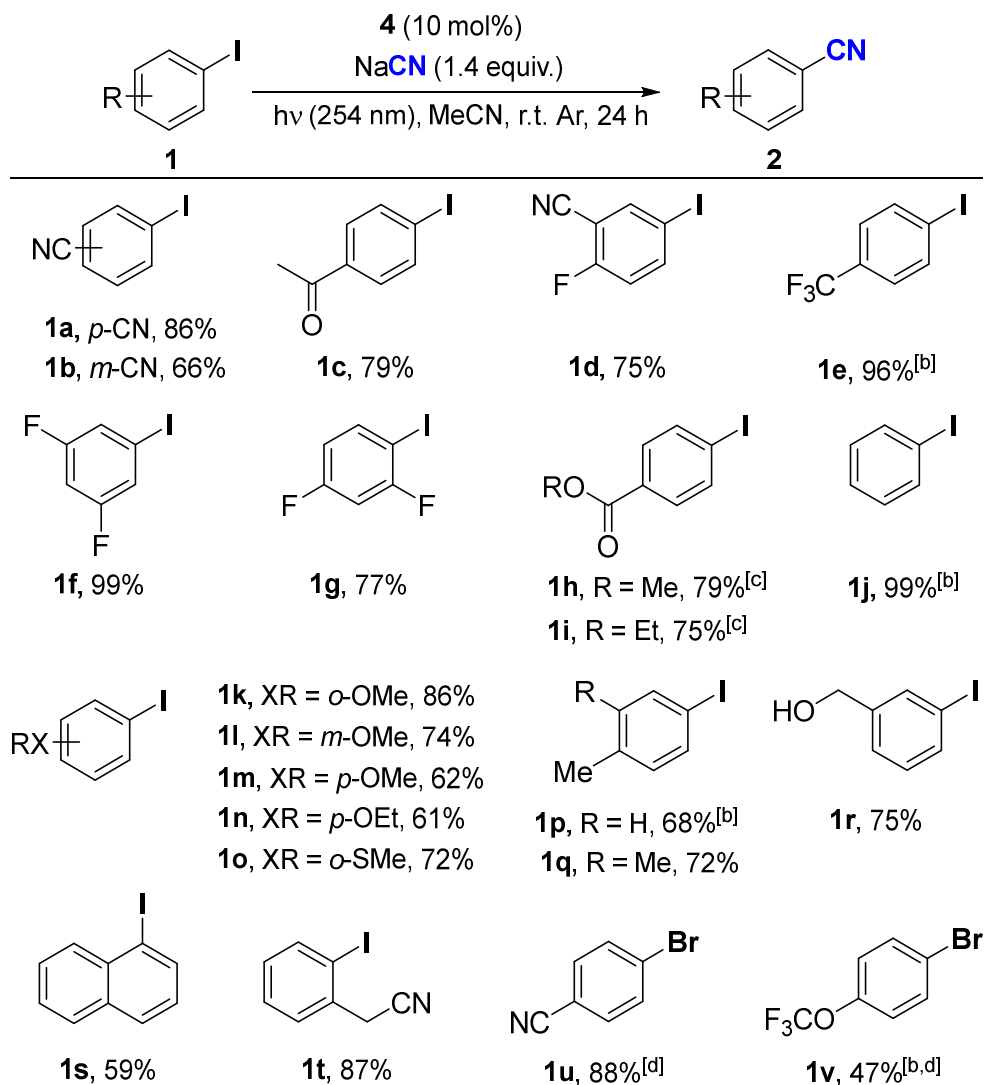
entry	Deviation from above	Conv [%]	<b>2a</b> [%]	<b>3a</b> [%]
1	2.0 equiv. TBACN instead of NaCN	100	59	41
2	none	100	88	12
3	[CuI] instead of <b>4</b>	100	84	16
4	[CuBr] instead of <b>4</b>	100	86	14
5	[CuCl] instead of <b>4</b>	100	74	26
6	$h\nu$ (visible light, 34W blue LED)	0	0	0
7	no [Cu]	0	0	0
8	no $h\nu$	0	0	0
9	no NaCN	59	0	0
10	under air	100	87	13
11	1.0 equiv. H <sub>2</sub> O	100	86	14
12	CD <sub>3</sub> CN instead of MeCN	100	82	0

<sup>[a]</sup> Conditions: **1a** (0.1 mmol), NaCN (1.4 equiv.), **4** (10 mol%), MeCN (0.4 mL), Ar, irradiation using four 15W UV germicidal CFL lamps, r.t. 20 h. Average of 3 runs; determined by NMR using 1,3,5-trimethoxybenzene as the internal standard.



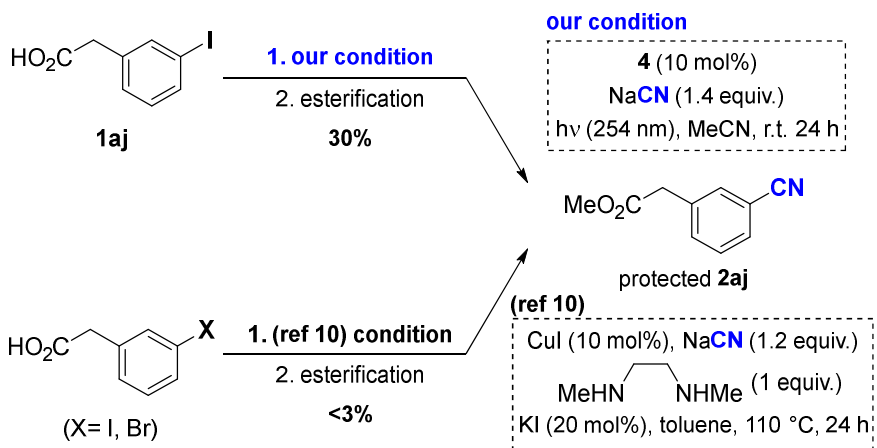
### 5.2.2 Substrate scope

With the optimized reaction conditions, diverse aromatic iodides and bromides were explored (Scheme 5.2). Both electron-rich and -deficient aromatic iodides reacted, affording the products in moderate-to-excellent yields regardless of substitution position. Electron-withdrawing cyano (**1a** and **1b**), acetyl (**1c**), trifluoromethyl (**1e**), fluoro (**1f** and **1g**), and ester groups (**1h** and **1i**) as well as electronically neutral iodobenzene (**1j**) were tolerated. In the case of electron-donating substituents, ether (**1k–n**), thioether (**1o**), alkyl (**1p** and **1q**), and alcoholic (**1r**) groups were compatible. In addition, the developed methods also afforded cyanation with aryl bromides (**1u** and **1v**) in the presence of 30 mol % NaI.

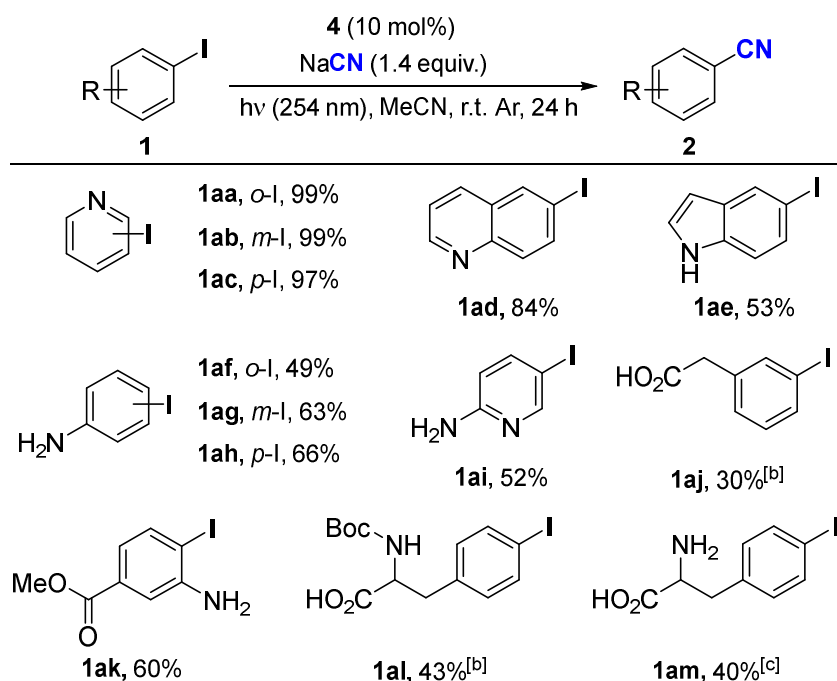


**Scheme 5.2** Scope of aryl halides.<sup>[a]</sup> <sup>[a]</sup> Conditions are same with a in Table 5.1. 0.3 mmol scale. Isolated yields. <sup>[b]</sup> NMR yield. <sup>[c]</sup> 36 h. <sup>[d]</sup> 2 equiv. NaCN and 30 mol% NaI were used.

A carboxylic acid, 3-iodophenylacetic acid (**1aj**), which was not compatible in the previously reported  $\text{Cu}^+/\text{Cu}^{3+}$ -based catalytic system,<sup>10</sup> was cyanated although the isolated yield (30%) after esterification was not so high (Scheme 5.3). Encouraged by the result, we applied the developed method to highly polar functional groups, which were usually less compatible in transition-metal catalysis. The developed method tolerated amino groups, free carboxylic acid, amino acids, and medicinally relevant heterocycles<sup>1c</sup> (Scheme 5.4). Pyridine derivatives including quinolone (**1aa–1ad**) successfully afforded the coupling products in good-to-quantitative yields despite their high affinity toward a transition metal center. Even free indole (**1ae**) and free anilines (**1af–1ai**) were smoothly transformed to the desired products in moderate yields. However, the reactions with thiophene derivatives such as 2-iodothiophene did not give any desired product, affording dehalogenated thiophene only. Notably, amino acid derivatives including unprotected amino acid (**1ak–1am**) were tolerated under the catalytic conditions. It is worthwhile to note that reactions with amino acids such as **1al** under the previously reported  $\text{Cu}^+/\text{Cu}^{3+}$ -based catalytic conditions did not afford the corresponding nitrile at all.



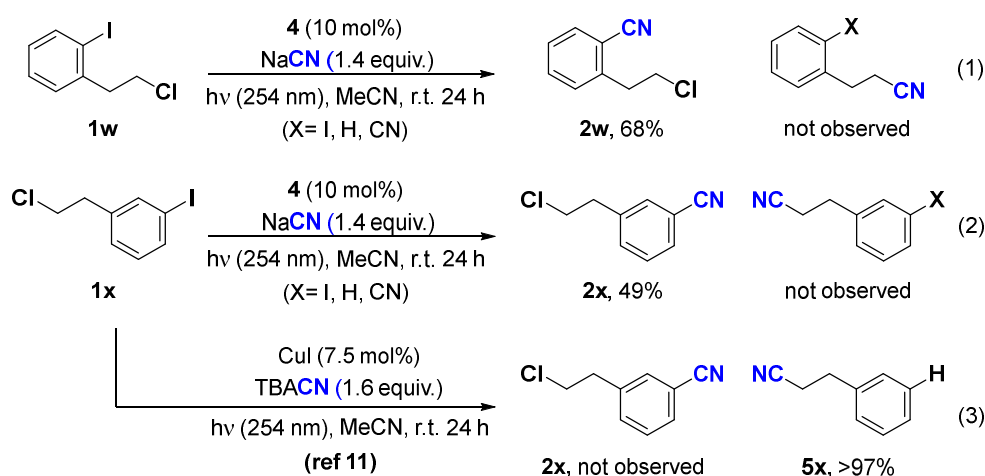
**Scheme 5.3** Cu-catalyzed cyanation: our method and the method in (ref 10)



**Scheme 5.4** Scope of aryl iodides with polar functional groups<sup>[a]</sup> [a] Conditions are same with a in Scheme 2. Isolated yields. <sup>[b]</sup> After the cyanation, the carboxylic acid was esterified <sup>[c]</sup> After the cyanation, the amine was Boc-protected, and then the carboxylic acid was esterified.

### 5.2.3 Chemoselectivity of the method

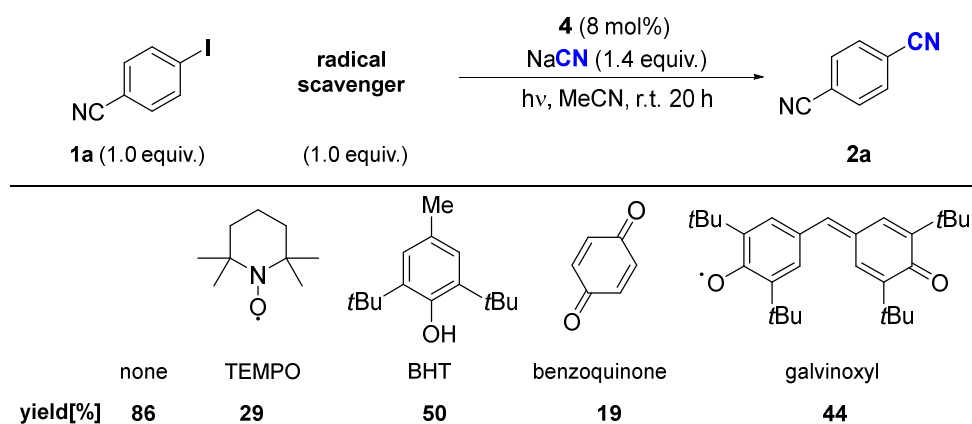
To illustrate the chemoselectivity of the method,<sup>18</sup> two reactions with S<sub>N</sub>2-reactive alkyl chlorides, substituted aryl iodides (**1w** and **1x**) were carried out [Eqs. (1) and (2), Scheme 5.5]. To our delight, this Cu(I) bisimine catalytic system selectively afforded C(sp<sup>2</sup>) cyanated products **2w** and **2x** without C(sp<sup>3</sup>) cyanation on alkyl chlorides, which is difficult to achieve with the previously reported catalytic systems operated at high temperatures. The reaction of **1x** under the reported photoinduced C(sp<sup>3</sup>) cyanation conditions<sup>11</sup> furnished only the C(sp<sup>3</sup>) cyanated and reductively dehalogenated product **5x** in a quantitative yield [Eq. (3), Scheme 5.5]. These results clearly indicate that this method can be used to selectively functionalize aryl rings differently from the traditional S<sub>N</sub>2 and recently reported photocatalytic C(sp<sup>3</sup>) cyanation protocols.



**Scheme 5.5** Chemoselectivity to C(sp<sup>2</sup>) cyanation over S<sub>N</sub>2

## 5.2.4 Mechanistic investigation

Photoirradiation is essential in the developed method as no conversion occurred without light (entry 8, Table 5.1). A light–dark experiment with **1a** further confirmed that the reaction proceeded only with irradiation (Figure 5.1A). The involvement of radical intermediates in photocatalysis was also investigated using four radical scavengers such as TEMPO (Scheme 5.6). All the reactions with **1a** were arrested in moderate-to-high degree (36–67% decrease in yield). Regarding the gradual conversion of aryl iodide (Figure 5.1B) and incomplete inhibition by radical scavengers, a catalytic amount of aryl radical may be present within the solvent cage following closed catalytic cycle rather than a rapid chain process.



**Scheme 5.6** Inhibition with radical scavenger

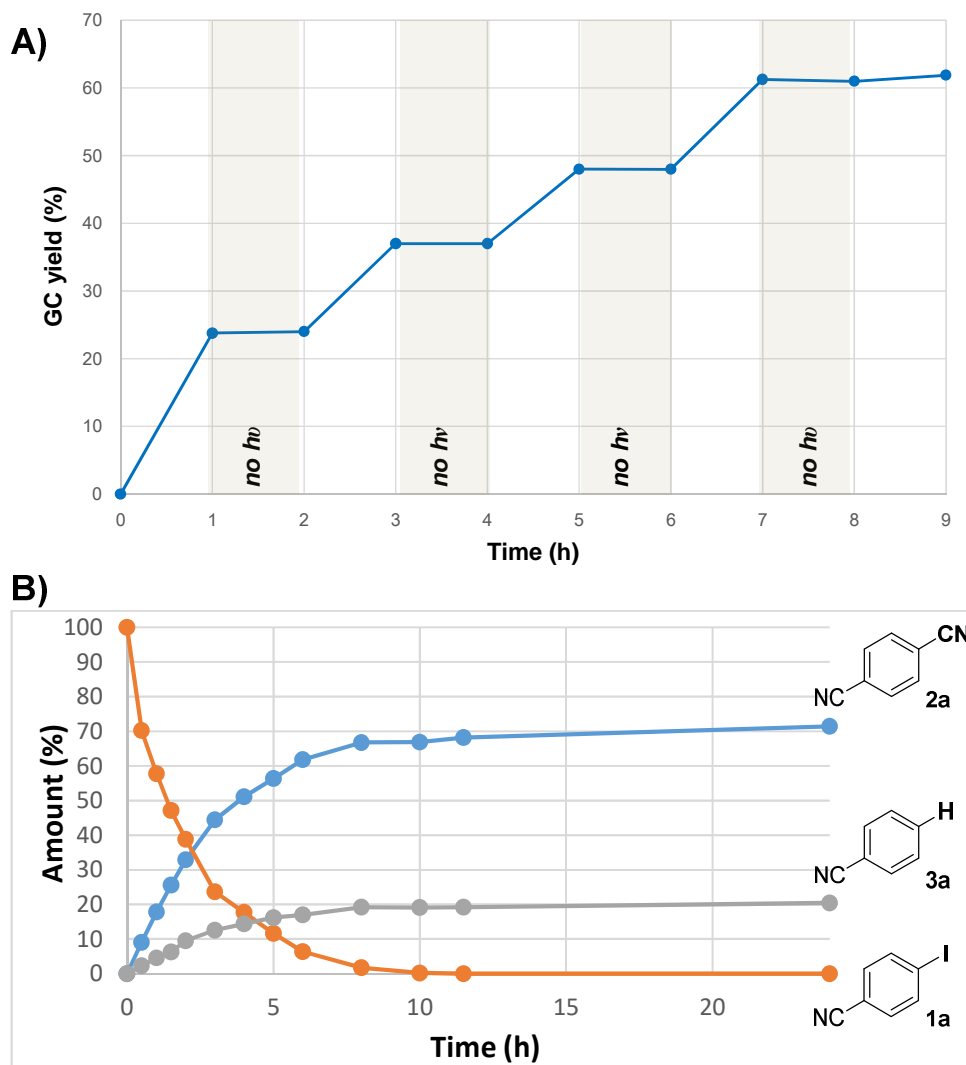
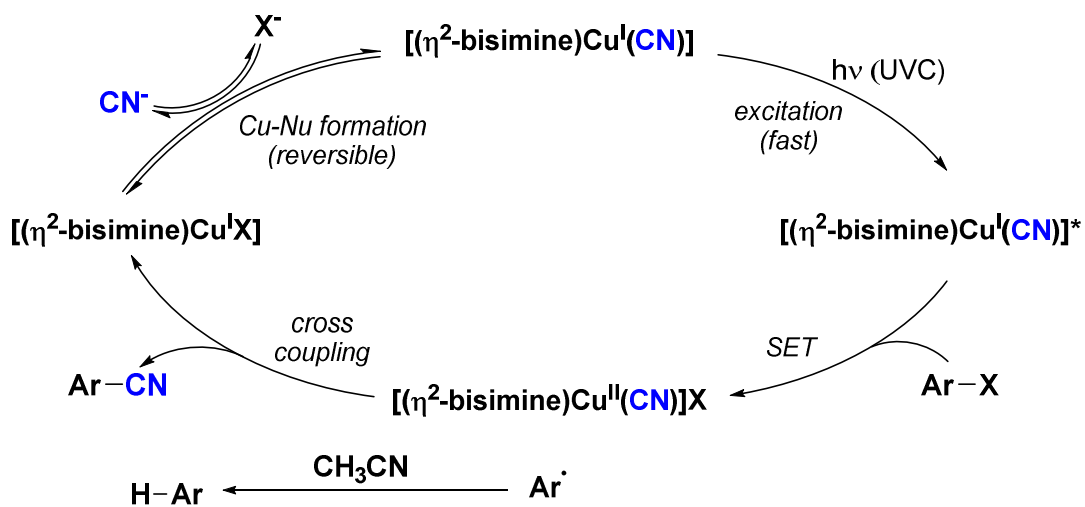


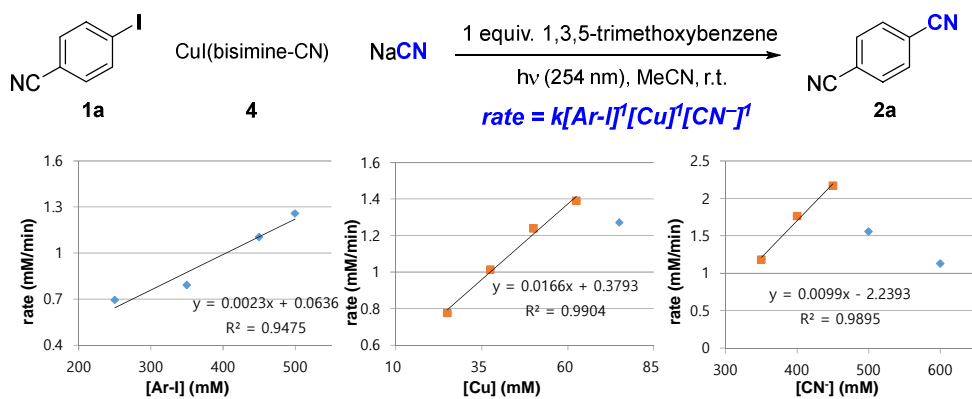
**Figure 5.1** Investigation of photocatalysis. A) light-dark experiment; B) reaction profile during catalysis

Based on the experiments and the previous reports,<sup>11,12h</sup> a plausible mechanism was proposed (Scheme 5.7).<sup>12h</sup> Cu(I) cyanide is formed from Cu(I) halide via anion exchange. The adduct is first photoexcited and then quenched with the aryl halide via SET, furnishing Cu(II) cyanide and an aryl radical. Next, they combine to generate an aromatic nitrile and Cu(I) halide. To gain a deeper mechanistic insight, a kinetic study was performed (Scheme 5. 8). All the reaction species (aryl iodide **1a**, Cu **4**, and cyanide) showed first-order dependence on the concentration. These results indicate that the reaction of copper cyanide adduct with aryl species is the turnover limiting step, which could be the SET or cross-coupling step in the proposed mechanism. Besides, Cu(I) halide seems to be a catalyst resting state in equilibrium via reversible cyanide exchange, regarding the first order of cyanide. Interestingly, a relatively large equivalence of cyanide (up to 1.8 equiv.) compared to copper catalyst did not hamper the reactions. Chelation of the bidentate bisimine ligand presumably inhibits the formation of a percyanide complex. Much higher concentrations of Cu and cyanide hindered the reactions. In high concentrations of Cu, comproportionation of Cu(I) might occur, giving catalytically inactive Cu(0) and Cu(II) species.<sup>19</sup> Similarly, In the presence of excess cyanides, Cu percyanide species could be formed as dead-end species similar to Pd catalysis.<sup>14a</sup>





Scheme 5.7 Plausible mechanism



Scheme 5.8 Kinetic study

### 5.3 Conclusion

In conclusion, we have developed a novel mild cyanation method for aryl halides at room temperature using a Cu(I) photocatalytic system. This method tolerates various functional groups including reactive free amino and carboxylic groups, which were previously incompatible in two-electron-based  $\text{Cu}^{n+}/\text{Cu}^{(n+2)+}$   $\text{C}(\text{sp}^2)$  cyanation reactions. The method also exhibited excellent chemoselectivity in the cyanation of aryl halides even in presence of  $\text{S}_{\text{N}}2$ -reactive alkyl chlorides.

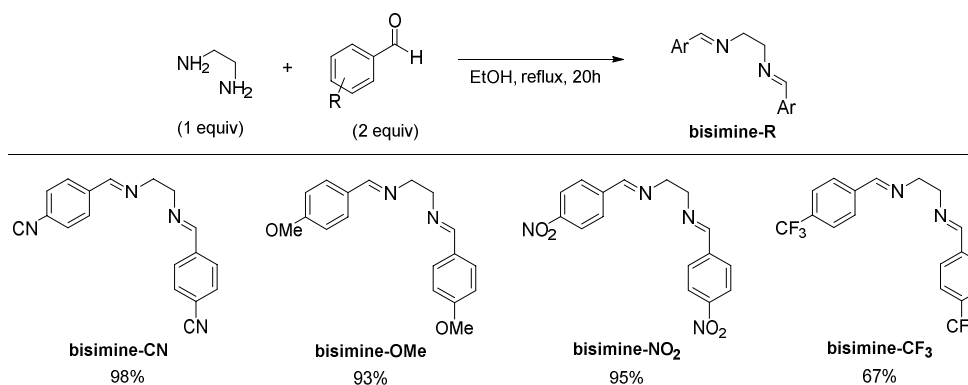
## 5.4 Experimental section

### 5.4.1 General considerations

Unless otherwise noted, reagents were purchased from commercial suppliers and used as received without further purification: CuI (Aldrich) and NaCN (Aldrich and Alfa) were ground using a mortar and dried in vacuum oven. Acetonitrile (anhydrous, Aldrich) was deoxygenated by bubbling argon without further drying. Unless otherwise specified, the reactions were carried out under magnetic stirring in an oven-dried quartz tube equipped with a rubber septum under an inert argon atmosphere. NMR spectra were recorded in CDCl<sub>3</sub>, dimethyl sulfoxide-*d*<sub>6</sub> and the residual solvent signals were used as the reference. The NMR spectral data were processed using the ACD/NMR Processor Academic Edition. Chemical shifts are reported in ppm, and coupling constants are reported in Hz. Multiplicity is indicated by one or more of the following: s (singlet), d (doublet), t (triplet), q (quartet), quin (quintet), and m (multiplet). High-resolution mass spectrometry (HRMS) was performed at Sogang University. GC analysis was carried out using a GC system equipped with an HP-5 column and FID detector and 1,3,5-trimethoxybenzene as the internal standard.

## 5.4.2 Catalyst and substrate preparation

### 5.4.2.1 Preparation of bisimines



Following the literature method,<sup>20</sup> the corresponding benzaldehyde (2 equiv) was added to an ethanolic solution (0.75 M) of ethylenediamine (1 equiv), and the solution was refluxed for 20 h. After the evaporation of the solvent, a yellow oil was obtained, which was crystallized from n-hexane, giving the desired bisimine as a solid.

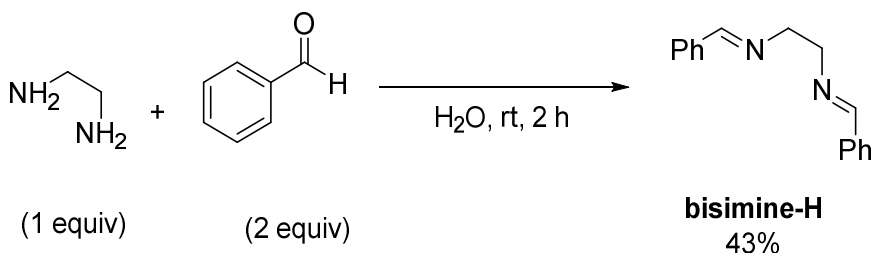
**N,N'-bis(4-cyanobenzylidene)ethylenediamine (bisimine-CN):** 98% isolated yield after reaction for 30 minutes <sup>1</sup>H NMR (CDCl<sub>3</sub>, 300MHz):  $\delta$  = 8.32 (s, 2 H), 7.80 (d,  $J$  = 8.3 Hz, 4 H), 7.69 (d,  $J$  = 8.5 Hz, 4 H), 4.04 ppm (s, 4 H) The spectral data were consistent with those reported in the literature.<sup>21</sup>

**N,N'-bis(4-methoxybenzylidene)ethylenediamine (bisimine-OMe):** 93% isolated yield after reaction for 20 h. <sup>1</sup>H NMR (CDCl<sub>3</sub>, 300MHz):  $\delta$  = 8.22 (s, 2 H), 7.65 (d,

$J = 8.9$  Hz, 4 H), 6.91 (d,  $J = 8.9$  Hz, 4 H), 3.92 (s, 4 H), 3.84 ppm (s, 6 H). The spectral data were consistent with those reported in the literature.<sup>21</sup>

**N,N'-bis(4-nitrobenzylidene)ethylenediamine (bisimine-NO<sub>2</sub>):** light pink solid. 95% isolated yield after reaction for 11 h. <sup>1</sup>H NMR (DMSO-d<sub>6</sub>, 499MHz):  $\delta = 8.52$  (s, 2 H), 8.28 (d,  $J = 8.8$  Hz, 4 H), 7.97 (d,  $J = 9.3$  Hz, 4 H), 3.99 ppm (s, 4 H). The spectral data were consistent with those reported in the literature.<sup>21</sup>

**N,N'-bis(4-trifluoromethylbenzylidene)ethylenediamine (bisimine-CF<sub>3</sub>):** white solid. 67% isolated yield after reaction for 16 h. <sup>1</sup>H NMR (DMSO-d<sub>6</sub>, 499MHz):  $\delta = 8.46$  (s, 2 H), 7.92 (d,  $J = 8.3$  Hz, 4 H), 7.79 (d,  $J = 8.3$  Hz, 4 H), 3.95 ppm (s, 4 H). The spectral data were consistent with those reported in the literature.<sup>21</sup>

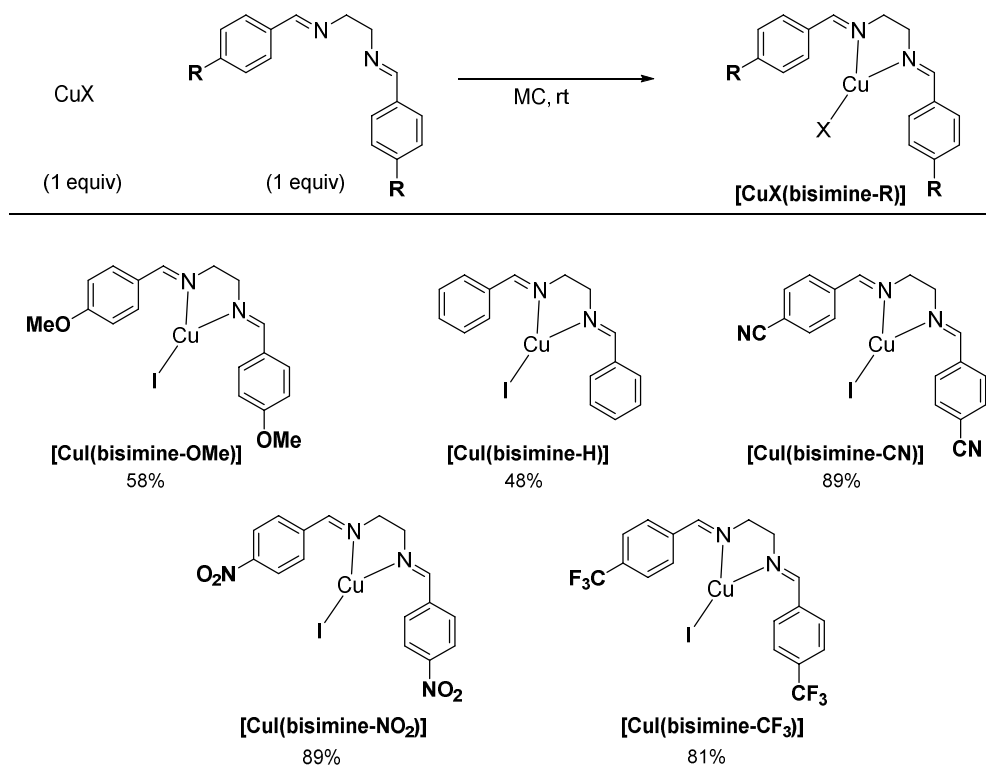


In the preparation of bisimine-H,<sup>22</sup> aldehyde (25 mmol) and water (8 mL) were added to a 100-mL round-bottom flask equipped with a stir bar. Ethylenediamine (12.5 mmol) was added in one portion and the flask was vigorously stirred magnetically at room temperature for 2 h. The crude mixture was filtered and

washed with hexane, giving the desired product.

**N,N'-bis(benzylidene)ethylenediamine (bisimine-H)**: light yellow solid. 43% isolated yield after reaction for 2 h.  $^1\text{H}$  NMR ( $\text{CDCl}_3$ , 499MHz):  $\delta$  ppm = 8.30 (s, 2 H), 7.70 (d,  $J = 7.3$  Hz, 4 H), 7.37 - 7.42 (m, 6 H), 3.99 (s, 4 H). The spectral data were consistent with those reported in the literature.<sup>22</sup>

### 5.4.2.2 Preparation of CuX-bisimine complexes



$[\text{CuI}(\text{bisimine-R})]$  ( $\text{R} = \text{OMe}, \text{H}, \text{CN}, \text{NO}_2, \text{CF}_3$ ) was prepared following the reported procedure.<sup>20</sup> A  $\text{CH}_2\text{Cl}_2$  solution (0.1 M) of bisimine-R (1 equiv) was reacted with  $\text{CuI}$  (1.0 equiv). After a sudden solubilization of the copper salt, the product was recrystallized as a microcrystalline solid using a mixture of diethyl ether and acetone.

**$[\text{CuI}(\text{bisimine-OMe})]$** : pale yellow solid. 58% isolated yield after reaction for 6 h.

$^1\text{H NMR}$  ( $\text{CDCl}_3$ , 499MHz):  $\delta = 8.34$  (s, 2 H), 8.18 (d,  $J = 7.8$  Hz, 4 H), 6.95 (d,  $J = 8.3$  Hz, 4 H), 3.98 (br. s, 4 H), 3.82 ppm (s, 6 H).

**[CuI(bisimine-H)]**: yellow solid. 48% isolated yield after reaction for 6 h.  $^1\text{H}$  NMR ( $\text{CDCl}_3$ , 300MHz):  $\delta = 8.35$  (s, 2 H), 7.82 - 7.91 (m, 4 H), 7.41 - 7.47 (m, 6 H), 4.00 ppm (s, 4 H).

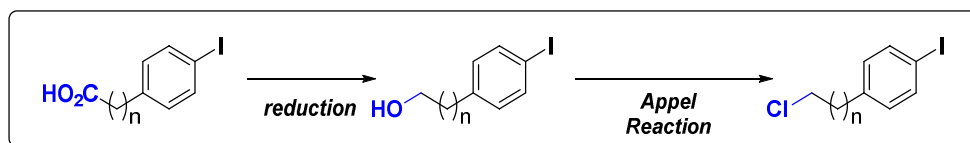
**[CuI(bisimine-CN)]**: orange solid. 89% isolated yield after reaction for 6 h.  $^1\text{H}$  NMR ( $\text{CDCl}_3$ , 499MHz)  $\delta = 8.33$  (s, 2 H), 7.84 (d,  $J = 7.8$  Hz, 4 H), 7.70 (d,  $J = 8.3$  Hz, 4 H), 4.05 ppm (s, 4 H)

**[CuI(bisimine-NO<sub>2</sub>)]**: brown solid. 89% isolated yield after reaction for 11 h.  $^1\text{H}$  NMR ( $\text{DMSO-d}_6$ , 499MHz):  $\delta = 8.61$  (br. s., 3 H), 8.29 (d,  $J = 8.3$  Hz, 4 H), 8.14 (d,  $J = 8.3$  Hz, 4 H), 4.00 ppm (s, 4 H)

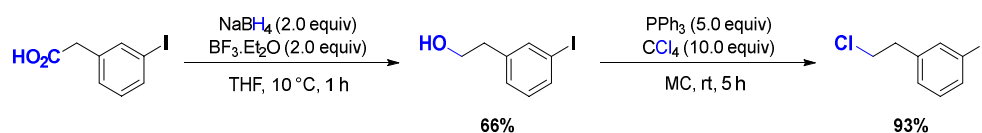
**[CuI(bisimine-CF<sub>3</sub>)]**: yellow solid. 81% isolated yield after reaction for 16 h.  $^1\text{H}$  NMR ( $\text{DMSO-d}_6$ , 499MHz):  $\delta = 8.66$  (s, 2 H), 8.10 (br. s., 4 H), 7.82 (d,  $J = 7.8$  Hz, 4 H), 4.00 ppm (s, 4 H).



### 5.4.2.3 Preparation of substrate



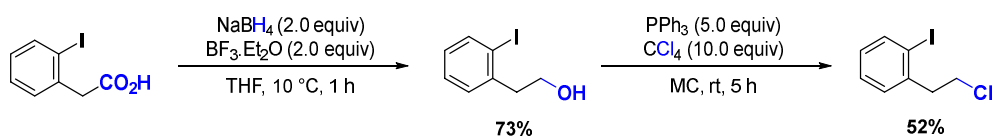
1-Iodo-3-(2-chloroethyl)benzene and 1-iodo-2-(2-chloroethyl)benzene were prepared from the corresponding carboxylic acids by the reduction of the carboxylic acids, followed by the chlorination of the resulting alcohols via Appel reaction.<sup>23</sup>



**1-Iodo-3-(2-chloroethyl)benzene:** a solution of 3-iodophenylacetic acid (1.91 mmol) in THF (2.5 mL) was added to  $\text{NaBH}_4$  (2 equiv) in one portion at 10 °C, followed by the slow addition of  $\text{BF}_3 \cdot \text{Et}_2\text{O}$  (2 equiv). The reaction mixture was stirred at 10 °C for 1 h. Then, methanol (1.5 mL) was slowly added, followed by 1 M HCl solution (1.5 mL). The reaction mixture was diluted with ethyl acetate (4 mL), and the organic phase was separated and dried over  $\text{MgSO}_4$ . The solvent was evaporated under reduced pressure, and the crude product was purified by column chromatography using a mixture of hexane/ethyl acetate (1:1 v/v), affording the corresponding alcohol, 2-(3-iodophenyl)ethanol [127201-31-4] as a colorless oil (315 mg, 66% yield).  $^1\text{H NMR}$  ( $\text{CDCl}_3$ , 499MHz):  $\delta$  = 7.62 (s, 1 H), 7.58 (d,  $J$  = 8.3 Hz, 1 H), 7.21 (d,  $J$  = 7.8 Hz, 1 H), 7.06 (t,  $J$  = 7.6 Hz, 1 H), 3.87 (q,  $J$  = 6.4 Hz, 2 H), 2.82 (t,  $J$  = 6.6 Hz, 2 H), 1.38 ppm (t,  $J$  = 5.6 Hz, 1 H).  $^{13}\text{C NMR}$  ( $\text{CDCl}_3$ , 75MHz):  $\delta$  = 141.1, 138.0, 135.6, 130.3, 128.3, 94.6, 63.3, 38.7 ppm. The spectral data were

consistent with those reported in the literature.<sup>24</sup>

PPh<sub>3</sub> (5 equiv) and CCl<sub>4</sub> (10 equiv) were added to a solution of 2-(3-iodophenyl)ethanol (1.2 mmol) in CH<sub>2</sub>Cl<sub>2</sub> (14 mL) at room temperature. The reaction mixture was stirred at room temperature for 5 h. The solvent was removed under reduced pressure, and the crude product was purified by column chromatography using a mixture of hexane/ethyl acetate (10:1 v/v). The title compound was obtained as a colorless oil (297 mg, 93% yield). <sup>1</sup>H NMR (CDCl<sub>3</sub>, 499MHz): δ = 7.58 - 7.62 (m, 2 H), 7.20 (d, *J* = 7.3 Hz, 1 H), 7.07 (t, *J* = 8.1 Hz, 1 H), 3.70 (t, *J* = 7.3 Hz, 2 H), 3.02 ppm (t, *J* = 7.3 Hz, 2 H). <sup>13</sup>C NMR (CDCl<sub>3</sub>, 75MHz): δ = 140.4, 137.8, 136.0, 130.2, 128.1, 94.5, 44.5, 38.5 ppm.



**1-Iodo-2-(2-chloroethyl)benzene** [1037075-33-4]: a solution of 2-iodophenylacetic acid (3.82 mmol) in THF (5.0 mL) was added to NaBH<sub>4</sub> (2.0 equiv) in one portion at 10 °C, followed by the slow addition of BF<sub>3</sub>·Et<sub>2</sub>O (2 equiv). The reaction mixture was stirred at 10 °C for 1 h. Then, methanol (3.0 mL) was slowly added, followed by 1 M HCl solution (3.0 mL). The reaction mixture was diluted with ethyl acetate (7 mL), and the organic phase was separated and dried over MgSO<sub>4</sub>. The solvent was evaporated under reduced pressure, and the crude product was purified by column chromatography using a mixture of hexane/ethyl acetate (3:1 v/v), affording the corresponding alcohol, 2-(2-iodophenyl)ethanol [26059-40-5] as a colorless oil (692

mg, 73% yield).  $^1\text{H}$  NMR ( $\text{CDCl}_3$ , 499MHz):  $\delta = 7.85$  (dd,  $J = 7.8, 1.5$  Hz, 1 H), 7.28 - 7.33 (m, 2 H), 6.94 (td,  $J = 7.6, 2.0$  Hz, 1 H), 3.88 (q,  $J = 6.8$  Hz, 2 H), 3.04 (t,  $J = 6.6$  Hz, 2 H), 1.38 ppm (t,  $J = 5.9$  Hz, 1 H). The spectral data were consistent with those reported in the literature.<sup>23</sup>

$\text{PPh}_3$  (5.0 equiv) and  $\text{CCl}_4$  (10 equiv) were added to a solution of 2-(2-iodophenyl)ethanol (2.0 mmol) in  $\text{CH}_2\text{Cl}_2$  (23 mL) at room temperature. The reaction mixture was stirred at room temperature for 5 h. The solvent was removed under reduced pressure, and the crude product was purified by column chromatography using a mixture of hexane/ethyl acetate (10:1 v/v). The title compound was obtained as a colorless oil (277 mg, 52% yield).  $^1\text{H}$  NMR ( $\text{CDCl}_3$ , 499MHz):  $\delta = 7.85$  (dd,  $J = 7.8, 1.0$  Hz, 1 H), 7.27 - 7.34 (m, 2 H), 6.96 (td,  $J = 7.3, 2.0$  Hz, 1 H), 3.72 (t,  $J = 7.6$  Hz, 2 H), 3.21 ppm (t,  $J = 7.3$  Hz, 2 H).  $^{13}\text{C}$  NMR ( $\text{CDCl}_3$ , 75MHz):  $\delta = 140.6, 139.7, 130.5, 128.8, 128.4, 100.3, 43.7, 43.3$  ppm. The spectral data were consistent with those reported in the literature.<sup>23</sup>

### 5.4.3 Experimental setup and general procedure for photoinduced copper catalyzed cyanation of aryl halides

#### 5.4.3.1 Photoreaction setup



**Figure 5.2** Pictures of reaction setup.

Following the literature protocol,<sup>11</sup> the experimental setup of photoreaction was carried out in a fume hood. Four 15W, UV germicidal CFL lamps were hanged around a ring clamp on an iron support stand surrounded by an aluminum folding screen to prevent the loss of irradiation (left, Figure 5.2). The lamps were spaced evenly around the circumference of the ring clamp. Using a second clamp underneath the ring clamp, a set of quartz test tubes were placed inside the lamps. A 25W-fan was installed facing towards the lamps to cool the heat generated from the lamps during the reaction (estimated temperature below 31 °C) (middle, Figure 5.2). The photoreactions were performed using a stirrer; the entire apparatus was covered with a paper box to prevent exposure to UV irradiation (right, Figure 5.2).

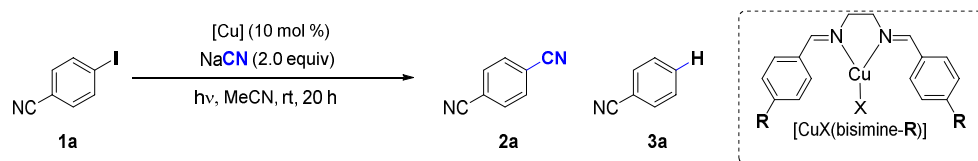
### 5.4.3.2 General procedure

To an oven-dried quartz tube (10 cm in height, fitted with a 14/20 septum) equipped with a stir bar, [CuI(bisimine-CN)] (10 mol%, 14.3 mg), NaCN (1.4 equiv, 20.6 mg), and (if solid) aryl halide (1 equiv, 0.3 mmol) were added in an Ar-filled glovebox. The quartz tube was capped with a 14/20 septum after CH<sub>3</sub>CN (1.2 mL) was added via a syringe. After removing from the glovebox, the reaction tube was sealed again with a black-vinyl-electrical tape (If the aryl halide is liquid, it was added via a microsyringe at this time). The resulting mixture was stirred vigorously and irradiated with light at room temperature for 24 h. Then, the reaction mixture was transferred to a round-bottom flask using acetone or CH<sub>2</sub>Cl<sub>2</sub> and then concentrated under reduced pressure. The residue was purified by column chromatography using a mixture of hexane/ethyl acetate, pentane/diethyl ether, or CH<sub>2</sub>Cl<sub>2</sub>/methanol.

[Note] Some of the resulting nitriles such as 4-tolunitrile are volatile under reduced pressure (~15 torr). The NMR yields were determined using 1,3,5-trimethoxybenzene as the internal standard, for quantitative analysis of those nitrile products.

## 5.4.4 Additional screening tables

**Table 5.2** Cu catalysts (variation of X and bisimine ligands)<sup>a</sup>



photoreactor	[Cu]	conv. (%)	2a(%)	3a(%)
Blue LED (vis)	CuI	0	0	0
	[CuI(bisimine-OMe)]	0	0	0
	[CuI(bisimine-Ph)]	0	0	0
	[CuI(bisimine-CN)]	0	0	0
LUZCHEM (UVC)	CuI	51	49	49
	[CuI(bisimine-OMe)]	100	64	36
	[CuI(bisimine-Ph)]	74	52	22
15W*4 UV lamp (UVC)	[CuI(bisimine-CN)]	95	77	9
	[CuI(bisimine-OMe)]	100	81	13
	[CuI(bisimine-Ph)]	100	76	16
	[CuI(bisimine-CN)]	<b>100</b>	<b>83</b>	<b>11</b>
	[CuI(bisimine-NO <sub>2</sub> )]	100	70	30
	[CuI(bisimine-CF <sub>3</sub> )]	100	19	81

(a) Estimated by NMR using 1,3,5-trimethoxybenzene as the internal standard.

**Table 5.3** Cyanide source (nucleophilic, neutral, and electrophilic) <sup>a,25</sup>

MCN	conv. (%)	2a(%)	3a(%)
NaCN	100	83	11
KCN	100	65	35
BrCN	77	4	22
TsCN	16	16	0
K <sub>3</sub> [Fe(CN) <sub>6</sub> ]	21	0	21
K <sub>4</sub> [Fe(CN) <sub>6</sub> ]	22	0	22
TMSCN	48	30	18
TBACN	100	59	41
HO-CN 	37	0	37

<p><i>nucleophilic CN</i></p> <p>metallic: KCN, NaCN, TMSCN, or K<sub>4</sub>[Fe(CN)<sub>6</sub>]</p> <p>non-metallic:</p> <div style="display: flex; justify-content: space-around; align-items: center;"> <div style="text-align: center;">  CN         </div> <div style="text-align: center;">             R=CH<sub>3</sub>, CH<sub>3</sub>CH<sub>2</sub>, PhCH<sub>2</sub>, CN         </div> </div>	<p><i>radical CN</i></p> <div style="text-align: center;">             O=S=O                         C<sub>6</sub>H<sub>4</sub> </div>	<p><i>electrophilic CN</i></p> <div style="text-align: center;"> </div>
---	--	---

(a) Estimated by NMR using 1,3,5-trimethoxybenzene as the internal standard.

**Table 5.4 Solvent <sup>a</sup>**

solvent	conv. (%)	2a(%)	3a(%)
MC	36	16	20
tBuCN	54	8	46
THF	100	2	98
1,4-dioxane	100	0	100
pentane	5	0	5
DMA	100	0	100
MeOH	100	17	48

(a) Estimated by NMR using 1,3,5-trimethoxybenzene as the internal standard.



### 5.4.5 Reactivity comparison ([CuI(bisimine-CN)] and [CuI])

**Table 5.5** Reaction with simple CuI catalyst<sup>a</sup>

Reaction scheme:  $\text{Ar-I} \xrightarrow[\text{MeCN, rt, 24 h}]{\text{[Cu] (10 mol \%), NaCN (1.4 equiv), } h\nu (254\text{nm})} \text{Ar-CN}$

<b>[CuI(bisimine-CN)] 4</b>	79%	86%	61%	66%
<b>[CuI]</b>	66%	79%	49%	51%

(a) Estimated by NMR using 1,3,5-trimethoxybenzene as the internal standard.

## 5.4.6 Mechanistic investigation (light-dark experiment, radical scavenger, kinetic profile, and kinetic order)

### 5.4.6.1 Light-dark experiment (Figure 5.1)

4-Iodobenzonitrile **1a** (70.1 mg, 0.3 mmol), CuI(bisimine-CN), **4** (14.3 mg, 0.03 mmol), NaCN (20.6 mg, 0.42 mmol), and 1,3,5-trimethoxybenzene (51.0 mg, 0.3 mmol) as the internal standard were added to a quartz tube equipped with a stir bar in an Ar-filled glovebox. The tube was filled with CH<sub>3</sub>CN (1.2 mL, 0.25M) and sealed with a rubber septum. The reaction tube was then evacuated and irradiated under constant stirring. The lights were turned off and the tube was completely covered in aluminum foil during the following duration (1–2, 3–4, 5–6, 7–8 h). Aliquots were taken via a syringe at 1 h intervals (till 9 h), filtered through a cotton-plugged filter filled with Celite and washed with CH<sub>2</sub>Cl<sub>2</sub>. The vial containing the aliquot was analyzed by GC for the formation of product. Quantitative analysis by GC was carried out in triplicate using 1,3,5-trimethoxybenzene as the internal standard.

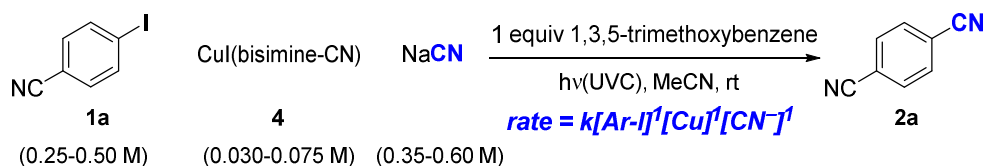
#### 5.4.6.2 Inhibition by radical scavenger

4-Iodobenzonitrile **1a** (70.1 mg, 0.3 mmol), radical scavenger (1 equiv, 0.3 mmol), CuI(bisimine-CN) **4** (11.4 mg, 0.024 mmol), NaCN (20.6 mg, 0.42 mmol), and 1,3,5-trimethoxybenzene (51 mg, 0.3 mmol) as the internal standard were added to a quartz tube equipped with a stir bar in an Ar-filled glovebox. The tube was filled with CH<sub>3</sub>CN (1.2 mL, 0.25M) and sealed with a rubber septum. The resulting mixture was stirred vigorously and irradiated for 20 h. Then, the reaction mixture was concentrated under reduced pressure. The yield of **2a** was analyzed by <sup>1</sup>HNMR using 1,3,5-trimethoxybenzene as the internal standard. \*BHT = 2,6-di-tert-butyl-4-methylphenol

#### 5.4.6.3 Kinetic profile (Figure 5.1)

4-Iodobenzonitrile **1a** (70.1 mg, 0.3 mmol), CuI(bisimine-CN) **4** (14.3 mg, 0.03 mmol), NaCN (20.6 mg, 0.42 mmol), and 1,3,5-trimethoxybenzene (51 mg, 0.3 mmol) as the internal standard were added to a quartz tube equipped with a stir bar in an Ar-filled glovebox. The tube was filled with CH<sub>3</sub>CN (1.2 mL, 0.25M) and sealed with a rubber septum. The reaction tube was evacuated and irradiated under constant stirring. Aliquots were taken via a syringe at 30 or 60 min time intervals (0 h, 0.5 h, 1 h, 1.5 h, 2 h, 3 h, 4 h, 5 h, 6 h, 8 h, 10 h, 11.5 h, 24 h). The aliquots were filtered through a cotton-plugged filter filled with Celite and washed with CH<sub>2</sub>Cl<sub>2</sub>. The vial containing the aliquot was analyzed by GC for the formation of product. Quantitative analysis by GC was carried out in triplicate using 1,3,5-trimethoxybenzene as the internal standard.

#### 5.4.6.4 Kinetic order



4-Iodobenzonitrile **1a**, CuI(bisimine-CN) **4**, NaCN, and 1,3,5-trimethoxybenzene as the internal standard were added to a quartz tube equipped with a stir bar in an Ar-filled glovebox. The tube was filled with CH<sub>3</sub>CN and sealed with a rubber septum. The reaction tube was evacuated and irradiated under constant stirring. Aliquots were taken via a syringe at 10 min time intervals. The aliquots were filtered through a cotton-plugged filter filled with Celite and washed with CH<sub>2</sub>Cl<sub>2</sub>. The vial containing the aliquot was analyzed by GC for the formation of product. Quantitative analysis by GC was carried out in triplicate using 1,3,5-trimethoxybenzene as the internal standard.

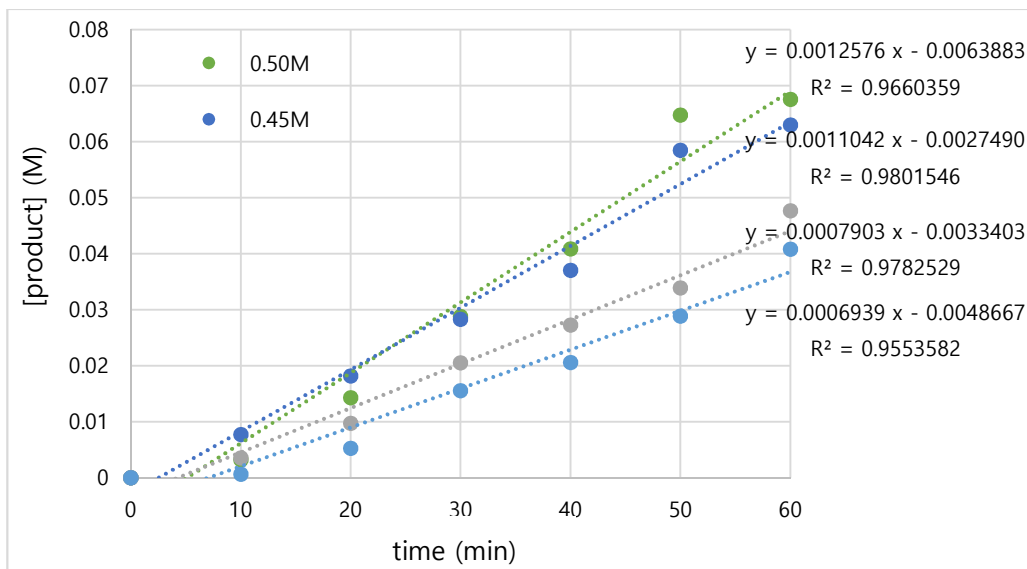


**Figure 5.3** [Ar-I] dependent initial reaction profile

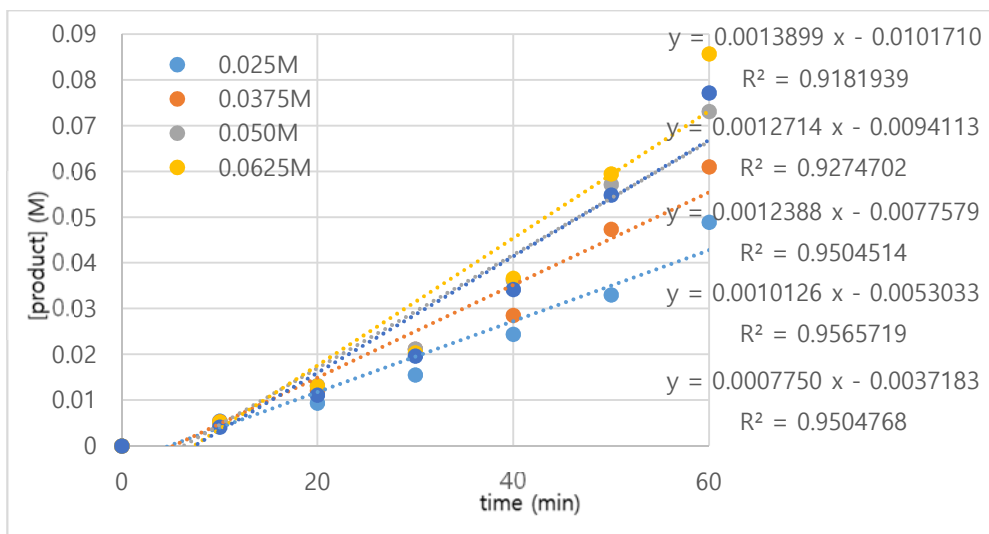


**Figure 5.4.** [Cu] dependent initial reaction profile

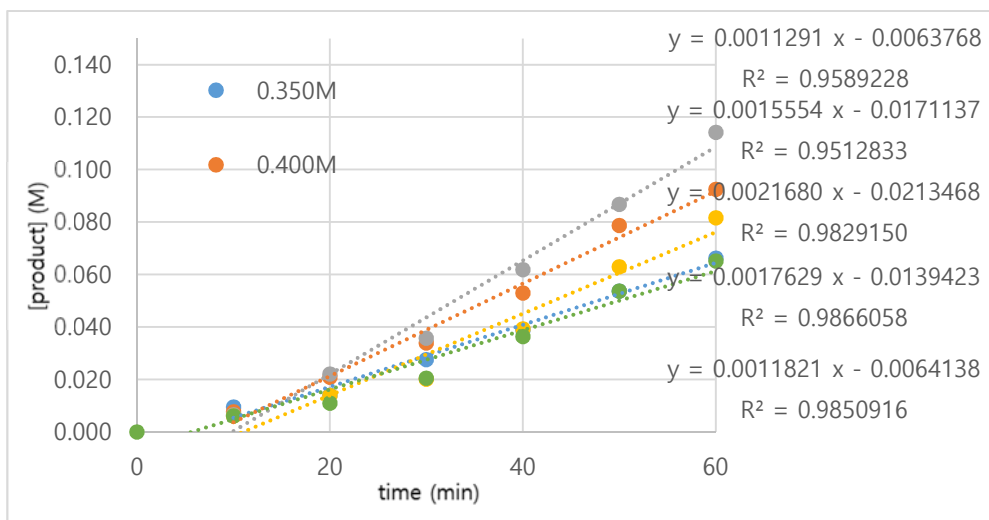
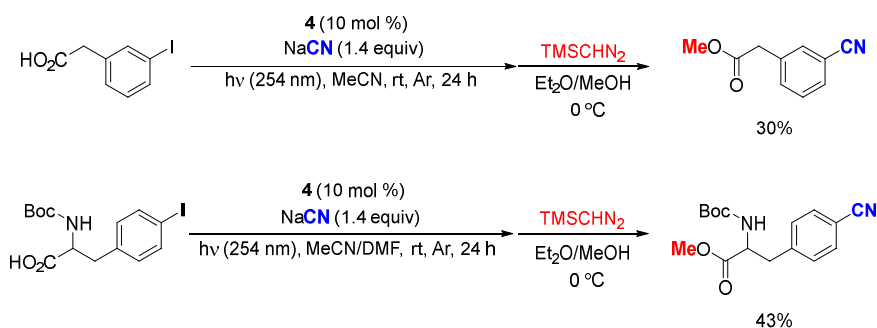


**Figure 5.5.** [CN<sup>-</sup>] dependent initial reaction profile

## 5.4.7 Characterization of products

### 5.4.7.1 Protection of carboxylic groups

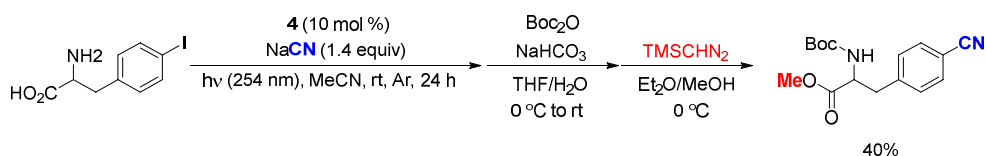
Because of the difficulty in the purification of crude reaction mixture with carboxyl-group-substituted compounds, further esterification<sup>26</sup> was conducted after the cyanation was completed.



To an oven-dried quartz-tube (10 cm in height, fitted with a 14/20 septum) equipped with a stir bar, [CuI(bisimine-CN)] (10 mol%, 14.3 mg), NaCN (1.4 equiv, 20.6 mg), and aryl halide (1.0 equiv, 0.3 mmol) were added in an Ar-filled glovebox. The quartz tube was capped with a 14/20 septum after CH<sub>3</sub>CN (1.2 mL) or a mixture of CH<sub>3</sub>CN/DMF (1.2 mL, 3:1 v/v) was added via a syringe. After removing from the glovebox, the reaction tube was sealed again with a black-vinyl-electrical tape. The mixture was stirred vigorously and irradiated in the center of the lamps at room temperature for 24 h. The crude mixture was esterified following a literature method. After the removal of the solvent under reduced pressure, the residue was treated with TMSCHN<sub>2</sub> (2 M solution in hexane, 7 equiv) in Et<sub>2</sub>O/MeOH (4:1 v/v, 0.25 M) at 0 °C in a 50 mL round-bottom flask under Ar. After 1 h, the solvent was removed under reduced pressure, and the residue was purified by silica gel column chromatography, giving the protected aromatic nitriles.

### 5.4.7.2 Protection of amino acid

Because of the difficulty in the purification of crude reaction mixture with amino acid, further protection of amine<sup>27</sup> and carboxylic acid<sup>26</sup> were conducted after the cyanation was completed.

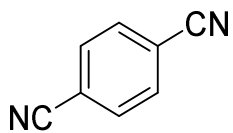


To an oven-dried quartz-tube (10 cm in height, fitted with a 14/20 septum) equipped with a stir bar, [CuI(bisimine-CN)] (10 mol%, 14.3 mg), NaCN (1.4 equiv, 20.6 mg), and aryl halide (1.0 equiv, 0.3 mmol) were added in an Ar-filled glovebox. The quartz tube was capped with a 14/20 septum after CH<sub>3</sub>CN (1.2 mL) or a mixture of CH<sub>3</sub>CN/DMF (1.2 mL, 3:1 v/v) was added via a syringe. After removing from the glovebox, the reaction tube was sealed again with a black-vinyl-electrical tape. The mixture was stirred vigorously and irradiated in the center of the lamps at room temperature for 24 h. The crude mixture was N-Boc protected and then esterified following literature methods. After the removal of the solvent under reduced pressure, the resulting mixture in a mixture of THF/H<sub>2</sub>O (3.6 mL, 1:1 v/v) was mixed with NaHCO<sub>3</sub> (3 equiv) and Boc<sub>2</sub>O (1.2 equiv) consecutively at 0 °C. After 30 min, the solution was stirred overnight at room temperature. The solution was extracted with Et<sub>2</sub>O (2×3 mL). The aqueous layer was acidified by careful addition of half sat. citric acid at 0 °C and then extracted with CH<sub>2</sub>Cl<sub>2</sub> (3×3 mL). The combined organic phase was dried (Na<sub>2</sub>SO<sub>4</sub>) and evaporated under reduced pressure to give the Boc-amino acids. These Boc-amino acids were used for next step without purification. The residue was treated with TMSCHN<sub>2</sub> (2 M solution in hexane, 7 equiv) in

Et<sub>2</sub>O/MeOH (4:1 v/v, 0.25 M) at 0 °C in a 50 mL round-bottom flask under Ar. After 1 h, the solvent was removed under reduced pressure, and the residue was purified by silica gel column chromatography, giving the protected aromatic nitriles.

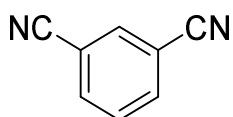


### 5.4.7.3 Characterization of products



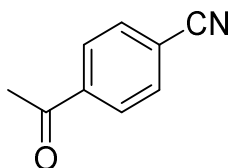
**2a**

**1,4-Dicyanobenzene (2a):** white solid (33.1 mg, 0.26 mmol, 86% isolated yield).  $^1\text{H}$  NMR ( $\text{CDCl}_3$ , 300MHz):  $\delta$  ppm = 7.80 (s, 4 H).  $^{13}\text{C}$  NMR ( $\text{CDCl}_3$ , 126MHz):  $\delta$  ppm = 132.8, 117.0, 116.7. The spectral data were consistent with those reported in the literature.<sup>28</sup>



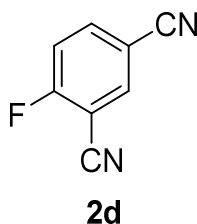
**2b**

**1,3-Dicyanobenzene (2b):** light yellow solid (25.4 mg, 0.20 mmol, 66% isolated yield).  $^1\text{H}$  NMR ( $\text{CDCl}_3$ , 499 MHz):  $\delta$  ppm = 7.67 (t,  $J$  = 8.07 Hz, 1 H), 7.91 (dd,  $J$  = 7.83, 1.47 Hz, 2 H), 7.96 - 7.98 (m, 1 H).  $^{13}\text{C}$  NMR ( $\text{CDCl}_3$ , 126MHz):  $\delta$  ppm = 136.0, 135.4, 130.3, 116.6, 114.2. The spectral data were consistent with those reported in the literature.<sup>28</sup>

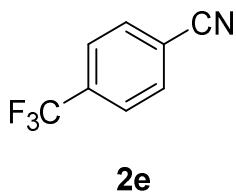


**2c**

**4-Acetylbenzointrile (2c)**: light yellow solid (34.4 mg, 0.24 mmol, 79% isolated yield).  $^1\text{H}$  NMR ( $\text{CDCl}_3$ , 499 MHz):  $\delta$  ppm = 8.05 (d,  $J$  = 8.31 Hz, 2 H), 7.79 (d,  $J$  = 8.31 Hz, 2 H), 2.66 (s, 3 H).  $^{13}\text{C}$  NMR ( $\text{CDCl}_3$ , 126MHz):  $\delta$  ppm = 196.5, 139.9, 132.5, 128.7, 117.9, 116.4, 26.8. The spectral data were consistent with those reported in the literature.<sup>29</sup>

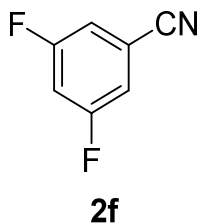


**2,4-Dicyano-1-fluorobenzene (2d)**: white solid (34.4 mg, 0.24 mmol, 79% isolated yield).  $^1\text{H}$  NMR ( $\text{CDCl}_3$ , 499 MHz):  $\delta$  ppm = 7.97 - 8.01 (m, 1 H), 7.94 (ddd,  $J$  = 8.68, 4.77, 2.20 Hz, 1 H), 7.41 (t,  $J$  = 8.31 Hz, 1 H).  $^{13}\text{C}$  NMR ( $\text{CDCl}_3$ , 126MHz):  $\delta$  ppm = 166.0, 163.9, 138.7, 138.6, 137.6, 118.3, 118.2, 115.8, 111.6, 110.2. The spectral data were consistent with those reported in the literature.<sup>30</sup>

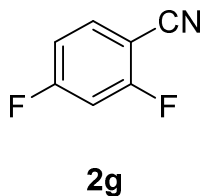


**4-Trifluoromethylbenzonitrile (2e)**: light yellow liquid (42.8 mg, 0.25 mmol, 83% isolated yield, 96% NMR yield). Due to its volatility, it's difficult to fully evaporate residual solvent from product mixture under reduced pressure. Therefore, NMR of

purified compound was mixed with residual solvent.  $^1\text{H}$  NMR ( $\text{CDCl}_3$ , 499 MHz):  $\delta$  ppm = 7.80 - 7.87 (m, 2 H), 7.74 - 7.79 (m, 2 H).  $^{13}\text{C}$  NMR ( $\text{CDCl}_3$ , 75 MHz):  $\delta$  ppm = 134.5(q), 132.7, 126.2(q), 123.0(q), 117.4, 116.0. The spectral data were consistent with those reported in the literature.<sup>7k</sup>

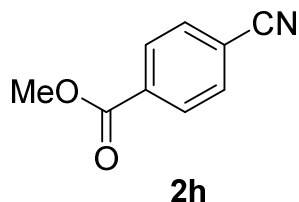


**3,5-Difluorobenzonitrile (2f)**: white solid (41.7 mg, 0.30 mmol, 99% isolated yield).  $^1\text{H}$  NMR ( $\text{CDCl}_3$ , 499 MHz):  $\delta$  ppm = 7.18 - 7.21 (m, 2 H), 7.08 ppm (tt,  $J$  = 8.6, 2.4 Hz, 1 H).  $^{13}\text{C}$  NMR ( $\text{CDCl}_3$ , 75 MHz):  $\delta$  ppm = 162.8 (dd,  $J$  = 253.3, 12.6 Hz), 116.4 (t,  $J$  = 3.6 Hz), 115.6 (m), 114.6 (t,  $J$  = 11.5 Hz), 109.4 (t,  $J$  = 24.9 Hz). The spectral data were consistent with those reported in the literature.<sup>31</sup>

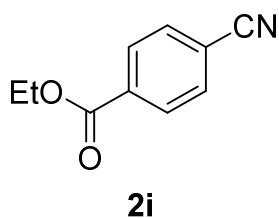


**2,4-Difluorobenzonitrile (2g)**: white solid (32.1 mg, 0.23 mmol, 77% isolated yield).  $^1\text{H}$  NMR ( $\text{CDCl}_3$ , 499 MHz):  $\delta$  ppm = 7.63 - 7.71 (m, 1 H), 6.97 - 7.06 ppm (m, 2 H).  $^{13}\text{C}$  NMR ( $\text{CDCl}_3$ , 75 MHz):  $\delta$  ppm = 165.8 (dd,  $J$  = 259.6, 11.5 Hz), 164.1 (dd,  $J$  = 274.1, 12.1 Hz), 135.0 (d,  $J$  = 10.7 Hz), 113.2 (m), 112.8 (d,  $J$  = 3.7 Hz), 105.5

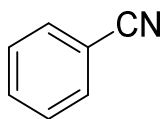
(dd,  $J = 26.1, 23.1$  Hz), 98.2 (m). The spectral data were consistent with those reported in the literature.<sup>32</sup>



**Methyl 4-cyanobenzoate (2h):** white solid (38.2 mg, 0.24 mmol, 79% isolated yield).  $^1\text{H}$  NMR ( $\text{CDCl}_3$ , 499 MHz):  $\delta$  ppm = 8.15 (d,  $J = 8.3$  Hz, 2 H), 7.76 (d,  $J = 8.3$  Hz, 2 H), 3.97 (s, 3 H).  $^{13}\text{C}$  NMR ( $\text{CDCl}_3$ , 75 MHz):  $\delta$  ppm = 165.4, 133.9, 132.2, 130.1, 118.0, 116.4, 52.7. The spectral data were consistent with those reported in the literature.<sup>32</sup>

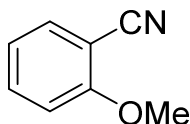


**Ethyl 4-cyanobenzoate (2i):** white solid (39.4 mg, 0.23 mmol, 75% isolated yield).  $^1\text{H}$  NMR ( $\text{CDCl}_3$ , 499 MHz):  $\delta$  ppm = 8.14 (d,  $J = 8.8$  Hz, 2 H), 7.74 (d,  $J = 8.3$  Hz, 2 H), 4.42 (q,  $J = 6.8$  Hz, 2 H), 1.41 ppm (t,  $J = 7.3$  Hz, 3 H).  $^{13}\text{C}$  NMR ( $\text{CDCl}_3$ , 75 MHz):  $\delta$  ppm = 164.9, 134.3, 132.2, 130.0, 118.0, 116.2, 61.8, 14.2. The spectral data were consistent with those reported in the literature.<sup>5e</sup>



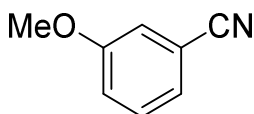
**2j**

**Benzonitrile (2j):** oil (0.30 mmol, 99% NMR yield).  $^1\text{H}$  NMR ( $\text{CDCl}_3$ , 499 MHz):  $\delta$  ppm = 7.67 (d,  $J$  = 8.3 Hz, 2 H), 7.62 (t,  $J$  = 7.6 Hz, 1 H), 7.49 (t,  $J$  = 7.8 Hz, 3 H).  $^{13}\text{C}$  NMR ( $\text{CDCl}_3$ , 75 MHz):  $\delta$  ppm = 132.7, 132.1, 129.1, 118.8, 112.4. The spectral data were consistent with those reported in the literature.<sup>28</sup>



**2k**

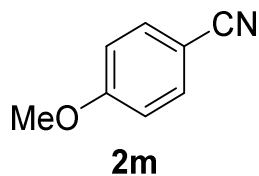
**2-Methoxybenzonitrile (2k):** yellow oil (34.4 mg, 0.26 mmol, 86% isolated yield).  $^1\text{H}$  NMR ( $\text{CDCl}_3$ , 499 MHz):  $\delta$  ppm = 7.56 (d,  $J$  = 9.78 Hz, 2 H), 6.98 (d,  $J$  = 8.31 Hz, 1 H), 7.01 (t,  $J$  = 7.83 Hz, 1H), 3.94 (s, 3 H).  $^{13}\text{C}$  NMR ( $\text{CDCl}_3$ , 75 MHz):  $\delta$  ppm = 161.2, 134.4, 133.7, 120.7, 116.5, 111.2, 101.7, 55.9. The spectral data were consistent with those reported in the literature.<sup>31</sup>



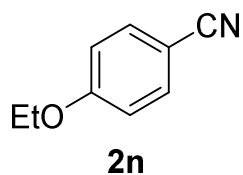
**2l**

**3-Methoxybenzonitrile (2l):** yellow oil (29.6 mg, 0.22 mmol, 74% isolated yield).

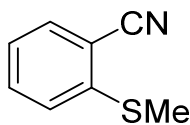
$^1\text{H}$  NMR ( $\text{CDCl}_3$ , 499 MHz):  $\delta$  ppm = 7.35 - 7.40 (m, 1 H), 7.22 - 7.26 (m, 1 H), 7.12 - 7.16 (m, 2 H), 3.83 (s, 3 H).  $^{13}\text{C}$  NMR ( $\text{CDCl}_3$ , 75 MHz):  $\delta$  ppm = 159.6, 130.3, 124.5, 119.3, 118.7, 116.8, 113.2, 55.5. The spectral data were consistent with those reported in the literature.<sup>31</sup>



**4-Methoxybenzonitrile (2m)**: white solid (24.8 mg, 0.19 mmol, 62% isolated yield).  $^1\text{H}$  NMR ( $\text{CDCl}_3$ , 499 MHz):  $\delta$  ppm = 7.58 (d,  $J$  = 8.80 Hz, 1 H), 6.95 (d,  $J$  = 8.80 Hz, 2 H), 3.86 (s, 3 H).  $^{13}\text{C}$  NMR ( $\text{CDCl}_3$ , 75 MHz):  $\delta$  ppm = 162.8, 134.0, 119.2, 114.7, 104.0, 55.5. The spectral data were consistent with those reported in the literature.<sup>31</sup>

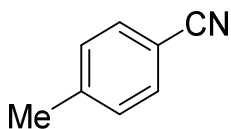


**4-Ethoxybenzonitrile (2n)**: yellow solid (26.9 mg, 0.18 mmol, 61% isolated yield).  $^1\text{H}$  NMR ( $\text{CDCl}_3$ , 499 MHz):  $\delta$  ppm = 7.58 (d,  $J$  = 8.80 Hz, 2 H), 6.94 (d,  $J$  = 8.80 Hz, 2 H), 4.09 (q,  $J$  = 7.01 Hz, 2 H), 1.45 (t,  $J$  = 7.09 Hz, 3 H).  $^{13}\text{C}$  NMR ( $\text{CDCl}_3$ , 75 MHz):  $\delta$  ppm = 162.2, 133.9, 119.3, 115.1, 103.7, 63.9, 14.5. The spectral data were consistent with those reported in the literature.<sup>33</sup>



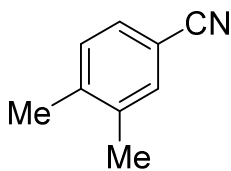
**2o**

**2-Cyanothioanisole (2o):** yellow oily solid (32.2 mg, 0.22 mmol, 72% isolated yield).  $^1\text{H}$  NMR ( $\text{CDCl}_3$ , 499 MHz):  $\delta$  ppm = 7.58 (dd,  $J = 8.80, 0.98$  Hz, 1 H), 7.52 (td,  $J = 7.83, 1.47$  Hz, 1 H), 7.31 (d,  $J = 8.31$  Hz, 1 H), 7.21 (td,  $J = 7.58, 0.98$  Hz, 1 H), 2.55 (s, 3 H).  $^{13}\text{C}$  NMR ( $\text{CDCl}_3$ , 75 MHz):  $\delta$  ppm = 143.6, 133.5, 132.9, 126.1, 125.1, 116.9, 111.6, 15.7. The spectral data were consistent with those reported in the literature.<sup>34</sup>



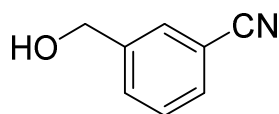
**2p**

**4-Methylbenzonitrile (2p):** yellow oil (0.20 mmol, 68% NMR yield).  $^1\text{H}$  NMR ( $\text{CDCl}_3$ , 499 MHz):  $\delta$  ppm = 7.52 (d,  $J = 8.31$  Hz, 2 H), 7.25 (d,  $J = 7.34$  Hz, 2 H), 2.40 (s, 3 H).  $^{13}\text{C}$  NMR ( $\text{CDCl}_3$ , 75 MHz):  $\delta$  ppm = 143.7, 132.0, 129.8, 119.1, 109.3, 21.8. The spectral data were consistent with those reported in the literature.<sup>28</sup>



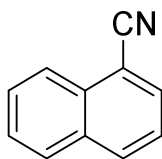
**2q**

**3,4-Dimethylbenzonitrile (2q)**: light yellow solid (28.3 mg, 0.22 mmol, 72% isolated yield).  $^1\text{H}$  NMR ( $\text{CDCl}_3$ , 499 MHz):  $\delta$  ppm = 7.42 (s, 1 H), 7.40 (d,  $J$  = 7.83 Hz, 1 H), 7.22 (d,  $J$ =7.83 Hz, 1 H), 2.33 (s, 3 H), 2.30 (s, 3 H).  $^{13}\text{C}$  NMR ( $\text{CDCl}_3$ , 126 MHz):  $\delta$  ppm = 142.4, 137.8, 132.8, 130.3, 129.6, 119.3, 109.5, 20.1, 19.5. The spectral data were consistent with those reported in the literature.<sup>35</sup>



**2r**

**3-(Hydroxymethyl)benzonitrile (2r)**: yellow liquid (30.0 mg, 0.23 mmol, 75% isolated yield).  $^1\text{H}$  NMR ( $\text{CDCl}_3$ , 499 MHz):  $\delta$  ppm = 7.68 (s, 1 H), 7.53 - 7.62 (m, 2 H), 7.47 (t,  $J$  = 7.58 Hz, 1 H), 4.75 (s, 2 H).  $^{13}\text{C}$  NMR ( $\text{CDCl}_3$ , 126 MHz):  $\delta$  ppm = 142.3, 131.1, 131.0, 130.1, 129.2, 118.8, 112.4, 63.9. The spectral data were consistent with those reported in the literature.<sup>36</sup>

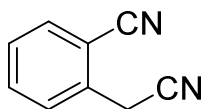


**2s**

**1-Naphthonitrile (2s)**: yellow liquid (27.1 mg, 0.18 mmol, 59% isolated yield).  $^1\text{H}$  NMR ( $\text{CDCl}_3$ , 499 MHz):  $\delta$  ppm = 8.26 (d,  $J$  = 8.31 Hz, 1 H), 8.10 (d,  $J$  = 8.31 Hz, 1 H), 7.94 (t,  $J$  = 7.83 Hz, 2 H), 7.68 - 7.74 (m, 1 H), 7.61 - 7.66 (m, 1 H), 7.54 (t,  $J$

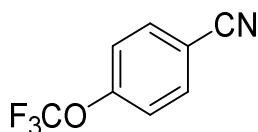


= 7.83 Hz, 1 H).  $^{13}\text{C}$  NMR ( $\text{CDCl}_3$ , 75 MHz):  $\delta$  ppm = 133.4, 133.0, 132.7, 132.5, 128.8, 128.7, 127.7, 125.3, 125.0, 117.9, 110.3. The spectral data were consistent with those reported in the literature.<sup>37</sup>



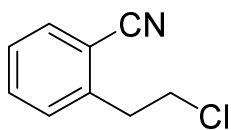
**2t**

**2-(Cyanophenyl)acetonitrile (2t)**: white solid (37.1 mg, 0.26 mmol, 87% isolated yield).  $^1\text{H}$  NMR ( $\text{CDCl}_3$ , 300 MHz):  $\delta$  ppm = 7.66 - 7.76 (m, 4 H), 7.45 - 7.54 (m, 1 H), 4.01 ppm (s, 2 H).  $^{13}\text{C}$  NMR ( $\text{CDCl}_3$ , 75 MHz):  $\delta$  ppm = 133.7, 133.5, 133.2, 129.0, 128.9, 116.5, 115.9, 112.1, 22.6. The spectral data were consistent with those reported in the literature.<sup>38</sup>



**2v**

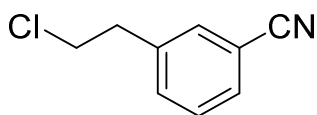
**4-(Trifluoromethoxy)benzonitrile (2v)**: oil (0.14 mmol, 47% NMR yield).  $^1\text{H}$  NMR ( $\text{CDCl}_3$ , 499 MHz):  $\delta$  ppm = 7.74 (d,  $J$  = 8.8 Hz, 2 H), 7.34 (d,  $J$  = 8.8 Hz, 3 H).  $^{13}\text{C}$  NMR ( $\text{CDCl}_3$ , 75 MHz):  $\delta$  ppm = 152.2, 134.2, 121.2, 119.9 (q), 117.7, 110.8. The spectral data were consistent with those reported in the literature.<sup>39</sup>



**2w**

**2-(2-Chloroethyl)benzonitrile (2w):** oil (33.6 mg, 0.20 mmol, 68% isolated yield).

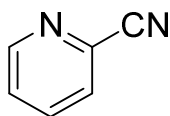
$^1\text{H NMR}$  ( $\text{CDCl}_3$ , 300 MHz):  $\delta$  ppm = 7.67 (d,  $J = 7.7$  Hz, 1 H), 7.54 - 7.62 (m, 1 H), 7.35 - 7.47 (m, 2 H), 3.82 (t,  $J = 6.9$  Hz, 2 H), 3.32 (t,  $J = 6.9$  Hz, 2 H).  $^{13}\text{C NMR}$  ( $\text{CDCl}_3$ , 75 MHz):  $\delta$  ppm = 141.7, 133.0, 132.8, 130.5, 127.6, 117.7, 112.7, 43.6, 37.3. HRMS-ESI ( $m/z$ )  $[\text{M}+\text{Na}]^+$  calcd for  $\text{C}_9\text{H}_8\text{ClNNa}$ , 188.0237; found: 188.0234.



**2x**

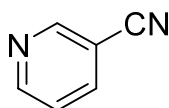
**3-(2-Chloroethyl)benzonitrile (2x):** oil (24.3 mg, 0.15 mmol, 49% isolated yield).

$^1\text{H NMR}$  ( $\text{CDCl}_3$ , 499 MHz):  $\delta$  ppm = 7.58 (d,  $J = 7.3$  Hz, 1 H), 7.54 (s, 1 H), 7.48 (s, 1 H), 7.46 (d,  $J = 7.3$  Hz, 1 H), 3.74 (t,  $J = 6.8$  Hz, 2 H), 3.12 ppm (t,  $J = 6.8$  Hz, 2 H).  $^{13}\text{C NMR}$  ( $\text{CDCl}_3$ , 126 MHz):  $\delta$  ppm = 139.5, 133.4, 132.4, 130.7, 129.3, 118.7, 112.7, 44.2, 38.3. HRMS-ESI ( $m/z$ )  $[\text{M}+\text{Na}]^+$  calcd for  $\text{C}_9\text{H}_8\text{ClNNa}$ , 188.0237; found: 188.0235.



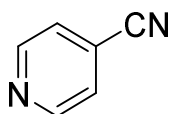
**2aa**

**2-Cyanopyridine (2aa)**: brown liquid (30.9 mg, 0.30 mmol, 99% isolated yield).  $^1\text{H}$  NMR ( $\text{CDCl}_3$ , 499 MHz):  $\delta$  ppm = 8.75 (d,  $J$  = 4.89 Hz, 1 H), 7.86 (td,  $J$  = 7.83, 1.96 Hz, 1 H), 7.72 (d,  $J$  = 7.83 Hz, 1 H), 7.54 (ddd,  $J$  = 7.83, 4.89, 1.47 Hz, 1 H).  $^{13}\text{C}$  NMR ( $\text{CDCl}_3$ , 75 MHz):  $\delta$  ppm = 151.2, 137.0, 134.1, 128.6, 126.9, 117.2. The spectral data were consistent with those reported in the literature.<sup>40</sup>



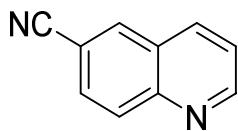
**2ab**

**3-Cyanopyridine (2ab)**: brown solid (30.9 mg, 0.30 mmol, 99% isolated yield).  $^1\text{H}$  NMR ( $\text{CDCl}_3$ , 499 MHz):  $\delta$  ppm = 8.91 (s, 1 H), 8.83 (d,  $J$  = 4.89 Hz, 1 H), 7.98 (dd,  $J$  = 8.07, 1.71 Hz, 1 H), 7.46 (t,  $J$  = 5.87 Hz, 1 H).  $^{13}\text{C}$  NMR ( $\text{CDCl}_3$ , 75 MHz):  $\delta$  ppm = 153.0, 152.5, 139.2, 123.6, 116.5, 110.2. The spectral data were consistent with those reported in the literature.<sup>41</sup>



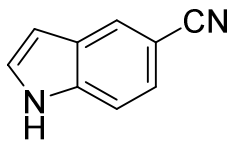
**2ac**

**4-Cyanopyridine (2ac)**: white solid (30.3 mg, 0.29 mmol, 97% isolated yield).  $^1\text{H}$  NMR ( $\text{CDCl}_3$ , 499 MHz):  $\delta$  ppm = 8.82 (d,  $J$  = 3.9 Hz, 2 H), 7.54 ppm (d,  $J$  = 3.4 Hz, 3 H).  $^{13}\text{C}$  NMR ( $\text{CDCl}_3$ , 75 MHz):  $\delta$  ppm = 150.8, 125.3, 120.4, 116.4. The spectral data were consistent with those reported in the literature.<sup>42</sup>



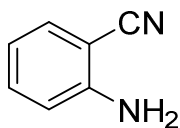
**2ad**

**6-Cyanoquinoline (2ad):** brown solid (38.9 mg, 0.25 mmol, 84% isolated yield).  $^1\text{H}$  NMR ( $\text{CDCl}_3$ , 499 MHz):  $\delta$  ppm = 9.01 - 9.09 (m, 1 H), 8.14 - 8.29 (m, 3 H), 7.84 (d,  $J = 8.31$  Hz, 1 H), 7.54 (dd,  $J = 8.07, 4.16$  Hz, 1 H).  $^{13}\text{C}$  NMR ( $\text{CDCl}_3$ , 75 MHz):  $\delta$  ppm = 153.2, 149.0, 136.3, 134.0, 131.0, 130.0, 127.5, 122.7, 118.4, 110.3. The spectral data were consistent with those reported in the literature.<sup>28</sup>



**2ae**

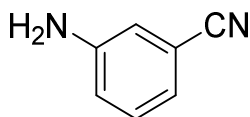
**1-H-indole-5-carbonitrile (2ae):** brown solid (22.6 mg, 0.16 mmol, 53% isolated yield).  $^1\text{H}$  NMR ( $\text{CDCl}_3$ , 499 MHz):  $\delta$  ppm = 8.72 (br. s., 1 H), 8.00 (s, 1 H), 7.40 - 7.50 (m, 2 H), 7.35 (s, 1 H), 6.64 ppm (s, 1 H).  $^{13}\text{C}$  NMR ( $\text{CDCl}_3$ , 75 MHz):  $\delta$  ppm = 137.5, 127.6, 126.5, 126.3, 124.8, 120.9, 112.0, 103.3, 102.6. The spectral data were consistent with those reported in the literature.<sup>5e</sup>



**2af**

**2-Aminobenzonitrile (2af):** brown liquid (17.4 mg, 0.15 mmol, 49% isolated yield).

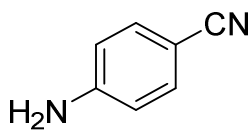
$^1\text{H}$  NMR ( $\text{CDCl}_3$ , 499 MHz):  $\delta$  ppm = 7.40 (d,  $J = 7.8$  Hz, 1 H), 7.34 (t,  $J = 7.8$  Hz, 1 H), 6.72 - 6.78 (m, 2 H), 4.39 ppm (br. s., 2 H).  $^{13}\text{C}$  NMR ( $\text{CDCl}_3$ , 126 MHz):  $\delta$  ppm = 149.5, 134.0, 132.3, 118.0, 117.6, 115.1, 96.1. The spectral data were consistent with those reported in the literature.<sup>33</sup>



**2ag**

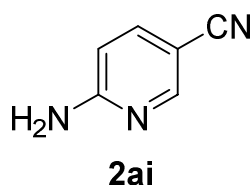
**3-Aminobenzonitrile (2ag):** brown liquid (22.3 mg, 0.19 mmol, 63% isolated yield).

$^1\text{H}$  NMR ( $\text{CDCl}_3$ , 499 MHz):  $\delta$  ppm = 7.21 (t,  $J = 7.83$  Hz, 1 H), 7.01 (d,  $J = 7.34$  Hz, 1 H), 6.90 (s, 1 H), 6.87 (d,  $J = 7.83$  Hz, 1 H), 3.91 (br. s., 2 H).  $^{13}\text{C}$  NMR ( $\text{CDCl}_3$ , 126 MHz):  $\delta$  ppm = 146.9, 130.0, 122.0, 119.2, 118.1, 117.4, 112.9. The spectral data were consistent with those reported in the literature.<sup>56</sup>

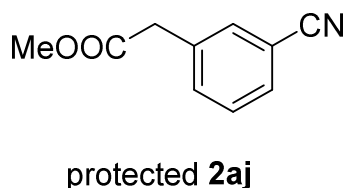


**2ah**

**4-Aminobenzonitrile (2ah)**: brown liquid (23.4 mg, 0.20 mmol, 66% isolated yield).  $^1\text{H}$  NMR ( $\text{CDCl}_3$ , 499 MHz):  $\delta$  ppm = 7.42 (d,  $J$  = 7.83 Hz, 2 H), 6.65 (d,  $J$  = 8.80 Hz, 2 H), 4.15 (br. s., 2 H).  $^{13}\text{C}$  NMR ( $\text{CDCl}_3$ , 126 MHz):  $\delta$  ppm = 150.3, 133.8, 120.1, 114.4, 100.2. The spectral data were consistent with those reported in the literature.<sup>29</sup>

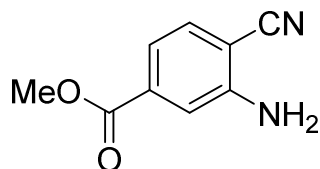


**6-Aminonicotinonitrile (2ai)**: brown solid (18.6 mg, 0.16 mmol, 52% isolated yield).  $^1\text{H}$  NMR ( $\text{CDCl}_3$ , 499 MHz):  $\delta$  ppm = 8.37 (d,  $J$  = 1.5 Hz, 1 H), 7.62 (dd,  $J$  = 8.8, 2.0 Hz, 1 H), 6.51 (d,  $J$  = 8.8 Hz, 1 H), 4.98 ppm (br. s., 2 H).  $^{13}\text{C}$  NMR ( $\text{CDCl}_3$ , 126 MHz):  $\delta$  ppm = 160.1, 153.1, 140.2, 118.1, 108.0, 98.4. The spectral data were consistent with those reported in the literature<sup>10</sup>



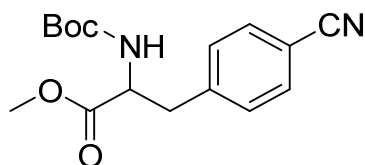
**Methyl 2-(3-cyanophenyl) acetate (protected 2ai)**: brown solid (18.6 mg, 0.16 mmol, 52% isolated yield).  $^1\text{H}$  NMR ( $\text{CDCl}_3$ , 499 MHz):  $\delta$  ppm = 8.37 (d,  $J$  = 1.5 Hz, 1 H), 7.62 (dd,  $J$  = 8.8, 2.0 Hz, 1 H), 6.51 (d,  $J$  = 8.8 Hz, 1 H), 4.98 ppm (br. s., 2 H).  $^{13}\text{C}$  NMR ( $\text{CDCl}_3$ , 75 MHz):  $\delta$  ppm = 170.8, 135.3, 133.9, 132.9, 130.9, 129.3, 118.5,

112.7, 52.3, 40.5 ppm. HRMS-ESI ( $m/z$ )  $[M+Na]^+$  calcd for  $C_{10}H_9NNaO_2$ , 198.0525; found: 198.0527.



**2ak**

**Methyl 3-amino-4-cyanobenzoate (2ak):** white solid (32.1 mg, 0.18 mmol, 60% isolated yield).  $^1H$  NMR ( $CDCl_3$ , 499 MHz):  $\delta$  ppm = 7.72 (d,  $J$  = 8.31 Hz, 1 H), 7.39 (d,  $J$  = 1.96 Hz, 1 H), 7.11 (dd,  $J$  = 7.83, 1.96 Hz, 1 H), 4.23 (br. s., 2 H), 3.90 (s, 3 H).  $^{13}C$  NMR ( $CDCl_3$ , 75 MHz):  $\delta$  ppm = 166.8, 146.8, 139.1, 131.3, 120.4, 115.4, 115.1, 89.9, 52.2. The spectral data were consistent with those reported in the literature.<sup>43</sup>



protected **2ai, 2am**

**Methyl-2-((tert-butoxycarbonyl)amino)-3-(4-cyanophenyl)propanoate**

(protected **2ai, 2am**): white solid (39.3 mg, 0.13 mmol, 43% isolated yield in the reaction of **1ai**).  $^1H$  NMR ( $CDCl_3$ , 499 MHz):  $\delta$  ppm = 7.28 - 7.33 (m, 2 H), 7.13 (d,  $J$  = 7.3 Hz, 2 H), 4.98 (d,  $J$  = 7.3 Hz, 1 H), 4.56 - 4.64 (m, 1 H), 3.72 (s, 3 H), 3.02 - 3.16 (m, 2 H), 1.43 (s, 9 H).  $^{13}C$  NMR ( $CDCl_3$ , 75 MHz):  $\delta$  ppm = 171.7, 154.9,

141.9, 132.2, 130.1, 118.7, 111.0, 80.2, 54.0, 52.4, 38.6, 28.2. The spectral data were consistent with those reported in the literature.<sup>5c</sup>



## 5.5 Notes and references

- (1) (a) M. Sundermeier, A. Zapf, M. Beller, *Eur. J. Inorg. Chem.* **2003**, 2003, 3513. (b) P. Anbarasan, T. Schareina, M. Beller, *Chem. Soc. Rev.* **2011**, 40, 5049. (c) F. F. Fleming, L. Yao, P. C. Ravikumar, L. Funk, B. C. Shook, *J. Med. Chem.* **2010**, 53, 7902.
- (2) G. P. Ellis, T. M. Romney-Alexander, *Chem. Rev.* **1987**, 87, 779.
- (3) K. W. Rosenmund, E. Struck, *Ber. Dtsch. Chem. Ges.* **1919**, 52, 1749.
- (4) S. Guo, G. Wan, S. Sun, Y. Jiang, J.-T. Yu, J. Cheng, *Chem. Commun.* **2015**, 51, 5085.
- (5) (a) T. Kentaro, S. Ken, S. Yasumasa, *Bull. Chem. Soc. Jpn.* **1991**, 64, 1118. (b) P. Y. Yeung, C. M. So, C. P. Lau, F. Y. Kwong, *Angew. Chem. Int. Ed.* **2010**, 49, 8918. (c) A. V. Ushkov, V. V. Grushin, *J. Am. Chem. Soc.* **2011**, 133, 10999. (d) T. D. Senecal, W. Shu, S. L. Buchwald, *Angew. Chem. Int. Ed.* **2013**, 52, 10035. (e) D. T. Cohen, S. L. Buchwald, *Org. Lett.* **2015**, 17, 202. (f) H. G. Lee, P. J. Milner, M. S. Placzek, S. L. Buchwald, J. M. Hooker, *J. Am. Chem. Soc.* **2015**, 137, 648.
- (6) (a) L. Cassar, *J. Organomet. Chem.* **1973**, 54, C57. (b) L. Cassar, M. Foà, F. Montanari, G. P. Marinelli, *J. Organomet. Chem.* **1979**, 173, 335. (c) S. Yasumasa, O. Fumio, S. Akira, K. Kunihiko, S. Mutsuji, U. Norito, T. Kentaro, *Bull. Chem. Soc. Jpn.* **1988**, 61, 1985. (d) S. Yasumasa, I. Yoshinori, S. Ken, S. Mutsuji, U. Norito, *Bull. Chem. Soc. Jpn.* **1993**, 66, 2776. (e) R. K. Arvela, N. E. Leadbeater, *J. Org. Chem.* **2003**, 68, 9122.
- (7) (a) J. X. Wu, B. Beck, R. X. Ren, *Tetrahedron Lett.* **2002**, 43, 387. (b) H.-J. Cristau, A. Ouali, J.-F. Spindler, M. Taillefer, *Chem. Eur. J.* **2005**, 11, 2483. (c) T. Schareina, A. Zapf, M. Beller, *Tetrahedron Lett.* **2005**, 46, 2585. (d) T. Schareina, A.

Zapf, W. Mägerlein, N. Müller, M. Beller, *Chem. Eur. J.* **2007**, *13*, 6249. (e) T. Schareina, A. Zapf, W. Mägerlein, N. Müller, M. Beller, *Synlett* **2007**, *2007*, 0555. (f) C. DeBlase, N. E. Leadbeater, *Tetrahedron* **2010**, *66*, 1098. (g) T. Schareina, A. Zapf, A. Cotté, M. Gotta, M. Beller, *Adv. Synth. Catal.* **2011**, *353*, 777. (h) G. Zhang, L. Zhang, M. Hu, J. Cheng, *Adv. Synth. Catal.* **2011**, *353*, 291. (i) G. Zhang, X. Ren, J. Chen, M. Hu, J. Cheng, *Org. Lett.* **2011**, *13*, 5004. (j) J. Kim, J. Choi, K. Shin, S. Chang, *J. Am. Chem. Soc.* **2012**, *134*, 2528. (k) Z. Wang, S. Chang, *Org. Lett.* **2013**, *15*, 1990. (l) A. B. Pawar, S. Chang, *Chem. Commun.* **2014**, *50*, 448. (m) Q. Wen, J. Jin, L. Zhang, Y. Luo, P. Lu, Y. Wang, *Tetrahedron Lett.* **2014**, *55*, 1271. (n) S.-L. Zhang, L. Huang, *Org. Biomol. Chem.* **2015**, *13*, 9963.

(8) (a) W. Zhou, L. Zhang, N. Jiao, *Angew. Chem. Int. Ed.* **2009**, *48*, 7094. (b) W. Zhou, J. Xu, L. Zhang, N. Jiao, *Org. Lett.* **2010**, *12*, 2888. (c) S. Ding, N. Jiao, *J. Am. Chem. Soc.* **2011**, *133*, 12374. (d) T. Shen, T. Wang, C. Qin, N. Jiao, *Angew. Chem. Int. Ed.* **2013**, *52*, 6677. (e) T. Wang, N. Jiao, *Acc. Chem. Res.* **2014**, *47*, 1137. (f) J. Kim, S. Chang, *J. Am. Chem. Soc.* **2010**, *132*, 10272. (g) A. B. Pawar, S. Chang, *Org. Lett.* **2015**, *17*, 660.

(9) S. R. Chemler, *Beilstein J. Org. Chem.* **2015**, *11*, 2252.

(10) J. Zanon, A. Klapars, S. L. Buchwald, *J. Am. Chem. Soc.* **2003**, *125*, 2890.

(11) T. S. Ratani, S. Bachman, G. C. Fu, J. C. Peters, *J. Am. Chem. Soc.* **2015**, *137*, 13902.

(12) (a) S. E. Creutz, K. J. Lotito, G. C. Fu, J. C. Peters, *Science* **2012**, *338*, 647. (b) A. C. Bissember, R. J. Lundgren, S. E. Creutz, J. C. Peters, G. C. Fu, *Angew. Chem. Int. Ed.* **2013**, *52*, 5129. (c) D. T. Ziegler, J. Choi, J. M. Muñoz-Molina, A. C. Bissember, J. C. Peters, G. C. Fu, *J. Am. Chem. Soc.* **2013**, *135*, 13107. (d) C. Uyeda,

Y. Tan, G. C. Fu, J. C. Peters, *J. Am. Chem. Soc.* **2013**, *135*, 9548. (e) H.-Q. Do, S. Bachman, A. C. Bissember, J. C. Peters, G. C. Fu, *J. Am. Chem. Soc.* **2014**, *136*, 2162. (f) Y. Tan, J. M. Munoz-Molina, G. C. Fu, J. C. Peters, *Chem. Sci.* **2014**, *5*, 2831. (g) Q. M. Kainz, C. D. Matier, A. Bartoszewicz, S. L. Zultanski, J. C. Peters, G. C. Fu, *Science* **2016**, *351*, 681. (h) M. W. Johnson, K. I. Hannoun, Y. Tan, G. C. Fu, J. C. Peters, *Chem. Sci.* **2016**, *7*, 4091.

(13) (a) S. Bloom, C. R. Pitts, D. C. Miller, N. Haselton, M. G. Holl, E. Urheim, T. Lectka, *Angew. Chem. Int. Ed.* **2012**, *51*, 10580. (b) C. R. Pitts, S. Bloom, R. Woltornist, D. J. Auvenshine, L. R. Ryzhkov, M. A. Siegler, T. Lectka, *J. Am. Chem. Soc.* **2014**, *136*, 9780.

(14) (a) S. Erhardt, V. V. Grushin, A. H. Kilpatrick, S. A. Macgregor, W. J. Marshall, D. C. Roe, *J. Am. Chem. Soc.* **2008**, *130*, 4828. (b) T. Schareina, M. Beller, in *Copper-Mediated Cross-Coupling Reactions*, John Wiley & Sons, Inc., **2013**, pp. 313.

(15) K. D. Dobbs, W. J. Marshall, V. V. Grushin, *J. Am. Chem. Soc.* **2007**, *129*, 30.

(16) Although CuI and CuBr exhibited comparable activity in the cyanation of **1a**, their efficiency decreased significantly with other substrates such as **1c**, **1k**, **1n**, and **1ah**. see the Supporting Information (Table 5.5).

(17) (a) Y. Zhu, L. Li, Z. Shen, *Chem. Eur. J.* **2015**, *21*, 13246. (b) M. Zhao, W. Zhang, Z. Shen, *J. Org. Chem.* **2015**, *80*, 8868.

(18) B. M. Trost, *Science* **1983**, *219*, 245.

(19) Z. Wang, in *Comprehensive Organic Name Reactions and Reagents*, John Wiley & Sons, Inc., **2010**.

(20) A. Toth, C. Floriani, M. Pasquali, A. Chiesi-Villa, A. Gaetani-Manfredotti, C.

- Guastini, *Inorg. Chem.* **1985**, *24*, 648.
- (21) M. Felderhoff, T. Smolka, R. Sustmann, *J. Prakt. Chem.* **1999**, *341*, 639.
- (22) A. Simion, C. Simion, T. Kanda, S. Nagashima, Y. Mitoma, T. Yamada, K. Mimura, M. Tashiro, *J. Chem. Soc., Perkin Trans. 1* **2001**, 2071.
- (23) A. Minatti, S. L. Buchwald, *Org. Lett.* **2008**, *10*, 2721.
- (24) WO2005014552 (A1)
- (25) J. Kim, H. J. Kim, S. Chang, *Angew. Chem. Int. Ed.* **2012**, *51*, 11948.
- (26) H. Mizuno, J. Takaya, N. Iwasawa, *J. Am. Chem. Soc.* **2011**, *133*, 1251.
- (27) D. M. Shendage, R. Fröhlich, G. Haufe, *Org. Lett.* **2004**, *6*, 3675.
- (28) U. Dutta, D. W. Lupton, D. Maiti, *Org. Lett.* **2016**, *18*, 860.
- (29) G.-Y. Zhang, J.-T. Yu, M.-L. Hu, J. Cheng, *J. Org. Chem.* **2013**, *78*, 2710.
- (30) WO2015/160636 A1
- (31) J. T. Reeves, C. A. Malapit, F. G. Buono, K. P. Sidhu, M. A. Marsini, C. A. Sader, K. R. Fandrick, C. A. Busacca, C. H. Senanayake, *J. Am. Chem. Soc.* **2015**, *137*, 9481.
- (32) A. Littke, M. Soumeillant, R. F. Kaltenbach, R. J. Cherney, C. M. Tarby, S. Kiau, *Org. Lett.* **2007**, *9*, 1711.
- (33) T. Shen, T. Wang, C. Qin, N. Jiao, *Angew. Chem. Int. Ed.* **2013**, *52*, 6677.
- (34) E. Jones-Mensah, J. Magolan, *Tetrahedron Lett.* **2014**, *55*, 5323.
- (35) Y. Zhu, M. Zhao, W. Lu, L. Li, Z. Shen, *Org. Lett.* **2015**, *17*, 2602.
- (36) N. Murai, M. Yonaga, K. Tanaka, *Org. Lett.* **2012**, *14*, 1278.
- (37) Q. Wen, J. Jin, Y. Mei, P. Lu, Y. Wang, *Eur. J. Org. Chem.* **2013**, *2013*, 4032.
- (38) A. P. Gaywood, H. McNab, *Org. Biomol. Chem.* **2010**, *8*, 5166.
- (39) Q.-W. Zhang, A. T. Brusoe, V. Mascitti, K. D. Hesp, D. C. Blakemore, J. T.

- Kohrt, J. F. Hartwig, *Angew. Chem. Int. Ed.* **2016**, *55*, 9758.
- (40) X. Zhang, J. Sun, Y. Ding, L. Yu, *Org. Lett.* **2015**, *17*, 5840.
- (41) S. Laulhé, S. S. Gori, M. H. Nantz, *J. Org. Chem.* **2012**, *77*, 9334.
- (42) B. Mondal, K. Acharyya, P. Howlader, P. S. Mukherjee, *J. Am. Chem. Soc.* **2016**, *138*, 1709.
- (43) J. Crosby, J. Moilliet, J. S. Parratt, N. J. Turner, *J. Chem. Soc., Perkin Trans. 1* **1994**, 1679.

## 국문초록

# 새로운 촉매적 유기 합성법 개발: 락탐 합성, 사이아노하이드린 탈수소화 반응, 아릴 할라이드의 사이안화 광촉매 반응

김기철

서울대학교 자연과학대학원 화학부

보다 녹색 화학적이면서도 효율적인 화학 합성법을 개발하는 것은, 유기 합성 분야뿐 아니라 인류 사회에 있어서 매우 중요한 화두이다. 널리 이용되는 대다수의 유기 합성법은 고효율이라는 장점은 있지만 1) 반응성 향상을 위한 반응물 전처리 과정이 필요하거나, 2) 고온, 고압의 혹독한 반응 조건, 3) 독성 시약 또는 4) 과량의 시약을 사용함으로써 5) 비용 및 이에 수반된 폐기물 처리 등의 문제가 있다. 화석 원료의 고갈, 기후 변화, 환경 문제에 직면한 국제사회는 이를 해결하기 위한 녹색화합적인 유기합성법 개발을 요구하고 있다. 한편, 고분자로 대표되는 상용품 생

산 공정 및 의약품 기능을 향상할 높은 선택성 및 효율을 가진 유기 합성법 개발 또한 끊임없이 요구되고 있는 실정이다.

따라서 지속 가능한 녹색 화학은 21세기 화학 연구에 있어서 필수적인 규율로 자리 잡았다. 이 개념은 분자 단위 수준에서 위험한 물질의 사용 및 생성을 줄이려는 노력에서 출발한다. 이 맥락에서 화학 공정은 다음과 같은 기준에 의거하여 수행해야 한다. 1) 폐기물 생성을 지양하고, 2) 에너지 효율과 3) 원자 및 반응 단계 경제성을 추구하고, 4) 가급적 덜 해로운 합성을 도모하고, 5) 반응물의 활성화 전처리를 피해야 한다. 이에, 유기금속 촉매법은 녹색 화학 및 효율적인 유기 합성 화학이라는 두 마리 토끼를 모두 잡을 수 있는 해결책으로 주목 받고 있다. 기존 전통적인 합성법과는 달리, 유기금속 촉매 반응은 전이 금속과 그 리간드의 상호 작용에 의한 독특한 메커니즘을 통해 촉매 조건에서 이뤄진다. 본 연구는, 정밀하게 구상된 유기 금속 촉매를 기반으로 한 알코올 활성화와 구리-광촉매 작용이라는 두 가지 반응물 활성화 방식을 도입하여, 기초 물질로부터 고부가 가치 물질을 합성하는 친환경적이면서도 효율적인 합성법 개발 과정을 다룬다. 구체적으로는 메커니즘에 기반하여 반응성 실현 전략을 구축하고 (유기화학), 핵심 단계를 매개하는 촉매와 리간드를 디자인하여 반응성을 구현하려는 과정이 담겨 있다 (유기금속화학). 더불어, 개발한 촉매 작용을 이해하고 궁극적으로 반응 개선을 위해 전자, 입체적 성질을 기준으로 수행한 메커니즘 연구 과정이

포함된다 (촉매작용).

**파트 1**은 총 3가지 챕터를 통해 알코올 활성화의 개념을 소개하고 ‘연쇄적인 탄소-질소 결합 형성 반응을 바탕으로 한 락탐 합성법 개발’ 및 ‘사이아노하이드린 탈수소화 반응 개발’이라는 두 적용 사례를 다룬다. 전이 금속 촉매에 의한 알코올 탈수소화 반응은 알코올 활성화 전략의 하나로서 유용한 합성 전구체인 카보닐 물질을 생성하여 추후 화학 반응에 적용할 수 있는 가능성을 열고 있다 (챕터 1). 알킬 할라이드나 산화제 등의 높은 반응성을 가진 시약을 배제한 조건에서도, 이를 적용함으로써 원자 경제적인 알코올의 탈수소화 관련 반응을 실현할 수 있다. 이에, 우리는 이리듐 촉매 하에 단계 경제적으로 질소-치환된 락탐을 합성하는 촉매법을 최초로 개발하였다 (챕터 2). 본 연구를 통해  $[Cp^*Ir]$  유기금속 착물이 락톤과 아민으로부터 탈수소화적인 탄소-질소 결합 형성 반응을 촉매적으로 매개할 수 있음을 밝혔다. 메커니즘 연구를 통해 본 반응은 기존의 비촉매적 락탐 합성법과는 달리, 세 가지 단계(락톤으로부터 아마이드 결합 형성, 하이드록시 아마이드 중간체의 N-알킬화 반응, 아미노 아마이드 중간체의 분자 내 아마이드 교체 반응)를 통해 락탐을 생성한다는 사실을 밝혔다. 챕터 3에서는 수소 반개 없이 알코올을 탈수소화는 전략을 기반으로, 염기 없이 루테튬 촉매를 이용하여 사이아노하이드린을 탈수소화하는 촉매 반응을 최초로 개발한 과정이 서술된다. 두 자리 포스핀 리간드를 지닌 루테튬(II) 아렌 착



물을 도입하여 열역학적으로 더 선호되는 방향 (시아노화수소 분출을 통한 알데히드 형성 반응) 대신 반응 속도론적 지배를 통한 탈수소화 반응을 이룩하였다. 또한 촉매 활성화도 및 반응 선택성 향상을 위해 루테튬 촉매를 구성하는 리간드, 배위 방식, 짝이온의 영향을 탐구하였다. 루테튬-알콕사이드 물질을 실험적으로 관찰함으로써 선택적인 탈수소화 반응이 베타-하이드라이드 제거 반응을 따름을 핵심 메커니즘으로 제시하였다.

**파트 2**는 두 챕터에 걸쳐 교차 짝지음 (cross-coupling) 반응을 매개하는 구리 광촉매 작용을 소개하고 방향족 할로젠 물질의 사이안화 반응에 대한 그 적용 사례를 다룬다. 전통적인 유기 반응에서 반응성 활성화를 위해 자주 사용되는 가열과는 달리, 광촉매 작용은 보다 환경 친화적인 방식으로 분자를 활성화시킬 수 있는 방법으로서 최근 주목 받고 있다. 이 방식은 빛의 조사를 통해 제공되는 광자를 이용해 광촉매를 활성화 시켜, 들뜬 광촉매로 하여금 에너지 전달 또는 단일 전자 전달 (SET) 과정을 촉매적으로 매개하도록 유도한다. 한편 이 분야에서 주로 쓰이는 루테튬 및 이리듐 기반의 광-산화환원 (photoredox) 촉매 작용과 비교하여, 구리 광촉매 작용은 비용, 안정성, 및 반응 활성화도 면에서 그 대안으로 주목 받고 있다. 특히, 특정 구리(I) 착물의 경우 온화한 조건에서 단일 전자 전달 반응 매개뿐 아니라 교차 짝지음 반응에 직접적으로 참여하는 반응성을 가진다고 알려져 있다. 이 점에 착안하여, 챕터 5에서는 쉽게 도입 가능한 구리(I)-비스이민 촉매 하에 상온에서 방향

족 할로젠 물질을 선택적으로 사이안화하는 최초의 광촉매 반응 개발을 소개한다. 기존에 개발된 이전자 전달 과정을 따르는 구리 촉매법과는 달리, 본 구리 광촉매법은 단일 전자 전달 과정을 통해 뛰어난 작용기-허용성(functional group tolerance)을 보여준다. 이 반응은 기존에 적용이 어려웠던 아민, 카르복실산 및 아미노산 등 여러 작용기의 적용이 가능하며, S<sub>N</sub>2 반응에 취약한 알킬 클로라이드에 대해 뛰어난 화학선택성(chemoselectivity)을 보인다.

본 연구 과정을 통해, 우리는 알코올 활성화와 광촉매 작용이라는 두 종류의 반응물 활성화 전략을 통해 보다 간단한 반응물로부터 고부가 가치 물질을 생성할 수 있는 효율적이면서도 새로운 세 가지의 합성법을 구축하였다. 또한 그 합성적 효용 및 메커니즘 연구를 통해 개발된 촉매 합성법의 적용 범위를 한층 넓힐 수 있는 가능성을 제시하였다.

**주요어:** 유기 화학, 유기금속 촉매법, 녹색 화학, 전이 금속 촉매, 촉매-리간드 디자인, 알코올 액티베이션, 광촉매 작용, 락탐, 아실 사이아니드, 방향족 나이트릴

**학번:** 2013-20256